RISØ

Risø-R-863(EN)

Annual Progress Report of the Department of Solid State Physics 1 January - 31 December 1995

Edited by M. Jørgensen, K. Bechgaard, K.N. Clausen, R. Feidenhans'l and I. Johannsen

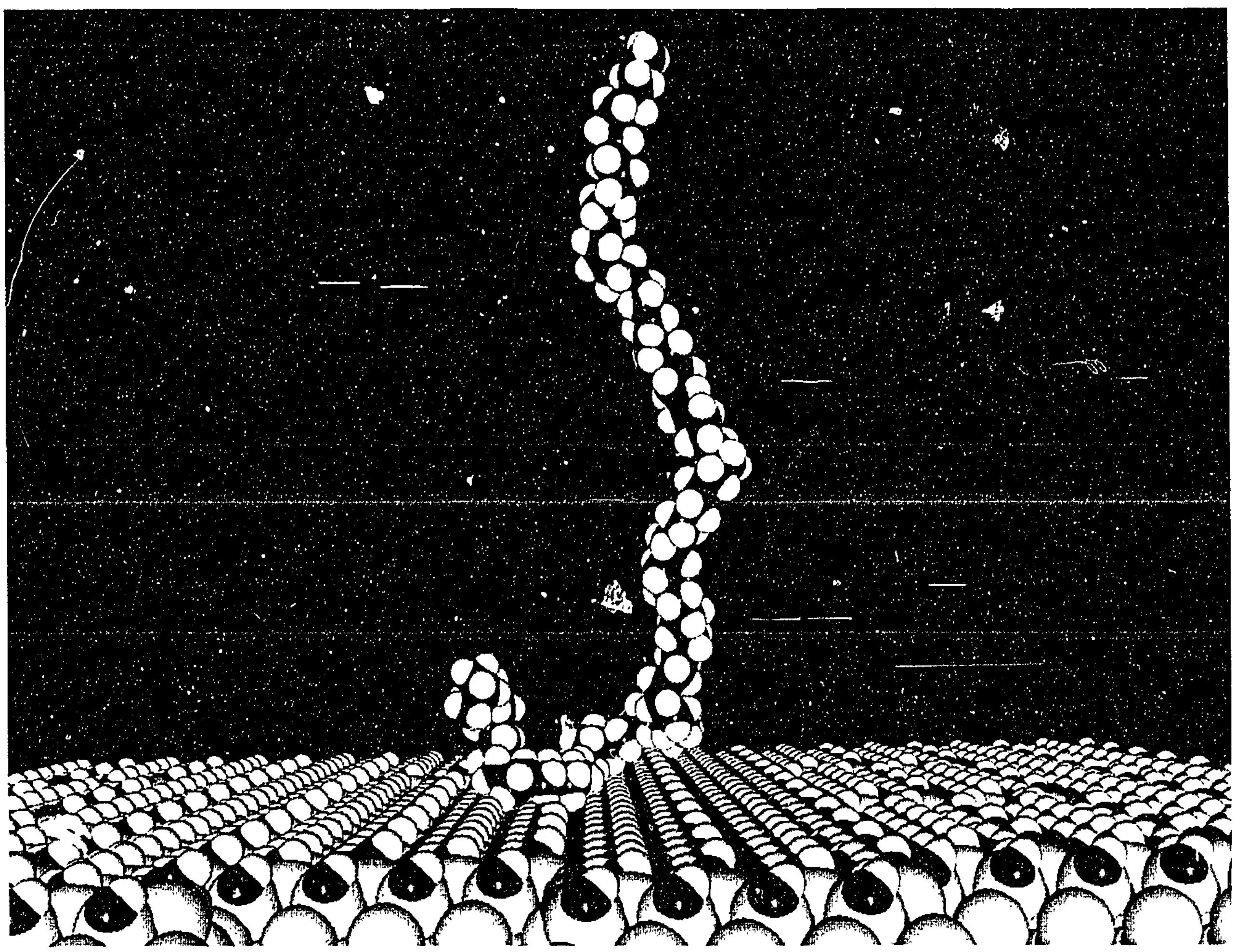

Risø National Laboratory, Roskilde, Denmark
January 1996

Annual Progress Report of the Department of Solid State Physics 1 January - 31 December 1995

Risø-R-863(EN)

Edited by M. Jørgensen, K. Bechgaard, K.N. Clausen, R. Feidenhans'l and I. Johannsen

Risø National Laboratory, Roskilde, Denmark
January 1996

Abstract
Research in the department is concerned with "Materials with Distinct Physical and Chemical Properties". The principal activities of the department in the period from 1 January to 31 December, 1995, are presented in this Progress Report.

Neutron and x-ray diffraction techniques are used to study a wide variety of problems in condensed matter physics and include: two- and three-dimensional structures, magnetic ordering, heavy fermions, high T_c superconductivity, phase transitions in model systems, precipitation phenomena, and nano-scale structures in various materials. The research in chemistry includes chemical synthesis and physico-chemical investigation of small molecules and polymers, with emphasis on polymers with new optical properties, block copolymers, surface modified polymers, and supramolecular structures. Related to these problems there is work going on in theory, Monte Carlo simulations, computer simulation of molecules and polymers and methods of data analysis.

Frontpage illustration:

Atomistic simulation of polyethylene adsorbed to a (1-1 0)-surface of quartz terminated with hydroxyl groups. The polymer is in a amorphous state. Only one polymer chain is shown.

ISBN 87-550-2142-5
ISSN 0106-2840
ISSN 0907-0249

Grafisk Service - Risø - 1996

Professor Allan Roy Mackintosh

December 20, 1995 was a very sad day for the Department of Solid State Physics. On his way home from Risø after delivering a splendid lecture on the 1995 Nobel Price in Physics, Professor Allan Roy Mackintosh was tragically killed in a car accident. Allan Mackintosh was one of the founders of modern Solid State Physics in Denmark in general and at Risø in particular. During the early sixties Allan Mackintosh and Hans Bjerrum Møller started inelastic neutron scattering at Risø. Their studies of the Rare Earth metals were truly outstanding and was later acknowledged with the 1986 Frank H. Spedding award. In 1966 Allan Mackintosh obtained a professorship at the Technical University in Denmark. A year later he moved to a Professorship at the University of Copenhagen. From 1971 to 1976 he served as Director of Risø, and from 1986 to 1988 as Director of NORDITA in Copenhagen. During the whole period he kept close links to the Department for Solid State Physics at Risø, and had a profound influence on the research carried out here.

From 1991 onwards Allan Mackintosh accepted new duties for Risø. He became a key person in the EC-supported neutron scattering user programme, was the secretary of our referee panel and acted as the link between Risø, the EC and the Users. Allan's extensive international contacts, his flair for international collaboration and strong emphasis on quality have been essential for establishing and running the user programme. In the same context, Allan acted as a consultant to the Commission of the European Commission on effective use of Large Scale Facilities in Europe. In the new EC-TMR programme scientific excellence will receive more emphasis at the expense of bureaucratic complexity.

Magnetism and neutron scattering has lost one of its finest scientists and we have lost a friend and a colleague, whose qualities as a human being were even more outstanding than his scientific career.

Contents

1 Introduction

The research of the Department of Solid State Physics is an integral part of Risø's long term programme "Materials with special physical and chemical properties".
This research aims at creating an understanding of the relation between the atomic and molecular structure of materials and their electrical, magnetic, optical, chemical, or biological properties. The activities in 1995 were organized in three programmes: Macromolecular Materials Chemistry, Magnetism and Superconductivity and Surfaces and interfaces. In addition the Department of Solid State Physics was in charge of a special programme under the Commission of the European Community (CEC) Human Capital and Mobility programme (HCM).
In 1995 Senior Scientist Kell Mortensen was appointed Research Professor by the Danish Natural Research Council. This appointment will further strengthen the departments' research in Soft Materials Science.

Macromolecular Materials Chemistry

The purpose of this programme is to investigate the properties of molecular materials with a view to prepare improved materials through integration of molecular design, synthesis, and knowledge of structure.

Part of the research projects are organized within the framework of the The Danish Polymer Centre (in collaboration with the Department of Chemical Engineering at the Technical university of Denmark, The Danish Polymer Centre (DPC) was established late 1994, and apart from the scientific activities the last year has been devoted to strengthening the industrial collaboration in the Centre. Seven industrial research projects on topics related to the general research themes of the Centre have commenced. Among the industrial partners are Novo Nordisk A/S, Danfoss A/S, Grundfos A/S, Nunc A/S and Hempel's Marine Paints A/S. Also in 1995 the renovation of the laboratories has been completed and several new instruments have been installed including NMR, MALDI-TOF-MS and GC-MS.

Some of the scientific highlights are:

- New Peptide-based materials for optical storage of information.

Recent work has demonstrated that suitably designed peptides, referred to as DNO oligomers, can be used as a new class of materials for holographic optical recording. By a number of measures, they perform better than polymers currently available. Diffraction efficiencies near 100% of the maximum achievable were obtained from laser-induced holographic gratings formed thin films of DNO oligomers containing two or more residues. The holograms formed are exceptionally stable and are not erased after exposure to 150 °C for extended periods. They can, however, be erased by exposure to circularly polarized light and reused several times without fatigue.

- Lifshitz Critical Point in a Complex Polymer blend.

Twenty years ago the concept of a multicritical Lifshitz point was introduced describing the critical phenomena associated with a continuous crossover between different types of critical phenomena. A variety of systems have been suggested to exhibit such Lifshitz point, including

magnetic systems and complex fluids. Up to the present, however, an isotropic Lifshitz point has never been realized experimentally. With the aim to experimentally investigate such Lifshitz critical point, Risø researchers in collaboration with the University of Minnesota have studied the phase behavior of a series of mixtures of symmetric diblock copolymers PE-PEP and a symmetric blend of the corresponding homopolymers PE and PEP, where PE is poly(ethylene) and PEP is poly(ethylene propylene). The studies were made using small-angle neutron scattering (SANS). The experiments clearly demonstrated that such polymer blends exhibit characteristics as theoretically predicted near the Lifshitz point, and thereby proved the utility of complex polymer systems to pursuit theoretically predicted critical behavior.

Magnetic and Superconductive Materials

The purpose of this programme is to investigate the relationship between atomic/molecular structure and properties of magnetic and superconducting materials.

Some scientific highlights are:

- Structural evidence for a two-step process in the depinning of the superconducting flux-line lattice.

A magnetic field penetrates a type II superconductor as a hexagonal lattice of quantised flux lines. In collaboration with AT&T Bell Laboratories small-angle neutron scattering has been used to image how, with increasing current, the static flux line lattice in $NbSe_2$ transforms via disordered plastic motion to a coherently moving flux crystal. The observations of these structural changes to the flux line lattice - close to the critical current - verify recent theoretical predictions.

- Antiferromagnetic order in long period antiferromagnets at low temperatures and high pressures.

Basic understanding of the magnetic order appearing in naturally occurring compounds forms the foundation for design of man-made compounds and super-lattices with predetermined magnetic properties In collaboration with Copenhagen University, Risø scientists have developed a method to extract the repeat distance of the antiferromagnetic order and the range of the antiferromagnetic correlation's, which yield information about the formation of order from small angle neutron scattering data. The method is general and not restricted to magnetic order. It allows researchers to extract physical important parameters from SANS data obtained by Bragg scattering from a wide variety of ordered systems, e.g. nearly ferromagnetic antiferromagnetic compounds, the magnetic flux line lattice formed in superconductors, long period order of clusters and aggregates etc.

- Studies towards development of high-T_c superconductor wires.

In recent years there has been significant progress towards technological applications of high- T_c superconductors. The Danish company NKT Corporation has a leading international position in the development of superconducting wires for power transmission cables based on the BISCCO type high-Tc materials. A development programme, which involves the Department of Solid State Physics and the Materials Department at Risø, has been established by support from the Danish Ministry of Energy and the electricity unions ELSAM and ELKRAFT. The texture of

wires was studied by high energy x-ray diffraction and it has been shown that the critical current is strongly dependent on the texture of the BISCCO material.

Surfaces and Boundary Layers

The purpose of this programme is to investigate the relationship between atomic/molecular structure and properties of surfaces, boundary layers and thin films.

Some scientific highlights are:

- Self-Organisation at Surfaces.

Chiral molecules (left or right handed) of biological origin have always only one chirality - it is a fascinating and unsolved problem how this breaking of symmetry have occurred during the evolution. Various mechanism that separates left and right-handed molecules are therefore of interest. By x-ray diffraction measurement performed at the synchrotron laboratory HASYLAB in Hamburg we have in collaboration with the Weizmann Institute in Israel discovered that a Langmuir-layer (a single monolayer on the surface of water) of long aminoacids spontaneously self-organises into domains of left-handed and domains of right-handed molecules. This is evident because the crystalline unit cell on the water surface can only contain one molecule with one chirality

Another example of self-organisation is from an completely different field. Nano-clusters can have very interesting electronic properties. An surprising example of self-organisation of nano-clusters occurs when a layer of indium is deposited on the (001) surface of germanium. The smooth surface spontaneously facets to a surface with completely different morphology consisting of an regular array of (103) facets like the roofs of attached houses all aligned in one direction. This work is a collaboration with the University of Hamburg and is an example of the how synchrotron x-ray diffraction measurements of reciprocal space go hand in hand with scanning tunnelling microscopy (STM) measurements of direct space.

- Artificial magnetic structures.

Artificial magnetic multilayers will be important for future generation of magnetic storage media. Multilayers are normally produced by sputtering techniques or molecular beam epitaxy. Magnetism in rare earth metals offers a rich variety of model systems for studying magnetic multilayers. The standard method of studying magnetism have traditionally been neutron diffraction, but synchrotron x-ray scattering offers a number of new possibilities. The project is a collaboration between Risø and Oxford University, where the superlattices are produced. The first experiments on light rare earth superlattices of Nd/Pr have been performed and the superlattices exhibit several novel features.

Neutron Programme

The special programme under the Commission of the European Community (CEC) Training and Mobility of Researchers (TMR) obtained in late 1995 a new contract covering the period 1996 until the end of 1998.

The construction of RITA (Reinvented triple axis spectrometer) proceeds as planned. In late 1995 a new cold source was installed at DR3. The spectrometer parts will be assembled in January and February of 1996 and test runs are expected to start around March 1 of 1996.

2 Research Projects in the Department

The work is divided into the following subject categories:

2.1 Theory

2.2 Magnetic and Metallic Structures

2.3 Superconducting Materials Phenomena

2.4 Structures and Defects

2.5 Surfaces and Interfaces

2.6 Langmuir Films

2.7 Microemulsions, Surfactants and Biological Systems

2.8 Polymers

2.9 Organic Chemistry

2.10 Human Capital and Mobility - Access to Large Installations

2.1 Theory

2.1.1 Calculation of Third Order Nonlinear Optical Properties of Molecules

P. Sommer-Larsen, *Department of Solid State Physics, Riso National Laboratory, Denmark*, J. Arentoft and T. Bjørnholm, *CISMI (Centre for Interdisciplinary Studies of Molecular Interactions), Chemistry Department, University of Copenhagen, Denmark*, M. Malagoli and J.-L. Bredas, *Service de Chimie des Matériaux Nouveaux et Centre de Recherche en Electronique et Photonique Moleculaire, Université de Mons-Hainaut, Mons, Belgium*

Molecules with stable delocalized polyconjugated π-electron systems have attracted considerable attention as constituents in materials for nonlinear optics. A series of Bis-1,3-Polymethine dyes has been synthesised and their third order nonlinear optical properties have been investigated both experimentally and theoretically.[1] Solid solutions of the molecules in thin polymeric films show very strong nonlinear optical effects. Several theoretical methods have been used in the calculations described here. Static molecular hyperpolarizabilities have been calculated with *ab initio* and semiempirical methods, whereas the dispersion of $\gamma(-3\omega;\omega,\omega,\omega)$ has been calculated with a sum over state (SOS) expression.

The molecules under study are shown in Fig. 1. The chain connecting the two 1,3-dithiole end groups extents from one to four alternating single/double bonds through the series. Calculations have been performed on free cationic molecules. The structure of all molecules is calculated to be cyanine-dye like. This means that all bonds in the chain are of equal length, so no single/double bond alternation occurs.

Calculated static hyperpolarizabilities are in general not in quantitative agreement with values measured at a laser wavelength of 1064 nm. Calculated and experimental values follow however the same scaling law for the hyperpolarizability as a function of molecular length. The dispersion of the hyperpolarizability has been calculated based on a SOS-expression and a free electron model fitted to the measured electronic absorption spectra for the molecules. The calculated values at 1064 nm are in much better agreement with experimental values. The dispersion curves in Fig. 2 show the reason: At $\bar{\nu}$ = 9398 cm^{-1} (corresponding to 1064 nm) the frequency has crossed the first reasonans at $\bar{\nu}_{01}/3$, where $\bar{\nu}_{01}$ is the frequency for the first molecular excitation.

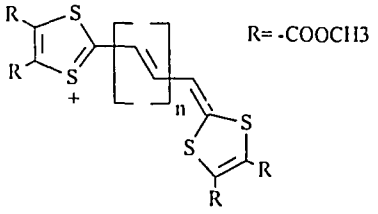

Fig. 1. Series of polymethine dyes studied. n = 0,1,2 or 3.

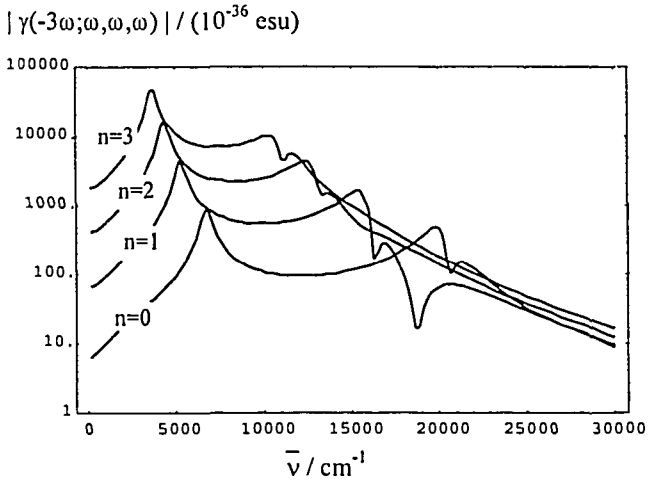

Fig. 2. The dispersion of the absolute value of gamma as a function of wave number for the four compunds n=0,1,2,3.

[1] K.B. Simonsen, T. Bjørnholm, T. Geisler, J.C. Petersen, J. Arentoft, P. Sommer-Larsen, D. Greve, C. Jacobsen, J. Becker, M. Malagoli, J.-L. Bredas. Manuscript in preperation.

2.1.2 Exact Enumeration of Protein Folds

P.-A. Lindgård, *Department of Solid State Physics, Riso National Laboratory, Denmark*, and H. Bohr, *Center for Biological Sequence Analysis, Department of Physical Chemistry, DTU, The Technical University of Denmark, Denmark*

The sequence information of several hundred thousands of proteins is by now known. The structural folding seems to be essential for their function. However, the determination of the protein structure in their "native", *i.e.* folded ground state is a very demanding x-ray task. Only about 100 different, typical structures have been determined of the "domains", which are subunits consisting of about 100 amino acid, folded up into about 10 secondary structures, α-helices or β-sheets, and about 10 connecting strands, in all about 20 elements. It is characteristic in this field of bio-inspired physics, that exact numbers are not meaningful, a certain flexibility is needed in the definitions. The homology problem in identifying two similar proteins has previously been suggested[1] to be solved by locally projecting the secondary structure elements onto a cubic lattice. A Hamiltonian model is constructed, which by its force constants in a unique way describes the fold (including the direction). We have by computer evaluated all possible folds on a cubic lattice in certain confinements. On Fig. 1. is shown all possible folds (thin line) with coordination number 4 in a (2 x 2 x 2) box. The full line shows the closed packed folds. It is interesting to observe the 'magic' numbers 7, 11 and 18 corresponding to complete filling of the sub-confinements (1 x 1 x 1), (2 x 1 x 1) and (2 x 2 x 1) boxes, respectively. The (2 x 2 x 2) box cannot be completely filled with all possible 25 elements using the coordination number 4. Of particular interest for a classification of proteins is that there for the typical domain size of about 20 elements is a plateau of around 4000 closed packed folds. The dashed line represents the mean field estimate[2] of the number of folds from a graph theoretical approach. We have also calculated the corresponding numbers for coordination number 5, including that two elements can continue in the same direction at a junction. This situation is relevant if we relax the projection conditions in the homology-constraint. This gives for 24 elements the large number of 292,334 closed packed folds. In this case, that with 25 elements exists with 79,517 closed packed folds.

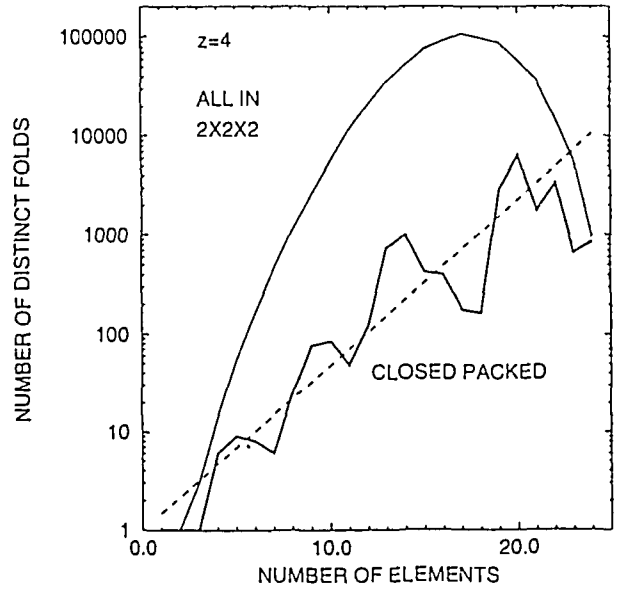

Fig. 1. Number of distinct folds in a (2 x 2 x 2) box containing up to 24 elements and coordination number 4 (thin line). Heavy line the closed packed folds and dashed line mean field teory.

[1] P. -A. Lindgård and H. Bohr, *Protein Folds*, Eds. H. Bohr and S. Brunak, CRC Press, New York, p. 98, (1995).
[2] H. Orland, C. Itzykson, and C. de Domenicis, J. Phys. (Paris), Lett. 46, L 353 (1985).

2.1.3 Theory of the Martensitic Transition Temperature in Alloys

P.-A. Lindgård, *Department of Solid State Physics, Riso National Laboratory, Denmark*

In practically interesting Martensitic materials the transition temperature is often close to room temperature. It is surprisingly easy to obtain a large range of transition temperatures, M_s, in the complicated alloys of three or more components. The question is why the transition temperature is so dramatically dependent on the alloy composition? The effect is much larger than conceivable from estimated consequences of changes in the electronic effects, in the inter atomic forces, in atomic radii or as a result of atomic ordering. In the complicated alloys, as for example Ni_xTi_{1-x} [1] and Cu_3AlBe_ε [2] a dramatic change in M_s is observed for $x \approx 0.5$ and $\varepsilon \approx 0.01$. In these interesting systems probably all the mentioned effects play a role, but still it is hard to understand the strong influence on M_s. A model including electronic effects was proposed [3] for the ternary NiTi-based alloys providing an interpolation formula between two elements of the type NiTi and MxTi, where Mx is an element which forms the B2 structure with Ti. Is was possible to account for a small downward deviation from a linear interpolation of M_s between the two pure systems, using two essentially free parameters (and including temperature influence on the electrons). However, in that model one totally neglects the thermal nature of the Martensitic transformation; and in most cases it is a high temperature transformation compared to the natural energy scale, the Debye temperature.

Previously we have developed a theory [4] relevant for the ideal pure model systems of the Group IV elements like Ti and Zr, for which also extensive neutron scattering measurements have been performed.

Based on one of the simplest possible model alloy systems, the Ti_cZr_{1-c} alloy system Fig. 1, a theory is developed including the effect of a disorder scattering of the phonons due to a mass difference between the elements. The depression of the Martensitic transition temperature, ΔM_s, is shown to depend parabolically on concentration c, as $c(1-c)$, for small depressions. For larger ΔM_s an enhancement at intermediate c is predicted. This gives rise to a more triangular dependence as a function of c. The theory contains only one phenomenological parameter [5].

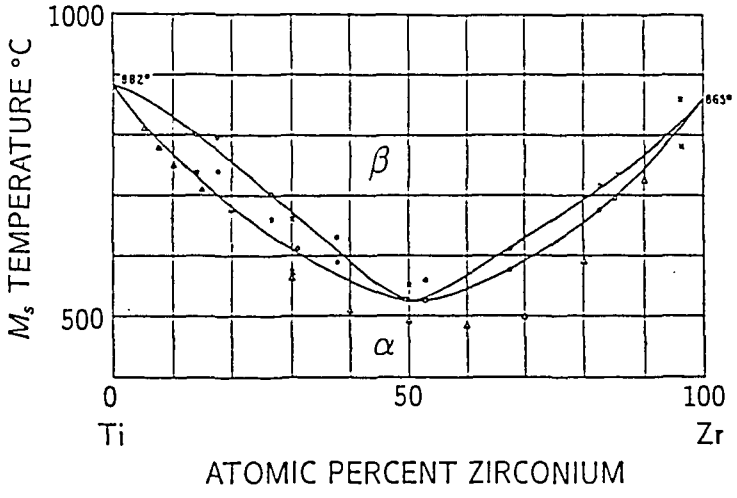

Fig. 1. Martensitic transition temperature for the Ti - Zr alloy system 1).

[1] Hansen, M., Constitution of Binary Alloys (McGraw-Hill Book Company, New York, 1958) p.1245.
[2] Belkahla, S. and Guenin, G., J. de Phys. IV, France, Colloque C4, **1**, C4-145 - C4-150 (1991).
[3] Huisman-Kleinherenbrink, P. M. and Beyer, J., J. de Phys. IV, France, Colloque C4, **1**, C4-47-C4-52 (1991).
[4] P. -A. Lindgård, J. de Phys. IV, France, Colloque C4, **1**, C4-3 (1991).
[5] P. -A. Lindgård, J. de Phys. IV, France, Colloque C2, **5**, C2-15 (1995).

2.1.4 Continuous Monte Carlo Simulation of Surfaces and of Interfaces of Mismatched Crystals

J. Baker, *Department of Physics, Florida State University, Tallahassee, Florida, U.S.A.*, and P.-A. Lindgård, *Department Solid State Physics, Riso National Laboratory, Denmark*

The relaxation phenomena encountered when an otherwise perfect crystal is terminated either by vacuum - *i.e.* at a surface, or by another crystal *i.e.* at an interface, is the topic of this study. The interface could be a grain boundary between two differently oriented crystals of the same material or between two different materials with different structures and/or lattice constants. In both cases there is an often incommensurate and large mismatch between the optimal atomic positions at the interface. The energy cost of this can be minimized by relaxing the atoms from the perfect positions in a region near the interface and sometimes in addition by a rotation of the adjacent crystals by a small epitaxial angle away from high symmetry relative orientation.
In recent papers by Vives and Lindgård[1] a continuous Monte Carlo method was developed and used to accurately describe the behavior of the ideal test example of rare gas mono layers on graphite. This is generalized to apply to 3d ionic systems. The ionic crystals pose an extra all important question of how to treat the unscreened Coulombic forces, which we have solved efficiently. We do not expect that the details in the forces are very important for the generic aspects of the interface relaxation, so the results may be instructive also for the behavior of at least simple binary alloys without strong angular forces. It should be interesting subsequently to study the interfaces between metals and ionic or covalent crystals, which is a problem of current technical interest. On the experimental side, KBr epitaxially grown on NaCl has been intensively studied by He-scattering[2] and a X-ray synchrotron study has been initiated. The lattice mismatch between KBr (a=6.592 Å) and NaCl (a=5.627 Å) is about 15% (very large). It is incommensurate with the nearest rational repeat distance behaving like 6:7. In spite of this large mismatch it is experimentally clear that KBr grows very well on NaCl although the first layer appears to be disordered, as judged from He-scattering. However, growth of perfect KBr surfaces is achieved after two or more layers, and remarkably the crystal is perfectly oriented according to the underlying NaCl crystal *i.e.* with no epitaxial rotation. Using known or fitted potentials we have calculated the real space structure and the corresponding scattering factor, $S(q)$, in a full plane in q-space. Systems up to 84 x 84 are used, partially to get high resolution in reciprocal space. Fig. 1 shows an obtained "rumpled" structure. The film and the two topmost layers of substrate are allowed to move.

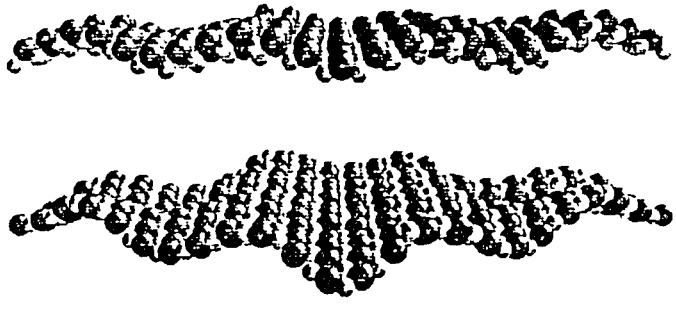

Fig. 1. The real space picture of the structure that results from the relaxation of two monolayers of KBr on NaCl(001) at 200K is shown on Fig. 1, viewed down the ⟨110⟩ direction. The scale perpendicular (z) to the surface is magnified by a factor of ten.

[1] E. Vives and P. -A. Lindgård, Surface Science Lett. 284: L449 (1993), E. Vives and P. -A. Lindgård, Phys. Rev. B 47, 7431 (1993).
[2] J. Duan, G. G. Bishop, E. S. Gillman, G. Chern, S. A. Safron, and J. G. Skofronick, *Surface Science* 272, 220 (1992).

2.1.5 Diffuse Scattering from Nano-Scale Structures

P.-A. Lindgård, *Department of Solid State Physics, Risø National Laboratory, Denmark*, and Gennadi Uimin, *Institut für Theoretische Physik, Universität zu Köln , Germany*

The phenomena on the nanoscale, for which it is of interest to calculate the diffuse scattering structure factor $S(q)$, may be results of equilibrium properties, but are more often related to non-equilibrium states of matter and occur in several different fields of physics. Some of the first problems considered were the stacking faults found as one of the most important defects in metals at low temperatures and in the Martensitic polytype materials which was considered by well known people.[1] It occurs in pattern formation under epitaxial growth of surfaces where terraced islands or huts may start to be formed. A presently very active field of research concerns self-organization, which is an equilibrium result of elastic relaxation in which almost ordered nano-scale structures spontaneously form on a crystal surfaces.
Other problems of relevance are found in artificially grown multilayer systems with some randomness or distribution in the layer thickness. Examples are also found in the phase separation problem in binary alloys or antiphase systems such as the high temperature superconductors $YBa_2Cu_3O_{6+x}$ (YBCO) and in Ising magnets. Related problems occur in bio-physics, and even in computer simulation physics. In a recent paper,[2] the diffuse scattering for such cases was discussed in terms of distribution probabilities of sizes for the various scattering objects, while neglecting the distribution of the space between the objects. We have here extended this work considerably by considering the distributions of all the space-filling objects. For these we derive the explicit scattering cross sections, taking into account the "excluded volume" effect exactly. The theory is based on a further development of that originally developed by Uimin[3] in order to describe the micro-structure of YBCO. To emphazise on the universal aspects of the problems, we focus on presenting the general theory, rather than on discussing a particular phenomena. We obtain the compact expression for the structure factor

$$S_{\text{diffuse}}(q) \propto \{ \langle F^*(1)F(1)\rangle + (\langle L|\mathbf{M}|R\rangle + \text{c.c.})\} , \qquad (1)$$

where the first term is the independent scattering from the involved substructures and the last term, is a term consisting of a 'bra' $\langle L|$, a matrix **M** and a 'ket' $|L\rangle$, which depend on the distribution functions and the internal structure of the substructures. This term represents the interference of the scattering between the sub-structures in a closed form. This may be very important. As an example we show the explicit expression for a distribution of terraces on a surface

$$S_{\text{diffuse}}(q) \propto \frac{1}{2(1-\cos qa)}\left\{1+\sum_{m=1}^{\infty}\left(\bar{\Gamma}^m+\bar{\Gamma}^{*m}\right)\overline{\sigma_i\sigma_{i+m}}\right\}, \quad \bar{\Gamma}=\frac{\sum_\ell e^{iqa\ell}D(\ell)}{\sum_\ell D(\ell)}. \qquad (2)$$

Here $D(\bullet)$ is the width distribution function and $\overline{\sigma_i\sigma_{i+m}}$ the step-step correlation function, a is the lattice constant.

---

[1] L. Landau, Phys. Z. Sow. **12**, 579 (1937), J. M. Lifshits, Phys. Z. Sow. **12**, 623 (1937), J. M. Hendriks and E. Teller, J. Chem. Phys. **10**, 147 (1939).
[2] T. Fiig, N.H. Andersen, J. Berlin and P.-A. Lindgård, Phys. Rev. B **51**, 12246 (1995). (Please note that in Table I. in that paper, κ should only refer to the half width, not the FWHM).
[3] G. Uimin, Phys. Rev. B **50**, 9531 (1994).

2.1.6 Magnetic Relaxation in Small Magnetic Particles

H. L. Richards, *Center for Materials Research and Technology, Supercomputer Computations Research Institute, and Department of Physics, Florida State University, Tallahassee, Florida, U.S.A.*, and P.-A. Lindgård, *Department of Solid State Physics, Riso National Laboratory, Denmark*

The ability of single-domain ferromagnets to preserve an accurate record of past magnetic fields has several important applications. Fine grains in lava flows preserve a record of the direction of the geomagnetic field at the time they cooled, giving valuable insight into continental drift and the dynamics of the earth's core. Of more direct technological importance is the potential application of single-domain ferromagnets to magnetic recording media, such as magnetic tapes and disks. During the magnetic recording process, different regions of the medium are briefly exposed to strong magnetic fields, so that each grain is magnetized in the desired direction. Since each grain can in principle store one bit of data, ithe interest points towards the smallest possible grains. However, in order to serve as reliable storage devices, the grains must be capable of retaining their magnetizations for long periods of time in weaker, arbitrarily oriented ambient magnetic fields - *i.e*, they must have a high coercivity and a large remanence. During both recording and storage, the relationships between the magnetic field, the size of the grain, and the lifetime of the magnetization opposed to the applied magnetic field are therefore of great technological interest.

A step towards a quantitative understanding of the nonequilibrium statistical mechanics in single-domain ferromagnets is a systematic study of the kinetic Ising model, the simplicity of which has made it amenable to many theoretical and numerical studies. In particular, the switching field for Ising 2-d systems with periodic boundary conditions (representing small particles with no boundary effects) has been shown[1] to have a peak with respect to system size near the "Thermodynamic Spinodal". Similar peaks seen in experiments are usually attributed to a crossover from single- to multi-domain equilibrium structure, but in the Ising model the peak is due solely to dynamic effects.

In this work we use Monte Carlo simulations of octagonal and circular systems and the droplet theory of metastability to study the effects of various boundary conditions on the switching field.

Since for an open boundary the droplets will form preferentially at the surface, we have designed a particular, uniform surface, where all spins have the same number of neighbors, see Fig. 1. It is found that the dynamic peak is not present in systems with surfaces unless the system is modified to discourage nucleation on the boundary. We have studied the effect of the addition of surface magnetic fields or anisotropy and the increase of the surface bonds. Both effects may occur as a result of surface reconstruction.

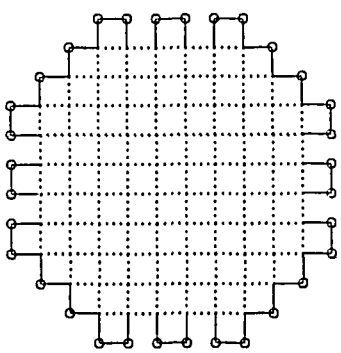

Fig. 1. An octagon with a boundary where all surface spins have two neighbor bonds (full lines), whereas the interior spins have four bonds (dotted lines).

[1] H.L. Richards, S.W. Sides, M.A. Novotny, and P. Rikvold, J. Magn. Magn. Mater. **150**, 37 (1995).

2.1.7 Scattering Functions of Semi-flexible Polymers With and Without Excluded Volume Effects

J. Skov Pedersen, *Department of Solid State Physics, Riso National Laboratory, Denmark,* and P. Schurtenberger, *Institut für Polymere, ETH Zürich, Switzerland*

Off-lattice Monte Carlo simulations on semi-flexible polymer chains with and without excluded volume interactions have been performed. The model used in the simulations is a discrete representation of the worm-like chain model of Kratky and Porod[1] applied in the pseudo-continuous limit. The ratio between the cross-section radius R of the chain and the statistical segment length b was chosen to be $R/b = 0.1$ which corresponds to the value found for polymer-like micelles. The ratio R/b is equivalent to a reduced binary cluster integral of $B = 0.30$, which is in accordance with the value for polystyrene in a good solvent.

The simulations have been performed using pivot moves[2] and subsequent coordinate corrections. Hard-spheres were placed along the chain and the "zippering" method was used for checking for chain overlap. Careful investigations of the finite size effects were carried out and it led to the conclusion that 32 spheres per b is required in order to reduce the effects to less than 1% up to $qb = 10$. During the simulation distance histograms were stroposcopically sampled for every 50 attempted Monte Carlo step. The total number of MC steps were 50000. The histograms were used for calculating the scattering functions. This procedure gave scattering functions for the semi-flexible chains with a precision of 1 - 2% for $L/b = 0.3$ to 640. Numerical approximations to these functions have been determined which interpolates between the simulated functions and these can be used in analysis of experimental scattering data.[3]

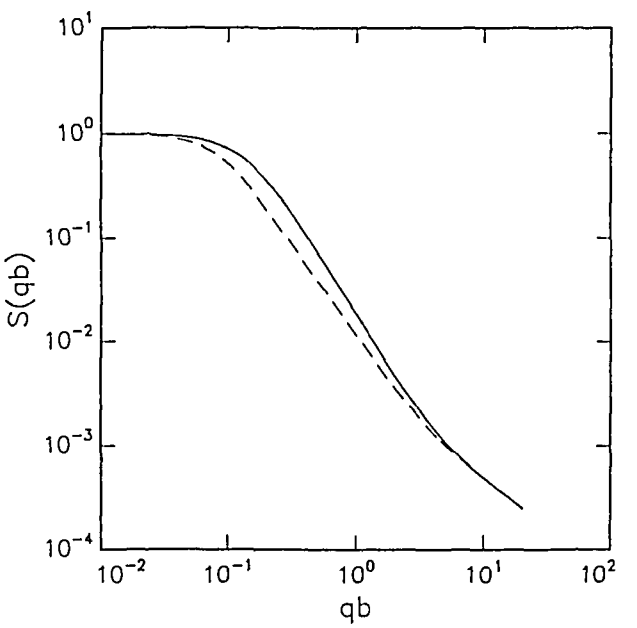

Fig. 1. Scattering functions for semi-flexible polymer chains in a double logarithmic representation. Monte Carlo simulations results for chains without excluded volume effects (full curve) and for chains with excluded volume effects (broken curve) for $L = 640\ b$.

[1] O. Kratky, G. Porod, Rev. Trav. Chim. Pay-Bas 68, 1105 (1947).
[2] S.D. Stellman, P.J. Gans, Macromolecules 5, 516 (1977).
[3] G. Jerke, C. Cavaco, P. Schurtenberger, J.S. Pedersen. *In preparation* (1995).

2.1.8 Dynamical Correlation Function of 1-D Quantum Chains in Applied Fields.

K. Lefmann, *Department of Solid State Physics, Risø National Laboratory, Denmark*, C. Rischel, *Ørsted Laboratory, Niels Bohr Institute, University of Copenhagen, Denmark.*

The one dimensional S=1/2 antiferromagnetic Heisenberg spin chain is one of the simplest non-trivial magnetic systems, and has therefore been widely studied during the last six decades. The spin model with only nearest-neighbour interactions (NNM) was the first one studied, but only few exact results have been obtained. Somewhat more tractable is the Haldane-Shastry model (HSM), where the interactions decay as $1/r^2$.

Our work concentrates on the dynamical correlation function, $S(q,\omega)$, in order to make direct and detailed comparisons with neutron scattering experiments on quasi-one-dimensional model systems. We have performed exact numerical diagonalizations of spin chains of different lengths up to N=26. To reduce the dimensionality of the problem we have made use of the inherent symmetries of the problem, which were enhanced by applying periodic boundary conditions. For the matrix diagonalization we used the Lanczos algorithm, which yields only the extreme eigenvalues of the matrix, corresponding to those low-lying excitations we want to study.

In zero field $S(q,\omega)$ has been studied extensively, and for the HSM it has been shown analytically to be confined within a continuum of excitations, having soft modes at q=0 and q=π.[1] A very similar expression was earlier conjectured by Müller et al. for the NNM on the basis of diagonalizations of chains of N=10.[2] Our results for the NNM shows a good agreement with this conjecture in the stronger, lower part of the continuum, but a small disagreement towards the upper continuum boundary.

With increasing field the continuum boundaries changes, and for the NNM one pair of soft modes of $S_{zz}(q,\omega)$ even moves away from the commensurate q=π position. Our calculations confirms this, and show in addition that the spectral weight of $S_{xx}(q,\omega)$ is distributed differently from what was earlier proposed.[2]

For the HSM the continuum boundaries have been calculated analytically to resemble the NNM result with the addition of another pair of soft modes in $S_{zz}(q,\omega)$, emerging from q=0.[1] Our data shows that this new pair of soft modes carries almost no weight, and that the dynamical correlation function for the HSM thus resembles that of the NNM.

[1] J.C. Talstra and F.D.M. Haldane, Phys. Rev. B, 50, 6889 (1994), and references therein.
[2] G.M. Müller, H. Thomas, H. Beck and J.C. Bonner, Phys. Rev. B, 24, 1429 (1981), and references therein.

2.1.9 Monte Carlo Simulations of the $YBa_2Cu_{3-y}M_yO_{6+x}$, M = (Al, Co, Fe) System

S. Mannstaedt, O.G. Mouritsen, *Department of Physical Chemistry, the Technical University of Denmark*, N.H. Andersen, T. Fiig and P.A. Lindgård, *Department of Solid State Physics, Riso National Laboratory, Denmark.*

It is well-known that M = Al, Fe and Co substitute mainly on the Cu(1) sites in the basal plane of the high-T_c superconductor $YBa_2Cu_{3-y}M_yO_{6+x}$ (YBCO), and that the changes in the structural and superconducting properties are strongly depending on the materials preparation method.[1] Previously, the structural changes and the reduction of T_c as function of doping level, y, for randomly distributed dopants have been studied by Monte Carlo simulations based on a modified version of the 2d ASYNNNI model, where an additional attractive model parameter, V_1^M, for the nearest neighbor oxygen interaction around the M-dopants was introduced,[2] and it was shown that this model can account for clustering of the M-dopants at low oxygen stoichiometry.[3]

We have extended the Monte Carlo simulation studies based on the modified version of the ASYNNNI model. The simulations have been carried out for different system sizes and values of the interaction parameter, V_1^M, under conditions that are in agreement with experiments. From analyses of the ordering properties it has been found that for $V_1^M = 0.38$ the model can account quantitatively for the experimental observations of the structural ordering properties. In Fig. 1 is shown the result of the orthorhombic order parameter as function of doping level under conditions corresponding to sample preparation in 1 bar of oxygen. As observed experimentally, the orthorhombic structure disappears for $y > 0.1$ both with $V_1^M = 0.12$ and 0.38, but not if V_1^M is zero. Under conditions simulating low oxygen pressure at high temperatures with mobile M-dopant and oxygen atoms, followed by oxidation at lower temperatures, where only the oxygen atoms are mobile, we find that only $V_1^M = 0.38$ reproduces the experimental observations. These show that the orthorhombic structure exists for high doping levels due to clustering of the M-dopants. Thus, the simple modified version of the ASYNNNI model with $V_1^M = 0.38$ appears to be a good starting model for studies of the structural ordering in M-doped YBCO.

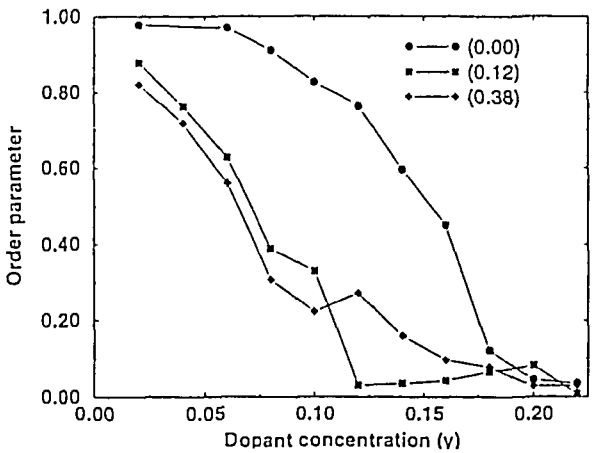

Fig. 1. The order parameter of the orthorhombic phase obtained by Monte Carlo simulations based on the modified version of the ASYNNNI model using standard interaction parameters for the Cu(1) atoms and $V_1^M = (0, 0.12, 0.38)$ for the M-dopants. The simulations have been carried out under conditions corrsponding to 1 bar of oxygen and with mobile oxygen and M-dopant atoms at high temperture, but only oxygen atoms are mobile at low temperature.

[1] S. Katsuyama, U. Ueda and K. Kosuga, Physica C **165**, 404 (1990).
[2] J.V. Andersen, N.H. Andersen, O.G. Mouritsen and H.F. Poulsen, Physica C **214**, 143 (1993).
[3] S. Mannstaedt *et al.*, Computational Materials Science **3**, 9 (1994).

2.2 Magnetic and Metallic Structures

2.2.1 The Interplay Between Structure and Magnetism in CeSb

D.F. McMorrow, J.-G. Lussier, B. Lebech, S.Aa. Sørensen, M. Christensen, *Department of Solid State Physics, Risø National Laboratory, Denmark,* and Doon Gibbs, *Department of Physics, Brookhaven National Laboratory, USA*

Resonantly enhanced x-ray magnetic scattering has now been observed in most of the rare-earth elements, with Ce being the most notable exception. Due to its tendency to form compounds that display various anomalous magnetic properties (heavy-fermion, intermediate valence, etc), there is obvious interest in exploring whether x-ray magnetic scattering is a useful probe of the magnetism of this element. This is further motivated by the fact that often it is difficult to obtain large enough single crystals for neutron scattering experiments. Here we report preliminary results of an x-ray scattering study of CeSb. The chemical and magnetic structures of CeSb have been investigated using high resolution x-ray scattering techniques. Experiments have been performed both in the non-resonant regime (x-ray energies of E=9.4 keV on BW2 at Hasylab) and in the vicinity of the L edges (E≈6keV on X22C at NSLS) of Ce. In the non-resonant regime, when the sample was cooled below its Neel temperature of ≈17 K peaks appeared with commensurate wave vectors q. (Of the two possible domains that could be detected in our scattering geometry, only the one with q parallel to the surface was observed.) From their polarisation and wave-vector dependence, the peaks are deduced to arise from a periodic lattice distortion. A summary of the temperature dependence of these peaks is shown in Fig. 1. In the resonant regime, when the energy was tuned to the L absorption edges of Ce weak, resonantly enhanced magnetic scattering was observed at the L_{II} edge (E=6.164 keV), with no scattering found at either of the other two edges Of the six possible zero-field commensurate structures reported in earlier neutron scattering experiments, we found the phase with q=2/3 and 4/7 only. Neutron scattering experiments on the same crystal confirmed that the absence of the other phases is a property of that particular crystal, but the single domain state is a feature of the near surface region.

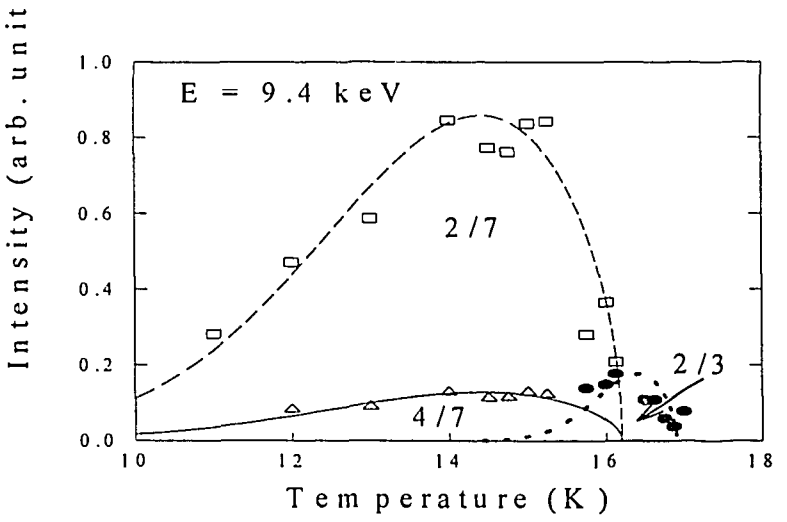

Fig. 1. Temperature dependence of the structural satellite peaks in CeSb.

2.2.2 High-Energy X-ray Scattering Study of the Critical Fluctuations in Rb_2ZnCl_4

D.F. McMorrow, *Department of Solid State Physics, Risø National Laboratory, Denmark,* M. Zinkin, *Clarendon Laboratory, Oxford University, UK,* and J.P. Hill, *Department of Physics. Brookhaven National Laboratory, USA*

X-ray scattering experiments performed at x-ray energies around 10 keV (typical penetration depth 10μm) have established that the critical fluctuations associated with a continuous phase transition occur on two length scales. The shorter length-scale fluctuations has been shown to be associated with the intrinsic critical fluctuations, whereas the second, longer one is anomalous and is not easily explained by any current theory. We have performed a transmission experiment using high-energy x-rays at 60 keV (penetration depth 2mm) from the superconducting wiggler on X17 at NSLS to investigate whether the second length scale comes from the bulk or is associated with the near surface region. We chose to study the normal-to-incommensurate phase transition in Rb_2ZnCl_4, as our earlier measurements at 9 keV had shown the presence of the second component. The critical scattering is summarised in Fig. 1, where it can be seen that the scattering is described by a single Lorentzian profile at all temperatures above T_c. These results show that the second length scale is not a feature of the bulk.

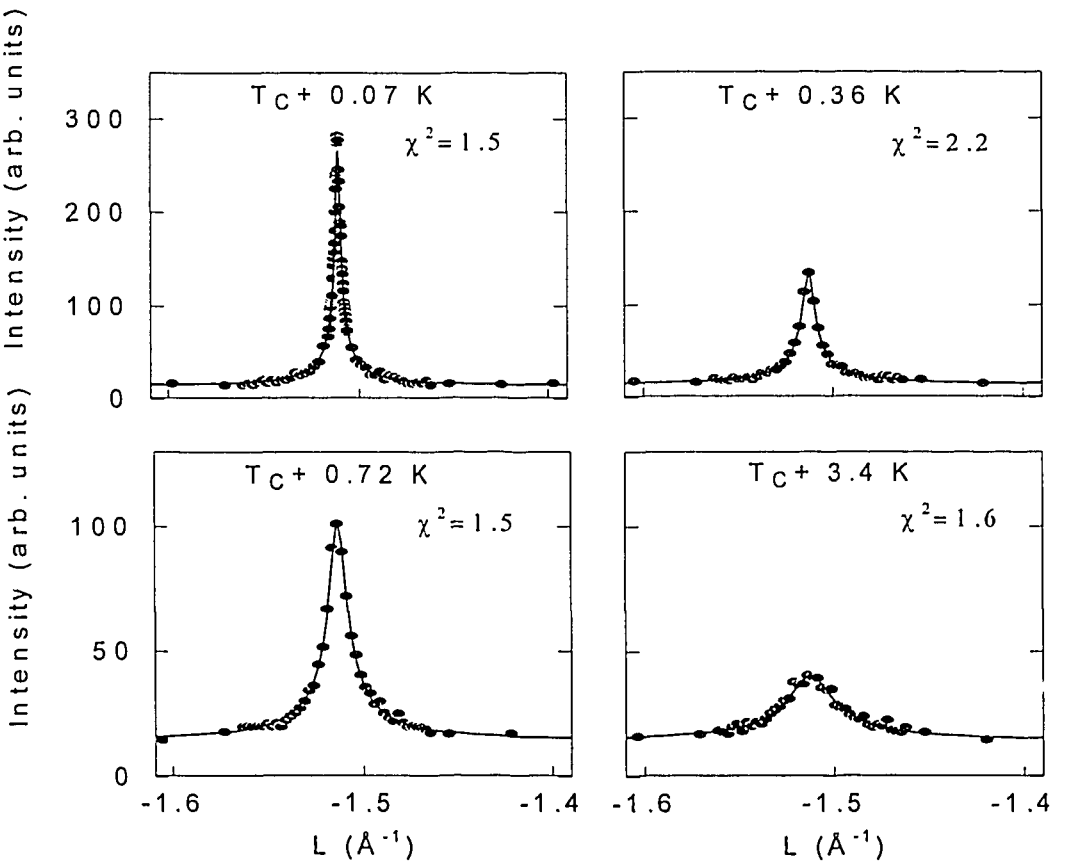

Fig. 1. The temperature dependence of the critical fluctuations in Rb_2ZnCl_4. The solid line is a fit of a 3D Lorentzian scattering function (convoluted with the instrumental resolution) to the data.

2.2.3 The Magnetic Structure of Er/Lu Superlattices

J.A. Simpson, R.A. Cowley, M.R. Wells, R.C.C. Ward, *Clarendon Laboratory, Oxford University, UK,* and D.F. McMorrow, *Department of Solid State Physics, Riso National Laboratory, Denmark*

As part of our continuing programme to elucidate the magnetic interactions in rare-earth superlattices, we have studied a series of Er/Lu superlattices using neutron scattering techniques. In total four superlattices were produced using the MBE facilities in Oxford, with chemical compositions of Er_{30}/Lu_{10}, Er_{20}/Lu_{20}, Er_{20}/Lu_{10}, Er_{10}/Lu_{10}, where the subscripts refer to the number of atomic planes in a bilayer. Bulk Er exhibits the most complex magnetic structures found in the heavy rare-earths, while Lu does not order magnetically. All the superlattice samples have transitions temperatures close to that of bulk Er (84 K), and the magnetic order of Er propagates coherently through the Lu spacer layers. The results for the Er_{30}/Lu_{10} sample are summarised in Fig. 1, where the wave-vector (or equivalently the turn angle) describing the magnetic structure of the Er layers is compared with the effective wave-vector of the response in the Lu layers. The wave-vector shown for Lu is a direct measure of the position of the peak in its conduction electron susceptibility, and its value is consistent with our earlier results on Ho/Lu superlattices. The overall temperature dependence of the Er layers is close to that of bulk, but several significant differences were found, including: the cone phase of bulk Er is suppressed in all of the superlattices; the q=1/4 c* phase is found at low temperatures in all of the samples; the turn angles deduced for the components of the moments parallel and perpendicular to the hexagonal basal plane are different.

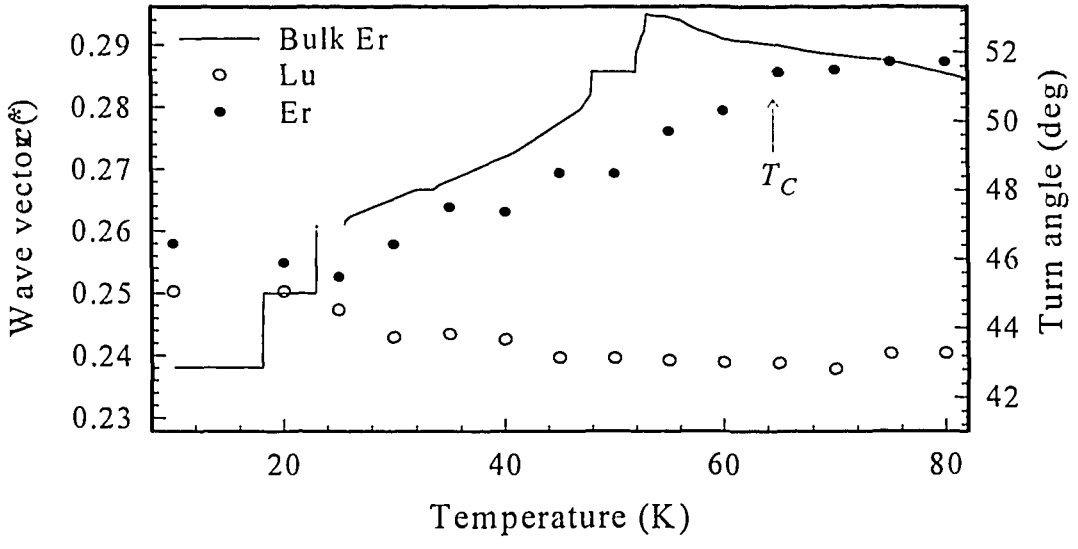

Fig. 1. The turn angles through Er and Lu for the Er_{30}/Lu_{10} superlattice. The solid line is the turn angle of bulk Er.

2.2.4 Magnetic Interactions in Nd/Pr Superlattices

J.P. Goff, C. Bryn-Jacobsen, *Clarendon Laboratory, Oxford University, UK*, and D.F. McMorrow, *Department of Solid State Physics, Risø National Laboratory, Denmark*

The magnetic properties of heavy rare-earth superlattices have been studied extensively. Here these investigations have been extended to light rare-earth Nd/Pr superlattices. The *4f* moments in Nd form a variety of multi-q incommensurate structures, whereas Pr has a singlet ground state down to very low temperatures. It is of interest to study in a superlattice whether the Nd magnetic order propagates coherently through the Pr, and whether the development of order in the Nd affects the magnetism of the Pr ions. Furthermore, the dhcp structure has two inequivalent sites, and there is the possibility that the magnetic order may propagate differently on the two sites. The samples were grown in Oxford using MBE, with compositions $Nd_{33}Pr_{33}$ and $Nd_{20}Pr_{20}$, where the subscripts refer to the number of atomic planes in one bilayer. The magnetic ordering was studied using neutron diffraction. The magnetic structures of $Nd_{33}Pr_{33}$ were simlar to those of bulk Nd, with the hexagonal sites ordering at T=19K and the cubic sites at T=7K. The behaviour was very different for $Nd_{20}Pr_{20}$, with the onset of hexagonal order at T=16K and the suppression of cubic ordering down to the lowest temperature. The width of the magnetic scattering along c^* gives information on the nature of the magnetic order in the growth direction, see Fig. 1., where the hexagonal order is seen to be coherent over many bilayer repeats, but the order on the cubic sites is only coherent across a single Nd block. For $Nd_{33}Pr_{33}$ the magnetic superlattice peaks either side of the hexagonal Bragg peak reflects the moment contrast between the Nd and Pr layers. The absence of such peaks for $Nd_{20}Pr_{20}$ indicates that order has been induced on the Pr hexagonal sites, so that in this case the entire superlattice exhibits a uniform magnetic structure.

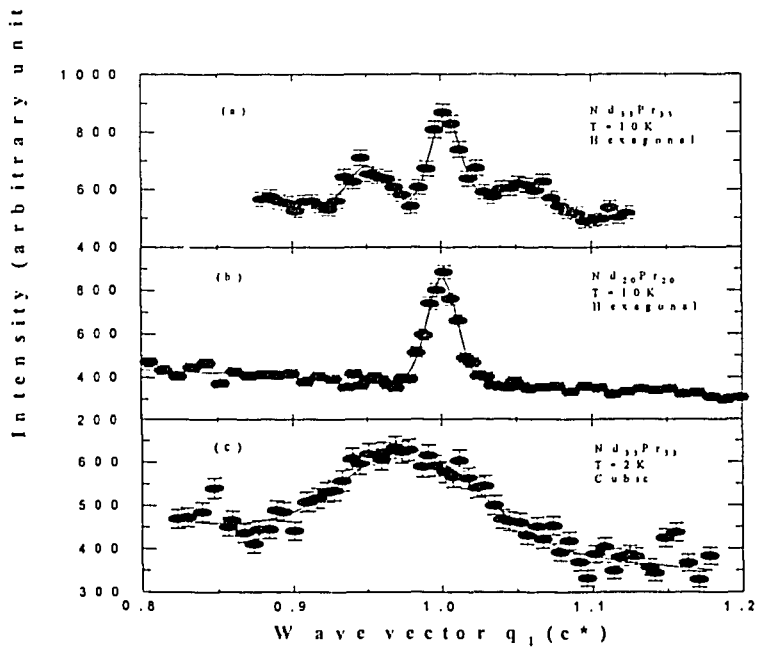

Fig. 1. The scattering at the hexagonal peak near (0.14 0 1) at T=10K is shown (a) for $Nd_{33}Pr_{33}$ and (b) for $Nd_{20}Pr_{20}$,and (c) at the cubic peak near (0.19 0 1) at T=2K for $Nd_{33}Pr_{33}$.

2.2.5 Nuclear Antiferromagnetic Phase Diagram of ^{109}Ag

J.T. Tuoriniemi, K.K. Nummila, R. Vuorinen, O.V. Lounasmaa, *Low Temperature Laboratory, Helsinki University of Technology, Finland*, A. Metz, K. Siemensmeyer, M. Steiner, *Hahn-Meitner Institut, Berlin, Germany*, K. Lefmann, K.N. Clausen, *Department of Solid State Physics, Riso National Laboratory, Denmark*, F.B. Rasmussen, *Niels Bohr Institute, University of Copenhagen, Denmark*

The system of nuclear spins in silver is a close realisation of the nearest neighbour antiferromagnetic Heisenberg model on an fcc lattice - a topologically frustrated system. At sufficiently low temperatures the spin system enters an antiferromagnetic phase. At zero applied field the critical temperature for natural Ag was found by NMR measurements to be 560 pK.[1] At the neutron scattering facility at the Hahn-Meitner Institut in Berlin, the nuclear ordered state in a single crystal of ^{109}Ag has been studied since the first successful experiment in October 1994. The experiments are planned to continue into 1996. We have observed that the nuclear spin system for all applied experimental fields below B_c = 100 μT shows type-I antiferromagnetic long range order. An (001) reflection is seen after the final demagnetisation has been performed from directions within a cone of 110 degrees around [001].[2] We conclude from this that the structure is of the 1-k type. This is in contradiction to earlier calculations which predict the existence of a 3-k structure for relatively high applied fields.[3] The nuclear spin entropy could be determined from the nuclear polarisation measured in fields large compared to B_c. The polarisation was in turn deduced from the transmission of unpolarised neutrons, taking advantage of the strong spin dependent absorption in ^{109}Ag. From the polarisation and the (001) signal measured in the same experiment, the critical entropy, S_c, was deduced. The resulting antiferromagnetic phase diagram is shown in Figure 1. It is surprising that the system seems more stable (higher S_c) when the field direction is close to the edge of the cone, [0.8 0.8 1], than when it is in the centre of the cone, [001].

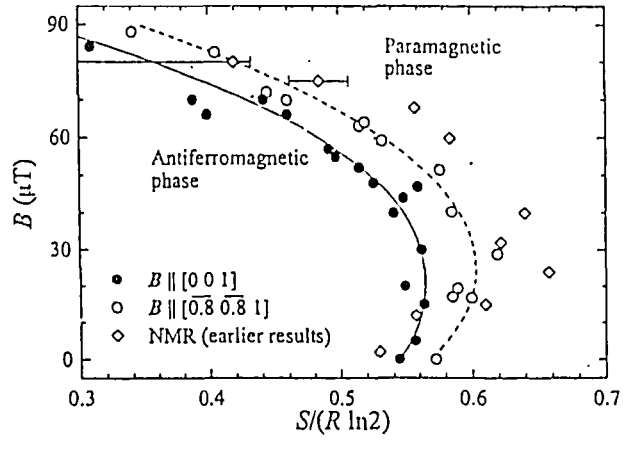

Fig. 1. Magnetic phase diagram of silver in the entropy-field plane. The critical entropy is systematically higher for fields along the [0.8 0.8 1] direction than for fields along [001]. The agreement with earlier NMR results (diamonds)[1] is reasonable.

[1] P.J. Hakonen, S. Yin, K.K. Nummila, Europhys. Lett. **15**, 677 (1991).
[2] J.T. Tuoriniemi et al. (authors as above), Phys. Rev. Lett. **75**, 3744 (1995).
[3] M. Heinila, A.S. Oja, Phys. Rev. B. **48**, 7227 (1993).

2.2.6 Insulator-Metal Transition in the Kondo Compound $CeNi_{1-x}Cu_xSn$

A. Schröder, *Department of Solid State Physics, Riso National Laboratory, Denmark,*
G. Aeppli, E. Bucher, *AT&T Bell Laboratories, Murray Hill, NJ, U.S.A.,*
T. E. Mason, *University of Toronto, Ontario, Canada*

CeNiSn is one of the few "Kondo insulators" which belongs to the Kondo compounds but exhibits a distinct charge[1] and spin gap.[2] Atomic replacement of 10% Ni by Cu drives this insulating compound into a metal.[3] Cold neutron investigations of a just-metallic sample, with x = 0.13, were performed at TAS7 in an orange cryostat and in a ^{3}He refrigerator to characterize the magnetic excitation spectrum. The characteristic spin gap at ΔE = 4 meV of the pure compound (x = 0), most pronounced at a particular wavevector Q = (0 ½ 1) (Fig.1a) disappears. The main magnetic excitations are at low-energy transfers and can be described by a quasielastic Lorentzian (Fig.1b), typical for metallic Kondo compounds. Below T_N = 1.4 K long-range static magnetic order occurs at wavevectors like Q = (0 ½ 1), which is the same as the particular Q of the main gap of the pure compound (Fig. 2). The neutron data show that the transition into a metallic state coincides here with a closing of the spin gap. This transition from a nonmagnetic insulating state into a magnetic metallic state, opposite to the Mott-Hubbard transition, is quite special for strongly correlated electrons systems and needs a new theoretical description.

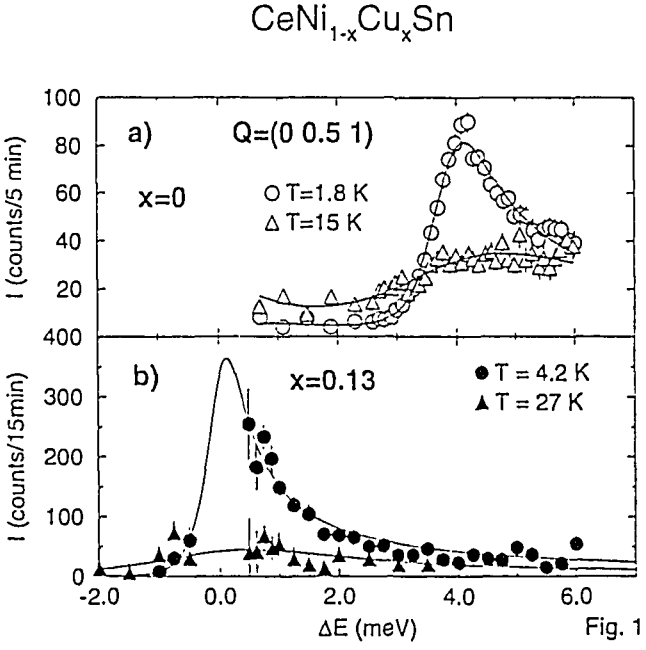

Fig. 1

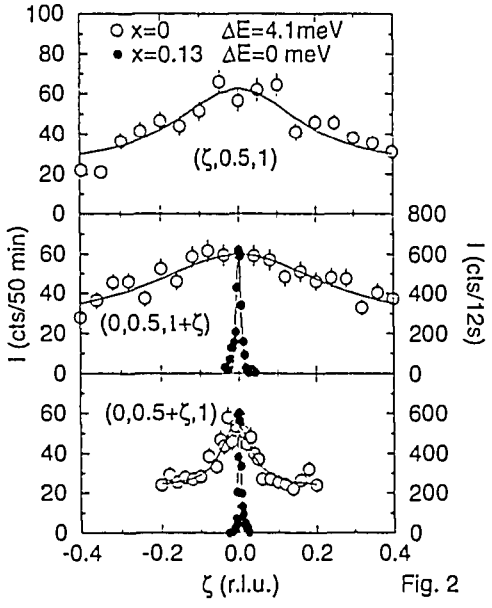

Fig. 2

Fig.1. Constant Q scan at Q = (0 0.5 1) for $CeNi_{1-x}Cu_xSn$ for the insulating compound with x = 0 (Fig.1a) and the just metallic compound x=0.13 (Fig.1b) at low temperatures.
Fig. 2. Constant E scans at the inelastic position ΔE = 4.1 meV for x = 0 at T = 1.7 K and at the elastic position ΔE = 0 meV for x = 0.13 at T = 0.4 K along the three main Q-directions centered at the same Q = (0 0.5 1).

[1] T. Takabatake et al., Phys. Rev. B **41**, 9607 (1990)
[2] T. E. Mason et al., Phys. Rev. Lett. **69**, 490 (1992)
[3] T. Takabatake et al., J. Magn. Magn. Mater. **76&77**, 87 (1988)

2.2.7 Magnetic Correlations of the Kondo Insulator CeNiSn in High Magnetic Fields

A. Schröder, *Department of Solid State Physics, Risø National Laboratory, Denmark,*
G. Aeppli, E. Bucher, *AT&T Bell Laboratories, Murray Hill, NJ, U.S.A.,*
T. E. Mason, *University of Toronto, Ontario, Canada*

Since the charge gap of the strongly correlated electron system CeNiSn is accompanied by a spin gap,[1] it should by affected by magnetic fields. In effect the low temperature insulating behaviour in the electrical resistivity dissappears, when a magnetic field parallel to the orthorhombic a-axis is raised up to 12 T.[2] With cold neutrons we investigated the main spin gap in high magnetic fields, using the 9T magnet at TAS7. The intensity of the 4 meV gap is reduced in B = 8.9 T compared to B = 0 T due to a broadening of the excitation (see Fig. 1) and a shortening of correlation length (see fig 2). As at 0T, the high field constant Q scan can be described by a combination of a gap (Δ) and a broad Lorentzian (with width Γ)[3] (see Fig. 2), where Δ remains the same and Γ becomes broader. The same effect was found at 0T for different temperatures T. The linear increase of Γ with B and T can be combined by (T(K) + 0.45 * B(T)) with an effective moment of $g\mu$ = 0.3 μ_B (Fig. 3). The change from a high T metallic like state into a low T insulating state can be reversed by a magnetic field at low T. A full understanding of the detailed structure of this modified excitation in high fields, caused by Zeeman splitting or change in lifetime, needs further studies.

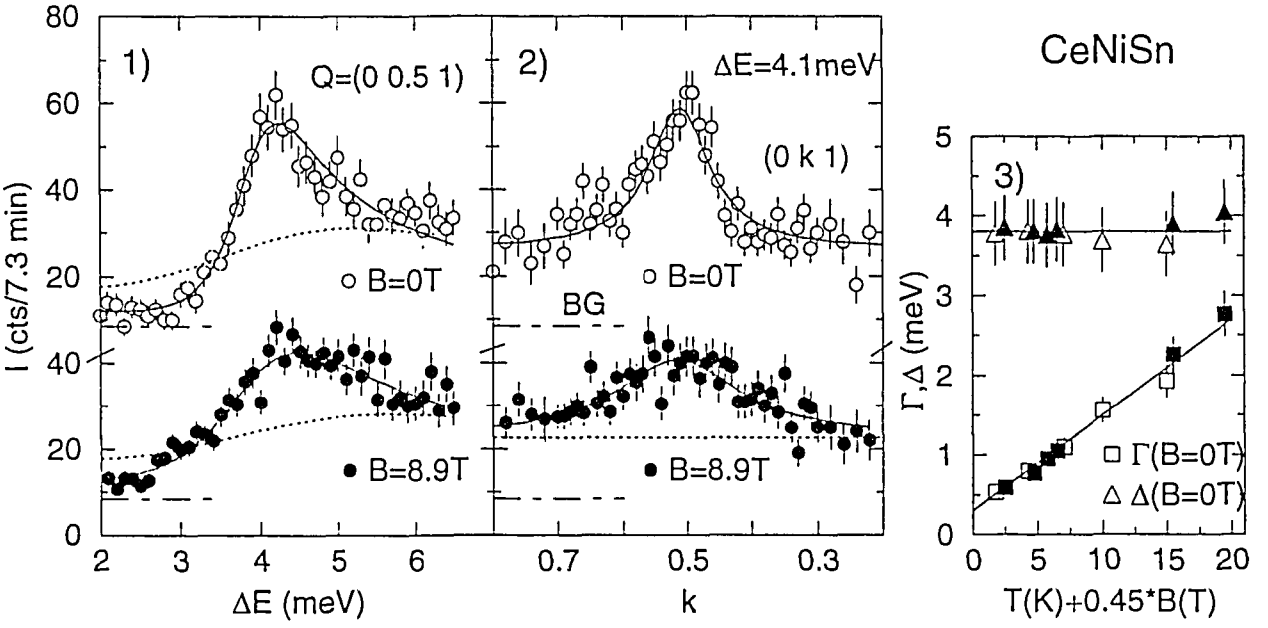

Fig.1. Consant Q scan at Q = (0 0.5 1) for B = 0 T and B = 8.9 T at T = 2.5 K. The straight lines are the fits containing the parameters Γ, Δ [3]. The fits describing the data for T=15.5 K are also shown as a broken line.
Fig.2. Constant E scan at ΔE = 4.1 meV along (0 k 1) for B = 0 T and B = 8.9 T at T = 2.5 K with Lorentzian fits.
Fig.3. The parameters gap Γ and width Δ vs T(K) + 0.45*B(T).

[1] T. E. Mason et al., Phys. Rev. Lett. 69, [illegible] (1992)
[2] T. Takabatake et al., Phys. Rev. B [illegible]0 (1992)
[3] explicit function s. in Ref.1)

2.2.8 Magnetic Order of the Heavy Fermion Compound $CeCu_{5.8}Au_{0.2}$

O. Stockert, H. v. Löhneysen, *Physikalisches Institut, Universität Karlsruhe, Germany*,
A. Schröder, *Department of Solid State Physics, Riso National Laboratory, Denmark*

The heavy fermion alloy $CeCu_6$ does not show long-range magnetic order down to 20 mK. Short range antiferromagnetic and incommensurate correlated fluctuations have been observed in inelastic neutron scattering at low temperatures.[1] Alloying with Au leads to magnetic order in $CeCu_{6-x}Au_x$ for $x > 0.1$ evidenced by sharp maxima at T_N in the specific heat C and susceptibility χ.[2] Here we report on neutron diffraction on a $CeCu_{5.8}Au_{0.2}$ single crystal with $T_N \approx 250$ mK determined by C and χ. The experiment was performed at TAS7 in the AT&T dilution refrigerator. Below $T \approx 400$ mK small magnetic reflections could be detected along the orthorhombic a^*-direction (Fig. 1), nothing was found along b^*. The magnetic structure is incommensurate with a wavevector $q = (0.79\ 0\ 0)$ which lies in between $q = (0.59\ 0\ 0)$[3] of the magnetic order of $x = 0.5$ and $q = (1\ 0\ 0)$ of the commensurate fluctuations of $x = 0$. The reflections are broader than the resolution consistent with a correlation length of 20 - 30 units cells. Also the intensity is very small giving a static magnetic moment of the order of $\mu = 0.01\ \mu_B$. In addition a weak temperature dependent sine modulated background occurs at low temperatures (Fig 1), which is presumably due to antiferromagnetic nearest neighbors interactions. The short time correlation observed at $x = 0.1$[4] seems to become static here. Already at the onset of magnetic order, the stronger correlations of $CeCu_6$ along b^* are less pronounced than the correlations along a^*, which drift away from the commensurate position upon alloying with Au.

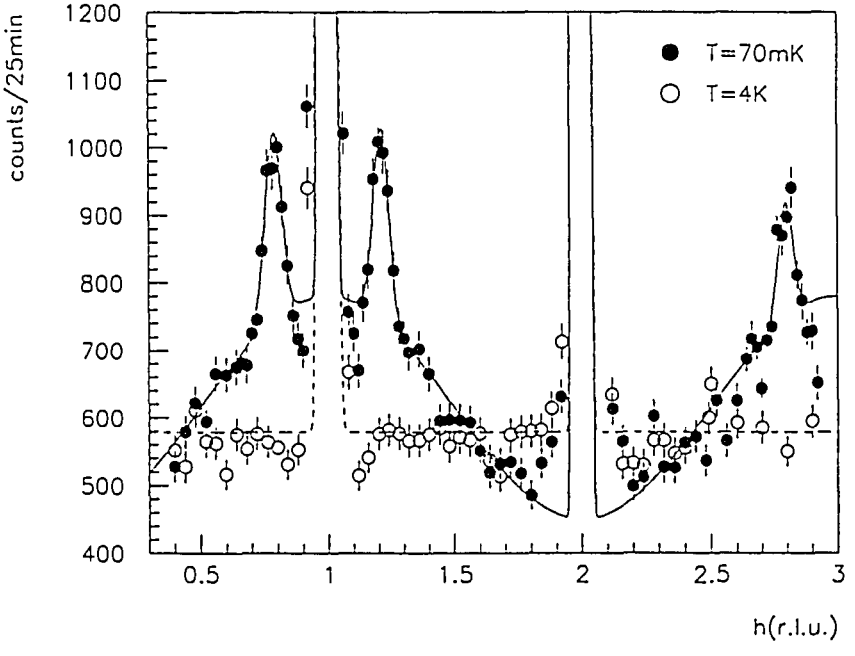

Fig. 1. Neutron diffraction intensity along (h 0 0) for $CeCu_{5.8}Au_{0.2}$ at T = 70 mK and T = 4 K.

[1] J. Rossat-Mignod et al., J. Magn. Magn. Mater. 76&77, 376 (1988)
[2] A. Germann et al., J. de Phys. 49, C8-755 (1988)
[3] A. Schröder et al., Physica B 199&200, 47 (1994)
[4] H. v. Löhneysen et al., unpublished

2.2.9 Neutron Scattering Studies of MnSi under High Pressure

S. A. Sørensen and B. Lebech, *Department of Solid State Physics, Risø National Laboratory, Denmark*

MnSi belongs to a family of intermetallic compounds with the cubic crystal structure ($P2_13$). This structure lacks a centre of inversion, and therefore an anti-ferromagnetic structure with a very long period may be stabilised.[1] From neutron diffraction data taken at ambient pressure, Ishikawa *et al.*[2] concluded that below the Néel-temperature 29 K, the magnetic structure of MnSi is a plane helix with modulation vector q along the <111>–directions and $|q| = 0.035$ Å^{-1}. Several measurements of bulk magnetisation and a.c. susceptibility under hydrostatic pressure in the range up to 15 kbar show a strong pressure dependence in the magnetic properties of MnSi. Bloch *et al.*[3] found a decrease of T_N with pressure at a $d\log T_N / dP = -3.9 \times 10^{-2}$ / kbar. In reference 4[4], Pfleiderer *et al.* report a suppression of the magnetic ordering at 14.5 kbar and a cross over from a second order to a first order phase transition at T_N around 12 kbar as the pressure is increased.

In the present experiment a single crystal of MnSi mounted in a McWhan type pressure cell was studied by Small Angle Neutron Scattering (SANS). The Risø SANS machine at the cold source of the DR3 reactor was operated in a configuration with 7 Å (18%) incoming neutrons collimated by two pinholes (16 mm at the source and 4 mm at the sample) at 3 meters distance. The sample-detector distance was 3 meters. In order to reduce the small angle background, a cylinder made from a single crystal sapphire was used to support the sample in the pressure cell. As the cell was attached to the cold tip of a closed cycle cryostat, the sample temperature could be controlled down to 8 K.

The measurements were carried out in two steps. First the unloaded pressure cell with the sample in Flourinert FC-75 was mounted in the cryostat to check, that the ambient pressure behaviour of the sample observed in a standard cryostat sample environment was reproduced. The features of the diffraction patterns as well as T_N agree with earlier results.[5] In the second step, the pressure cell was loaded in a hydraulic press to a pressure of 5 kbar.

At 5 kbar hydrostatic pressure, the modulation vector q is observed in the [100]–[001] plane of the reciprocal lattice. However, the width of the magnetic satellites perpendicular to the direction of q is significantly increased relative to this width at ambient pressure. The angle between q and [001] measured in the [100]–[001] plane *vs.* temperature is shown in Fig. 1. Note, that q is aligned along <101>–directions just below $T_N \approx 24$ K.

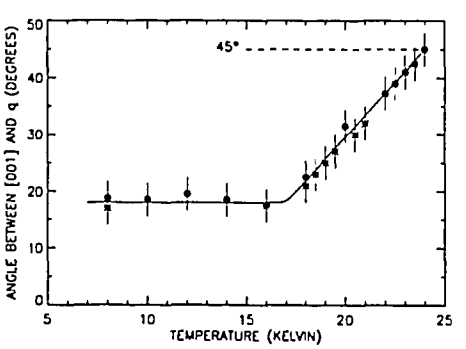

Fig. 1. The full curve is a guide to the eye.

[1] P. Bak and M. H. Jensen ,J. Phys. C.: Solid St. Phys. **13**, L881 (1980).
[2] Y. Ishikawa, K. Tajima, D. Bloch and M. Roth , Solid State Comm., **19**, 525(1976).
[3] D. Bloch, J. Voiron, V. Jaccarino and J. H. Wernick , Phys. Lett., **51A**, 259 (1975).
[4] C. Pfleiderer, G. J. McMullan and G. G. Lonzarich, Physica B, **199**, 634 (1994).
[5] P. Harris, Risø Report **R-747** (1994).

2.2.10 Magnetic Scattering in the Critical Region from MnSi

S. A. Sørensen and B. Lebech, *Department of Solid State Physics, Risø National Laboratory, Denmark*

Several authors[1,2] have reported on anomalous magnetic neutron scattering from the cubic intermetallic compound MnSi at temperatures just above the Néel-temperature. In wave vector space, this scattering is reported to be ring shaped, centred around nuclear peaks with a radius q ~ 0.038 Å^{-1}. New experiments have been carried out at the triple-axis spectrometer TAS7 and the small angle neutron scattering facility SANS at Risø.

A nearly cylindrical sample (approximately 4 mm in diameter and 30 mm in height) of MnSi was mounted with the [0 -1 1] direction vertical to bring the [1 0 0] – [0 1 1] plane into the horisontal scattering plane of the triple axis spectrometer. At the SANS instrument, the sample could be rotated around the vertical direction so that any reciprocal lattice plane containing the [0 -1 1] was accessible at this instrument. For the experiments we used partly a ^{4}He Orange Cryostat and partly a closed cycle refrigerator. With the triple-axis spectrometer in the elastic mode, q-scans were made at each chosen temperature to form a rectangular grid around the (0 1 1) nuclear peak. At the SANS instrument diffraction patterns were collected in steps of 5° of rotation of the sample around the [0 -1 1] vertical direction.

Figure 1 shows a typical data set from TAS7 at the temperature 30.2 K. It is clear, that the scattering has the shape of two ridges rather than the above mentioned ring shape. Detailed studies of the data indicate a peak in the intensity in the [0 1 1] directions, suggesting the existence of a second magnetically ordered phase with modulation vector q along <0 1 1> directions at temperatures just below T_N. The existence of such a phase is apparently contradicting with symmetry considerations.[3] Further analysis of the collected data and more experiments are in progress.

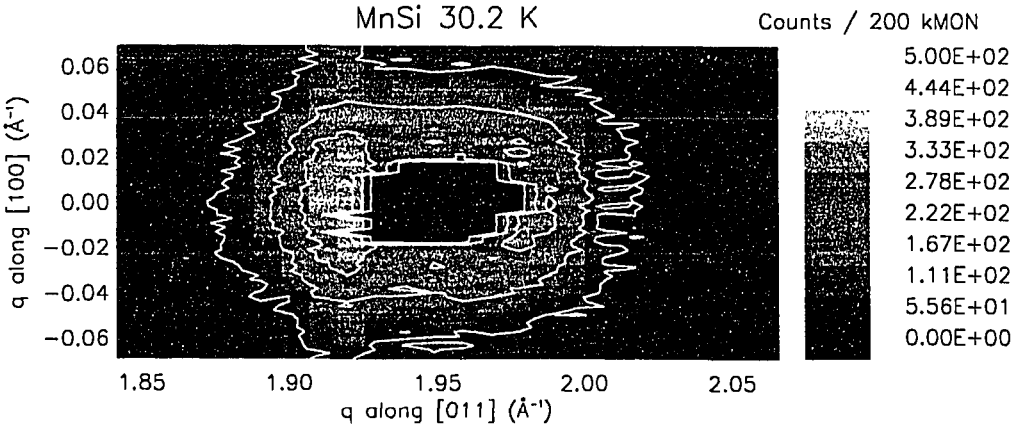

Fig. 1. MnSi at 30.2 K. The background measured at 40 K was subtracted from the data.

[1] Y. Ishikawa, Y. Noda, C. Fincher and G. Shirane (1982). Phys. Rev. **B25**, 254.
[2] S. A. Brown (1990). Ph.D. thesis, Cavendish Laboratory, University of Cambridge, UK.
[3] P. Bak and M. H. Jensen (1980). J. Phys. C.: Solid State Phys. **13**, L881.

original contains color illustrations

2.2.11 Small Angle Neutron Scattering Studies of FeGe

S. A. Sørensen and B. Lebech, *Department of Solid State Physics, Risø National Laboratory, Denmark* and S. Lloyd, *School of Physics and Space Research, University of Birmingham, Birmingham, U.K.*

The magnetic structures of the cubic isomorph of the intemetallic compound FeGe have earlier been investigated by the small angle neutron scattering (SANS) technique.[1] Among the key features reported in reference 1 are a Néel-temperature of 278.7 K and a magnetic modulation vector q of length ~0.0095 Å^{-1}. In the temperature region 278.7 K > T > 211 K, q is observed along the <1 0 0> reciprocal lattice directions. Below 211 K, q is directed along the <1 1 1> space diagonals of the cubic crystal structure. There are, however still open questions concerned with the spatial arrangement of the magnetic moments in the ordered phases. In particular, it is not clear whether the structure is to be interpreted as a single-q multi domain structure or a single domain multi-q structure.

A new computer program[2] for the analysis of single crystal SANS data has been developed at Risø. This program makes it possible to extract position, intensity and width of diffraction peaks from SANS data recorded at different orientations of the sample crystal. The correlation lengths associated with the magnetic satellites are important parameter informations when trying to resolve the above mentioned single-q multi-q question. In order to take full advantage of the new data analysis programme, a new series of SANS data from FeGe has been collected at the Risø SANS facility. The sample (approximately 1 mm^3) was mounted in a closed cycle refrigerator with the [0 -1 1] – direction vertical. Diffraction patterns were recorded in 5° steps of rotation around the vertical axis. The SANS instrument was operated in a mode with 16.5 Å (18 %) incoming neutrons.

The data analysis is still in progress, so only preliminary results are available at the moment. Figure 1 shows the intensity integrated in masks corresponding to the satellite positions of the $q \parallel$ [1 0 0] and the $q \parallel$ [0 1 1] phases, respectively. Note, that the two phases are coexisting in a broad temperature region and that in this region a significant diffuse magnetic scattering is observed.

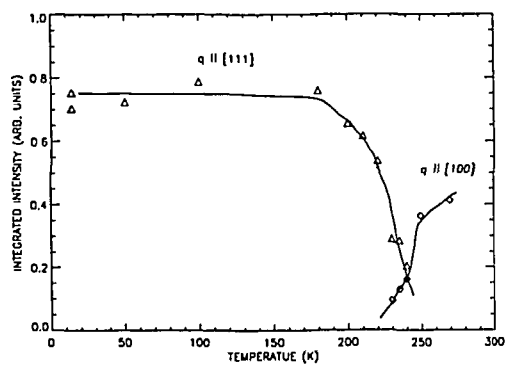

Fig. 1. FeGe — Magnetic satellite intensities versus temperature (heating).The solid curves are guides to the eye

[1] B. Lebech, J. Bernhard and T. Freltoft, J. Phys.:Condens. Matter **1**, 6105 (1989).
[2] P. Harris,Risø Report R-747 (1994).

2.2.12 Neutron Scattering Response in UFe_2

L. Paolosini, *EITU Karlsruhe, Germany and CEN, Grenoble, France,* G. H. Lander, *EITU Karlsruhe, Germany,* R. Caciuffo, *University of Ancona, Ancona, Italy* S. M. Shapiro, *Brookhaven National Laboratory, New York, USA* and B. Lebech, *Department of Solid State Physics, Riso National Laboratory, Denmark*

UFe_2 (Laves phase, fcc crystal structure) is a ferromagnet with T_c = 165 K. Elastic neutron diffraction studies have shown small moments on both sites[1,2] with approximately zero moment on the U-sites because of almost equal spin and orbital moments. There is a strong hybridisation between the U 5*f* and the Fe 3*d*-electrons, and the present inelastic neutron scattering studies were initiated in order to examine how the hybridisation between the 5*f*-electrons of the U atoms and the 3*d* of the Fe atoms affects the magnetic exchange parameters and the spin wave spectrum.

A large untwinned[2] single crystal (0.7 cm^3) grown by Czochralski technique at CEN-Grenoble was used to characterise the magnetic response by neutron scattering and Mössbauer studies.[3] The inelastic neutron scattering studies have been difficult and have involved the use of thermal triple-axis spectrometry at the Siloë reactor (Cen-G, Grenoble) and the High-Flux beam reactor at Brookhaven National Laboratory, cold neutron triple-axis spectrometry at DR3 at Risø National Laboratory, (unpolarised) and at the Institute Laue Langevin, Genoble (unpolarised and polarised). The early measurements at Siloë showed that there are no well-defined spin waves beyond ~5 meV. Subsequent measurements at the cold neutron triple-axis TAS6 using 5 meV neutrons and a cooled Be filter to reduce higher order contamination revealed magnetic response was primarily near the longitudinal acoustic [1 1 1] phonon branch (LA).

As an example, Fig. 1 shows the temperature dependence of $\chi''(q,\omega)$ for constant E = 1 meV longitudinal scans around the [1 1 1] zone centre. The positions of the phonon peaks (LA and TA) obtained at much higher Q values are shown by arrows. The phonon scattering may be reduced by the Bose factor and decreases substantially below 150 K. Note further that because of a small elastic structure factor the longitudinal acoustic phonon is weak around [1 1 1]. The response at h = 1.02 shows a strong temperature dependence which almost disappears above T_c. Assuming that this is the spin wave response, the gap is found to be ~0.4 meV, which is in good agreement with the small anisotropy found in the magnetisation measurements.[4] The response disappears at ~3 meV, presumably because of the Stoner modes from the *d*-electrons. Polarised neutron measurements at ILL have confirmed that the response shown in Fig. 1 is indeed magnetic.[3]

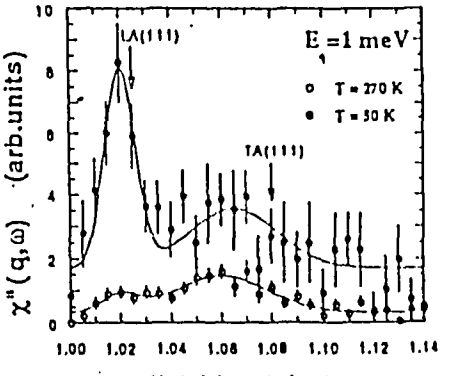

Fig. 1. $\chi''(q,\omega)$ of UFe_2 derived from the experiments at Risø.

[1] M. Wulff, G. H. Lander, B. Lebech and A. Delapalme, Phys. Rev. B39 ,4719 (1989).

[2] B. Lebech, M. Wulff, G. H. Lander, J. Rebizant, J.C. Spirlet and A. Delapalme, J. Phys.: Condens. Matter **1**, 10229 (1989).

[3] L. Paolasini, G. H. Lander, S. M. Shapiro, R. Caciuffo, B. Lebech, B.Roessli and J.-M. Fournier. Magnetic excitations in the itinerant ferromagnet UFe_2, to be published.

[4] A. T. Alred, J. Magn. Magn. Mat. **10**, 42 (1979).

2.2.13 Temperature Dependence of the Spin-Peierls Energy Gap in $CuGeO_3$

J.-G. Lussier and D.F. McMorrow, *Department of Solid State Physics, Riso National Laboratory, Denmark*, S.M. Coad and D. McK. Paul, *Department of Physics, University of Warwick, Coventry, CV4 7AL, UK.*

$CuGeO_3$ is the only inorganic compound, to date, to exhibit a spin-Peierls (SP) transition (T_{SP}≈14K). Such a state occurs when the 1D magnetic correlations induce a dimerization of the lattice along the chain direction leading to the formation of a non-magnetic ground-state. Experimentally, the SP state in $CuGeO_3$ is revealed by the onset of structural superlattice reflections at (h+½,k,l+½) (h, l: all odd, k: integer), and by the creation of an energy gap in the excitation spectra (≈1.93 meV at 1.5K). We performed several measurements at TAS6 and TAS7 to study the relationship between the magnitude of the SP energy gap (Δ) and the intensity of the structural superlattice peak (I) vs. temperature (Fig. 1). According to the theory of Cross-Fischer for the SP transition, the magnitude of the gap should follow the intensity of the superlattice reflection such that: $\Delta \approx I^{1/3}$. Recent numerical models[1,2] have considered the inclusion of next-nearest-neighbor intrachain interactions (frustration) in the Bonner-Fischer model for Heisenberg spin-1/2 chains to better fit the magnetic susceptibility above T_{SP}. In the high frustration regime, a scaling relationship $\Delta \approx I^{1/2}$ is predicted and a new low-lying secondary gap (≈0.2meV) should appear above T_{SP}[1]. Our study extends previous work by Nishi *et al.* (Fig. 2a) and confirms, within errors, that Cross-Fischer scaling better fit the data (Fig. 2b). Further studies are necessary to determine whether a low-lying energy gap is indeed observed above T_{SP}.

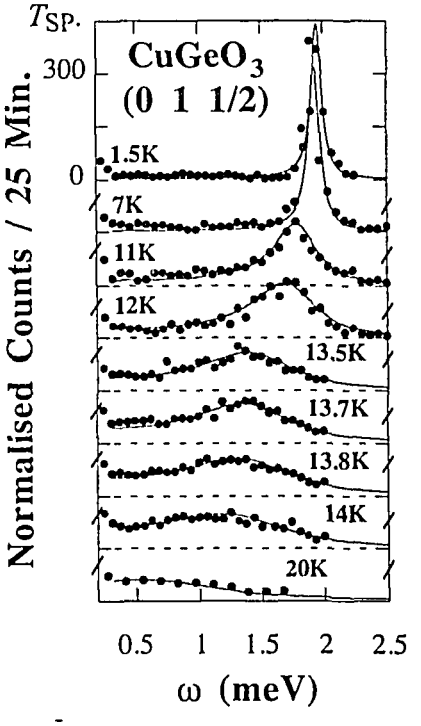

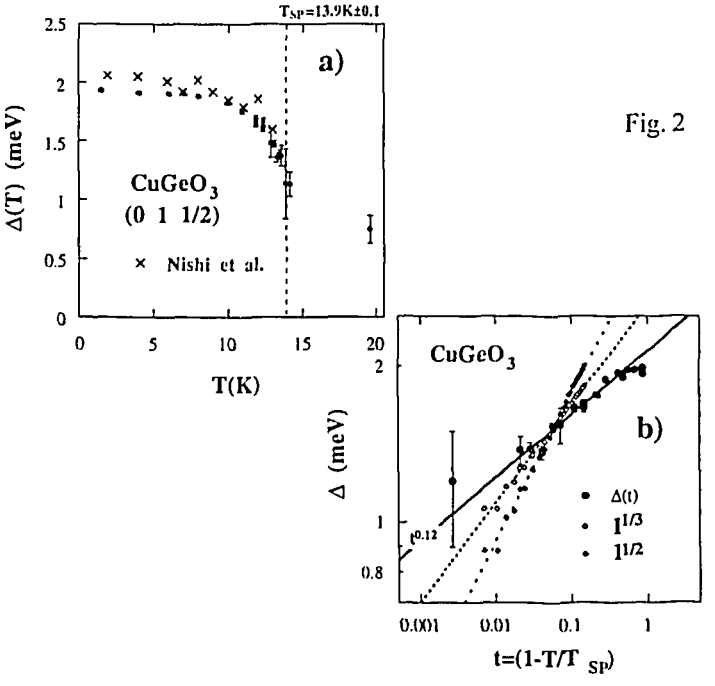

Fig. 2

Fig. 1. Scattered neutron intensity observed in constant-Q scans at (0,1,½) for several temperatures.
Fig. 2. a) The magnitude of the SP gap at (0,1,½) (●). The × are thermal neutron data previously published.[3]
b) Comparison in the critical regime between the magnitude of the SP gap Δ(t) and the intensity of the superlattice reflection from a synchrotron measurement (✧,◆).

[1] Riera *et al.*, Phys. Rev. B, **51**, 16098 (1995).
[2] Castilla *et al.*, Phys. Rev. Lett., **75**, 1823 (1995).
[3] Nishi *et al.*, Phys. Rev. B, **50**, 6508 (1994).

2.2.14 Observation of the Néel State in Doped $CuGeO_3$

S.M. Coad and D. McK. Paul, *Department of Physics, University of Warwick, Coventry, CV4 7AL, UK*, J.-G. Lussier and D.F. McMorrow, *Department of Solid State Physics, Riso National Laboratory, Denmark.*

The spin-Peierls state in $CuGeO_3$ is very sensitive to the introduction of small levels of impurities.[1] The substitution of Cu (S=1/2) by a few percent magnetic Ni (S=1) or non-magnetic Zn (S=0) is sufficient to suppress the spin-Peierls ground state and to drive the system into a new phase transition at low temperature. The nature of this new phase transition was however unclear as initial reports claimed the observation of an hysteresis in the susceptibility below 4K which could indicate the creation of a spin-glass state.[1]

Our measurements performed on two single crystals of Zn and Ni doped $CuGeO_3$ at TAS7 show that the new phase transition is into a Néel state. In Fig. 1, we show that this new phase transition is associated with the onset of a superlattice reflection at (0, 1, ½) at T_N=4.2K (Zn 4%) and T_N=2.8K (Ni 1.5%). The magnetic Bragg peaks are resolution limited and correspond to long range order, as shown in Fig. 2. In Fig. 3, we extended the measurement of Fig. 1 for the Zn 4% to lower temperatures using a ^{3}He-cryostat. This measurement confirms the remarkable linear shape of the order parameter and the saturation of the magnetic intensity at low temperatures.

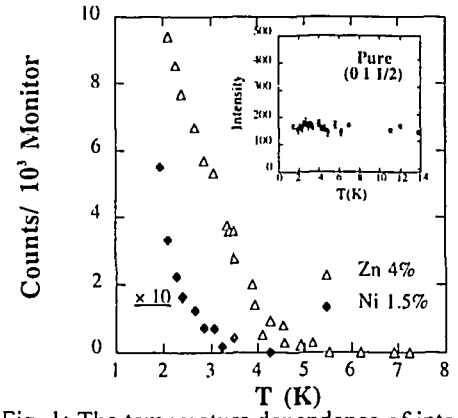

Fig. 1: The temperature dependence of integrated intensity at the (0,1,½) reflection in 4% Zn (Δ) and 1.5% Ni samples (◆). The inset shows the temp-erature dependence of integrated intensity at the same wave vector in the pure sample.

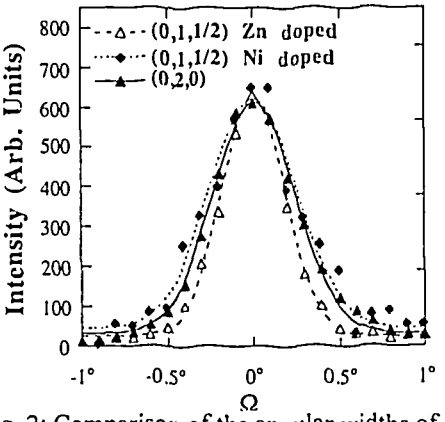

Fig. 2: Comparison of the angular widths of the magnetic reflection (0,1,½) (Δ) and the nuclear reflection (0,2,0) (▲) as measured in the 4% Zn, and in the 1.5% Ni (◆) samples.

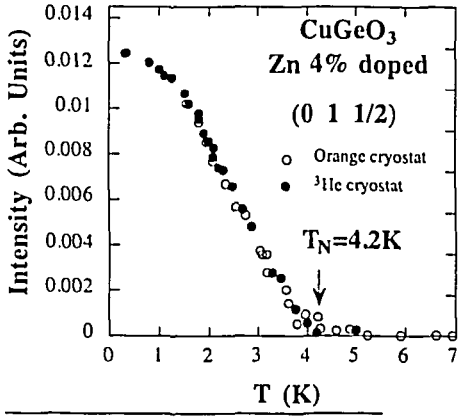

Fig. 3: The temperature dependence of the integrated intensity at the (0,1,½) reflection in 4% Zn obtained with a He^3-cryostat.

[1] M. Hase, I. Terasaki and K. Uchinokura, Phys. Rev. Lett. 70, 3651 (1993).

2.2.15 Neutron Scattering Measurements on Single Crystals of $Cu_{1-x}A_xGeO_3$ (A=Ni,Zn)

S.M. Coad and D. McK. Paul, *Department of Physics, University of Warwick, Coventry, CV4 7AL, UK*, J.-G. Lussier and D.F. McMorrow, *Department of Solid State Physics, Risø National Laboratory, Denmark*

We extended our study of the effect of doping into the spin-Peierls (SP) system $CuGeO_3$ by taking a series of single crystals with dopant concentrations of 1.2% to 2.4% Zn and 1.7% to 6% Ni ions. Our aim was to study the effect of impurities on the structural phase transition and to better characterize the low temperature antiferromagnetic state.

We performed several elastic neutron scattering measurements at the superlattice position $Q=(1/2,3,1/2)$ using the TAS VI and TAS VII spectrometers. The values of T_{SP} extracted from power law fits to the order parameter are plotted against dopant concentration and compared with the linear suppression predicted by a mean-field model[1] (Fig. 1).

Another significant effect of the substitution of Ni^{2+} or Zn^{2+} for Cu^{2+} in $CuGeO_3$ is the appearance of a Néel state at low temperature. We find that the value of T_N increases with the impurity level until a maximum is reached near 3 to 4% (Fig. 2). To study the magnetic structure within the Néel state, we measured the intensity of the magnetic reflections $Q=(0,1,1/2)$, $(0,1,3/2)$ and $(0,3,1/2)$ in both Zn and Ni-doped samples. Assuming a simple antiferromagnetic collinear model for the spin structure and using the $\vec{Q}\times\vec{s}\times\vec{Q}$ dependence of the magnetic neutron cross-section, our results suggest a different spin-orientation for Zn and Ni doped samples (Fig. 3). For the Zn^{2+} doped crystals, the intensity pattern is compatible with an orientation along the c-axis while for the Ni^{2+} doped crystals a preferred orientation along the a-axis is observed.

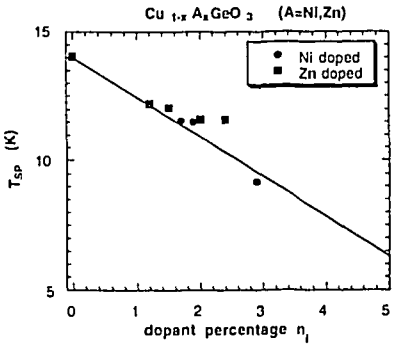

Fig. 1. Variation of T_{SP} as a function of the impurity concentration (Zn and Ni).

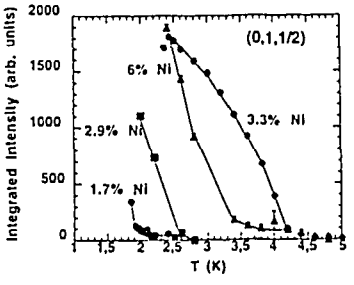

Fig. 2. Intensity of the magnetic Bragg peak (0,1,1/2) vs. temperature for the 1.7%, 2.9%, 3.3% and 6% Ni-doped samples.

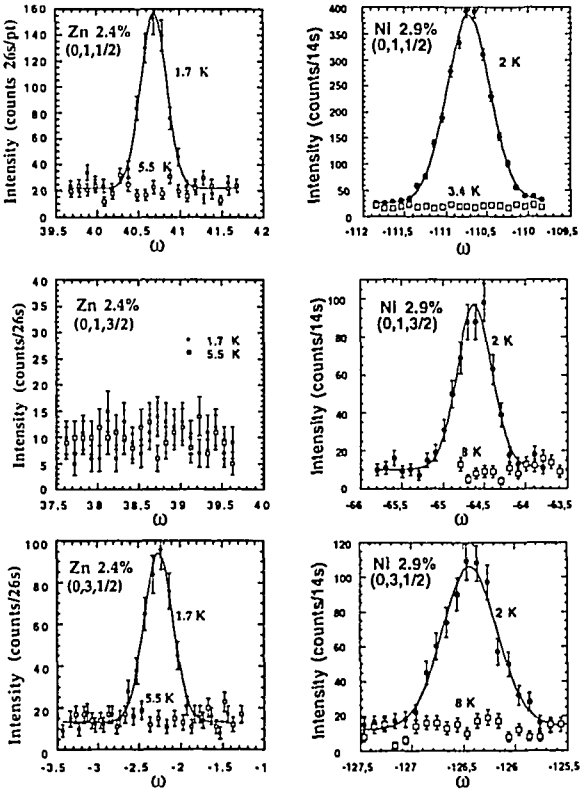

Fig. 3. Ω-scans at (0,1,1/2), (0,1,3/2) and (0,3,1/2) for the Zn and the Ni-doped samples. The open symbols are the same scans taken above T_N.

[1] Lu Zhong-Yi and Su Zhao-Bin, Phys. Rev. Lett., 72, 1276 (1994).

2.2.16 The Effect of Er Solute Atoms on the Magnetic Structure of Ho

H.M. Rønnow, J. Jensen and A.R. Mackintosh, *Niels Bohr Institute, Ørsted Laboratory, University of Copenhagen, Denmark*, D.F. McMorrow, Department of Solid State Physics, *Riso National Laboratory, Denmark*

The magnetic structures of Ho have been studied in great detail[1] and therefore provide an ideal starting point for examining the effect of perturbations such as solute atoms on the ordering of the moments. We have embarked on an investigation of the influence of Er atoms by performing neutron diffraction measurements on the TAS1 spectrometer on single crystals of $Ho_{90}Er_{10}$ between 10 K and the ordering temperature of 125 K. As illustrated in the figure, the low-temperature structure differs markedly from the regular q=1/6 c* configuration observed in Ho, and there are also indications that the ferromagnetic c-axis component is modified. In order to interpret these results in detail, we have developed a virtual-crystal model, using the magnetic interactions deduced for the pure elements as a starting point. As may be seen in the figure, the q=7/36 c* structure gives a good general account of the data, although there are substantial discrepancies in the intensities of some of the peaks. The increase of q is consistent with the periodicities observed in the elements. By carrying out the measurements with improved resolution and refining the model, we should be able to investigate the extent to which the structure can be represented in terms of an average magnetic configuration on each ion, and explore possible effects associated with differences between the Ho and Er sites.

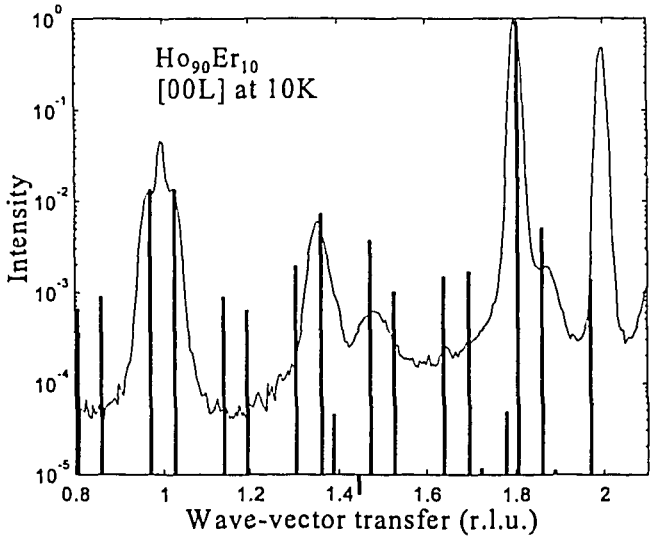

Fig. 1. Neutron diffraction along 00L in a $Ho_{90}Er_{10}$ alloy at 10 K. The lines depict the intensities predicted by the virtual-crystal approximation for a structure with Q = 7/36.

[1] R.A.Cowley and S. Bates, J. Phys. C.: Solid State Phys. **21**, 4113 (1988); J. Jensen and A.R. Mackintosh, Rare Earth Magnetism (Oxford University Press 1991); J.A. Simpson, D.F. McMorrow, R.A. Cowley and D.A. Jehan, Phys. Rev. B **51**, 16073 (1995).

2.2.17 Finite Temperature Effects in the S=1/2 Heisenberg Antiferromagnetic Chain $Cu(C_6D_5COO)_2 \cdot 3D_2O$

D. C. Dender, D. H. Reich, C. Broholm, *Johns Hopkins University, Baltimore, Maryland, USA*, K. Lefmann, *Solid State Physics, Risø National Laboratory, Denmark*, G. Aeppli, *AT&T Bell Laboratories, Murray Hill, New Jersey, USA*

Quasi-one-dimensional magnetic materials provide the opportunity totest rigorously theories of non-classical behavior for simple,interacting many-body systems.Through measurements of the zero-field excitation spectrum at TAS7, $Cu(C_6D_5COO)_2 \cdot 3D_2O$ (copper benzoate) has previously been shown to be a good model system of the S=1/2 Heisenberg antiferromagnetic (AFM) chain.[1] With an excitation bandwidth of 5 meV, this material is ideal for studying the behavior of this model quantum system using cold neutron triple-axis spectometry. Using TAS6, we have measured the temperature evolution of magnetic excitations for wave vectors in the vicinity of the antiferromagnetic reciprocal lattice plane of the one dimensional magnet.

It is known that true long-range order cannot exist for any 1D or 2D quantum system at finite temperature, and that classical 1D AFM systems exhibit a linear temperature dependence of their spin-spin correlation length κ. An interesting experimental question is the behavior of a quantum system at finite temperatures. Constant - $\hbar\omega$ scans across the antiferromagnetic point provide a direct measure of κ vs. temperature. We measured κ over the range 1.7-15 K, corresponding to $0.1J < k_B T < 0.8J$ for the copper benzoate coupling strength J=18.2 K. Over this range, the plot of κ vs. T extrapolates to zero at T=0 K. Further measurements at lower temperatures will be necessary to determine the behavior of κ as T approaches zero.

The evolution of the spinon continuum of the 1D S=1/2 antiferromagnetic chain is another interesting field of experimental work. It is interesting to compare the measurements in this region to the field theory predictions of H. J. Schulz.[2] At $q = \pi$, this prediction simplifies to $S(q,\omega) \propto 1/T * f(\omega/T)$, where $f(\omega/T)$ is a universal function that does not contain any sample-dependent parameters. Combining this with the definition of the generalized susceptibility, we can write $\chi''T \propto f(\omega/T)$. In this scaled form, according to the theory, the data should fall onto a single curve. Preliminary data analysis supports this conjecture. Figure 1 shows this scaling of the magnetic scattering.

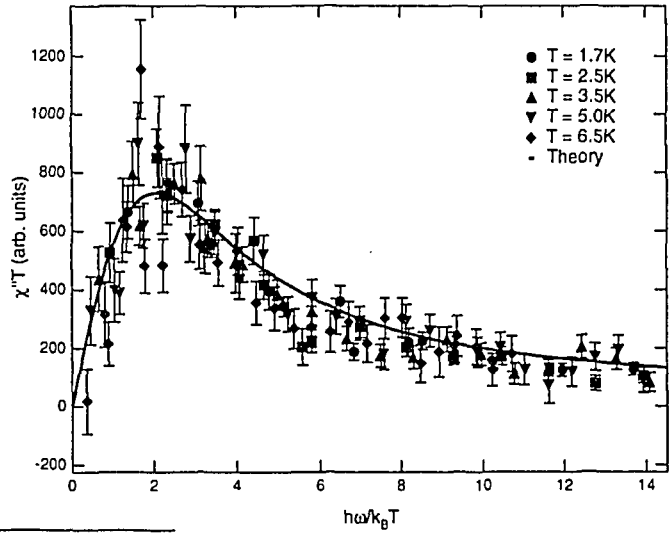

[1] D. C. Dender, D. H. Reich, C. Broholm, K. Lefmann, G. Aeppli, to appear in Phys. Rev. B, 1.Feb 1996

[2] H. J. Schulz, Phys. Rev. B 34, 6372 (1986).

2.3 Superconducting Materials and Phenomena

2.3.1 Structural Evidence for a Two-Step Process in the Depinning of the Superconducting Flux-Line Lattice

U. Yaron, P.L. Gammel, D.A. Huse, R.N. Kleiman, C.S. Oglesby, E. Bucher, B. Batlogg, D.J. Bishop, *AT&T Bell Laboratories, New Jersey, USA.* K. Mortensen and K.N. Clausen *Department of Solid State Physics, Riso National Laboratory, Denmark*

A magnetic field penetrates a type II superconductor as a hexagonal lattice of quantised flux lines. With a current through the superconductor, a Lorentz force acts on these flux lines, but below the so-called critical current I_c, the motion of the lattice is inhibited by pinning to materials defects. When the current exceeds I_c, the lattice breaks free and starts to flow, dissipating energy and destroying superconductivity. The microscopic nature of this - technologically crucial effect - is still poorly understood. We have used small-angle neutron scattering to image how, with increasing current, the static flux line lattice in $NbSe_2$ transforms via disordered plastic motion to a coherently moving flux crystal.[1] Our observations of these structural changes to the flux line lattice - close to the critical current - verify recent theoretical predictions.[2]

The width of the Bragg spots from the flux-line lattice can be measured in three perpendicular directions. From these data the correlation length for the flux lines can be determined, along the flux-line, radial to the line and in the shear direction. The two latter correlation lengths are always resolution limited - i.e. order extends beyond a lower bound of 0.5 μm. The order along the flux-line is however strongly depending on history, as can be seen from fig.1. A FWHM of 0.20 deg, 0.25 deg and 0.11 deg (resolution limit) corresponds to correlation length of ≈ 12μm, ≈ 9 μm and > 50 μm respectively.

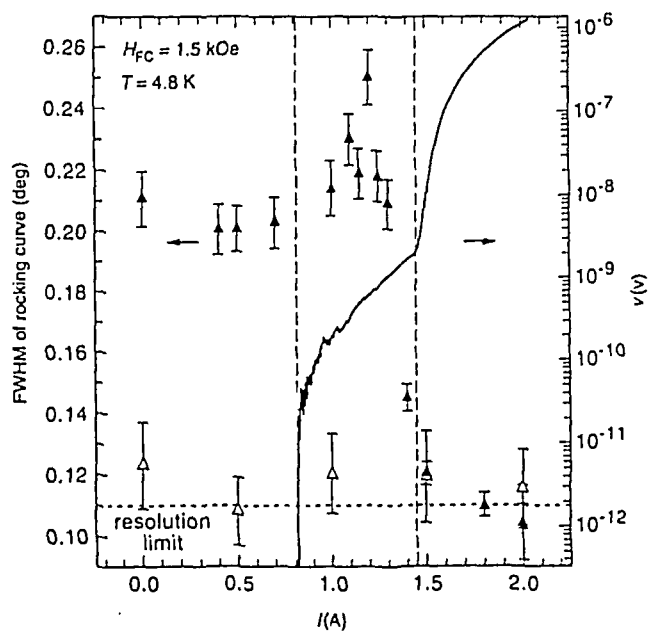

Fig. 1. The FWHM for the rocking curves for a sample cooled to 4.8 K in an applied magnetic field H_{FC} = 1.5 kOe as a function of current I for both increasing (filled triangles) and decreasing (open triangles) current. The solid line is the measured voltage V across the sample. The vertical dashed lines separate the three regimes: pinned lattice, plastic motion and flowing crystal.

[1] U. Yaron, P.L. Gammel, D.A. Huse, R.N. Kleiman, C.S. Oglesby, E. Bucher, B. Batlogg, D.J. Bishop, K. Mortensen and K.N. Clausen. Nature 376, 753-755 (1995).
[2] A.V. Koshelev & V.M. Vinokur. Phys. Rev. Lett. 73, 3580-3583 (1994).

2.3.2 Structural Changes Induced by Room Temperature Chemical Oxidation in T/O-Phases of $La_{2-x}Nd_xCuO_4$ ($0 \le x \le 0.5$)

C.Rial, E.Morán, M.A.Alario-Franco, *Dpto.Q.Inorgánica, Universidad Complutense de Madrid, Spain*, U.Amador, *C.A.I. Difracción de Rayos-X, Universidad Complutense, Spain*, and N.H. Andersen, *Department of Solid State Physics, Riso National Laboratory, Denmark.*

In recent papers we reported the modifications induced in the structure and the superconducting properties of $La_{2-x}Sr_xCuO_4$ by room temperature chemical oxidation, using a sodium hypobromite aqueous solution.[1] The insertion of extra oxygen in the position (¼,¼,≈¼) provides a mechanism of releasing the internal stress of the *T/O* structure at room temperature. This effect is similar to that caused by the substitution of La^{3+} by Sr^{2+}. The amount of oxygen inserted by chemical oxidation increases with the degree of distortion of the rock-salt layer in the starting material, such that all the oxidized phases show the same distortion of the NaCl layer.

Following these ideas we have initiated a neutron diffration study on starting and oxidized materials in the $La_{2-x}Nd_xCuO_{4+\delta}$ ($0 \le x \le 1$) system, using the multi-detector diffractometer at the DR3 reactor at Risø National Laboratory. The structural changes induced by the oxidation process include the following results: Since Nd^{3+} ions are smaller than La^{3+} and Sr^{2+} the T/O phase becomes more unstable upon substitution. Thus, for $x = 0.5$ two phases can be isolated depending on the synthesis temperature: the *T/O* and the so-called *T"*. For $x > 0.5$, the samples are mixtures of two phases, *T"* and *T'*, in proportions depending on the neodymium content. As expected, the progressive partial substitution of La^{3+} by Nd^{3+} in the *T/O* phase induces a decrease of the *c* parameter; however, the Cu-O_{apical} distance remains constant with *x*. Thus the perovskite blocks seem to be "rigid", while the distance between two rock-salt layers becomes shorter. Since the extra oxygen will be located in between two NaCl layers, only a small amount of interstitial oxygen is expected. The refinement of our powder neutron diffraction data confirms this point. Even more, since the degree of distortion of the NaCl layer is about the same in all the starting samples, though the whole structure is less stable with increasing *x*, the content of extra oxygen in the oxidized $La_{2-x}Nd_xCuO_{4+\delta}$ ($0 \le x \le 0.5$) materials is also similar $\delta \approx 0.05$.[1] On the other hand, this small amount of extra oxygen seems to introduce holes in the CuO_2 planes. Like in $La_{2-x}Sr_xCuO_4$ samples, the removal of anti-bonding electrons from the CuO_2 sheets induces a shortening of the distance Cu-O_{basal} (see Fig. 1). This, and the improvement of the geometry of the CuO_2 planes, buckling and scissors angles closer to 180° and 90°, respectively, are related to the improvement of the superconducting properties observed in materials with the T/O structure.[1] Thus, the title compounds are expected to become superconducting after oxidation.

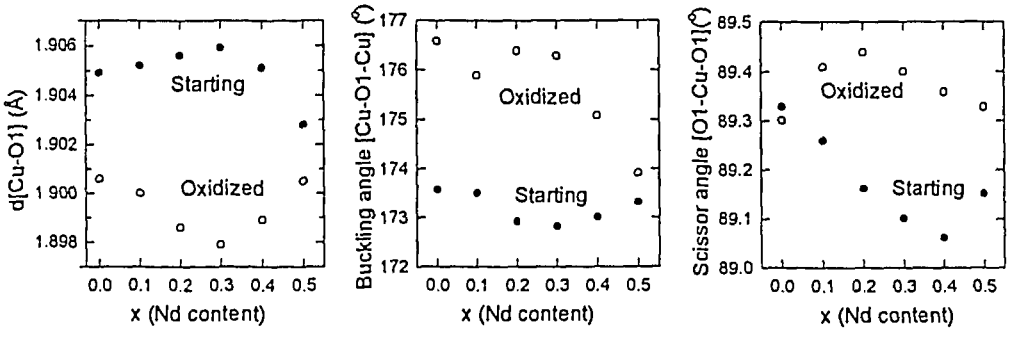

Fig. 1: The distance Cu-O_{basal},, and the buckling and scissors angles in the CuO_2 planes of $La_{2-x}Nd_xO_{4+\delta}$

[1] C. Rial *et al.*, Physica C **234**, 237 (1994), and C. Rial *et al.*, Physica C **254**, 233 (1995).

2.3.3 Reversible T/O ↔ T" Structural Phase Transition in $La_{1.5}Nd_{0.5}CuO_4$

C. Rial, E. Morán, M.A. Alario-Franco, *Dpto. Q. Inorgánica, Universidad Complutense de Madrid, Spain*, U. Amador, *C.A.I. Difracción de Rayos-X, Universidad Complutense, Spain*, and N.H. Andersen *Department of Solid State Physics, Risø National Laboratory, Denmark*

Compounds with structures related to those of superconducting materials like the so-called *T/O* (K_2NiF_4-type) and *T'* structures have been extensively studied and their crystal-chemistry is well established. In the *T/O* structure the copper atoms are located in the center of an elongated octahedron giving rise to a perovskite block. In the *T'* phase the copper atoms present a square-planar coordination, where the "O_{apical}" is shifted towards tetrahedral sites giving a fluorite layer instead of a rock-salt one in the *O/T* phase. A structural change from *T/O* to *T'* occurs for increasing Nd content along the series $La_{2-x}Nd_xCuO_4$, but the existence of the so-called *T"* phase has been suggested. We have observed the *T"* phase for $x \geq 0.5$. The difference between the two phases seems to be that for a given Nd content *T"* has a slightly larger unit cell than *T'*, and it has been suggested that this may result from an ordering of the La and Nd in the *T"* phase.

We have studied the structural phase transition in $La_{1.5}Nd_{0.5}CuO_4$. Powder materials were prepared by the sol-gel method which allowed synthesis at quite low temperatures. For materials synthesized at 800°C (LTP) the *T/O* phase, as observed for materials with $x < 0.5$, was obtained, but when the synthesis was carried out at 1050°C the sample showed a different structure (HTP). The x-ray diffractogram of HTP is indexed with a unit cell slightly larger than that expected for a *T'* phase. The materials were studied by neutron powder diffraction experiments, using the multi-detector diffractometer at the DR3 reactor at Risø National Laboratory, and TGA and DTA measurements.

The atomic positions of the *T'* phase were used as a starting model for the refinement of the neutron diffraction data of the HTP sample. We found no evidence to support a long-range ordering between La and Nd, but some La-Nd short-range order cannot be discarded in the *T"* phase. A structural model for *T"* considering partial occupation of positions equivalent to the O_{apical} of the *T/O* phase gives the best fit to our data. This might explain the larger unit cell. Final atomic parameters of the *T"* phase are collected in Table1. The transition from the *T/O* phase to the *T"* phase has been studied by DTA in argon. The phase transition appears to be a reversible endothermic process taking place at ≅ 870°C with an energy gain of ≅ 5.3 KJ/mole. The TGA measurements under argon showed a small weight loss that could be associated with the phase transition, giving a material with an oxygen content of 3.97, which is in agreement with the results from neutron diffraction data (Table 1). TGA experiments performed in air showed the weight loss to be reversible (oxygen loss on heating and oxygen gain on cooling), though it takes place at higher temperature than in argon (≅ 1030°C).

Table 1: Structural parameters for T"-$La_{1.5}Nd_{0.5}CuO_{4-\delta}$
Composition: $La_{1.51(1)}Nd_{0.49(1)}Cu_{1.00(2)}O_{3.95(3)}$ a=5.6443(2) Å, c=12.4718(6) Å.
S.G:F4/mmm, R_p=6.7%, R_{wp}=8.7%, R_{exp}=5.6%, R_B=4.0%, χ^2=2.5

Atom	*x/a*	*y/b*	*z/c*	Occupation	B_{iso} (Å^2)
La	0.0	0.0	0.3517(1)	1.51(1)	0.28(3)
Nd	0.0	0.0	0.3517(1)	0.49(1)	0.28(3)
Cu	0.0	0.0	0.0	1.00(2)	0.29(5)
O1	¼	¼	¼	2.00(1)	0.52(3)
O2	¼	¼	¼	1.90(3)	0.36(5)
O3	0.0	0.0	0.194(7)	0.05(1)	0.36(5)

2.3.4 Domain Wall Scattering from Twin-Structure in $YBa_2Cu_3O_{6+x}$

M. von Zimmermann, J.R. Schneider, *HASYLAB, Hamburg, Germany*, H.F. Poulsen, *Materials Department, Risø National Laboratory, Denmark*, N.H. Andersen, T. Frello, M. Käll, J. Madsen, O. Schmidt, *Department of Solid State Physics, Risø National Laboratory, Denmark*, R. Liang, P. Dosanjh, and W.N. Hardy, *UBC, Vancouver, Canada*

In the $YBa_2Cu_3O_{6+x}$ (YBCO) high-T_c superconductor twin-structures are formed in the orthorhombic phases due to a ferroelastic transition governed by the oxygen ordering in the CuO_x basal plane of the structure. The twin-domains have significant influence on the superconducting properties as they may act as pinning centers for the magnetic flux lattice, and they may influence the oxygen ordering and thereby T_c. We have studied the twin-domain wall scattering in YBCO for four oxygen stoichiometries, x = 0.35, 0.50, 0.67 and 0.96, by synchrotron x-ray diffraction using the high energy (90 keV) triple axes diffractometer at beam-line BW5 at HASYLAB. $SrTiO_3$ (2 0 0) crystals with 15" mosaicity (HWHM) were used as monochromator and analyzer for the experiment on the x = 0.50 crystal; for the other three samples perfect Si (2 2 0) crystals were used. At the YBCO (2 0 0) reflection the corresponding resolutions in HWHM r.l.u. (longitudinal, transverse) are: (3.7×10^{-3},1.4×10^{-4}) and (1.2×10^{-4},1.2×10^{-5}), respectively.

In Fig. 1 is shown the results from the x = 0.35 crystal of a full contour map of the scattering around the four-fold degenerate (2 0 0)/(0 2 0) Bragg reflection which result from twinning along the ⟨1 1 0⟩ directions. It is uncertain whether the scattering density in the middle of the four main (0 2 0)/(2 0 0) Bragg peaks is from the domain walls or results from a small (4%) tetragonal component in the crystal. A similar scattering density is found in the x = 0.67 crystal, but not in the x = 0.96 and x = 0.5 crystals, from which a scan in the [1 1 0] direction between two of the (0 2 0) and (2 0 0) reflections is shown in Fig. 2. The full line in Fig. 2 is a model calculation of the domain wall scattering following Chrosh and Salje[1] but extended to include strain field displacements both along the a and b directions. The model calculation is based on a tangens-hyperbolic variation of the strain field over the domain wall with an extension of 20 Å. The domain size is taken to have a Gaussian distribution with an average size of 1350 Å and a width of 500 Å.

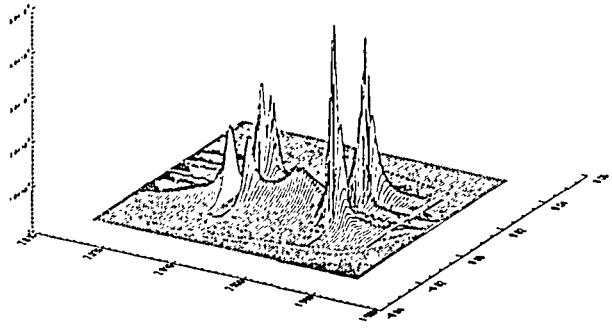

Fig. 1 Contour map of the domain wall scattering around the (2 0 0)/(0 2 0) Bragg peaks of $YBa_2Cu_3O_{6.35}$. The scattering in the center of the map may be a small tetragonal component.

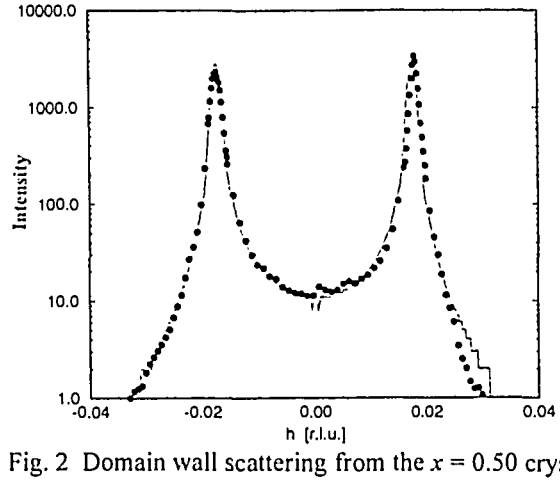

Fig. 2 Domain wall scattering from the x = 0.50 crystal along the (1 1 0) direction between two (0 2 0) and (2 0 0) Bragg reflections. The full line is the result of a model calculation as described in the text.

[1] J. Crosh and E.K.H. Salje, Physica C **225**, 111 (1994).

2.3.5 Antiferromagnetic Ordering of Reduced $NdBa_2Cu_3O_{6+x}$ Single Crystals

E. Brecht, W. W. Schmahl, H. Fuess, *FB Materialwissenschaft, TH Darmstadt, Germany*, N.H. Andersen, B. Lebech, *Department of Solid State Physics, Risø National Laboratory, Denmark*, Th. Wolf, *Institut für Technische Physik, Forschungszentrum Karlsruhe, Germany*

It has been well established that the $YBa_2Cu_3O_{6+x}$ (YBCO) compound shows a transition from the metallic and superconducting phase to an isolating and antiferromagnetically ordered phase when oxygen is removed from the Cu(1) chain layer (*i.e.* for $x < 0.35$). Two antiferromagnetic ordered phases, which differ with respect to the stacking of the moments on the Cu(2) sites along the *c*-axis, have been observed. In the pure system the antiferromagnetic phase AFI, which correspond to an ordering vector Q_1=(½½0), is stable over the whole antiferromagnetic region[1], whereas a small amount of trivalent ions like Al^{3+} on Cu(1) sites results in a reordering at low temperatures to the AFII phase with an ordering wave-vector Q_2=(½½½).[2] However, in the pure $NdBa_2Cu_3O_{6+x}$ (NdBCO) system the magnetic properties seem to be completely different compared to the YBCO compound. In this context Moudden *et al.*[3] have reported that the AFII phase is exclusively present in their NdBCO single crystal with x =0.10, whereas Li *et al.*[4] observed a reordering from the AFI to the AFII phase far below T_N (*c.f.* Table I).
To elucidate this problem we have studied two undoped NdBCO single crystals with x=0.08 and x=0.23. Both samples gave magnetic peaks at low temperatures which correspond to the AFI phase, and no reordering to the AFII phase was observed down to 2 K. The transition temperatures, T_N, from the paramagnetic phase to the AFI phase and the corresponding ordered magnetic moments on the Cu(2) site are qouted in Table 1. The ordered magnetic moment for x = 0.08 is in full agreement with the values observed in the Y-compound.[1,2] The lower values of T_N and $\mu_{Cu(2)}$ for x = 0.23 indicate that charge has been transferred from the Cu(1) layer to the Cu(2) layer. In both crystals the spins are found to be oriented within the *ab* plane and thus in agreement with the spin-direction in the YBCO compound. Table I compares the results of our magnetic studies to results found in the literature. The discrepancies may be related to the fact that the magnetic Nd-ions are known to occupy also the Ba-sites, which can modify the magnetic structure. However, refinement of a full nuclear Bragg data set gave no evidence for Nd on the Ba-sites in our crystals. Therefore, we conclude that the intrinsic magnetic behavior of the pure NdBCO system is similar to that found in the pure YBCO system, which means that the AFI phase is stable over the whole range of the antiferromagnetic ordering, and that most likely the AFII phase observed by Moudden *et al.* and Li *et al.* is caused by impurities.

Table I: Transition temperatures T_N (Nèel temperture) and T_2 (transition to the AFII phase), and the ordered magnetic moment on the Cu(1) and Cu(2) sites for different $NdBa_2Cu_3O_{6+x}$ samples.

Sample	T_N	T_2	$\mu_{Cu(2)}$	$\mu_{Cu(1)}$
$NdBa_2Cu_3O_{6.08}$[a]	387 K	-	0.54 μ_B (T=20 K)	-
$NdBa_2Cu_3O_{6.23}$[a]	289 K	-	0.34 μ_B (T=30 K)	-
$NdBa_2Cu_3O_{6.10}$[b]	-	385 K	0.40 μ_B (T=80 K)	0.54 μ_B (T=80 K)
$NdBa_2Cu_3O_{6.10}$[c]	430 K	80 K	0.83 μ_B (T=20 K)	0.32 μ_B (T=20 K)
$NdBa_2Cu_3O_{6.35}$[c]	230 K	10 K	0.27 μ_B (T=5 K)	0.23 μ_B (T=5 K)

[a]This work, [b]Moudden *et al.*, [c]Li *et al.*

[1] H. Casalta *et al.*, Phys. Rev. B **50**, 9688 (1994).
[2] E. Brecht *et al.*, Phys. Rev. B **52**, 9601 (1995).
[3] A.H. Moudden *et al.*, Phys. Rev. B **38**, 8720 (1988).
[4] W.H. Li, J.W. Lynn and Z. Fisk, Phys. Rev. B **41**, 4089 (1989).

2.3.6 Neutron Diffraction Study of $HoNi_2B_2C$[1]

L.J. Chang, C.V. Tomy, and D.McK. Paul, *Department of Physics, University of Warwick, England,* N.H. Andersen, *Department of Solid State Physics, Risø National Laboratory, Denmark,* and M. Yethiraj, *Solid State Division, Oak Ridge National Laboratory, USA*

RNi_2B_2C (R=rare earth) compounds exhibit a considerable degree of interaction between their superconducting and magnetic properties. Of these compounds, $HoNi_2B_2C$ shows extremely interesting properties. This compound becomes superconducting with a $T_c = 9$ K, but shows anomalous behaviour in the low field magnetisation around 5 K (increasing susceptibility with decreasing temperature), below which a more conventional behaviour is regained. This anomalous behaviour is directly linked to the nature of the magnetic ordering of the Ho moments in this compound. Neutron diffraction measurements were performed to investigate the correlations between the anomalous superconducting properties and the magnetic ordering.

At low temperatures (T < 5 K), the observed magnetic peaks can be indexed simply with the condition that $h+k+l$ is an odd integer. This implies that for this body-centred tetragonal compound, the magnetic unit cell has the same size as the chemical cell. A model with ferromagnetic planes antiferromagnetically coupled along the c-axis is capable of explaining the observed intensities if the Ho moments are aligned at $75^\circ \pm 5^\circ$ to the c-axis. At high temperatures (5 K < T < 8.5 K) the same set of principal Bragg reflections is observed but each reflection is accompanied by two satellites, corresponding to a modulation of the magnetic order along the c-axis with a modulation wavelength of 136 Å, 13 unit cells in the c-direction (Fig. 1). In the intermediate temperature range (5 K < T < 7 K), an additional set of Bragg reflections occur which correspond to a modulation along the c-axis with a period of 2.4 unit cells for the Ho moments (Fig. 2). The low temperature AFM commensurate structure of the ordered Ho magnetic moments is capable of coexisting with the superconductivity. However, at high tempeatures (5 - 8.5 K), it would appear that the existence of a spiral modulation is adopted in order to coexist with the superconducting state. This may be due to the fact that the interactions which lead to the ferromagnetic correlations in the a-b plane are stronger than the AFM coupling along the c-axis. The high temperature state probably has Ho moments arranged on the surface of a cone with a cycloidal spiral in the a-c plane, as this configuration permits the observed Bragg reflections with the period of the spiral and the commensurate spacing.

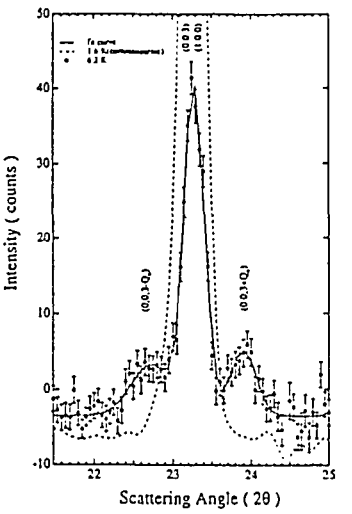

Fig. 1 Magnetic satellites peaks showing c-axis modulations of the Ho ordering.

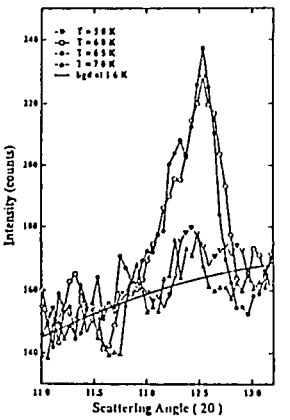

Fig. 2. Magnetic Bragg peak showing additional modulations along the a-axis

[1] C.V. Tomy, L.J. Chang, D.M^{c}K. Paul, N.H. Andersen and M. Yethiraj, Physica B **213&214**, 139 (1995).

2.3.7 Magnetic Order in HoNiBC and ErNiBC

L.J. Chang, C.V. Tomy, D.McK. Paul, *Department of Physics, University of Warwick, England,*
N.H. Andersen, *Department of Solid State Physics, Riso National Laboratory, Denmark,* and
M. Yethiraj, *Solid State Division, Oak Ridge National Laboratory, USA.*

The RNi_2B_2C (R = Y or Rare Earth) compounds show interesting properties which include superconductivity with relatively high T_C's for magnetic as well as non magnetic rare earths (16.5 K for Lu and 11 K for Tm), magnetic ordering of the R moments and the coexistence of magnetic ordering with superconductivity. In addition, they have a layered structure with alternate layers of R-C and Ni_2-B_2. The quaternary RNiBC compounds form with a similar structure as that of RNi_2B_2C but with an additional R-C layer in between the Ni_2-B_2 layers, and they are metallic but do not show superconductivity. Band structure calculations show that the density-of-states (DOS) at the Fermi level is less for RNiBC than for RNi_2B_2C compound. This reduced DOS is thought to be the primary reason for the absence of superconductivity in RNiBC compounds. Even though the RNiBC compounds do not show superconductivity, they exhibit magnetic ordering of the R moments. This provides an interesting comparison with the magnetic properties of the structurally related RNi_2B_2C compounds. Furthermore, since RNiBC may form as impurity phases in RNi_2B_2C compounds, it is of importance to have information about the magnetic nature of the RNiBC compounds in analysing the magnetic properties of the RNi_2B_2C compounds.

We have carried out neutron powder diffraction measurements on HoNiBC and ErNiBC to study the nature of magnetic interaction in these compounds. Below the ordering temperature (T_N = 10 K), the magnetic peaks for HoNiBC can be indexed if the chemical unit cell is doubled along the *c*-axis, as illustrated in Fig. 1b. The magnetic structure consists of ferromagnetic planes of Ho moments coupled antiferromagnetically along the *c*-direction. However, the magnetic Bragg peaks of ErNiBC were observed at the same positions as the nuclear Bragg peaks, corresponding to a ferromagnetic ordering of the Er moments (Fig. 1a) below T_C = 4.5 K. In both RNi_2B_2C and RNiBC compounds, the planes undergo ferromagnetic ordering of the rare earth moments. It is the subtle changes in the interactions along the *c*-direction, which give rise to different magnetic behaviour indicating the importance of the interplane over the intraplane interactions. Even though the absence of superconductivity in RNiBC can simply be related to the reduction in the density of states at the Fermi level, the difference in magnetic interactions between the RNiBC and RNi_2B_2C compounds can be assumed to arise from the difference in the interplane interactions and the changes in the band structure of these compounds.

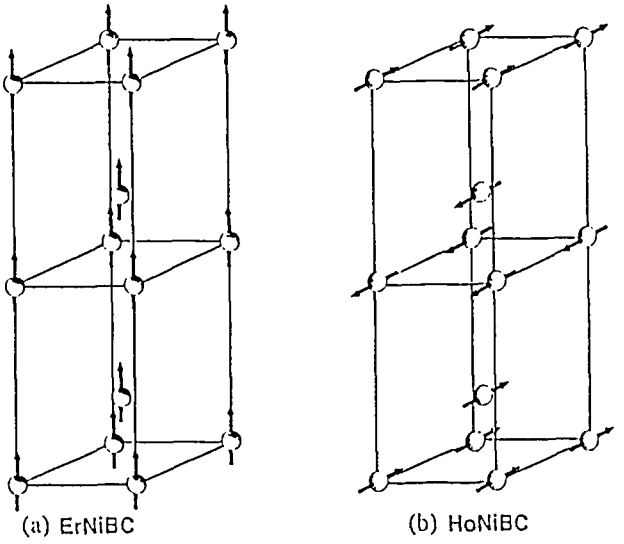

Fig. 1. The magnetic structures of the ordered rare earth moments:
(a) ErNiBC - ferromagnetic
(b) HoNiBC antiferromagnetic

2.3.8 Neutron Diffraction Studies of $Ho_{1-x}Y_xNi_2B_2C$ Compounds

L.J. Chang, C.V. Tomy, D.McK. Paul, *Department of Physics, University of Warwick, England,*
N.H. Andersen, *Department of Solid State Physics, Risø National Laboratory, Denmark.*

$HoNi_2B_2C$ (T_c ~ 9 K) shows commensurate antiferromagnetic (AFM) ordering of the Ho moments below 5 K. Above this temperature (5 K < T < 8.5 K), the commensurate nature changes over to a complex type of ordering with *a*- and/or *c*-modulations.[1] Even though it is not clear which of these modulations gives rise to the anomaly in the magnetisation, the observed *a*-modulation coincides well with the temperature region where the anomaly occurs. In order to investigate the nature of these modulations, neutron powder diffraction measurements were carried out in $Ho_{1-x}Y_xNi_2B_2C$ ($x = 0.1$ and 0.2) compounds. By substituting Y for Ho, T_N is expected to decrease and the T_c to increase. This in turn increases the interval between the T_c and T_N and is thus expected to change the nature of the magnetic modulations. For the $x = 0.1$ sample, the commensurate AFM ordering is observed below 2 K. As, the temperature increases (T > 2 K), satellite peaks appear which correspond to a modulation of the magnetic order along the *c*-axis with a wave vector, $q_c = 0.09$ Å^{-1}. Fig. 1 shows the (001) magnetic peak at $T = 3.5$ K, along with the satellite peaks. The temperature at which the maximum in the intensity of the satellite peaks (3.5 - 4 K) agrees well with the anomaly seen in the magnetisation for this compound. For $x = 0.2$, the principal magnetic Bragg peaks are absent above 1.6 K and only satellite peaks corresponding to a *c*-modulation ($q_c = 0.104$ Å^{-1}) appears (Fig. 2). The results show that the *c*-modulation is responsible for the anomalies in the magnetisation of the Ho compound. In $HoNi_2B_2C$, the AFM commensurate structure (T < 5 K) of the ordered Ho moments is able to coexist with superconductivity. However, at high temperatures (5 K < T < 8.5 K) where the superconductivity also sets in, a correlation between the superconducting order parameter and the onset of magnetic order may force the Ho moments to adapt a spiral configuration along the *c*-axis to coexist with superconductivity giving rise to the modulations in the magnetic order. This may also be due to the build up of ferromagnetic correlations in the *a-b* planes. When the non-magnetic Y is doped for the Ho, the correlations between the Ho moments are expected to be reduced. With $x = 0.1$, the interactions in the *a-b* planes are not strong enough to build a stable commensurate ordering down to 2.0 K. Increasing x to 0.2 weakens the correlations of Ho moments in such a way that only the *c*-axis incommensurate peaks are observed.

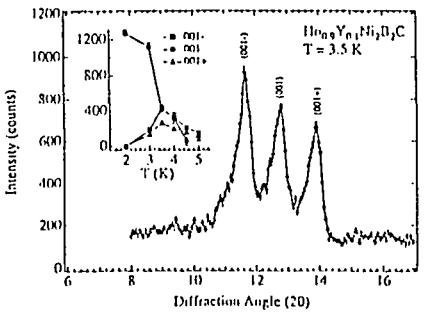

Fig. 1. Magnetic (001) peak with its satellites (001±) at 3.5 K for the x=0.1 compound. The inset shows the variation of the integrated intensities of the peaks with temperature.

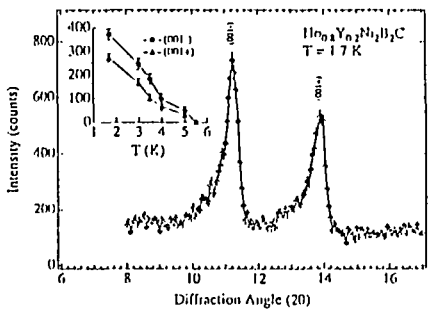

Fig. 2. The (001±) satellite peaks at 1.7 K for x = 0.2. Note the absence of the principal (001) peak. The inset shows the variation of the integrated intensity of the satellites with temperature.

[1] C.V. Tomy, L.J. Chang, D.McK. Paul, N.H. Andersen and M. Yethiraj, Physica B **213&214**, 139 (1995), and contribution 2.3.6 in this Annual Report.

2.3.9 Model for the Low Temperature Antiferromagnetic Phase of $YBa_2Cu_3O_{6+\delta}$ Materials

G. Uimin, *Landau Institute for Theoretical Physics, Chernogolowka, Moscow, Russia*, and N.H. Andersen, *Department of Solid State Physics, Riso National Laboratory, Denmark*

The antiferromagnetic ordering observed in the CuO_2 double layer planes of the $YBa_2Cu_3O_{6+\delta}$ (YBCO) high-T_c superconductor for $x < 0.3$ is characterized by a simple antiferrromagnetic alignment of the Cu^{2+} spins on all nearest neighbour sites in the double layer structure. The two magnetic phases reported: a high temperature AFI phase with Nèel temperature up to T_N=410 K, and a low temperature AFII phase differ only in the way the double layers are aligned relative to one another. In the AFI phase the coupling between adjacent planes of two neighbouring double layers is antiferromagnetic, whereas it is effectively ferromagnetic in the AFII phase. Accordingly, the periodicity along the *c* axis is one unit cell for AFI and two unit cells for AFII. Recently, it was found that in high purity YBCO crystals only the AFI phase exists, whereas crystals containing non-magnetic Al ions in the CuO_x basal plane develop the AFII phase at low temperatures (up to 18 K), but without forming an ordered magnetic moment in the CuO_δ chain structure. In an intermediate temperature region the Bragg peaks from both magnetic phases are observed, and it has been speculated whether the two phases co-exist or there exists an intermediate phase, called the TA (Turn-Angle) phase, where the spins turn continuously from the AFI to the AFII configuration.

We have established a model that explains the existence of the AFII phase at low temperature in Al-doped YBCO. The model is based on the conclusion that isolated Cu^+ ions and singlet pairs of Cu^{2+} ions bridged by an O^{2-} ion in the CuO_δ chain structure are non-magnetic and mediate an antiferromagnetic coupling between Cu^{2+} spins on the adjacent CuO_2 double layer planes. However, free Cu-spins may be formed next to Al-dopants, where excess oxygen is always present. From statistical mechanics it is shown that an effective ferromagnetic type of coupling is established via polarization of the free spins, and that this coupling becomes ineffective as temperature is raised. In agreement with experiments the model predicts continuous phase transitions, the stability of the TA phase in a temperature range between AFI and AFII and the suppression of the AFII phase at low doping levels (see Fig. 1). Using realistic values for the model parameters we obtain transition temperatures in good agreement with experimental values. If an in-plane anisotropy for rotation of Cu^{2+} spins in the CuO_2 planes is introduced a first order transition directly from AFI to AFII results for high concentrations of free spins.

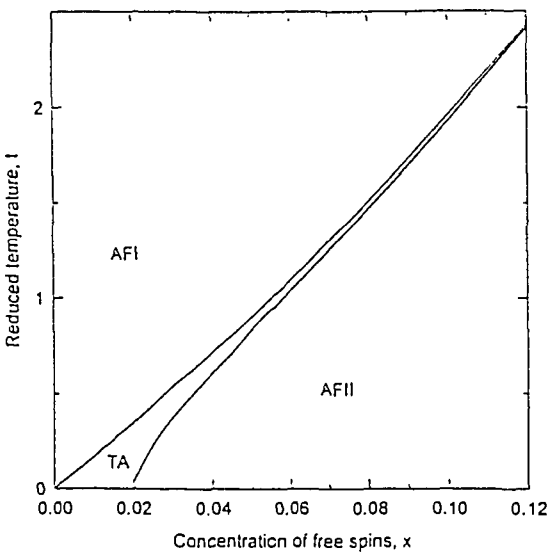

Fig. 1. Model calculation of the magnetic phase diagram of Al-doped $YBa_2Cu_3O_{6+\delta}$ containing the antiferromagnetic phases AFI, AFII and the turn angle phase, TA, as described in the text. For low doping levels the concentration of free spins, *x*, is estimated to be approximately two times the concentration of Al ions in the CuO_δ chain structure. The reduced temperature, *t*, is normalized to the strength of the magnetic coupling between the Cu^{2+} spins in the CuO_2 double layer and the free Cu^{2+} spins in the CuO_δ chain structure, which is estimated to be about 10 K. The indirect antiferromagnetic interaction between Cu^{2+} ions on adjacent double layers via non-magnetic or singlet pair sites in the CuO_δ chain structure is estimated to be 0.1 K

2.3.10 Evidence of Photoinduced Oxygen Ordering in $YBa_2Cu_3O_{6.77}$?

M. Käll, N.H. Andersen, *Department of Solid State Physics, Riso National Laboratory, Denmark,* L. Börjesson, *Department of Applied Physics, Chalmers University of Technology, Sweden,* R. Liang, P. Dosanjh, and W.N. Hardy, *Department of Physics, University of British Colombia, Canada*

We have performed Raman spectroscopy investigations of a detwinned single-crystal $YBa_2Cu_3O_{6.77}$ superconductor (T_c = 84 K) with local OIII order. The experimental technique involves the inelastic scattering of visible monochromatic laser light by elementary crystal excitations, in this case optical phonons. Fig. 1a) shows Raman spectra of the $YBa_2Cu_3O_{6.77}$ sample for two different scattering geometries, where the electric fields of the incident and scattered light are either parallell (denoted *e//b*) or perpendicular (denoted *e//a*) to the crystallographic *b*-axis. The sharp peaks in the *e//a* spectrum are due to scattering by even-symmetry q=0 optical phonons. In addition to these Raman-allowed phonons, the *e//b* spectrum exhibits intense disorder induced scattering from normaly Raman forbidden phonons localized in the CuO-chains. In Fig. 1b) we show that the intensity of the disorder induced phonons rapidly decrease with the ilumination time t. The effect is observed at all investigated sample temperatures (10K - 300K) and power densities. The effect is ireversible, i.e. the intensity does not return when the illumination stops, and only occurs for *e//b* and not for *e//a*. The intensity decay is well aproximated by a power-law, $i(t) = At^{-\alpha}$, with $^1/_3 \leq \alpha \leq {}^1/_2$. The fact that the intensity of the disorder induced scattering decrease as a function of illumination time indicate that the incident light somehow improves the translational order of the CuO-chains. The details of such a process is however unclear at present. One possibility is that the photons (λ=5145 Å, E=2.41 eV) give rize to an electronic excitation that removes the energy barrier for chain oxygen diffusion (E=1.6 eV) and that the orthorhombic strain-fields drives the oxygen ordering. It is most probable that the results described here are related to the phenomenon of "persistent photoconductivity" which has been reported in oxygen-deficient $YBa_2Cu_3O_{6+x}$ (x < 1).

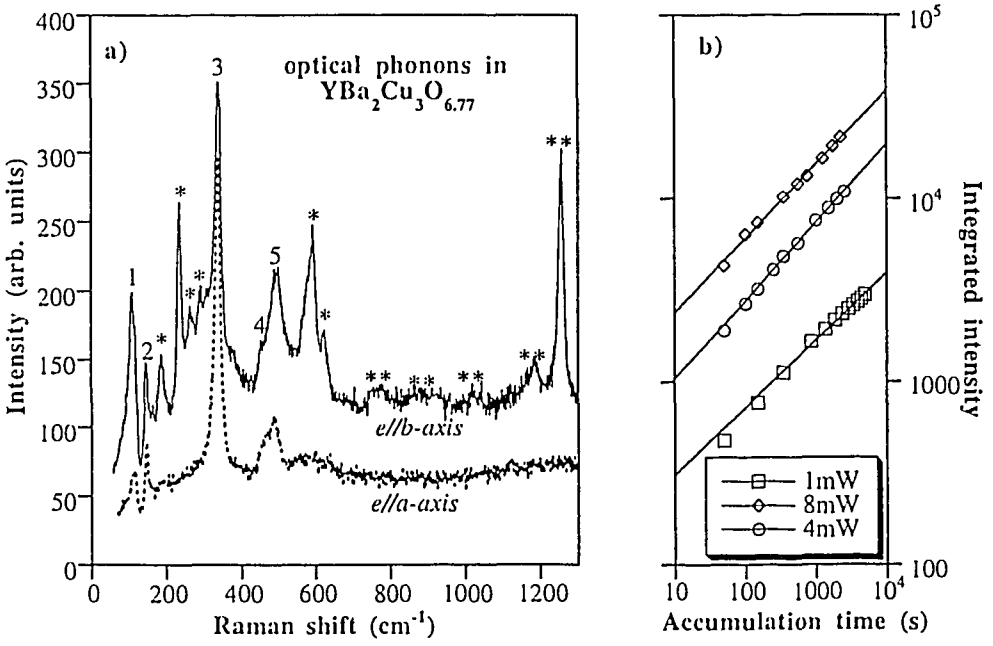

Fig. 1. a) Room-temperature Raman spectra of $YBa_2Cu_3O_{6.77}$. Numbers 1-5 marks symmetry-allowed phonons. Stars and double-stars marks disorder induced one-phonon and two-phonon scattering, respectively. b) The time integrated intensity of the disorder-induced scattering vs. time for various incident photon intensities, measured at 100 K. Lines are best fits with a power-law $I(t) = \int i(t)\, dt \sim t^{1-\alpha}$ ($\alpha \approx 1/3$).

2.3.11 Superstructures in Pure and Doped $YBa_2Cu_3O_{6+x}$ High-Tc Superconductors

M. von Zimmermann, J.R. Schneider, *HASYLAB, Hamburg, Germany*, N.H. Andersen, T. Frello, M. Käll, J. Madsen, O. Schmidt, *Department of Solid State Physics, Riso National Laboratory, Denmark*, H.F. Poulsen, *Materials Department, Riso National Laboratory, Denmark*, , R. Liang, P. Dosanjh, W.N. Hardy, *UBC, Vancouver, Canada,* and Th. Wolf, *Institut für Technische Physik, Forschungszentrum Karlsruhe, Germany.*

Despite many studies the mechanisms governing the oxygen ordering process in the CuO_x basal plane of the high-T_c superconductor $YBa_2Cu_3O_{6+x}$ (YBCO) and how it influences the superconducting properties are still not satisfactorily settled. Previously we have found that the superstructure for oxygen stoichiometries x = 0.36 and x = 0.50 were the double-cell ortho-II structure, whereas the triple-cell ortho-III structure was observed for x = 0.77.[1] A central question in these studies is the reason why long range ordered superstructures do not appear and why the transition temperatures to the superstructure phases are strongly suppressed compared to the expectations from most theoretical model calculations. In the detailed study on a high purity crystal with the ideal composition for ortho-II, x = 0.50, the longest correlation length ever reported for this superstructure was observed (see Table 1, marked *), and it was suggested that the finite correlation lengths result from random field-effects due to impurities.[1]
To study the phase properties further, we have prepared single crystals with different purity and oxygen stoichiometry using a gasvolumetric technique, determined their superconducting T_c from ac-susceptibility data, and measured superstructures by high-energy (90 keV) synchrotron x-ray diffraction on the triple crystal diffractometer at the BW5 beam-line at HASYLAB using $SrTiO_3$ (2 0 0) with 15" HWHM mosaicity as monochromator and analyzer crystals. Superconducting T_c, structural ordering temperature, $T_{OII/OIII}$, and room temperature correlation lengths, $\xi = 1/q_{HWHM}$, of different crystals are given in Table 1. Notice that two high purity crystals with x = 0.50 (grown by different groups) have similar correlation lengths, and that the correlationn lengths of the superstructures decrease with increasing impurity or doping levels, as expected from freezing due to random fields. With only 6 % Al in the CuO_x basal plane the ortho-II superstructure disappears. It is also interesting to note that the high purity crystal with ideal oxygen stoichiometry for ortho-III structure, x = 0.67, does not show any superstructure.

Table 1: Composition, superconducting T_c, structural ordering and transition temperature, and the correlation lengths at room temperature along the *a*, *b* and *c* directions of pure and doped $YBa_2Cu_3O_{6+x}$

Oxygen x	Doping	T_c K	Ordering	$T_{OII/OIII}$ K	ξ_a Å	ξ_b Å	ξ_c Å
0.35	High purity	41	Ortho-II	360	12	---	7
0.36	High purity	23	Ortho-II	360	12	97	4
0.50	High purity*	59	Ortho-II	398	57	223	28
0.50	High purity	---	Ortho-II	360	64	198	30
0.50	Pure, no Al	50	Ortho-II	395	15	---	9
0.50	6% Al-doped	30	None	None	None	None	None
0.67	High purity	64	None	None	None	None	None
0.72	High purity	68	Ortho-III	330	18	51	3
0.77	High purity	84	Ortho-III	350	20	58	≈ 0

[1] Contributions 2.3.1, 2.3.2 and 2.3.3 in: Annual Progress Report 1994: Department of Solid State Physics, Riso National Laboratory, January 1995, and P. Schleger *et al.*, Phys. Rev. Lett. **74**, 1446 (1995), and Physica C **241**, 103 (1995).

2.3.12 AC-Susceptometer for Studies of High -T_c Superconductors

J. Madsen and N.H. Andersen, *Department of Solid State Physics, Risø National Laboratory, Denmark*

One of the characteristic properties of a superconductor (SC) is its ability to exclude magnetic fields from the bulk of the material, the so-called *Meissner effect*, below the superconducting transition temperature, T_c. Thus, ideally the superconductor (SC) behaves as a perfect diamagnet with a magnetic susceptibility $\chi = -1$ (SI units), whereas it is weakly paramagnetic above T_c. *Measurements of the magnetic susceptibility of an SC at different temperatures, will* reveal information about the temperature dependence of the superconducting phase transition.
An ac-susceptometer system for studies of high-T_c superconductors has been developed. It is based on a low temperature closed cycle He-refrigeration cryostat: Displex® CS-202, equipped with a mutual inductance coil system. The cryostat is top-loaded for easy sample exchange and may be controlled from 12 K to 320 K within ± 0.01 K by use of a Risø Digital Temperature Controller, type A1931a. The electronics consist of a two-channel digital lock-in amplifier (LIA), Stanford Research Systems type SR850, with an SR552 preamplifier (gain 100), and a voltage/current (V/C) converter manufactured by NKT Research Center A/S. The schematics of the equipment is shown in Fig. 1.
In an ac-susceptometer two identical oppositely wound pick-up coils are connected in series and placed in an applied alternating magnetic field supplied by an external primary coil which is charged by the LIA via the V/C converter. The two pick-up coils are balanced to give zero signal without sample. When a "magnetic" sample is placed in one of the pick-up coils an *emf*, proportional to the applied magnetic field, the frequency and the magnetic moment of the sample, is induced in the pick-up coils. Since the LIA detects both the in phase and 90° out of phase signal with respect to the applied magnetic field, information about the real and imaginary part of the susceptibility: $\chi = \chi' + i\chi''$ is supplied. In practice, applied magnetic fields up to 15 mT and frequencies up to 10 kHz may be used. At 0.3 mT and 20 Hz *Meissner effect* may be detected in a 10^{-3} mm^3 sample. Temperature regulation and data acquisition are controlled from a PC by the TASCOM command language. An example of an ac-susceptibility measurement on a 59 mg single crystal of $YBa_2Cu_3O_{6.67}$ is shown in Fig. 2. The ac-susceptometer has been tested against a commercial Lake Shore 7000 Series Susceptometer/Magnetometer, which has become available in the Department of Solid State Physics. Complete agreement has been established within the experimental uncertainty. The Lake Shore susceptometer/magnetometer covers the temperature range from 1.3 K to 300 K and may supply dc-magnetic fields up to 5 T.

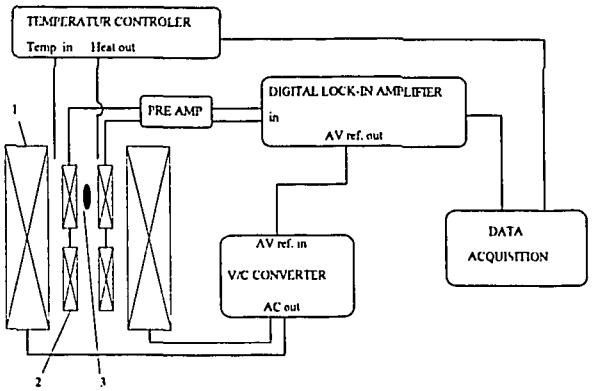

Fig. 1. Block diagram of the ac-susceptometer:
1) primary coil, 2) Secondary pick-up coil, 3) sample.
Electronics are explained in the diagrams.

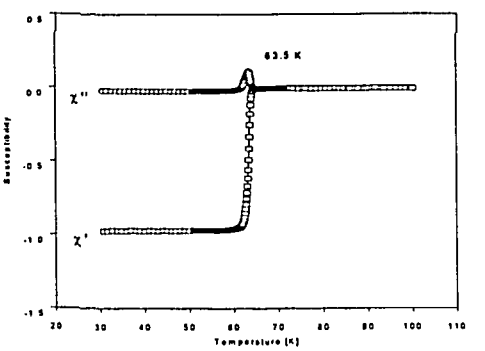

Fig. 2. Temperature dependence of the real, χ', and imaginary, χ'', components of the volume susceptibility of a 59 mg $YBa_2Cu_3O_{6.67}$ single crystal.

2.3.13 Characterization of Superconducting $Bi_2Sr_2Ca_1Cu_2O_{8+x}$ Powder by Neutron Powder Diffraction and Mass Spectroscopy

T. Frello, N. H. Andersen, and R. Hadfield, *Department of Solid State Physics, Riso National Laboratory, Denmark*

High-T_c superconducting cables for current transport is made by the powder-in-tube technique, where the superconducting compound $Bi_2Sr_2Ca_1Cu_2O_{8+x}$ (the 2212 phase with T_c=85 K) plus additional unreacted components are needed as starting composition. The powder is filled into a silver tube, and after proper heat treatment it is transformed into the 2223 phase (T_c=110 K). Contaminants like Nitrogen and Carbon in the starting powder can be released as gases by heating the powder, and it is highly undesirable if this gas release takes place in the silver matrix. If subjected to proper heating procedures, the contaminants can be removed from the starting powder before loading it into the tube. We have undertaken neutron diffraction studies and mass spectrometry studies in order to establish what temperatures and heating times are necessary for removing the contaminants without destroying the 2212 phase.

Neutron diffraction was made at the TAS3 powder diffractrometer at Risø from room temperature to 800 °C. The diffraction data show that the 2212 phase is stable for temperatures less than ≈700 °C. During pre-heating the temperature must therefore be kept below ≈700 °C.

The mass spectrometry was made with a quadrupole mass spectrometer. The powder was heated in an evacuated furnace. The gases expelled from the powder during heating was CO_2, NO_2, N_2O, N_2 and O_2. The partial pressures of these gases were recorded as a function of time and temperature. An example is shown in Fig. 1. It was found that CO_2 and NO_2 was released at 550 °C and 650 °C, while the O_2 pressure decreased at 550 °C and increased at 650 °C.

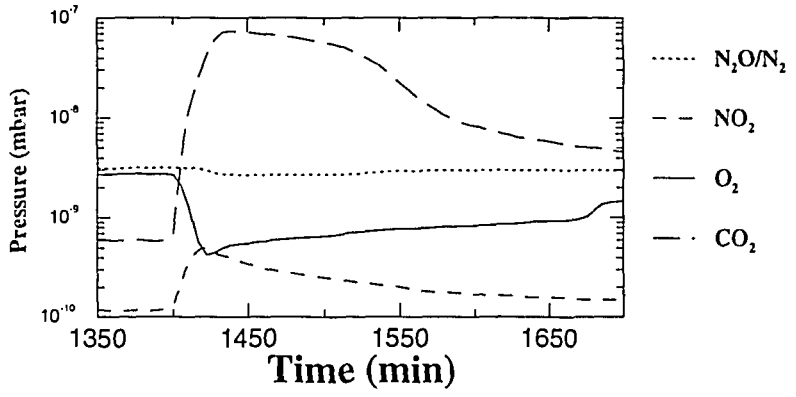

Fig. 1. At 1400 min., the temperature was raised from 550 to 650 °C. The CO_2 and NO_2 pressure is increasing, while the O_2 pressure drops. The N_2O/N_2 pressure is almost unaffected by the temperature increase.

The observations shown in Fig. 1 can be explained by a simple reaction between carbon and oxygen at 550 °C: $C+O_2 \rightarrow CO_2$, thus accounting for the drop in O_2 pressure. However, other reactions involving oxygen may also take place. If carbon is released as CO_2 together with O_2 at 650 °C, this gives rise to increase in both CO_2 and O_2 pressure.

Our data also show that the chemical reactions did not come to an end, even after heating at more than 650 °C for more than five days. Thus prolonged heat treatment is necessary to remove as much contamination as possible from the starting powder.

This project is part of a development program conducted by the Danish company NKT Research Center A/S.

2.3.14 Texture Studies of BiSCCO Crystallites in Ag-tape by High-Energy Synchrotron X-ray Diffraction

H.F. Poulsen, *Materials Department, Risø National Laboratory, Denmark,* T. Frello, N.H. Andersen, *Department of Solid State Physics, Risø National Laboratory, Denmark,* M. Bentzon, *NKT Research Center, Denmark,* R.F. Jensen, *The Technical University of Denmark, Denmark,* J. Süssenbach and D. Nowikow, *HASYLAB, Hamburg, Germany*

It is well established that the epitaxy is a crucial parameter for obtaining high critical current densities in high-T_c superconducting films[1], and it is believed that this is also the case for superconducting tapes, where $Bi_2Sr_2Ca_2Cu_3O_{10+x}$ (BiSCCO) crystallites are imbedded in a silver cladding. We have investigated superconducting tapes made by the Danish company NKT by high-energy x-ray diffraction. The synchrotron beamlines CEMO and BW5 were used as x-ray sources. Photons of energy 90 keV have sufficient penetration power to be transmitted through the Ag-tape (thickness ≈ 160 μm). Diffraction patterns were recorded by a 2-dimensional detector. The scattering vectors lying on almost flat Debye-Scherrer cones are characterized by their polar angles χ. The angle between the incoming beam and the normal to the surface of the tape is called ω. By analyzing the scattering intensity as function of χ for different ω, the texture of the crystallites can be determined. The diffracted signal from BiSCCO clearly showed that the crystallites were aligned with the *c*-axis preferentially normal to the surface of the tape, and the *a-b* plane was randomly oriented within the plane of the tape. Fig. 1 shows the intensity distribution along χ for an (0,0,*l*) reflection giving a measure of the *c*-axis orientation distribution. The critical current I_c for this tape was 18.6 A. Decent fits could be made with simple Gaussians, as indicated in Fig. 1.

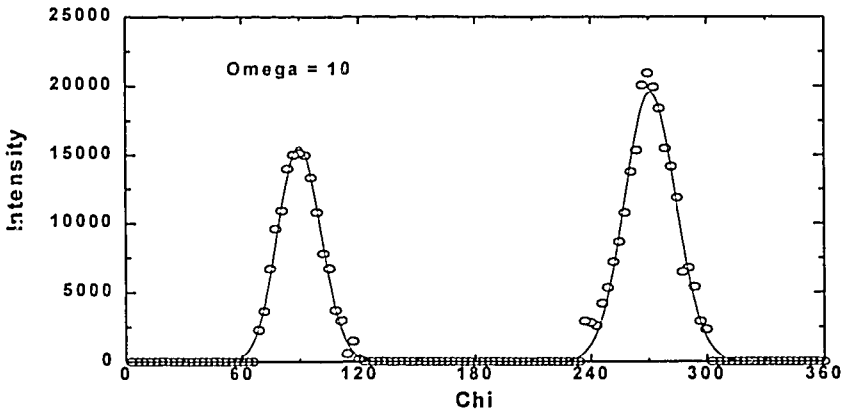

Fig. 1. The distribution of the diffracted signal from a (0,0,*l*) reflection along χ for a superconducting tape with critical current I_c = 18.6 A. Full lines show Gaussian fits to the data points.

The FWHM for the Gaussians in Fig. 1 was ≈ 28°. Similar measurements for a tape with I_c = 10.8 A gave a FWHM of ≈ 40°. In conclusion, we have demonstrated that it is possible to measure the alignment of the crystallites in the bulk of the tape with high-energy synchrotron diffraction. To our knowledge, this is the only technique that can give direct information about the bulk distribution in the tape. We also see that there is a relation between the critical current through the HTCS tape and the epitaxy of the superconducting grains.

[1] R. Kromann, J.B. Bilde-Sørensen, R. de Reus, N.H. Andersen, P. Vase and T. Freltoft, J. Appl. Physics 71, 3419-3426 (1992).

2.3.15 Disordering of the Flux Line Lattice in Nb below H_{C2}

U. Yaron, P. L. Gammel, D.A. Huse, A.P. Ramirez, E. Bucher and D. Bishop, *AT&T Bell Laboratories, USA*, M.R. Eskildsen and K. Mortensen, *Department of Solid State Physics, Risø National Laboratory, Roskilde, Denmark.*

Small-angle neutron scattering, SANS, was used to study the magnetic flux line structure in a very high quality Nb single crystal. Fig. 1 shows snapshot of the diffraction pattern at four fields at $T = 6.4$ K. The ring of scattering observed at $H = 1.48$ kOe, only 50 Oe below H_{C2}, is the first SANS observation of a total loss or orientational correlations as H_{C2} is approached.

The horizontal field SANS scattering geometry allows us to extract three correlation lengths. Translational and orientational correlation lengths in a plane perpendicular to the flux lines are extracted from the radial and azimuthal widths of the Bragg peaks, respectively, whereas the longitudinal correlation length ξ_L, which is a measure of the correlations along the field direction, is extracted from the widths of the rocking curves. Shown in Fig. 2 is the field dependence of the translational correlation length, R_C (a), the azimuthal width (b) and the longitudinal correlation length (c). Approaching H_{C2} from below, the lattice loses translational and orientational correlations, whereas the correlations along the lines remain rather large ($\xi_L \approx$ 100 a_0, where a_0 is the flux lattice constant). A thermodynamic melting of the flux lattice and static disordering due to a peak effect are being considered as mechanisms leading to the observed structural changes.

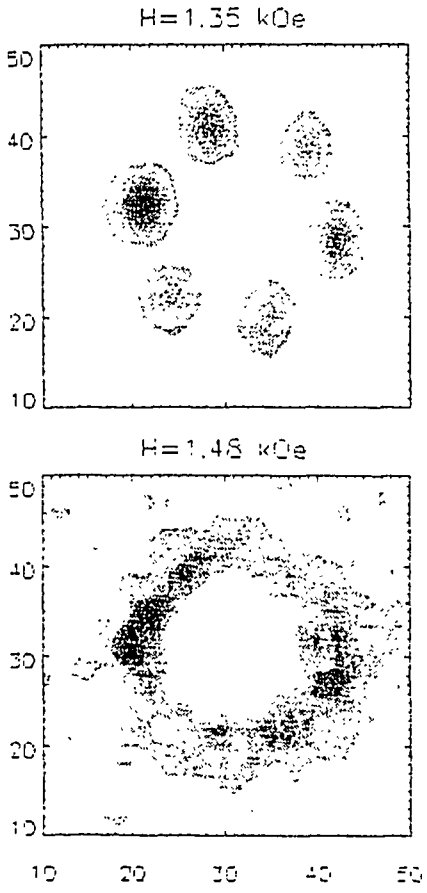

Fig. 1 Snapshots of the diffraction pattern at two fields at $T = 6.4$ K.

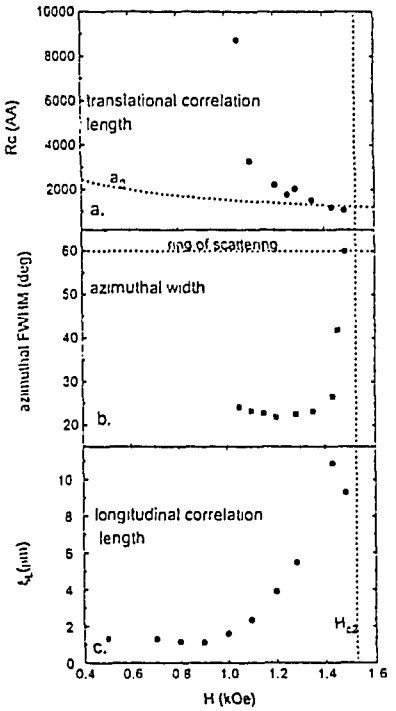

Fig. 2 Field dependence at T=6.4K of a) translational correlation length, approaching H_{C2}, $R_C \approx a_0$, indicative of loss of translational correlations. b) Azimuthal width (azimuthal width of 60° per peak corresponds to a ring of scattering resulting from loss of orientational correlations). c) longitudinal correlation length.

2.3.16 Small-Angle Neutron Scattering of the Magnetic Flux Line Lattice in $NdBa_2Cu_3O_{6+x}$

M. R. Eskildsen, N. H. Andersen, K. Mortensen, *Department of Solid State Physics, Riso National Laboratory, Denmark*, U. Yaron, P. L. Gammel, D. Bishop, *AT&T Bell Laboratories, USA*, and Th. Wolf, *Institut für Technische Physik, Forschungszentrum Karlsruhe, Germany*

We have performed SANS studies of the magnetic flux line lattice (FLL) in $NdBa_2Cu_3O_{6+x}$ (NdBCO), one of the family of Re-BCO materials which exhibits high-temperature superconductivity. The motivation for looking at NdBCO in stead of the more widely studied YBCO[1,2,3] is partly due to the difference in magnetic moment of Nd and Y, and partly due to the fact that NdBCO is more easily grown into large single crystals. One disadvantage of Nd123 however is that it seems to be more fragile than YBCO, and in fact the crystal used in this experiment fell apart at some point during the measurements. The sample used in the experiment was a 253 mg single crystal of dimensions 4x7x1.7mm^3 grown in a ZrO_2/Y crucible with T_c = 94.0 K and a width of less than 1 K. The FLL was studied at a number of fields and temperatures. The following results can be derived from the measurements. The magnetic flux line lattice shows 4-fold symmetry with additional intensity in a square structure, as shown in Fig. 1. This is similar to what is reported in ref. 2. The resolution used in the experiment does not allow us to resolve additional structure apart from the four major peaks. Considering the reflectivity of the FLL versus the applied field, it is possible to extract values for the penetration depth and the superconducting coherence length. One finds $\lambda = 950\pm100$ Å and $\xi = 16$ Å. The observed penetration depth is thus smaller than the 1500 Å usually quoted for YBCO. Finally the reflectivity versus temperature is shown in Fig. 2. The temperature dependence is quite similar to what is found for YBCO.[1,2,3]

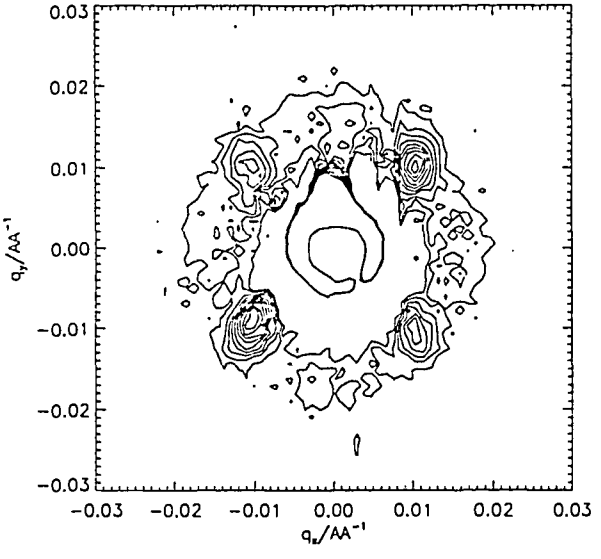

Fig. 1. Example of the magnetic flux line lattice of NbBCO. The picture is the sum of a rocking curve going through the lower left and upper right Bragg peak.

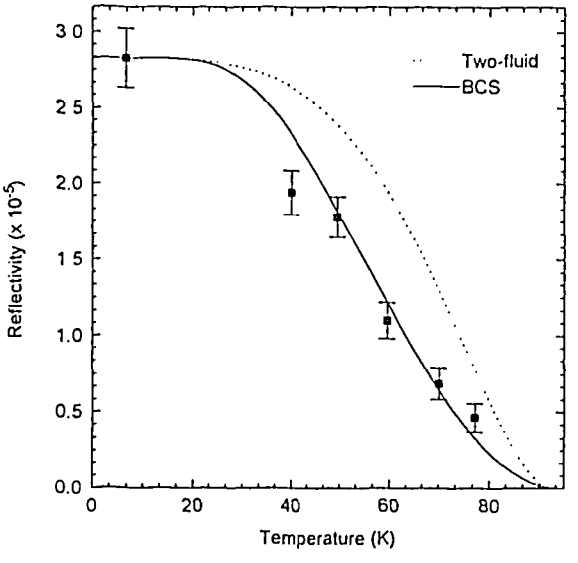

Fig. 2. The reflectivity of one Bragg peak of the magnetic flux line lattice vsersus temperature.

[1] E. M. Forgan et al., Nature **343**, 735 (1990).
[2] B. Keimer et al., Phys. Rev. Lett. **73**, 3459 (1994).
[3] M. Yethiraj et al., Phys. Rev. Lett. **70**, 857 (1993).

2.3.17 Magnetic Ordering in High-Purity Single Crystals of $PrBa_2Cu_3O_{6+x}$

A.Longmore, A.T. Boothroyd, *Department of Physics, Oxford University, UK*, N.H. Andersen, *Department of Solid State Physics, Riso National Laboratory, Denmark*, E. Brecht, *FB Materialwissenschaft, Technische Hochschule Darmstadt, Germany*, and Th. Wolf, *Institut für Technische Physik, Forschungszentrum Karlsruhe, Germany*

Lanthanide ions are contained in many of the high-*Tc* superconductors, and usually the superconductivity is independent of whether the lanthanide is magnetic or not. A notable exception is praseodymium, which often suppresses high-*Tc* superconductivity. The most famous material of this genre is $PrBa_2Cu_3O_{6+x}$.

Our first diffraction studies of the magnetic ordering in this compound employed crystals which contained dissolved Al from the crucible. This impurity influences the magnetic coupling in the *c*-direction. Our latest studies used crystals with much lower levels of impurities, and in particular they contained no Al. We studied oxygenated (x=0.92) and reduced (x=0.35) crystals, and compared the results with our Al-doped crystals and with the $YBa_2Cu_3O_{6+x}$ system.

The onset of the Cu antiferromagnetic ordering was found to occur at temperatures of 266 K and 347 K for x=0.92 and x=0.35 respectively, rather lower than in the Al-doped samples. Further, only one magnetic phase (AFI) was observed for the Cu sublattice in the pure crystals, whereas a second phase (AFII) had been found at low temperatures in the Al-doped crystals.

The most interesting results, however, were associated with the Pr ordering, which was observed below 19 K and 11 K respectively for the two oxygen values. Fig. 1 displays the temperature variation of the (1/2 1/2 0) magnetic Bragg peak which arises from the Pr sublattice ordering in the x=0.92 crystal. Also shown is the variation of the Cu contribution to the (1/2 1/2 2) magnetic Bragg peak. It will be seen that as the Pr ordering develops, the Cu ordering is diminished. Fig. 2 shows that the width of the (1/2 1/2 0) peak in the *c*-direction also correlates with the Pr ordering. We deduce from these observations that there must be a strong coupling between the Cu and Pr moments, and a conflict between the ordering on the Pr and Cu sublattices leads to a reduction in the size of the Cu ordered moment and a limitation on the coherence of the Pr order in the *c*-direction.

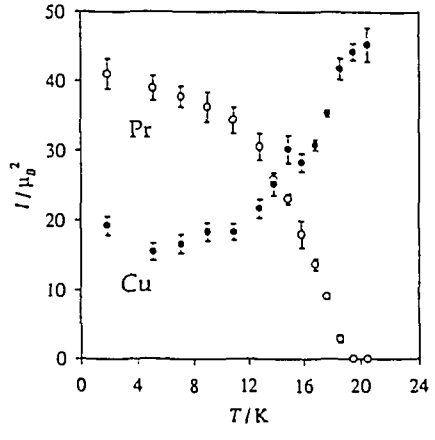

Fig. 1. Temperature variation of the intensity of the (1/2 1/2 0) magnetic Bragg peak (open circles) from the Pr sublattice antiferromagnetic ordering, and the Cu contribution to the (1/2 1/2 2) peak (filled circles), which reflects the magnetic ordering of the Cu sublattice. Data from the oxygenated (x = 0.92) crystal.

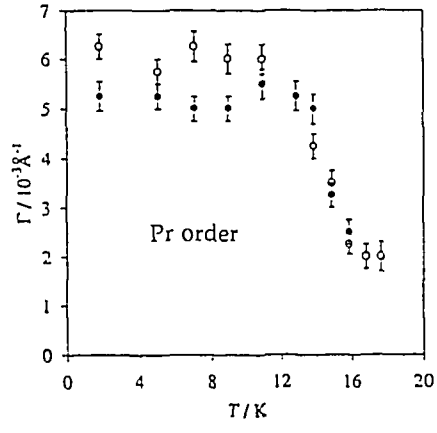

Fig. 2. Variation in the intrinsic half-width of the (1/2 1/2 0) magnetic Bragg peak which is Lorentzian-broadened parallel to the *c*-direction. The open and filled circles correspond to heating and cooling cycles.

2.3.18 Critical Thickness of $SmBa_2Cu_3O_7$ Films on $SrTiO_3$ Substrates

D.-M. Smilgies, R. Feidenhans'l, M. Nielsen, *Department of Solid State Physics, Riso National Laboratory, Denmark,* Q.D. Jiang, A. Kazimirov, and J. Zegenhagen, *Max-Planck-Institut für Festkörperforschung, Stuttgart, Germany*

Thin films of $SmBa_2Cu_3O_7$ grow pseudomorphicly, i.e. with the substrate lattice constant, on $SrTiO_3$ substrates up to a thickness of 500Å. Films of more than 800Å are twinned and display the bulk orthorhombic structure. The Bragg reflections from pseudomorphic films are characterized by satellite peaks at constant $q \approx (0.01, 0.01, 0)$. We observe these satellite peaks both on films lesser than 100Å thick which have a smooth surface (as seen in STM and by the thin film oscillations of the diffraction rods) and on films between 100Å and 500Å which display a columnar surface morphology in the STM scans. These satellites are presumably caused by some density modulation within the film, which could be due to the formation of domain boundaries. We have measured the intensities of the satellites at a number of film Bragg reflections and hope to be able to derive information about the density modulation.
We also tried to find the critical thickness between pseudomorphic and twinned films. A 600Å film displayed a very interesting behavior: The intensities of the satellite peaks are higher than the pseudomorphic peak, although the film does not yet show any reflections characteristic of twinning. In this film domain walls seem to be the dominant feature and only a small amount of the material is still in registry with the substrate. This behavior may be an indication that the domain boundaries and the twin boundaries, which are both along the [1,1,0] direction of the substrate, are related to each other. For a full understanding of the structure of the pseudomorphic phase, a local probe, like HRTEM or LEEM, could provide useful additional information.

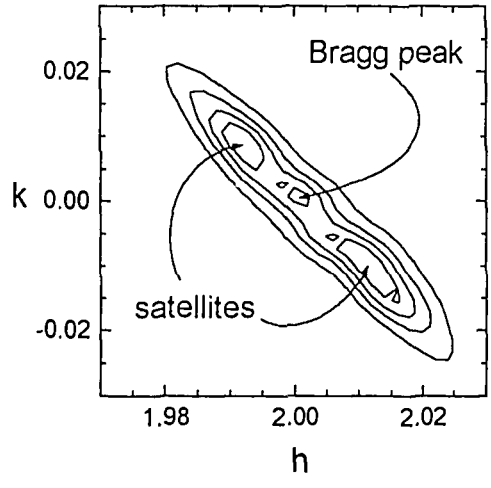

Fig. 1. (201) reflection of a 600 Å thick $SmBa_2Cu_3O_7$ film grown on a $SrTiO_3$ substrate in a cut parallel to the film surface. The satellite peaks are stronger than the film Bragg reflection. The film is still pseudomorphic, however, dominated by the domain boundaries that give rise to the satellites.

2.4 Structures and Defects

2.4.1 Nuclear Motion in Borax and MADMA for Charge Density Studies

H. Birkedal, D. Madsen, P. Harris, S. Larsen, *Centre for Crystallographic Studies, University of Copenhagen, Denmark* and B. Lebech, *Department of Solid State Physics, Riso National Laboratory, Denmark*

Intermolecular interactions, especially hydrogen bonds, play an important role in the determination of the most important topological features of chemically interesting systems. Among these are protein/DNA folding and molecular recognition. One of the main interests at the Centre for Crystallographic Studies is therefore to obtain a detailed level of understanding of intra- and intermolecular interactions in molecular crystals. This may be done by investigations of the electron charge density in the regions of interaction. For such studies, it is essential to have detailed information about nuclear positions and motion, but when using x-ray diffraction data this information can only be obtained for heavier atoms. This poses a problem for compounds containing hydrogen/deuterium, because their electron distribution is almost totally removed from the nuclei by chemical bonding. Furthermore hydrogen/deuterium atoms are often engaged in the parameters (positions and nuclear motion) are taken from a neutron experiment while the some of the most important interactions – hydrogen bonds. Thus a very important feature cannot be accurately studied by x-ray diffraction alone, but needs to be supplemented by neutron diffraction data. We are presently engaged in obtaining accurate X-ray diffraction data on MADMA (methylammonium deuterium maleate) and deuterated borax ($Na_2B_4O_7 \cdot 10\ D_2O$). To obtain an accurate description of especially the hydrogen/deuterium nuclear parameters we have collected single crystal neutron diffraction data at the four-circle diffractometer TAS2. Figure 1 shows the resulting refined crystal structure of MADMA with the 50% nuclear probability ellipsoids. We are currently processing the borax data. The obtained nuclear parameters for the hydrogen/deuterium atoms will be used in a so-called X-N refinement[1] of the x-ray data in a multipolar formalism[2] for the electron charge density. In the X-N method some or all nuclear parameters (positions and nuclear motion) are taken from a neutron experiment while the electronic parameters are based on X-ray diffraction data. In the multipolar formalism the X-ray scattering factors are based on an expansion of the electron density, that makes it possible to model electronic deformation due to interatomic interactions (*e. g.* chemical bonding).

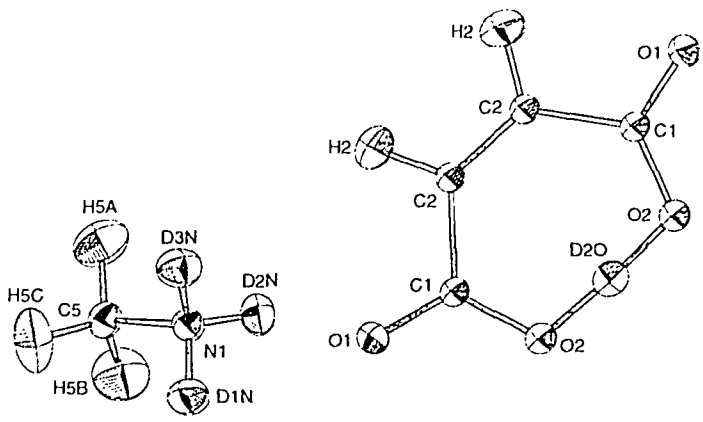

Fig 1. Refined neutron structure of MADMA shown with the 50% nuclear probability ellipsoid.

[1] P. Coppens. In Electron Distributions and the Chemical Bond, P. Coppens and M. B. Hall (*eds.*), Plenum Press p. 61 (1982).
[2] R. F. Stewart, J. Chem. Phys. **51**, 4569 (1969).

2.4.2 Morphological Characterization of Partially Crystallized $Fe_{78}Si_9B_{13}$ Amorphous Alloy

A. Deriu, *INFM - Dipartimento di Fisica, University of Parma, Italy,* F. Malizia, F. Ronconi, *INFM - Dipartimento di Fisica, University of Ferrara, Italy,* J. Skov Pedersen, *Department of Solid State Physics, Riso National Laboratory, Roskilde, Denmark*

Iron-based metallic glasses produced by rapid solidification tecniques have been the object of extensive studies since their soft magnetic properties are important for technological applications. These properties are to a large extent modified by even partial crystallization, moreover such properties depend critically on the dimensions and shape of crystalline phases embedded in a still amorphous matrix. It is therefore important to have a good knowledge and control of the morphology of such crystalline products in order to produce stable partially crystallized materials with structural characteristics tailored to specific applications. In particular, it was shown that the primary crystallization of $Fe_{78}Si_9B_{13}$ gives rise to the precipitation of α-Fe crystals, with dimensions in the nanometric range, whose morphology depends on the preparation conditions of the amorphous precursor. The purpose of our work is to investigate the mechanism of the primary crystallization of $Fe_{78}Si_9B_{13}$ studying the morphological evolution of the α–Fe clusters which are formed at the various stages of the devitrification process as a function of the thermal treatments during the crystallization process as well as the preparations conditions of the amorphous precursors. For this study we have produced a series of samples with different degree of crystallization coming from amorphous precursors with different preparation conditions and we have used the small-angle neutron scattering (SANS) technique in order to characterize these samples from a morphological point of view. The figure shows the radially averaged scattering intensities of the amorphous ribbon and of two samples heated to different temperatures. A different shape of scattering profiles as a function of crystallization degree is evident in the low-Q region. The same effect can be seen in the scattering profiles of samples with the same degree of crystallization but different from each others in the preparation conditions of the starting glassy material. A quantitative analysis of the SANS data will be performed by fitting the measured intensities to a model derived from the morphological information provided by transmission electron microscopy of the same samples.

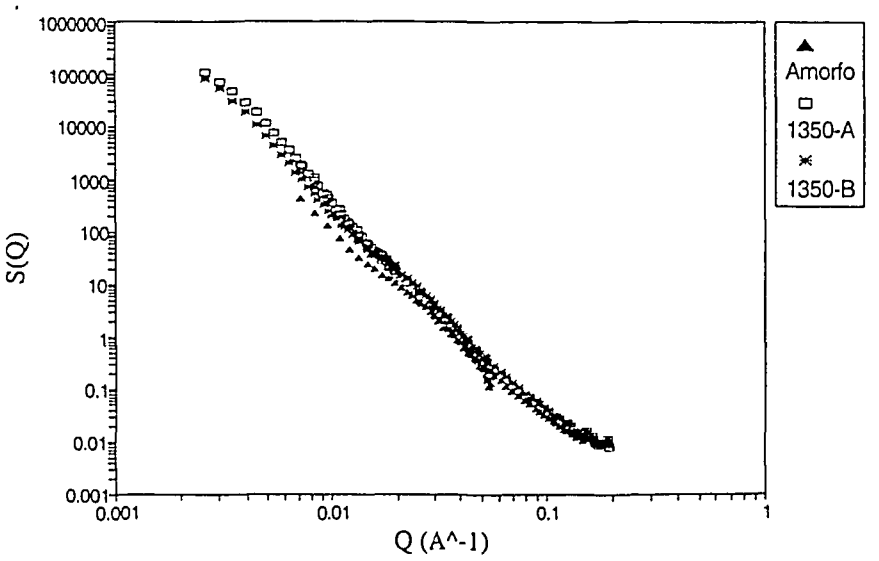

2.4.3 Small-angle Neutron Scattering Study of $Fe_{91}Zr_9$ Glass in Magnetic Field

L. Fernandez Barquin, J. Gomez Sal, P. Gomez Plaza, *CITIMAC, University of Cantabria, Santander, Spain*, S.N. Kaul, *School of Physics, University of Hyderabad, India*, J.M. Baradiaran, P. *Depart. Elec. Electronica, UPV, Bilbao, Spain*, J. Skov Pedersen, *Department of Solid State Physics, Riso National Laboratory, Denmark*

Zero-field and in-field small-angle neutron scattering measurements over a wide range of scattering vectors (q) have been performed for the $Fe_{91}Zr_9$ metallic glass in the 10 - 290 K temperature range. Two transitions are observed at 210 K and around 60 K and these are related to the T_c and re-entrant transition temperature, respectively. The spectra $I(q)$ (0.003 $Å^{-1} < q <$ 0.5 $Å^{-1}$) reveal the exsistence of an important contribution at the lowest q values and at least two humps in the entire curves. The application of the magnetic field results in a anisotropic signal, and a global decrease of intensity. The magnetic field drastically reduces $I(q)$ in the region for q < 0.04 $Å^{-1}$, but not so strongly at larger q values (even at H = 4 T), but with the results that the remaining hump becomes more evident. Its origin can so far be uniquely explained by models dealing with the exsistence of clusters embedded in a ferromagnetic matrix.

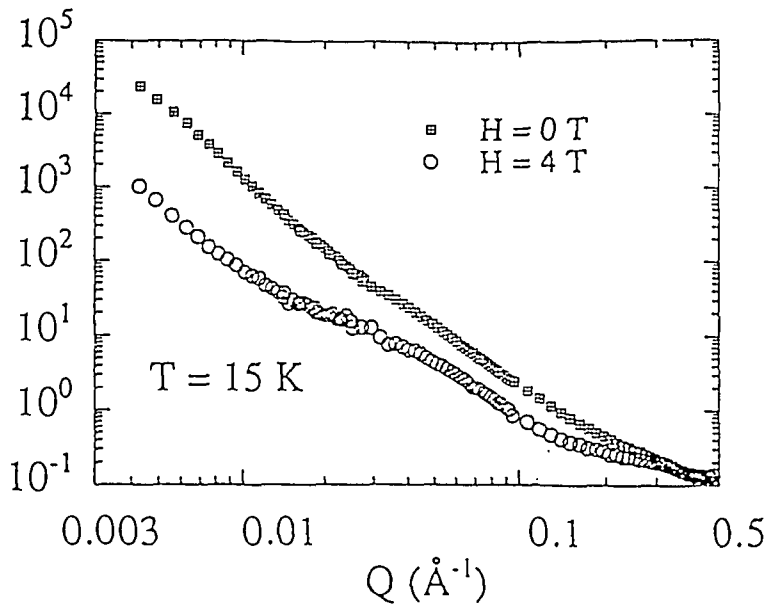

Small-angle neutron scattering spectra in a log-log representation with and without magnetic field in the re-entrant spin-glass state at T = 15 K.

2.4.4 Small-angle X-ray and Neutron Scattering Studies of Kr Inclusions in Ni

A.M. Hussain, J. Skov Pedersen, *Department of Solid State Physics, Risø National Laboratory, Denmark,* M. Eldrup, *Materials Department, Risø National Laboratory, Denmark*

Bulk samples of Ni containing about 3 at.% Kr, prepared[1] at Harwell, U.K., by the combined sputtering and deposition technique have been investigated. The samples have been isochronally annealed for 30 min at each of several temperatures up to 1270°C in order to study the development of the size distribution of the Kr inclusions. A sample with a relatively large size of about 10 x 10 x 0.8 mm^3 was used for the SANS measurements, whereas several smaller samples with a diameter of about 3 mm and a thickness of about 0.1 mm were used for SAXS measurements. The same sample was used throughout the SANS measurements. The samples for the SAXS measurements were annealed together with the SANS sample and taken out one by one to have samples with identical annealing histories. For the SANS measurements the sample was mounted in a magnetic field of 0.25 T in order to identify the possible magnetic contribution to the scattering, but no influence of the magnetic field was detected. The SANS measurements were performed at the Risø instrument and covered scattering vectors, q, in the range 0.01 - 0.25 $Å^{-1}$. The SAXS measurements were performed at the newly installed instrument at the rotating anode in the Department and covered the range 0.012 - 0.12 $Å^{-1}$. Most of the data sets have two contributions to the scattering: One from 10 - 70 Å large Kr inclusions at relatively large q, and an additional power law contribution (q^{-4}) at low q, which originates from large heterogeneties in the samples. The data were analysed by several different approaches: Indirect Fourier transformation[2], model fitting and size distribution determinations.[3] The indirect Fourier transformation provides information on the distance distribution function $p(r)$ and the radius of gyration R_g. The model used in the model fitting consisted of one or two components of spherical inclusions with different sizes. The analysis showed the following behaviour: In the as-prepared sample an inclusion radius of 10 - 15 Å is found. An increase of the size of the inclusions sets in around 300°C. For annealing temperatures in the range 350 - 700°C one observes the presence of two main components of sizes: one with a radius of about 10 Å and another with a radius of about 30 Å. Above 700°C the size of the largest inclusions gradually increases until about 900°C where the inclusions no longer can be observed due to the increase in the power law contribution. Measurements of the sample weight show that gas loss sets in at around 650°C and at the same time a strong increase in the prefactor of the power law contribution occurs. The volume fraction of the inclusions increases by about a factor of three from the as-prepared state to 650°C, above which an abrupt decrease is observed which is associated with the gas loss.

---

[1] D.S. Whitmell, R.S. Nelson, K.J.S. Smith and G.J. Bauer, Eur. Res. Reports Nucl. Science and Techn. 4, 513, (1983).

[2] O. Glatter, J. Appl. Cryst. 10, 415 (1977).

[3] J. S. Pedersen, J. Appl. Cryst. 27, 595 (1994).

2.4.5 Coarsening of Bimodal Coherent γ' Particles Size Distributions in Ni-Al-Mo Alloys

J.J. Cruz, H.A. Calderon, *Departamento de Ingenieria, E.S.I.Q.I.E.-I.P.N.*, Mexico, J. Skov Pedersen, *Department of Solid State Physics, Riso National Laboratory, Denmark*

The coarsening kinetics of bimodal distributions of coherent γ' (Ni_3Al) particles in Ni-base alloys is investigated. Molybdenum is added to vary the lattice parameter mismatch which affects the elastic interactions between particles during the ripening process. In solids, the elastic strain energy can affect the coarsening process of particles as theoretically suggested by several investigators (see for example[1]) and experimentally shown by Sequeira et al.[2] The bimodal distribution of particles is created by aging at two different temperatures. Aging close to the solvus line produces large particles in relatively short times. Aging at lower temperatures gives rise to the formation of a second set of smaller particles. The alloys investigated have the following compositions: Ni-14 at.% Al, Ni-10 at.%Al-5 at.%Mo and Ni-6.5 at.%Al-10 at.%Mo. Small angle neutron scattering (SANS) experiments have been carried out to determine the size, shape and arrangement of particles as a function of aging time for the smaller particles. Single crystalline specimens oriented with the plane (110) parallel to their surface have been used for the experimental measurements. The SANS patterns obtained are anisotropic showing interference peaks along directions [001] and cuboidal shapes at large scattering vectors (q). This indicates that the particles are not spherical and that they are spatially arranged along directions <001>. Fig. 1 shows curves of absolute intensity versus scattering vector q obtained after averaging the measurements along two different directions of the anisotropic patterns of the alloy Ni-10 at.%Al-5 at.% Mo. These anisotropic patterns are more complicated to analyse than those of spherical particles oriented at random (isotropic). Sequeira et al. attempted evaluation from anisotropic patterns using a technique developed for isotropic patterns[2] and they found somewhat large inconsistencies with measurements from transmission electron microscopy. A better evaluation technique is needed for anisotropic patterns which is being currently developed.

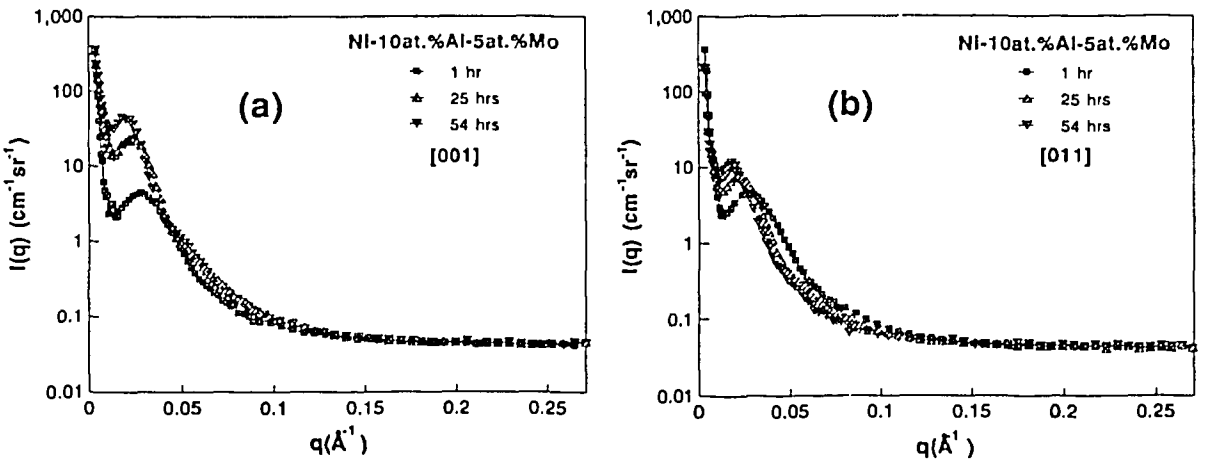

Fig. 1. SANS intensity versus scattering vector in Ni-10 at.%Al-6 at.%Mo (a) [001] and (b) [011].

[1] W.C. Johnson, Act. Metall. 32, 465 (1984).
[2] A.D. Sequeira, H.A. Calderon, G. Kostorz, J.S. Pedersen, Acta Metall. Mater. 43, 3427 (1995).

2.4.6 Corsening of γ' Coherent Particles in Fe-Ni-Al Alloys

H.J. Dorantes, H.A. Calderon, *Departamento de Ingenieria, E.S.I.Q.I.E.-I.P.N.*, Mexico, J. Skov Pedersen, *Department of Solid State Physics, Risø National Laboratory, Denmark*

Fe- 10 at.% Ni- 15 at.%Al and Fe-10at.%Ni-15 at.%Al-1 at.%Mo have been investigated. These alloys can be hardened by coherent γ' (NiAl) precipitates which have a B2 structure in the bcc matrix. Mo has been added to vary the lattice parameter mismatch δ between particles and matrix. δ affects the elastic interactions between particles which are important for the coarsening process of particles in solids. Single crystals with a cylindrical form, having the direction [100] parallel to the long axis have been prepared for measuring the coarsening kinetics of γ' particles by means of small angle neutron scattering. The SANS patterns have anisotropic shapes, i.e. they show interference peaks along [001] directions and they do not have a circular symmetry. The distribution of particles is not homogeneous in space as shown by the interference peaks in the pattern. The shape of the pattern at large scattering vectors q shows that the particles are not spherical. Fig. 1 shows scattering curves of absolute intensity versus scattering vector q obtained after averaging along specific crystallographic directions. Fig. 1a shows averaging along a [010] direction and Fig. 1b after averaging along [011]. The differences in the curves can be converted into quantitative parameters of the microstructure if the anisotropic patterns can be analyzed and modeled. An appropriate technique for analysis is currently being developed.

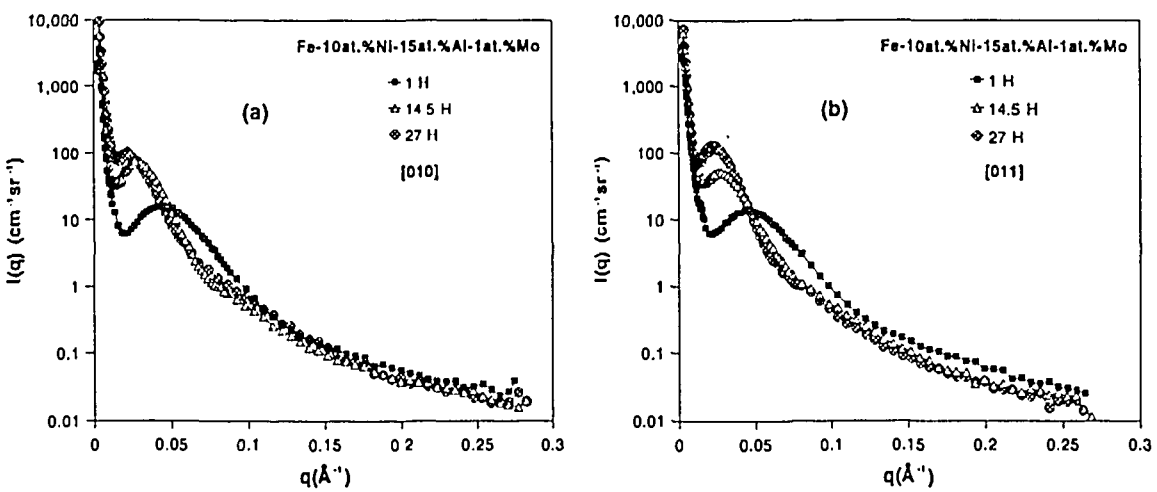

Fig. 1. Curves of absolute intensity versus scattering vector for the alloy Fe-10Ni-15Al-1Mo. (a) [010] and (b) [011].

2.5 Surfaces and Interfaces

2.5.1 Formation of Tilted Clusters in the Electrochemical Deposition of Copper on *n*-GaAs(001)

D.-M. Smilgies, R. Feidenhans'l, *Department of Solid State Physics, Riso National Laboratory, Denmark*, G. Scherb, D.M. Kolb, *Abteilung Elektrochemie, Universität Ulm, Germany*, A Kazimirov, and J. Zegenhagen, *Max-Planck-Institut für Festkörperforschung, Stuttgart, Germany*

Using synchrotron x-ray diffraction, we have investigated thin copper films (about 50 monolayers) which were deposited onto a *n*-doped GaAs(001) substrate in an *in-situ* electrochemical cell. We found the following epitaxial relations: Cu(001) || GaAs(001) and Cu[100] || GaAs[110]. Copper has a large lattice mismatch of 10% with the substrate and it is known that copper grows under these conditions as 3D islands.[1] Hence it was no surprise to find a large in-plane mosaic of 5.5°. However, we found furthermore that the (111)Cu reflection was smeared out into a ring. This can only be explained by assuming that the copper clusters are tilted by about 6°, without any preference for the azimuth of the tilt. A simple geometrical model describes the observed shape of the (111) ring (see Figure) as well as the transverse scans through the (200)Cu and (202)Cu reflections. It may be speculated that the relatively large substrate roughness of 5Å, in combination with the large lattice mismatch give rise to this peculiar tilt.

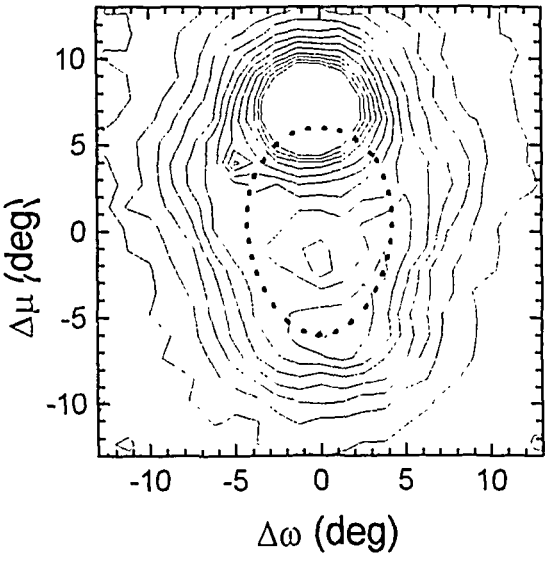

Fig.1. Contour of the ring-shaped (111)Cu reflection on the constant-q sphere. The angle μ corresponds to the latitude and the transverse scan direction ω to the longitude on the sphere. The calculated shape of the reflection is shown as a dotted line, assuming a tilt angle of 6° without any azimuthal preference. The intense peak at the upper part of the figure is the (20*l*)GaAs crystal truncation rod of the substrate.

[1] G. Scherb and D.M. Kolb, J. Electroanal. Chem (1995), in press.

2.5.2 Structure of the c(2×8) Reconstructed InSb(001) Surface

D.-M. Smilgies, E. Landemark, R. Feidenhans'l, M. Nielsen, *Department of Solid State Physics, Risø National Laboratory, Denmark,* G. Falkenhagen, L. Seehofer, L. Lottermoser, and R.L. Johnson, *II. Institut für Experimentalphysik, Universität Hamburg, Germany*

A number of structural models for the c(2×8) reconstruction of the (001) surfaces of III-V semiconductors have been proposed in literature. However, the in-plane data set we took last year for InSb(001) proved to be incompatible with all of these models, including the presently favored model of this surface.[1] Furthermore, the (00l) crystal truncation rod shows a wide maximum around the (002) reflection, whereas all the existing models would predict a lowering of the rod intensity. Furthermore, a careful re-examination of this rod revealed an interesting interference behavior close to the (002) Bragg peak (see Fig 1). Both observations indicate that there should be a layer of material with different enough stoechiometry on top of the substrate which behaves like a thin film of about 2 layers. This is not unreasonable for a surface prepared by sputtering, since preferential sputtering of one atom species can give rise to a changed surface composition. In fact, recent ion scattering results[2] also indicate a change in the stoechiometry close to the surface.

Additionally, we have taken a large set of fractional-order rods. Since we knew from the in-plane Patterson function, that the surface is almost (4×1), we restricted the set to the fourth-order superstructure rods and ignored the very weak eighth order reflections. We obtained a 3D Patterson function from these rods which shows clearly some out-of plane interatomic vectors. Hence this reconstruction is not confined to a single lattice plane.

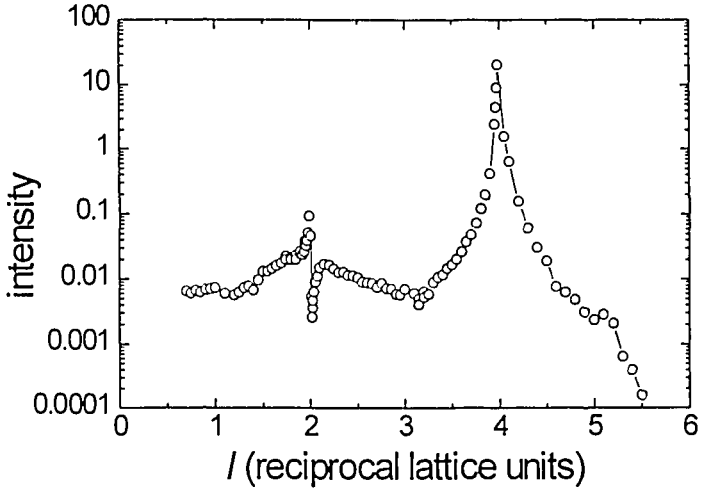

Fig. 1. (00l) crystal truncation rod of the c(2x8) reconstructed InSb(001) surface. Note the wide maximum around (002) and the interference effects close to the (002) reflection. These findings indicate that there is a thin layer with changed chemical composition at the surface.

[1] C.F. McConville *et al.*, Phys. Rev. B **50**, 14 965 (1994).
[2] J. Falta *et al.*, Phys. Rev. Lett. 69, 3068 (1992); Phys. Rev. B 48, 5282 (1993).

2.5.3 A Dynamic Phase Transition in Sputtering of Ge(001)

D.-M. Smilgies, E. Landemark, M. Nielsen, *Department of Solid State Physics, Risø National Laboratory,* and P.J. Eng, *Center for Advanced Radiation Sources, University of Chicago, USA*

Dynamic scaling theory is a concept of describing systems far from thermal equilibrium. An example is sputtering of a single crystal surface. Sputtering removes atoms from the surface at random positions. Fluctuations in the sputter flux density give rise to the formation of a randomly rough surface. However, at high enough temperatures, surface diffusion tries to bring the surface morphology back to the thermal equilibrium shape, the smooth surface. Depending on which of the processes, fluctuations or diffusion, is dominant, the surface will be randomly rough or smooth. However, when both processes are of equal importance, a *dynamical* equilibrium forms which is characterized by the *dynamic scaling exponent* β of the root-mean-square roughness and the so-called *static scaling exponent* α of the in-plane correlations. The line-shape of the crystal truncation rods is characterized by a sharp component which decays with sputter time and a broad diffuse component which appears at long sputter times. We were able to find appropriate surface temperatures and sputter fluxes to observe this behavior in sputtering of Ge(001).

In order to measure β properly from the decay of the sharp component, it is necessary to perform *in-situ* and *real-time* measurements which was possible at the Surface Diffraction Beamline of the ESRF. We found β values of about 0.2 for the dynamic scaling regime. At higher ion fluxes or lower surface temperatures, the system moved into the random-ablation regime which is characterized by $\beta = 0.5$. Surprisingly, the transition between the two regimes is sharp. In the figure, temperature scans of the rod intensity are shown at various ion fluxes. A theoretical description for the observed behavior does not yet exist.

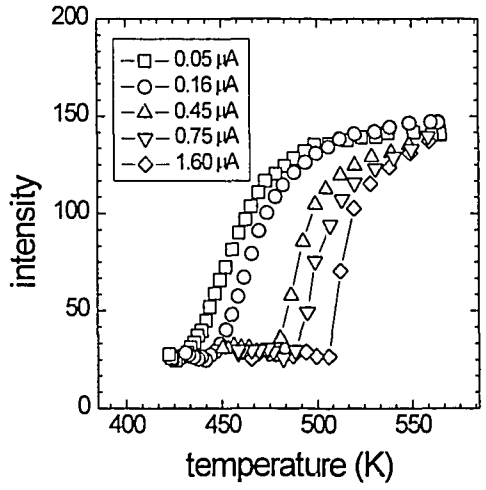

Fig. 1. Rod intensity at (2,0,1.7) versus substrate temperature at various ion currents, as indicated. At temperatures above 520 K the system is in a dynamic scaling regime with a β of about 0.2. When the temperature is lowered, the system moves into the random ablation regime with $\beta = 0.5$. The transition temperature depends on the ion current.

2.5.4 STM Investigations of Self-Assembled Monolayers of Dialkoxyanthracene Derivatives

S. B. Wilkes and K. Bechgaard, *Department of Solid State Physics, Risø National Laboratory, Denmark*, T. Hansen, S. Itoua, T. Bjørnholm and K. Schaumburg, *Centre for Interdisciplinary Studies of Molecular Interactions, University of Copenhagen, Denmark*

It has been demonstrated by many authors that anthracenes photodimerise over the 9-,10-positions of the benzenoid ring structure. In addition, Rabe *et al.* have recently reported the lamellae-forming properties of structures derived from hydroquinone ethers and 1,4-dialkoxybenzenes.[1] It was therefore decided to synthesise a series of 2,6- and 1,4-dialkoxyanthracene derivatives in order to investigate lamellae-forming properties and the possibility of STM-induced chemical reactivity at the liquid-graphite interface.

The STM image of one of the anthracene derivatives, 2,6-didodecyloxyanthracene (2,6-DDOA) (see Fig. 1), at the interface between highly ordered pyrolytic graphite (HOPG) and a high boiling organic solvent (octylbenzene, *bp.* = 261-263°C), is shown in Fig. 2. In the STM image, the anthracene moieties are represented by bright areas (high tunnelling current). Generally, alkyl chains in a molecule give a lower tunnelling current and therefore, the dodecyl chains are represented by the red shaded areas. The darker lines between the rows stem from van der Waals gaps between the rows of molecules. The compound 2,6-DDOA self-assembles from solution in less than two hours giving a physisorbed monolayer at the solid-liquid interface. The molecule has lattice parameters, a = 8.5 Å and b = 23.5 Å, fitting the size of the molecule well. The smallest a-b angle in the 2D unit cell is measured to be 40°. The dislocation in the monolayer along the b-axis from row to row has been investigated and is so far believed to be an intrinsic property of this compound under these specific conditions. Attempts to initiate a photochemical reaction within the 2,6-DDOA monolayer under pulsed conditions have, so far, been unsuccessful.

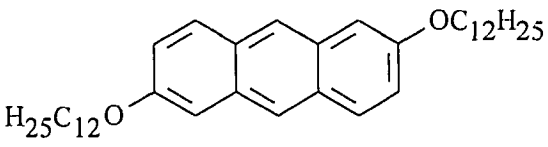

Fig.1. 2,6-Didodecyloxyanthracene (2,6-DDOA).

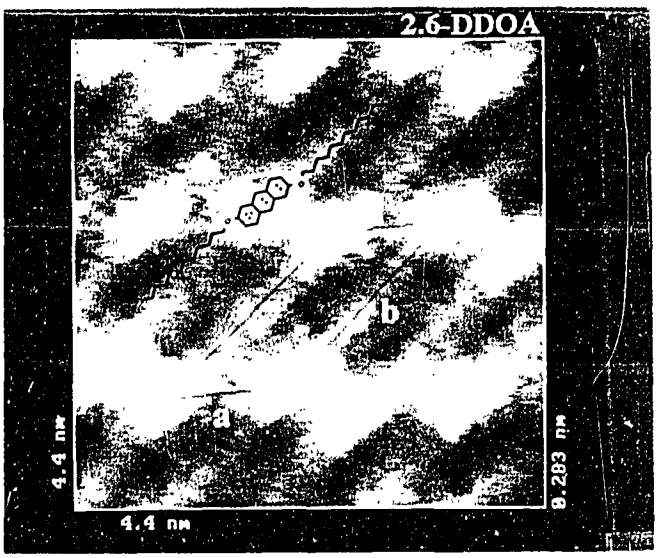

Fig 2. The STM image of a 2,6-DDOA monolayer.

[1] R. Heinz, A. Stabel, J.P. Rabe, G. Wegner, F.C. De Schryver, D. Corens, W. Dehaen, C. Suling, Angew. Chem. **106**, 2154 (1994).

original contains color illustrations

2.5.5 Self-Assembled Amide-Containing Overlayers on Silicon and Gold for E-Beam Lithography Studies

S. B. Wilkes and K. Bechgaard, *Department of Solid State Physics, Riso National Laboratory, Denmark*, T. Bjørnholm and K. Schaumburg, *Centre for Interdisciplinary Studies of Molecular Interactions, University of Copenhagen, Denmark*

The modification of solid surfaces by spontaneously self-assembling monolayers (SAM's) is a model system for the study of biomembranes and is of technical interest for the fabrication of sensors, transducers and protective layers. SAM's have also found direct practical use in patternable materials for cell growth, protein adhesion and microlithography.[1,2] E-beam lithography has been employed for the fabrication of such materials although over the last decade or so, the ultimate resolution of organic resists has remained around 10 nm. Various reasons for this have been proposed including, among others, the sensitivity of the organic resist to low energy secondary electrons. One way of addressing this problem is to synthesise a molecule in which selected functional groups within the SAM are able to absorb the low energy electrons without a fundamental change in the molecular structure. It is hoped the efficient absorption of the low energy electrons would prevent excessive straggling of the secondary electrons within the resist and so confine the exposure more accurately. A number of recent reports have used amide-containing SAM's as a means of monitoring photoinduced electron damage to the organic material occurring on exposure to X-rays.[3] As such, a number of molecules have been synthesised for investigating the nature and degree of damage occurring by the interaction of electrons with the organic film using E-beam lithography. All the molecules contain an alkyl chain, an amide function and in some cases a reactive group allowing chemical bonding to a silicon or gold surface. For the octadecanoic amide derivatives, the amide function may be placed either close to the surface using LB-deposition on a hydrophilic substrate, or in a distance given by the alkyl chain (*ca.* 20 Å) by deposition on a hydrophobic substrate (*eg.* HF dipped Si). A fairly high degree of order is expected in these layers as indicated by synchrotron radiation diffraction studies of Langmuir films of similar molecules.[4] The amide-containing molecules possessing a reactive end group, such as silicon ($-SiCl_3$, $-Si(OCH_3)_3$) or sulphur (–SH), allow coverage by one self-assembled monolayer of a hydrophilic silicon wafer or gold surface respectively. It has been possible to vary the position of the amide function along the alkyl chain in relation to the reactive end group, thereby placing the amide function either at the air-substrate interface or closer to the desired surface.

---

[1] A. Ulman, An Introduction to Ultrathin Films, Academic Press: San Diego, CA (1991).
[2] L.H. Dubois and R.G. Nuzzo, Annu. Rev. Phys. Chem. 43, 437 (1992).
[3] R.L. Graham, C.D. Bain, H.A. Biebuyck, P.E. Laibinis and G.M. Whitesides, J. Phys. Chem. 97, 9456 (1993).
[4] S.P. Weinbach, D. Jacquemain, F. Leveiller, K. Kjaer, J. Als-Nielsen, *et al.*, J. Am. Chem. Soc. **115**, 11110 (1993).

2.5.6 Monitoring *in-situ* Crystal Growth and Dissolution by AFM and GIXD

D. Gidalevitz, S. Matlis and L. Leiserowitz, *Department of Materials and Interfaces, Weizmann Institute of Science, Rehovot, Israel*, D.-M. Smilgies, M. Christensen and R. Feidenhans'l, *Department of Solid State Physics, Riso National Laboratory, Denmark*

The crystals of β-alanine and α-form of glycine were choosen to study the atomic structure at the liquid/solid interface while the crystals were growing or dissolving. The crystals are composed of zwitterioninc molecules, which form a molecular crystals with properties very much alike to those of ionic crystals. Both compounds consist of hydrogen bonded bilayers parallel to the (010) crystal face.

During *in-situ* Atomic Force Microscopy (AFM) measurements we performed a series of snapshots, taken in equal periods of time, of the same region of the surface of the crystal face following either its growth or dissolution. It was observed that both dissolution and growth processes occur as a step flow with the minimal step size equal to ~7±0.5Å in the case of β-alanine and ~5.5±0.5Å in the case of glycine. These values appeared to be very close to the bilayer height of corresponding crystals.

The calculated intensities along the crystal truncation rods (CTR) revealed a dramatic depending on how crystal surfaces are truncated. Therefore, grazing incidence x-ray diffraction (GIXD) measurements were performed at wiggler BW2 beamline at HASYLAB, Hamburg using the surface diffractometer.

The GID data were collected from dry cleavage surfaces of both crystals, from pure ethanol-β-alanine surface interfaces (dissolution), and from saturated ethanol-water solution-glycine interfaces (growth).

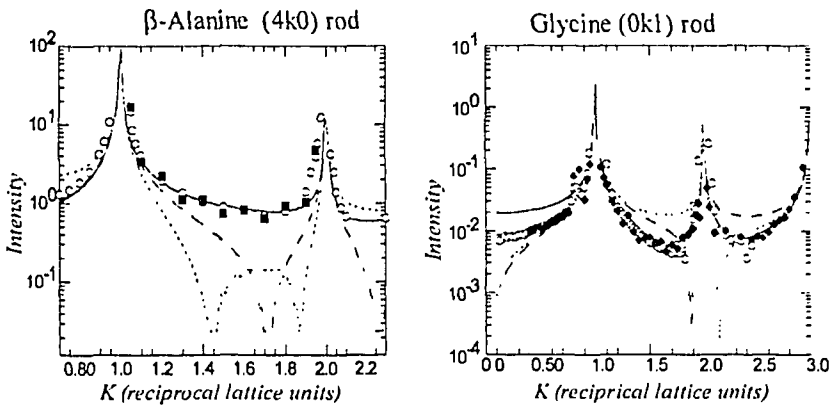

Fig. 1 The GIXD data of in-situ dissolution of β-alanine and growth of glycine. The models corresponding the expected cleavage plane through the van der Waals bonded bilayers (solid line) fits the measured data points (squares). The dashed lines corresponds to other possible truncations.

The results of the experiments unambiguously showed that during all performed measurements the truncation of the β-alanine and glycine crystals remained constant. Together with result of AFM measurements this suggests that the processes of the growth and the dissolution of (010) crystal face of α-form of glycine and β-alanine occur at the steps on the surface.

2.5.7 The Surface X-ray Scattering Study of Stereospecific Adsorption of (S)-Methionine onto the Surface of Glycine

D. Gidalevitz and L. Leiserowitz, *Department of Materials and Interfaces, Weizmann Institute of Science, Rehovot, Israel*, M. Christensen and R. Feidenhans'l, *Department of Solid State Physics, Riso National Laboratory, Denmark*

Over the past decade control over nucleation, polymorphism, growth, dissolution and habit of molecular crystals has been achieved with the use of tailor-made molecular additives. The essence of this approach is based on selective binding of the additive to particular crystal faces and effect thereof on macroscopic crystal properties. The nature of the additive binding was generally deduced from macroscopic data, such as the habit and shape of the resulting crystal, but it had nor been possible to observe the surface-bound "foreign" molecules. Here direct evidence is presented by surface X-ray diffraction of attachment of a layer of (S)-methionine molecules additive to two opposite {010} faces of α-glycine, following growth from an aqueous solution.

Crystals of the α-form of glycine are monoclinic, space group $P2_1/n$. Large crystals can be grown from pure aqueous solution with well expressed {110}and {011} faces and poorly developed {010} faces. Only an (R)-methionine additive can substitute a glycine molecule at the (010) face, whereas only (S)-methionine can substitute a glycine molecules on the $(0\,\bar{1}\,0)$ face. Surface X-ray scattering experiments were carried out at the wiggler BW2 beamline at HASYLAB, DESY, Hamburg. The (0k0), (0k1), and (2k0) crystal truncation rods (CTR) were measured from the (010) face of the freshly cleaved glycine crystal and (010) and $(0\,\bar{1}\,0)$ faces of a glycine crystals whose cleaved faces was further grown in a saturated glycine solution containing 9% (S)-methionine. Intensity calculations of the CTR's of the $(0\,\bar{1}\,0)$ face yielded reasonable fits where (S)-methionine molecules are hydrogen-bonded to the glycine surface molecule via pseudo centers of inversion (as in the bulk) forming a monolayer, with two molecular conformations.

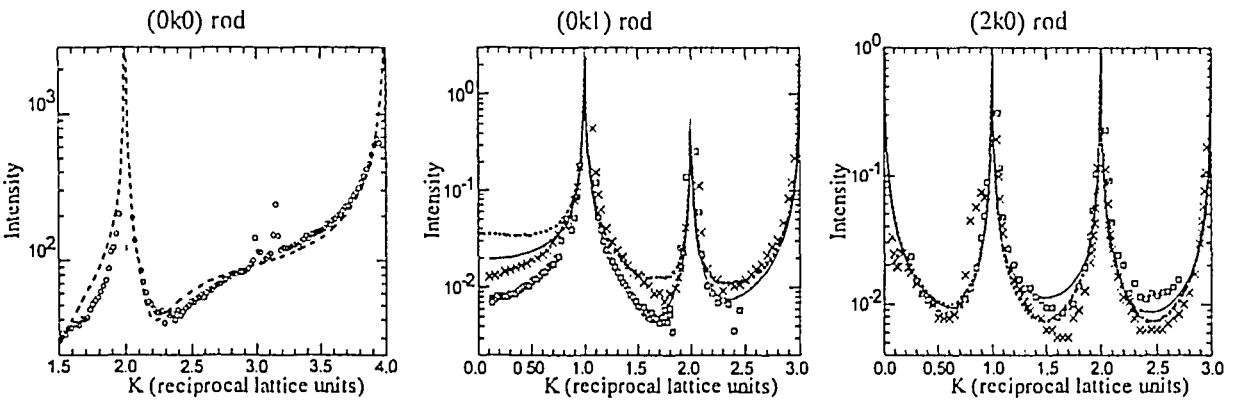

Fig.1 The measured and calculated CTR profile for the truncated bulk glycine surface (circles and solid line) and with adsorbed (S)-methionine (crosses and dashed line).

These two conformations are similar to those found in the 3-D crystal structure of (S)-methionine. The analysis yielded a molecular layer of (S)-methionine with an occupancy of 50%-80%. The structural model of the (010) face consists of a layer of (S)-methionine less strongly bound to the glycine surface via a pseudo twofold axis, occupying approximately 70% of the surface sites.

2.5.8 X-ray Diffraction Study of Fe/V Superlattices

A. Madsen, R. Feidenhans'l and M. J. Christensen, *Department of Solid State Physics, Riso National Laboratory, Denmark*

Fe/V superlattices were grown under UHV-conditions in a MBE-chamber with base pressure 2 × 10^{-10} Torr. The Fe and V layers were electrongun-evaporated and deposited on a MgO(001) crystal surface used as substrate. The deposition rate was controlled by an oscillating quartz crystal. The actual system consists of 20 repetitions of the bilayer: 30Å Fe and 9Å V, plus a 25Å thick Au cap layer to protect the superlattice against oxidation. The superlattices were grown at five different substrate temperatures to compare the quality.

The X-ray diffraction mwasurements on the superlattices were performed at the wiggler beamline BW2 in HASYLAB at DESY, Hamburg. The analysis show that the orientation of the Fe/V superlattice on MgO was: MgO(001) ‖ V/Fe(001) and the inplane orientation MgO[100] ‖ Fe/V [110]. This is as expected, since the Fe/V lattice constant a_0 almost equals a_0 (MgO) /$\sqrt{2}$. The orientation relationship predicts, that the Fe/V superlattice reflections is seen along the MgO(11*l*) rod in reciprocal space and the superlattice rodscan is shown in Fig. 1. The rodscan shows the superlattice reflections as satellite peaks around the center peak. The distance between the satellite peaks reflects the superlattice period, in this case 39Å. In Fig 1 one can see several quite narrow peaks showing, that the structure is coherent in three dimensions, i.e. that it is a superlattice. The width of the peaks is inversely proportional to the coherence length of the superlattice, so the width Δl (FWHM) of the peaks is a measure of the quality of the superlattice. In Fig. 2 Δl of the centerpeak is plotted as a function of growth temperature. This indicates, that the optimal growth temperature of this system is around 300°C. In-plane scans show, that generally this superlattice does not lock to the substrate, i.e. it does not get the same inplane lattice constant as MgO. However, one can see in Fig. 1, that there are some 'extra' peaks, and scans along the (11) in-plane direction show, that these peaks comes from a component of the superlattice locked to the substrate. Further analysis is in progress.

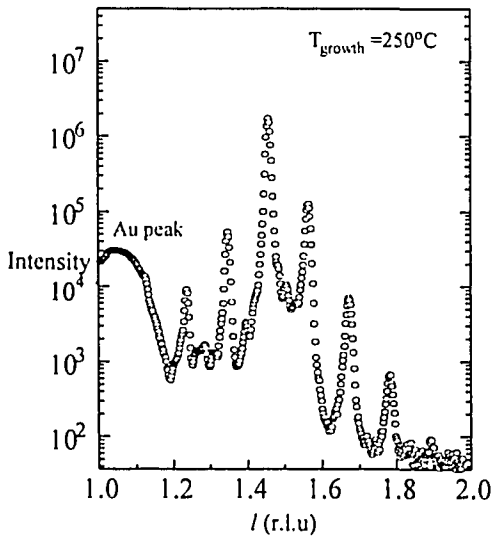

Fig. 1 The superlattice rodscan as described above. 1 r.l.u = 1.488 Å^{-1}
r.l.u = reciprocal lattice units

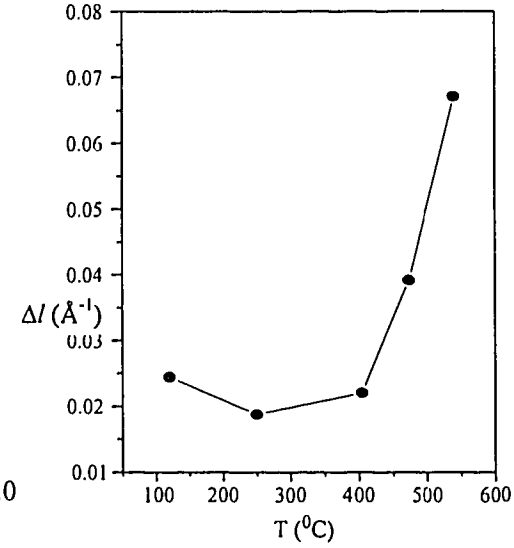

Fig. 2 Δl (FWHM) of the center peak as a function of growth temperature

2.5.9 Surface X-Ray Diffraction Studies of the Li and Na induced Si(111)3x1 Structures

E. Landemark, M. Nielsen, D.-M. Smilgies and R. Feidenhans'l, *Department of Solid State Physics, Riso National Laboratory, Denmark,* L. Lottermoser, L. Seehofer, G. Falkenberg, R. L. Johnson, *II. Institut für Experimentalphysik, Universität Hamburg, Germany*

We have continued our efforts to solve the puzzling 3x1 reconstructions of the Si(111) surface. Similar 3x1 reconstructions are induced by sub monolayer coverages of different adsorbates, such as Li, Na, K, Ag, and maybe also Mg and CaF_2. Despite an extensive amount of studies by different experimental methods and theory presented during the last years, the atomic structure of the Si(111)3x1 surfaces is still controversial.[1]

Our previous X-ray diffraction measurements of the 3x1-Ag and 3x1-Na surfaces included inplane data and rodscans with a restricted range of perpendicular momentum transfer. We found that our data sets were not large enough to unambiguously determine the atomic structure by least-square fitting refinements of different models. The 3x1 structure seems to be quite complex and involve major rearrangements of the substrate atoms, as well as deep relaxations in the subsurface layers, which leads to a large number of parameters to be determined in the fitting procedure. The new detector arm installed on the X-ray diffractometer at the HASYLAB, BW2 beamline, allows us to perform extensive rodscans while still keeping a grazing incidence angle, in order suppress the background intensity. The new set-up turned out to be very useful for our measurements of the Si(111)3x1 Na and Li surfaces, where the scattered intensity in the fractional order rods is relatively weak. A few examples of the measured fractional order rods are shown in Fig.1. Note that a large part of the diffracted intensity comes up as peaks at large l values. We have not been able to reproduce the data by calculating the diffracted intensity from models proposed in the literature. New structural models for the Si(111)3x1 surfaces is in progress.

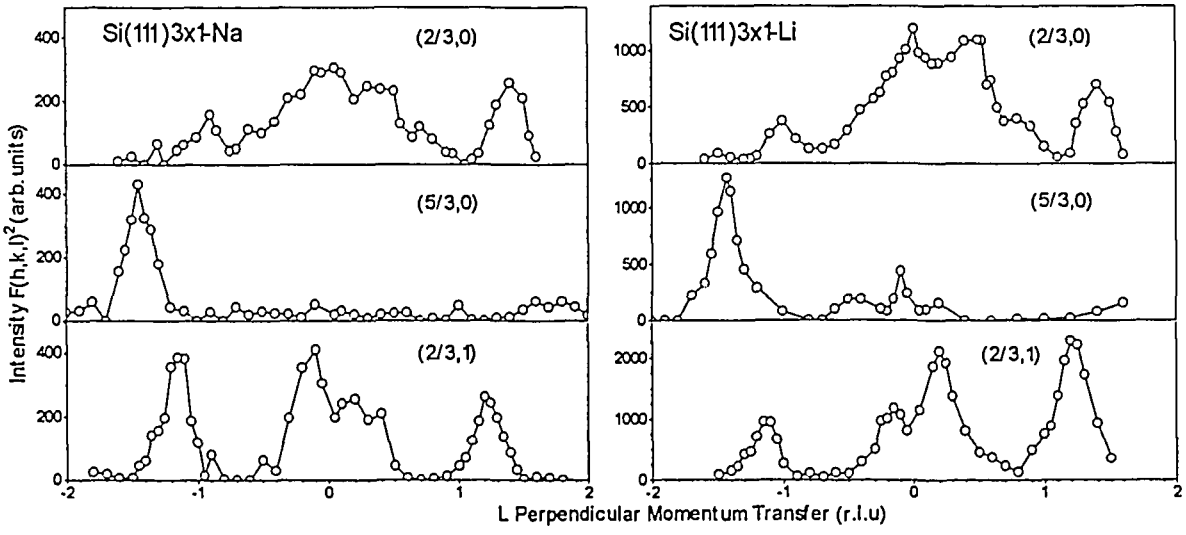

Fig. 1. Fractional order X-ray diffraction rodscans of the 3x1-Na and 3x1-Li surfaces. The X-axis units correspond to an inverse Si(111) bilayer distance (1 r.lu.=2.0 $Å^{-1}$). Each data point is the integrated intensity of an ω-scan.

[1] Steven C. Erwin, Phys. Rev. Lett. 75, 1973 (1995).

2.5.10 Topologic Study of a Ag Monolayer on a Cu(111)

B. Aufray, J.M. Gay, M. Gothelid *CRMC2-CNRS, Marseille, France* Erik Landemark, *Department of Solid State Physics, Risø National Laboratory, Denmark*, G.Falkenberg, *II Institut für Experimental Physik, Universität Hamburg, Germany*

The atomic structure of a Ag monolayer deposited on Cu(111) has been determined from theoretical calculations using an extended tight-binding quenched molecular dynamics simulations.[1] These calculations show that the first layer is strongly corrugated (1Å) and that the perturbation extends up to the first ten surface layers. In order to check experimentally this theoretical simulation we have studied by both Surface X-Ray Diffraction (SXRD) and Scanning Tunneling Microscopy (STM), the structure of one monolayer of Ag deposited on Cu(111).

The experiments were performed in a UHV multichamber, containing an Omicron STM, a Low Energy Electron Diffraction (LEED), a sputtering chamber and a MBE chamber for silver deposition and annealing. One monolayer of Ag was deposited and the sample was annealed at about 100°C for a few minutes. At room temperature the LEED pattern showed the expected superstructure which is a p(9±1x9±1). The samples were then transferred either in a portable UHV baby chamber for X ray measurement or in the STM UHV system.

From the STM images with atomic resolution (see Fig.1) we find that the structure of the Ag monolayer is made of a periodic frame of two kinds of triangles: those of 5 atomic rows width with 3 atoms in the centre and those of 4 atomic rows width with one atom in the centre. The corrugation between atomic rows far from triangles is about 0.05Å while between the centre and the outside of triangles it is about 0.5Å. The periodicity of triangles with 3 atoms in the centre is about 10 times the Cu unit cell while it is 9 times the Cu unit cell for triangles with 1 atom in the center.

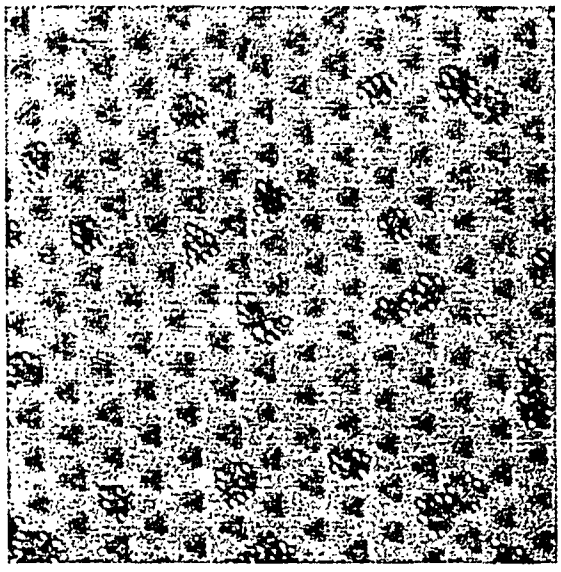

Figure 1. STM Image

By SXRD essentially from both scans along the main symmetry axis and in-plane ω-scans around the superstructure reflections we determined very accurately the periodicity of the surface unit cell. We find that the "average" Ag surface unit cell is (9.43x9.43) times the Cu(111) surface unit cell without any rotation in good agreement with first STM observations.

[1] C. Mottet, G. Tréglia et B. Legrand, Phys. Review B 46 (1992) 16018.

2.5.11 Local Residual Strain Determinations around a Single Inclusion in an Al/W Metal Matrix Composite

H.F. Poulsen, T. Lorentzen, Y.-L. Liu, *Materials Department, Riso National Laboratory, Denmark,* and R. Feidenhans'l, *Department of Solid State Physics, Riso National Laboratory, Denmark*

An X-ray technique for local measurements of the internal residual strain gradients near inclusions in metal matrix composites has been investigated. The technique utilizes medium to high energy monochromatic X-rays from a synchrotron source and a combination of slits on the entry and exit sides of the sample in order to determine the strains from small volumes deep within the composite sample. By varying the sample orientation the various strain components are determined. An analyzer is introduced in order to avoid well-known systematic errors related to direct space geometry and stability of the beam. The experiments were done at beamline BW2, HASYLAB, with perfect Si (1,1,1) crystals and a focused 26 keV beam. The surroundings of single W fiber inclusions in Al matrix pellets of 4.5 mm diameter were investigated. The typical gauge volume was 10x10x170 μm^3 with resulting countrates of order 10000 cps and an accuracy in the strain measurements of $\Delta d/d \leq 5x10^{-5}$. This should be compared with typical residual strains of order 10^{-4} - 10^{-3}.
Samples were investigated with Al grain sizes ranging from 1 mm to 50 μm (grains larger than and smaller than the W fiber dimensions). In all cases a complete debounding was found to take place at the interface, likely due to some minor amount of chemical reaction. Intra-grain strain fluctuations of the order of $\Delta d/d = 2x10^{-4}$ were observed to build up close to grain boundaries. In the 'polycrystalline cases', that is for small grain sizes, we find that sampling data from 15 grains at the same distance to the fiber is sufficient to allow for averaging out the inter-grain fluctuations. Furthermore, effects from the sample preparation (cutting by a diamond saw) were clearly evident up to 400 μm from the surface, emphasizing the need for use of a bulk technique.

The present technique provides a considerable better accuracy on the strain than previous attempts with white-beam methods.[1] It should also be noted, that replacing the monochromator and analyzer crystals with imperfect crystals could increase intensities by up to two orders of magnitudes, leading to spatial resolutions close to 1 μm.

[1] T.A. Kuntz, H.N.G. Wadley, and D.R. Black. Metall. Trans. **A 24** , 1117-1124 (1993).

2.5.12 Structure of the Si(111)(2 $\sqrt{3}$ x2 $\sqrt{3}$)R30°-Sn Reconstruction

A. H. Levermann, P. B. Howes, K. A. Edwards, J. E. Macdonald, *Department of Physics and Astronomy, Cardiff University, UK*, C. L. Nicklin, *Department of Physics and Astronomy, University of Leicester, UK*, R. Feidenhans'l, *Riso National Laboratory, Denmark*, R. L. Johnson, L. Seehofer, G. Falkenberg, L. Lottermoser, *Institute für Experimentalphysik, Universität Hamburg, Germany*

The Sn/Si(111) interface is a prototypical, non reactive metal--semiconductor interface and has been studied by a variety of techniques. It is particularly interesting because a number of different Sn/Si(111) surface reconstructions exist with different Schottky barrier heights (SBH). One of these reconstructions, the (2 $\sqrt{3}$ x 2 $\sqrt{3}$) is poorly understood. Törnevik *et al.*[1] a structure model based on their STM study, containing a two-layer structure with 14 Sn atoms. Other groups have proposed slight modifications.

We performed surface x-ray diffraction measurements from the Si(111)(2 $\sqrt{3}$ x 2 $\sqrt{3}$)R30°-Sn reconstruction at beamline BW2, HASYLAB. In total, 338 in-plane reflections were measured of which 181 were inequivalent. Peaks in the Patterson function calculated from these data correspond to interatomic vectors (Figure 1 left). The Patterson map calculated for the Törnevik model is shown for comparision in figure 1 right. It is clear that the two Patterson maps contain few peaks in common and therefore this model is inconsistent with our data.

Certain features of the correct structural model can be deduced from our data set. The (5/6, 5/6) peak was the strongest and this is consistent with diffraction from (220) planes of α-Sn. The experimental Patterson function is dominated by a grid of peaks at 1/5 order positions. Reasonable agreement was found between our data and models in which a number of atoms (10 to 19) were distributed on a such a grid allowing only a few atoms to move away from 1/5 order positions. Several variants of the atomic arrangement give reasonable agreement with the experimental data and further analysis is underway.

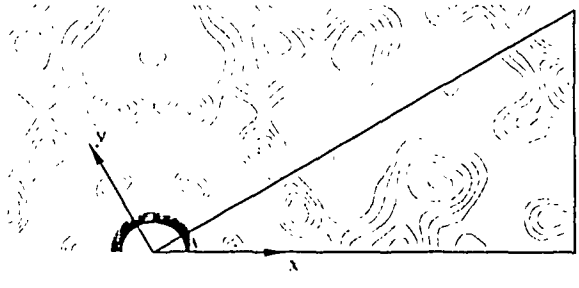

Figure 1. Left: measured Patterson function.

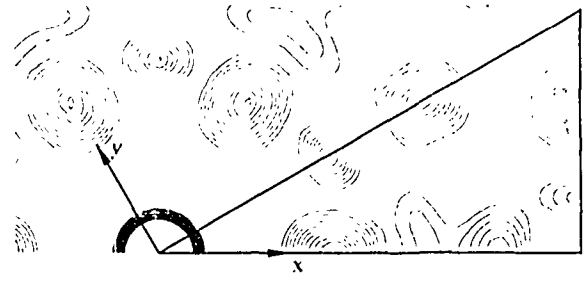

Right: Patterson calculated from Törnevik model. The triangle is the irreducible unit.

[1] C. Törnevik, M. Hammar, N. G. Nilsson and S. A. Flodström, Phys. Rev. **B44**, 13144 (1991).

2.5.13 Large Defect Structure of Epitaxial Cr_2O_3 Overlayers on Cr(110) Films

A. Stierle, T. Koll, and H. Zabel, *Institut für Experimentalphysik/Festkörperphysik, Ruhr-Universität Bochum, Germany*, M. Nielsen, R. Feidenhans'l, *Department of Solid State Physics, Riso National Laboratory, Denmark*

We have studied the defect structure of (0001) oriented Cr_2O_3 layers,which were grown by thermal oxidation of Cr (110) films prepared by molecular beam epitaxy (MBE).[1] In order to develop microscopic models of oxidation reactions, it is essential to know the defect structure of the oxide, because defects determine the oxidation kinetics. In addition, thin ordered oxide layers are used as model catalysts and defects may have a decisive impact on the cataytic reactions.

Orthorhombic α-Cr_2O_3 exhibits a layered structure in (0001) direction. Hexagonal closed packed O^{2-} layers and 2/3 filled Cr^{3+} layers alternate, where every third atom row in the (11$\bar{2}$0) direction is missing. The O^{2-} layers have an ABAB... stacking sequence known from hcp crystals, the Cr^{3+} layers are abc stacked, according to the three inequivalent positions where the atom row in (11$\bar{2}$0) direction can be missing. This stacking is formally identical to the ABC... stacking of fcc crystals in the (111) direction. To reproduce the structure in the (0001) direction, 12 layers are needed forming the stacking sequence AaBbAcBaAbBc.

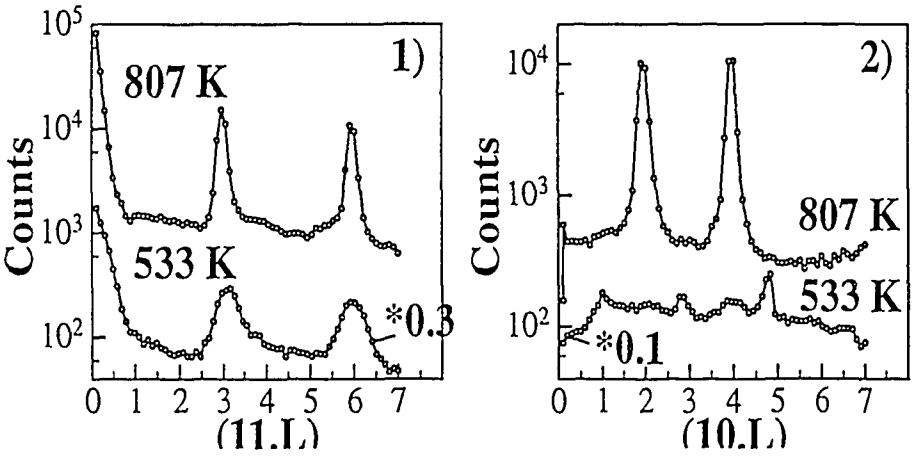

Figure 1. Left: Scan along the (11$\bar{2}$L) rod. Right: Scan along the (10$\bar{1}$L) rod.

We performed scans along the oxide reciprocal lattice rods perpendicular to the surface at BW2 (HASYLAB). In Fig. 1 a scan along the (11$\bar{2}$L) rod is shown, which is sensitive to the stacking of the O^{2-} layers. For both high and low temperatures the reflections at L=3 and L=6 appear, indicative for the ABAB stacking of the O^{2-} layers. The peak broadening for low temperatures is manly due to the finite thickness of the oxide layer of 3.2 nm; in comparison the high temperature sample has a thickness of 11.8 nm. The rod scan along the (10$\bar{1}$L) direction, which is sensitive to the stacking of the Cr^{3+} layers, is also shown in Fig. 1. At higher temperatures we find reflections at L=2 and L=4, compatible with abc- and cba- stacked twins. For low temperatures only broad features are observed which is a direct evidence for stacking faults of Cr^{3+} layers in (0001) direction. The grain boundaries between differently stacked domains can serve as ion diffusion paths during the oxidation reaction. Future rod scans on Cr_2O_3 layers prepared at different temperatures are planned.

[1] A. Stierle, P. Bödeker, and H. Zabel, Surf. Sci 9, 327 (1995).

2.5.14 A new Bi/Cu Alloy on Cu(110) Determined by X-ray Diffraction

L. Lottermoser, T. Buslaps, and R.L. Johnson, *II. Institut für Experimentalphysik, Universität Hamburg, Germany*, R. Feidenhans'l, M. Nielsen, E. Landemark, and D. M. Smilgies, *Department of Solid State Physics, Riso National Laboratory, Denmark*, H.L. Meyerheim and W. Moritz, *Institut für Kristallographie und Mineralogie, Universität München, Theresienstrasse 41, Germany*

The growth of submonolayer Bi films on Cu(110) has been investigated by surface X-ray diffraction. In the case of the p(4x1)reconstruction formed at a coverage of 0.75 monolayer both the in-plane and out-of plane data are compatible with a model in which every fourth Cu row in the [001]- direction of the top-most layer are substituted by Bi atoms as shown in Fig. 1. The direction of the atomic displacement of the Cu atoms are shown schematically with arrows.

The extensive structural data set, including in-plane scans as well as several fractional and crystal truncation rods, were measured at the beamline BW2 at Hasylab. As representative examples the structure factor intensities along the $(\frac{1}{4}0l)$ and $(10l)$ rod are shown in Fig. 2. The solid curves in Fig. 2 are obtained by the final structural model. We obtained χ^2=1.1 for a least-square analysis if both the fractional in-plane and out-of plane intensities are refined. The good agreement between the model and the crystal truncation rods indicate that nearly 100 % of the surface is reconstructed. The formation of a ordered surface alloy in spite of the immiscibility of bulk Cu and Bi is in good agreement with recent studies on adsorption of Pb on low index copper surfaces.[1]

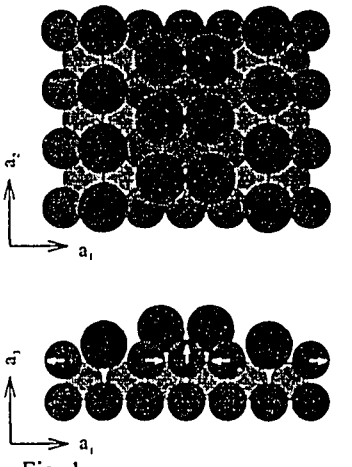

Fig. 1
The Cu(110)p(4x1)-Bi structure

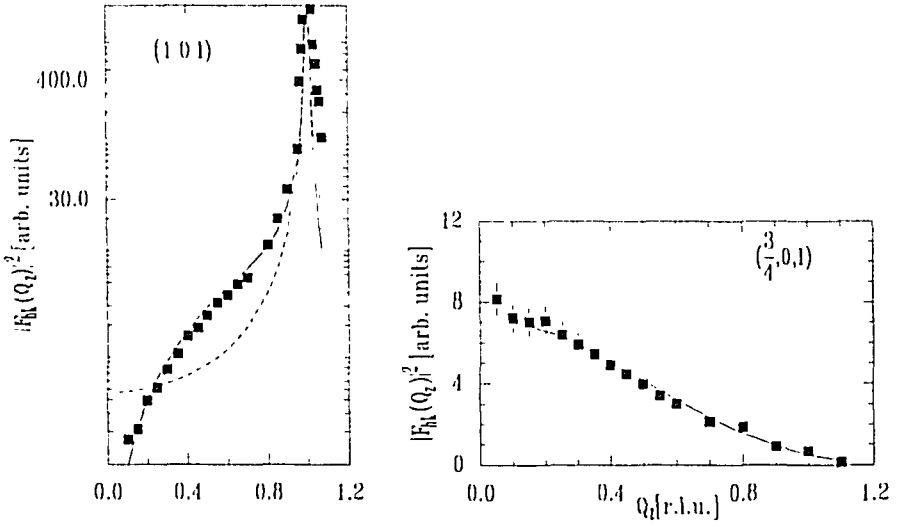

Fig. 2
Rods for (h,k)= $(\frac{1}{4}0)$ and (1,0). The dash curvesponds to an ideally terminated crystal and the solid lines obtained for the model.

[1] C. Nagl, E. Platzgummer, O. Haller, M.Schmid, and P.Varga, Surf. Sci. **831**, 331-333 (1995).

2.5.15 Submonolayer Growth of Bismuth on Cu(111) Determined by Surface X-ray Diffraction

L. Lottermoser and R.L. Johnson, *II. Institut für Experimentalphysik, Universität Hamburg, Germany*, R. Feidenhans'l, M. Nielsen, E. Landemark, and D. M. Smilgies, *Department of Solid State Physics, Riso National Laboratory, Denmark*

Grazing incidence X-ray diffraction has been used to analyze the adlayer structures of Bi on Cu(111) for submonolayer coverages at room temperature. The experiments were performed at the Wiggler beamline BW2 at Hasylab in Hamburg. For bismuth coverages around 0.3 ML deposited on a clean Cu(111) surface an ordered structure with $\sqrt{3} \times \sqrt{3}$ periodicities was observed. At coverages around 0.5 ML a more complicated incommensurate phase exists. Scans along high symmetry directions in reciprocal space were performed in order to characterize the incommensurability. For the structural analysis of the Cu(111) $\sqrt{3} \times \sqrt{3}$ -Bi surface we have taken subsequently an extensive in-plane and out-of plane data set. 90 in-plane reflection, 6 fractional-order rods and five crystal truncation rods were measured. As representative examples the measured intensities along the $(\frac{2}{3}\frac{5}{3}l)$ and $(20l)$ rod are shown in Fig. 1.

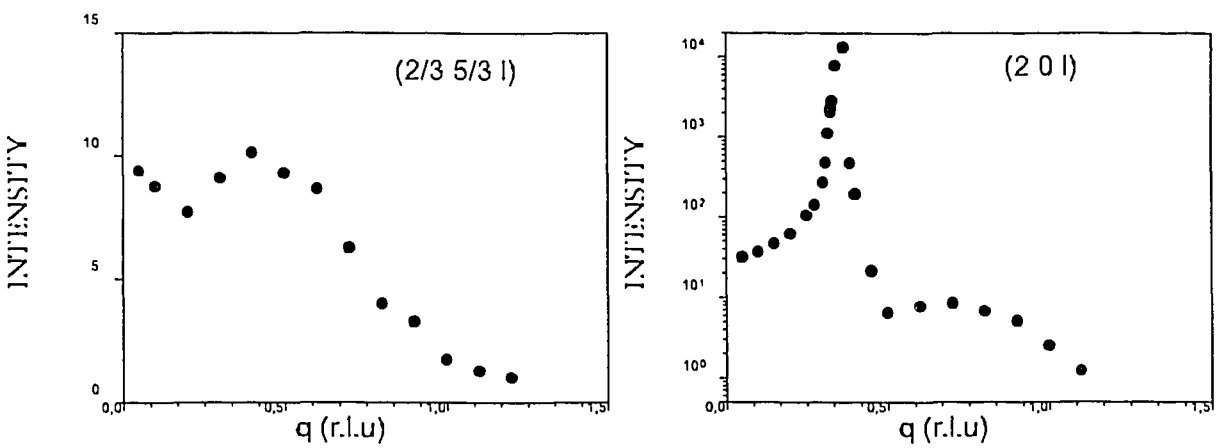

Fig. 1. The structure factor intensities along the $(\frac{2}{3}\frac{5}{3}l)$ and $(20l)$ rod for the Cu(111 $\sqrt{3} \times \sqrt{3}$ -Bi surface.

The intensity variation, especially the feature in the $(\frac{2}{3}\frac{5}{3}l)$rod, indicates that deeper layers are involved in the reconstructions. Similar to our work on Bi on Cu(110) the features in the rods could signaling the formation of a Bi/Cu surface alloy. A new formation of a Pb/Cu alloy on a close packed Cu(111) in the submonolayer coverage range was reported recently by Varga[1] although Pb and Cu are immiscible in bulk. A more detailed data analysis is in progress.

[1] C. Nagl, O. Haller,E. Platzgummer,M. Schmid and P. Varga, Surf. Sci. **321**, 237 (1994).

2.5.16 X-ray Diffraction Analysis of the (1x1)-phase of Bi/GaSb(110)

L. Lottermoser, T. van Gemmeren, and R.L. Johnson, *II. Institut für Experimentalphysik, Universität Hamburg*, R. Feidenhans'l, M. Nielsen, E. Landemark and D. M. Smilgies, *Department of Solid State Physics, Riso National Laboratory, Denmark*

Ordered nonreactive systems provide the best starting point for studying the surface structural and electronic properties of metal-semiconductor interfaces. Skeath *et al.*[1] observed that a monolayer (ML) of Sb deposited on GaAs(110) at room temperature forms zigzag chains of Sb atoms bonded alternately to Ga and As atoms. Bi deposited on GaSb(110) at room temperature also shows an ordered (1x1) reconstruction consisting of Bi zigzag chains.[2]
In order to obtain structural information about the GaSb(110)1x1-Bi structure we have performed scans at beamline BW2, Hasylab, along the specular reflectivity and six crystal truncation rods. As a representative example the structure factor intensities along the (00*l*) is shown in Fig. 1. Starting points for the structure determination were the two favored structures discuss in the literature, -namely the epitaxy continued-layer structure (ECLS) and the epitaxy on-top structure (EOTS). Along the (00*l*)- rod the momentum transfer is only in the direction normal to the surface and hence independent of the in-plane atomic arrangement. Assigning the Bi atoms to normal structural positions as expected from covalent radii arguments yielded the solid line for the ECLS model and the dash line for the EOTS model in Fig. 1.

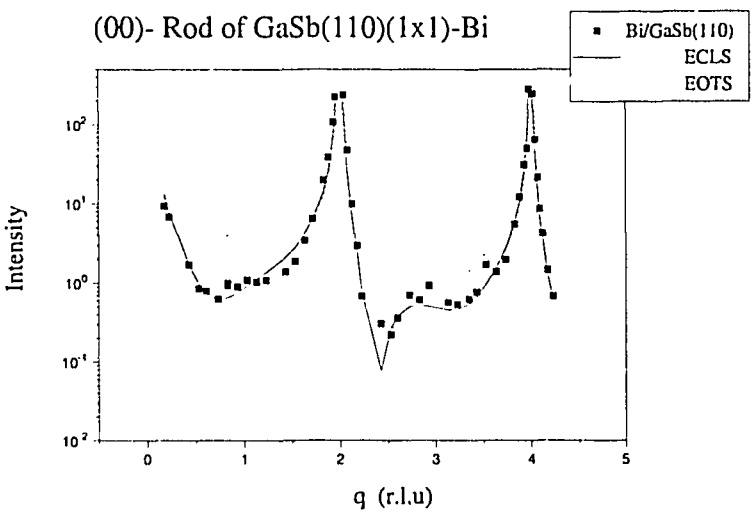

Fig1 The specular reflectivity for Bi on the GaSb(110) surface.

The analysis of the integer-order truncation rods were consistent. Along these rods momentum transfer is also in laterally directions to the surface and hence sensitive to the in-plane arrangement of the Bi atoms. The in-plane coordinates of the Bi atoms are found in good agreement with a shifted ECLS registry and also exclude an epitaxial on-top structural model. All measured rods can only be fitted in the same accuracy by the shifted ECLS model, which is compatible with a previous determination of the Bi registry on GaAs(110).[3] A more detailed description of the structural model is in preparation.

[1] P. Skeath, I. Lindau, C. Y. Su, and W. E. Spicer, J. Vac.Sci. Technol. **19**, 556 (1981).
[2] T. van Gemmeren and R.L. Johnson, Surf. Sci. **331-333**, 613 (1995)
[3] A. Ruocco, N. Jedrecy, R. Pinchaux, M. Sauvage-Simkin, A. Waldhauer, M. Betti, and C. Mariani, Phys. Rev. B50, 8004 (1994).

2.5.17 X-Ray Diffraction and STM Studies of the Ge(103) Surface

G. Falkenberg, R.L. Johnson, L. Lottermoser, L. Seehofer, *II. Institut für Experimentalphysik, Universität Hamburg, Germany* , M. Nielsen, and R.K. Feidenhans'l, *Riso National Laboratory, Denmark*

The Ge(100) surface is unstable under deposition of less than one monolayer of In atoms. The surface breaks up into regular facets and eventually the entire surface consists of arrays of{103} facets. This facetted surface resembles the {105} hut-cluster observed in epitaxial growth of Ge on Si(100), where all surfaces are {105} facets. Two parameters dominantly control the stability of these huts, namely the strain energy associated with the misfit between hut and substrate and the surface energy of the facets.

To investigate the surface energy of the {103} facets, we have prepared a Ge sample, which is cut so that the top surface is parallel with a (103) surface, and studied this with STM and synchrotron x-ray diffraction, both before and after deposition of In atoms. As a first result we found that the pure (103) Ge surface is stable and has a well ordered 4x1 reconstruction. A full x-ray data set including rod scans has been measured for this and is under analysis. The (103) surface is stable against faceting at least up to 750°C, and at 430°C there is a reversible phase transition between the 4x1 and a 1x1 structure.

The unit cell of the reconstructed 4x1 structure may in cubic coodinates of the bulk crystal be expressed as (3 0 $\bar{1}$) and (0 4 0). The STM picture below shows the well ordered 4x1 structure. The (3 0 $\bar{1}$) direction runs from upper left to lower right in the figure. There is complete order within each terrace, which is about 200Å in the (3 0 $\bar{1}$) direction and larger along (0 4 0).

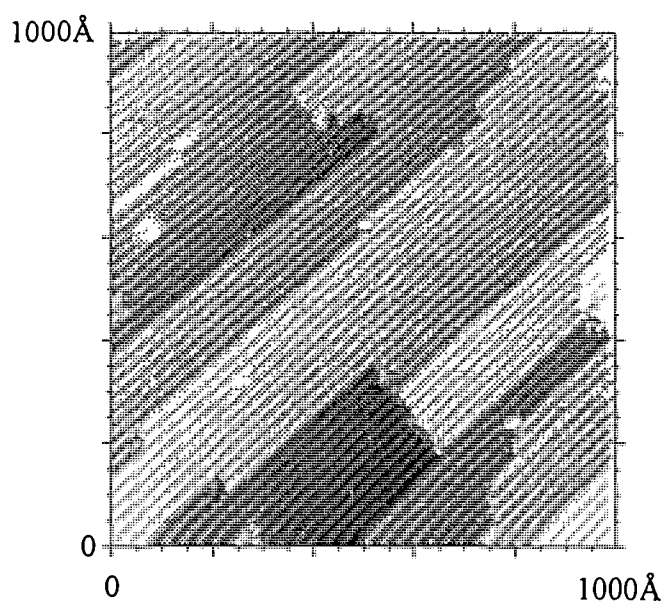

Fig. 1. STM picture of the 4x1 reconstructed surface of the Ge(103) crystal. The sample bias voltage was 2.2 V and the tunnelling current 0.5 nA.

2.5.18 Faceting of the Ge(100) Surface, studied by STM and X-ray Diffraction

M. Nielsen, and R.K. Feidenhans'l, *Risø National Laboratory, Denmark,*
G. Falkenberg, R.L. Johnson, L. Lottermoser, L. Seehofer, *II. Institut für Experimentalphysik, Universität Hamburg, Germany*

Small nanoscale clusters are spontaneously created on Ge(100) surfaces when about a monolayer of In atoms is deposited at a temperature between 350°C and 500°C. A detailed x-ray study has been carried out at the BW2 beamline diffractometer in HASYLAB at DESY in Hamburg, in order to characterize the structures and to study the mechanism behind their formation. The aspect ratio and the size of the clusters vary with the preparation, but all facets are {103} surfaces. The samples used in the present measurements were annealed after In deposition at 350°C for 5 min, which produced surfaces completely covered with a superstructure of huts all near 11Å high and 66Å wide and on average 1000Å long. The same samples were studied both with STM and x-ray diffraction techniques.
It is concluded from the results that the {103} facets are energetically stabilized by In atoms which are chemisorbed at the surfaces, saturating all the dangling bonds of the Ge(103) facets. This is illustrated in the figure below, where the large white circles show the positions of the In atoms. It is also found that the internal structure of the hut clusters is very weakly strained relative to the bulk Ge crystal, and no interface was observed. A surprising feature of the structure is the uniformity of the clusters and the high degree of order in the superstructure. This can hardly be explained by the surface energy term alone, but further analysis of the existing data may indicate the origin.

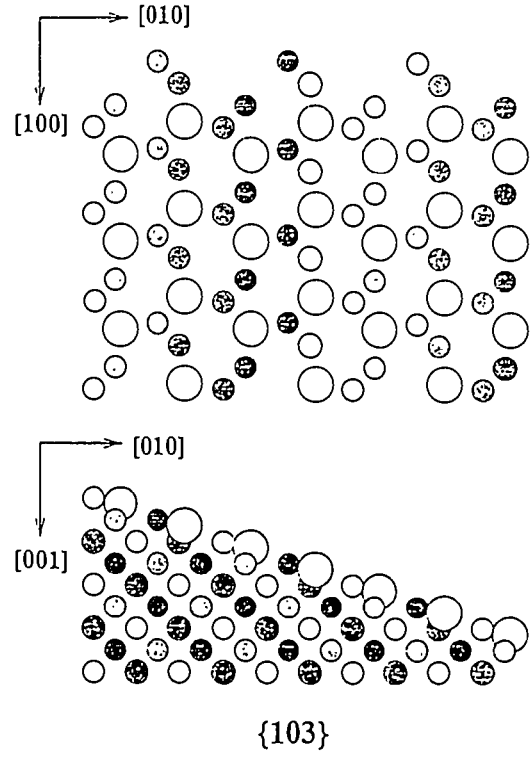

Fig.1 Model drawing of the {103} facets illustrating how the In atoms, the large white circles, are chemisorbed with one row of atoms on each terrace and each In atom saturating three Ge dangling bond.

2.5.19 Hut Clusters of Ge on Si(100)

M. Nielsen, and R.K. Feidenhans'l, *Riso National Laboratory, DK-4000 Roskilde, Denmark*, G. Falkenberg, and R.L. Johnson, *II. Institut für Experimentalphysik, Universität Hamburg, Germany*, A.J. Steinfort, P.M.L.O. Scholte, A.H.H.F. Ettema, and F. Tuinstra, *Physical Crystallography group, Dept. of Applied Physics, Delft, The Netherlands*

Epitaxial growth of Ge on Si(100), at temperatures below 550°C, proceeds from layer by layer growth for the first two layers to growth of coherent structures, the so-called hut clusters, for coverages up to about 9 layers, and thereafter 3-dimensional crystallization takes over.[1] The hut clusters have the shape of elongated prisms with canted ends, and all top surfaces are {105} facets. We have carried out a series of STM and synchrotron x-ray measurements in order to determine in particular the internal strain in the huts. The strain relaxation is the important property for understanding the growth of the huts.

The samples studied with x-ray diffraction have about 70 percent of the Si(100) surface covered with almost monodispersed huts, all about 13Å high, 140Å wide and a few hundreds Å long. All huts are aligned along the (100) direction. The x-ray scattering intensity is concentrated around the "rods" from the {105} facets and from the (100) interface between huts and Si substrate, although the individual {105} facets are quite small. The interface is free of dislocations and therefore the first layer of Ge atoms at the interphase is considerably compressed relative to the packing of Ge atoms in bulk material. This compression is gradually relaxed towards the top of the huts. X-ray diffraction rods extends from the bulk Bragg points at angles 11.3 and 0 degrees to the [001] direction, and accurate data were measured out to the (501) Bragg point, where the scattering profiles are very sensitive to the strain field. The data have been interpreted on the basis of a computer model of the huts. Fig. 1 illustrates the scattering profiles.

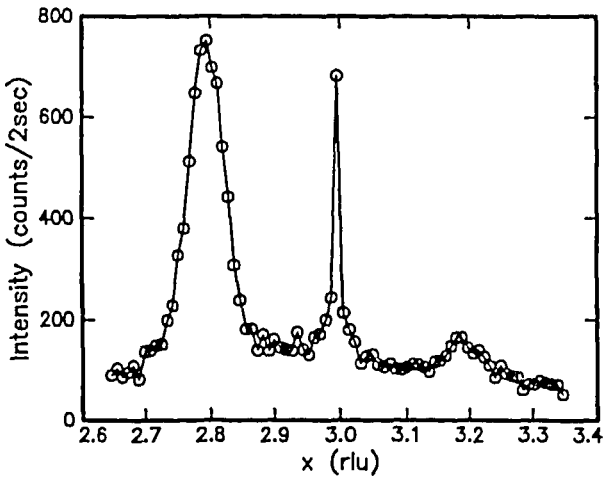

Fig. 1. X-ray scattering profile from a scan in x-direction through the (3,1,z) point at z=0.027. The "rods" originate from the (311) point. The strong asymmetry is a measure of the strain in the huts.

[1] Ref.1 Y.-W.Mo, D.E.Savage, B.D.Swartzentruber, and M.G.Lagally, Phys.Rev.Lett.65,1020 (1990)

2.5.20 Diffraction Studies of the Weakly Incommensurate Phases in the Systems Pb/Ge(111) and Pb/Si(111)

R.L. Johnson, G. Falkenberg, L. Lottermoser, L. Seehofer, *II. Institut für Experimentalphysik, Universität Hamburg, Germany*, R.K. Feidenhans'l, and M. Nielsen, *Riso National Laboratory, Denmark*

Monolayers of Pb on Ge(111) and on Si(111) surfaces form closely packed two-dimensional hexagonal lattices with either the commensurate $\sqrt{3} \times \sqrt{3}$, R30 structure or weakly incommensurate variants of this. Relative to the bulk lattice of Pb, the commensurate monolayer requires 1 percent compression on Ge and 5 percent on Si. With increasing coverage the Pb on Ge(111) layer undergoes a phase transition from commensurate to an incommensurate slightly denser structure with positive misfit parameter, whereas Pb on Si never make a completely commensurate phase, but the maximum density corresponds to a negative misfit of 2.6 percent. The two weakly incommensurate structures have domain wall lattices with respectively heavy and light walls which accomodate the misfit.

The domain wall lattices have been studied with both STM and x-ray diffraction. The x-ray measurements were performed at the *in situ* diffractometer at beamline ID-3 in ESRF, Grenoble. Here it was possible to follow by diffraction the development of monolayer structures in real time when switching on and off the Pb deposition. The light walls of Pb/Si(111) form an uniaxial striped lattice, whereas the heavy walls of Pb/Ge(111) order in a hexagonal superstructure. Both wall lattices, and especially the striped phase show spatial fluctuations of the walls away from ideal order, and by x-ray scattering this has been characterized by recording mesh scans in regions of reciprocal space around the Bragg points corresponding to the ordered wall structure. Examples of this is shown in the figure below. The commensurate positions are indicated by hexagons; no scattering intensity is measured there.

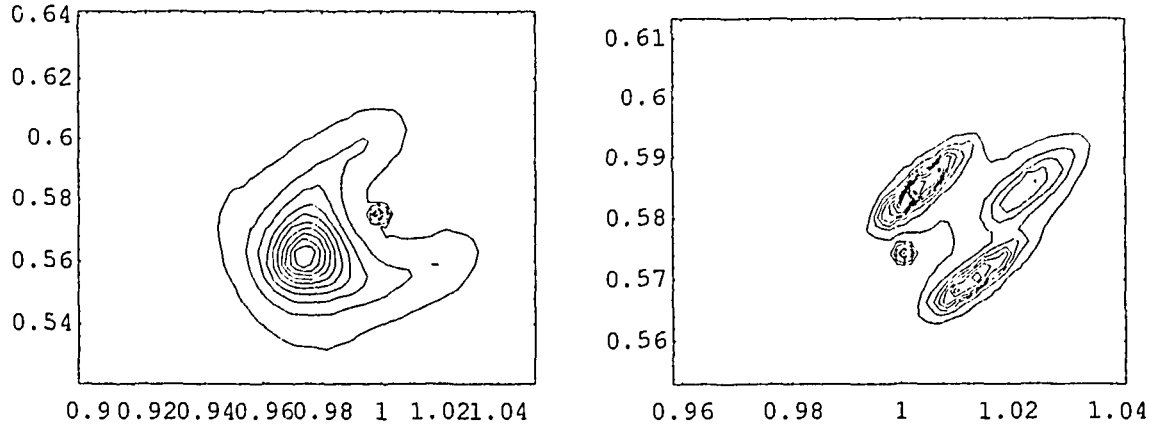

Fig. 1. Contour plots of the x-Ray scattering intensity from weakly incommensurate Pb monolayers on i(111), left panel, and Ge(111), right panel. Commensurate reciprocal lattice points are indicated by small hexagons. The units of the axes are those of the Si and Ge 1x1 surface structures.

2.6 Langmuir Films

2.6.1 Monolayers of Enantiomeric and Racemic 4-Hexadecyloxy-butane-1,2-diols

R. Rietz, *Inst. of Physical Chemistry, University of Halle, Germany,* G. Brezesinski, H. Möhwald, *Max-Planck-Institute for Colloids and Interfaces, Berlin, Germany*, F. Bringezu, *Inst. of Pharmaceutical Chemistry, University of Halle, Germany,* B. Struth, *Inst. of Physical Chemistry, University of Mainz, Germany*, W.G. Bouwman, and K. Kjær, *Department of Solid State Physics, Risø National Laboratory, Denmark*

Derivatives of optically active (chiral) 1,2-diols are currently of interest as potential ferroelectric amphiphiles which can form thermotropic and lyotropic mesophases in the bulk and stable monolayers at the air/water interface. Moreover, monolayers have been shown to be useful for investigating chiral recognition. In an ongoing effort to study the influence of chemical changes on chiral recognition near the chiral centre in the hydrophilic head group, we have characterized the phase behaviour of the (S) 4-hexadecyloxy-butane-1,2-diol ($C_{16}H_{33}$-O-CH_2-CH_2-C*HOH-CH_2OH, S-HOBD), the racemic HOBD ($x_R = x_S = 0.5$) and a mixture with $x_S = 0.75$ using pressure-area-isotherms, fluorescence microscopy as well as synchrotron grazing incidence X-ray diffraction (GIXD) experiments at the liquid-surface diffractometer on the undulator beamline BW1 at HASYLAB, DESY, Hamburg, Germany.

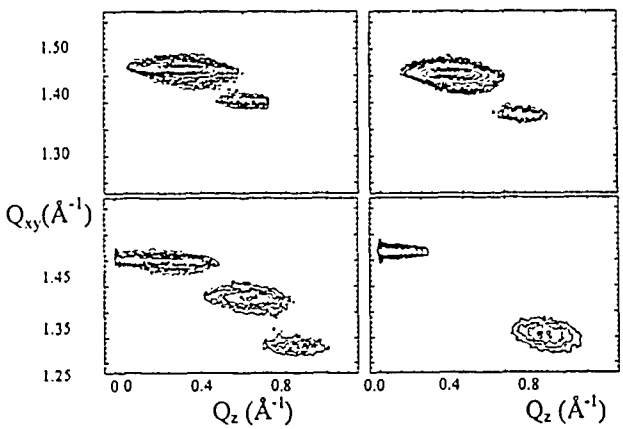

Figure 1 shows contour plots of the corrected X-ray intensities as function of in-plane scattering vector component Q_{xy} and of out-of-plane scattering vector component Q_z at different surface pressures and 20 °C. At all pressures investigated two diffraction peaks only were observed for the racemate indicating a centred-rectangular unit cell. In the low pressure phase (below 15 mN/m) the molecules are tilted in a symmetry direction towards nearest neighbours (NN) such that the single peak n (non-degenerate) is at the horizon ($Q_z^n = 0$ Å^{-1}) and the doublet peak d (twofold degenerate) is above the horizon ($Q_z^d > 0$ Å^{-1}), while in the high pressure phase the tilt is in the alternative symmetry direction - towards next-nearest neighbours (NNN): Both peaks are above the horizon with $Q_z^n = 2 * Q_z^d$. The tilt angle decreases with increasing pressure. At lower surface pressures both the pure enantiomer and the mixture with $x_S = 0.75$ exhibit three diffraction peaks, indicating an oblique structure with only translational symmetry relating the chiral molecules. Above 22 mN/m two peaks merge together, to give the same intensity distribution as observed for the racemate. At the highest pressure the molecules are still strongly tilted (21 °) and the cross section amouts to 19.9 Å^2 indicating a rotator phase. While the NN-NNN transition (jump in tilt direction) of the racemate occurs at a well defined lateral pressure π_S, the oblique-NNN transition of both the pure enantiomer and of the mixture ($x_S = 0.75$) is connected with a continuous change of the tilt direction from a non-symmetry direction to NNN between π_C and π_S. The rectangular NNN-phase of the enantiomer occurs at higher lateral pressures than does that of the racemate.

2.6.2 Two-Dimensional Crystalline Packing Arrangement of Zwitterionic Optically Pure and Racemic Straight Chain α-Amino Acids on a Water Surface

I. Weissbuch, M. Lahav, L. Leiserowitz, *Department of Materials & Interfaces, The Weizmann Institute of Science*, K. Kjær, *Department of Solid State Physics, Riso National Laboratory*, J. Als-Nielsen, *Niels Bohr Institute, H.C. Ørsted Laboratory, Copenhagen*

A systematic study of the two-dimensional crystalline packing arrangements (on water and on aqueous glycine ($CH_2(NH_3^+)CO_2^-$) solution) of a series of α-amino acid monolayers, $C_nH_{2n+1}CH(NH_3^+)CO_2^-$, n=10,12,16, (both optically pure and racemic mixtures) as determined by grazing incidence X-ray diffraction (GIXD) using synchrotron radiation, shows that the racemic amphiphiles with straight chains aggregate into racemic crystalline domains. From the GIXD patterns we derived for the racemic 2-D domains a rectangular cell of dimensions a=4.9Å, b=9.7Å (molecular area 23.3Å^2) and for the optically pure counterparts an oblique cell of dimensions a=4.9Å, b=5.2Å γ=111.6°. The formation of racemic crystalline domains is in contrast with the behavior of racemic α-amino acids bearing an *amide* functional group, $C_nH_{2n+1}CONH(CH_2)_4CH(NH_3^+)CO_2^-$ n=11,17,21. These spontaneously separate into enantiomorphous crystalline domains, *cf.* contribution 2.6.3.

Comparison of the measured Bragg rod profiles with calculations using atomic coordinate models show that in the optically pure domains the molecules (tilted by 37° from the surface normal) are related by translation symmetry whereas in the racemic domains the two molecules in the cell are related by glide parallel to the b axis. The latter packing arrangement and the hydrogen-bonding pattern are very similar to the layer structure in 3-D crystals of racemic α-aminobutyric acid and norleucine, $C_nH_{2n+1}CH(NH_3^+)CO_2^-$ n=2,4.

Spreading the monolayers on saturated aqueous solutions of glycine does not change the monolayer structure according to the GIXD pattern. It does make the system less susceptible to beam damage and high order diffraction peaks can be measured even for the compound $C_{10}H_{21}CH(NH_3^+)CO_2^-$ which on water gave a single very weak Bragg peak.

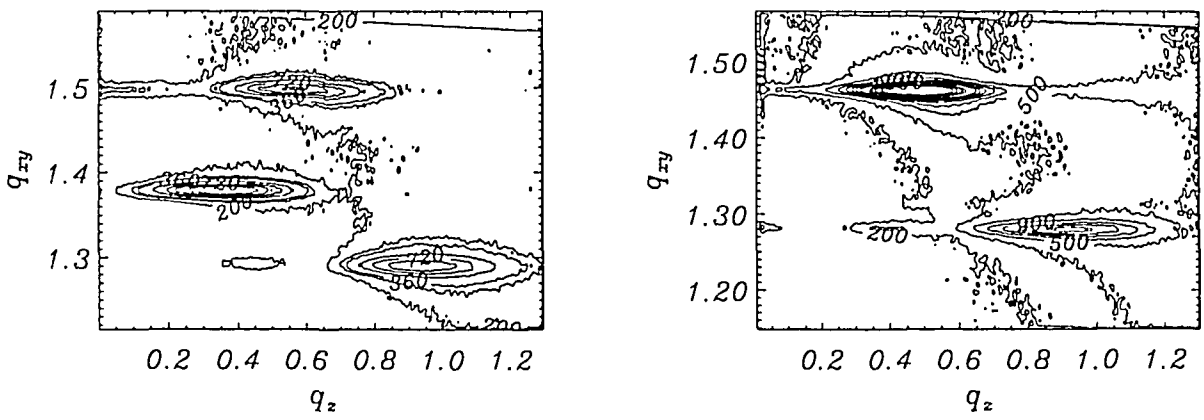

Fig. 1. Typical GIXD patterns from the optically pure (left) and racemic (right) monolayer spread on glycine solution.

2.6.3 The Effect of an Amide Functional Group on the Spontaneous Segregation of Racemic α-Amino Acids into Chiral Two-Dimensional Crystalline Domains on the Water Surface

I. Weissbuch, M. Berfeld, M. Lahav, L. Leiserowitz, *Department of Materials & Interfaces, The Weizmann Institute of Science, Israel*, W.G. Bouwman, K. Kjær, *Department of Solid State Physics, Risø National Laboratory, Denmark*. J. Als-Nielsen, *Niels Bohr Institute, H.C. Ørsted Laboratory, Copenhagen, Denmark*

The two-dimensional crystalline packing arrangements on water surfaces of a series of racemic α-amino acid monolayers, $C_nH_{2n+1}CONH(CH_2)_4CH(NH_3^+)CO_2^-$, 'C_n-lysine', n=11,17,21, as determined by grazing incidence X-ray diffraction (GIXD) using synchrotron radiation, are consistent with the separation of the molecules into enantiomorphous domains. Based on the analysis of the GIXD pattern, we demonstrate that the $-HC(NH_3^+)CO_2^-$ head groups of the monolayers of C_n-lys (n=11,17,21), both optically pure and racemic, are related by translational symmetry and interlinked by a network of hydrogen bonds. This arrangement is similar to the almost isostructural layer structures in 3-D crystals of α-glycine ($CH_2(NH_3^+)CO_2^-$) or of the water-soluble hydrophobic α-amino acids leucine ($(CH_3)_2CHCH_2CH(NH_3^+)CO_2^-$) and valine ($(CH_3)_2CHCH(NH_3^+)CO_2^-$) The GIXD results are supported by the efficiently induced oriented nucleation of α-glycine crystals under these monolayers.
The C_{29}-lys monolayers, both optically pure and racemic, are very poor nucleators of α-glycine, consistent with the large mismatch between the packing arrangements of the monolayer head groups and that of the α-glycine layer, in agreement with the analysis of the GIXD pattern.

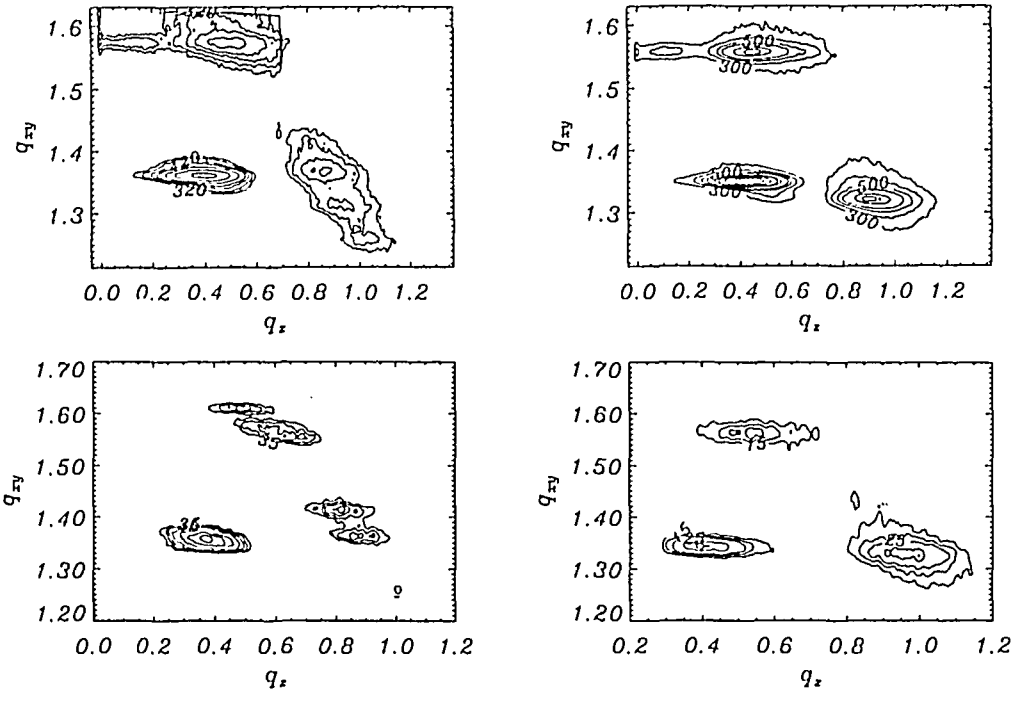

Fig. 1. Typical GIXD patterns from the optically pure (*left*) and racemic (*right*) monolayer spread on water surface for C_{17}-lys (*top*) and C_{21}-lys (*bottom*).

2.6.4 Chiral Discrimination in a Monolayer of a Triple-Chain Phosphatidylcholine

F. Bringezu, *Institute of Pharmaceutical Chemistry, University of Halle, Germany,* G. Brezesinski, H. Möhwald, *Max-Planck-Institute for Colloids and Interfaces, Berlin, Germany,* B. Struth, *Institut of Physical Chemistry, University of Mainz, Germany,* W.G. Bouwman, and K. Kjær, *Department of Solid State Physics, Riso National Laboratory, Denmark,* D. Bahr, *Hasylab at DESY, Hamburg, Germany*

Chiral interactions are of interest in physics and biology. Here we are predominantly interested in the fact that slight chemical changes at the hydrophilic/hydrophobic interface (in the chirality of the glycerol backbone) can have a profound influence on tail ordering in phospholipid monolayers. To further elucidate this question we have studied the enantiomer (one handedness only) and the racemate (1:1 mixture of the two handednesses) of a phosphatidylcholine with three aliphatic tails (3H-2-($2C_{16}$-18:0)-*sn*-1-PC, see Fig. 1.). The structure of the racemate is discussed in contribution 2.6.5.

Synchrotron grazing incidence X-ray diffraction (GIXD) experiments were performed at 5 °C, 15 °C and 25 °C using the liquid-surface diffractometer at the undulator beamline BW1 at HASY-LAB, DESY (Hamburg, Germany). Fig. 1. depicts the diffracted intensity as a function of the in-plane scattering vector component Q_{xy} of the enantiomer at 7 mN/m. The width of the maximum for $Q_z > 0$ Å^{-1} indicates that two peaks contribute. The fitted maximum positions of these diffraction peaks are marked by bars. There is a large overlap between the two peaks with higher Q_z. Between 13 mN/m and 30 mN/m the two peaks at higher Q_z merge, indicating a transition from an oblique to a centered rectangular unit cell with chains tilted in a symmetry direction towards nearest neighbours (NN). While the enantiomer forms a chiral (oblique) lattice at lower lateral pressures, at all pressures the racemate exhibits only two diffraction peaks. Although the area per three tails exceeds that per head, the chiral carbon atom obviously has an influence on tail ordering. Hence it is not sufficient to consider molecular area requirements. The extension of the head group into specific directions must be considered. However, even at the lowest pressure the deviation from a rectangular unit cell (due to the chiral carbon of the glycerol) is not very pronounced. Increase of the lateral pressure suppresses this influence completely. Comparing the structures at medium pressure and different temperatures one observes a change in distortion from NN (nearest neighbours) to NNN (next-nearest neighbours) with decreasing temperature. Such a change was also observed in the L_{2h} phase of simple fatty acids.

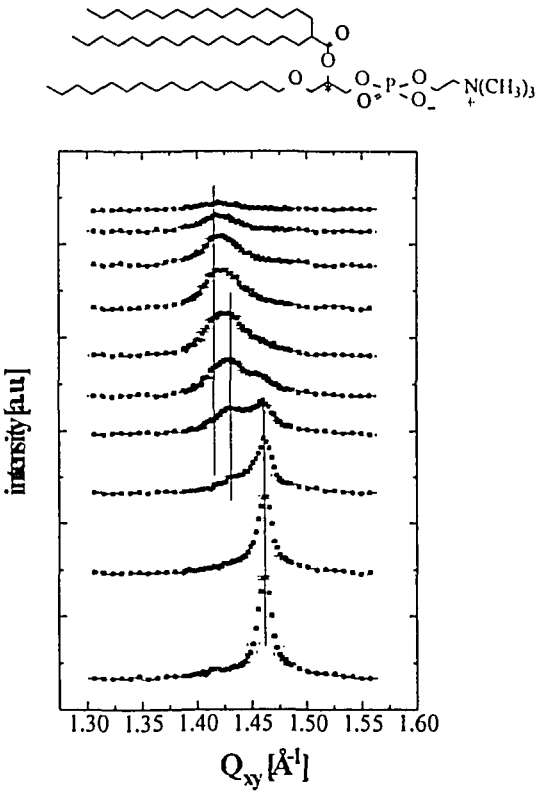

Fig.1. Scattering intensity as a function of Q_{xy} for different Q_z intervals (0.08 Å^{-1} each), with increasing Q_z from bottom to top, for monolayers of the enantiomeric 3H-2-($2C_{16}$-18:0)-*sn*-1-PC at 25 °C and 7 mN/m.

2.6.5 Influence of Chain Length Differences on the Monolayer Structure of Triple-Chain PCs

G. Brezesinski, H. Möhwald, *Max-Planck-Institute for Colloids and Interfaces, Berlin, Germany*, F. Bringezu, *Inst. of Pharmaceutical Chemistry, University of Halle, Germany*, A. Dietrich, B. Struth, *Inst. of Physical Chemistry, University of Mainz, Germany*, W.G. Bouwman, and K. Kjær, *Department of Solid State Physics, Riso National Laboratory, Denmark*, D. Bahr, *Hasylab at DESY, Hamburg, Germany*

Although the richness of mesophases of amphiphile monolayers at the air/water interface has been extensively characterized many open questions remain as regards the underlying interactions. One of these questions concerns the interplay between forces involving the head group and the tail regions, which is an important issue for understanding phospholipid monolayers. Two racemic (1:1 mixture of the enantiomers) triple-chain phosphatidylcholines (1H-2-($2C_{14}$-16:0)-PC and 1H-2-($2C_{16}$-18:0)-PC, see Fig. 1) which differ in the length of the branched chain have been investigated by grazing incidence X-ray diffraction using the liquid-surface diffractometer at the undulator beamline BW1 at HASYLAB, DESY, Hamburg.

At all pressures investigated 1H-2-($2C_{16}$-18:0)-PC exhibits a centered-rectangular (distorted-hexagonal) lattice with chains tilted in a symmetry direction towards nearest neighbours (NN). At lower surface pressures the lattice is distorted from hexagonal packing in the NN direction ($Q_{xy}^{n} > Q_{xy}^{d}$), where Q_{xy}^{n} is the position of the non-degenerate peak and Q_{xy}^{d} that of the twofold degenerate peak. With increasing pressure the distortion decreases and at 40 mN/m the lattice is undistorted (see Fig. 1.): We observe a hexagonal in-plane unit cell in spite of a large tilt angle (t = 13°). In contrast to this behaviour 1H-2-($2C_{14}$-16:0)-PC shows a very rich polymorphism. At lower surface pressures a centered-rectangular packing with chains tilted towards next-nearest neighbours (NNN) was found: Both the non-degenerate and the twofold degenerate peaks are above the horizon. The lattice distortion azimuth is also in the NNN direction. Between 20 mN/m and 30 mN/m both directions change to NN. At 40 mN/m only one diffraction peak at Q_z = 0 Å^{-1} was found, indicating a hexagonal packing of upright chains. Comparing the phase behaviour of these two molecules one could expect that the pressure of the transition NNN - NN increases with increasing temperature (roughly equivalent to decreasing the chain length), whereas that of the transition NN - upright hexagonal packing decreases. Apparently, the temperature dependence of these transition pressures is so steep that for 1H-2-($2C_{16}$-18:0)-PC only the NN phase is observed in the pressure range from 0 mN/m up to 50 mN/m.

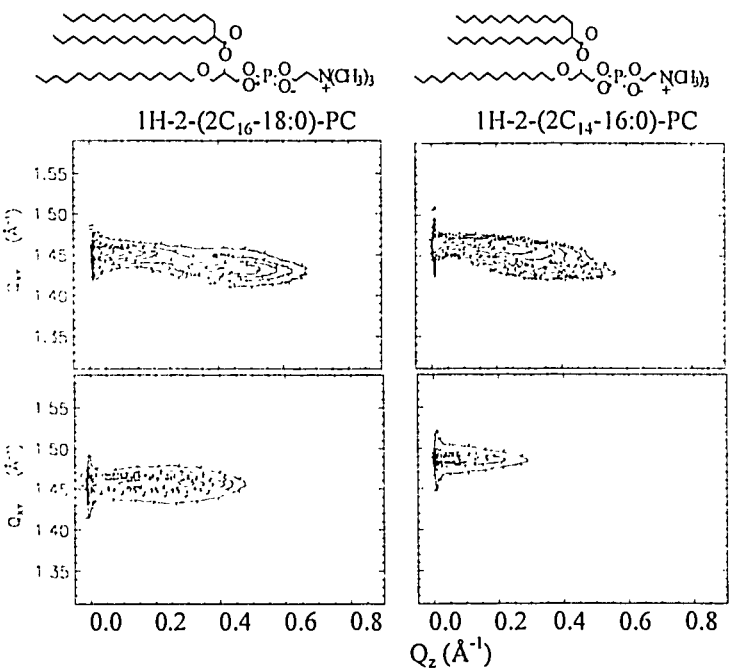

Fig.1. Contour plots at 14 mN/m (above) and 40 mN/m (below.

2.6.6 GIXD Studies of Glycerophosphoethanolamine Monolayers at the Air/Water Interface

F. Bringezu, *Institute of Pharmaceutical Chemistry, University of Halle, Germany,* G. Brezesinski, H. Möhwald, *Max-Planck-Institute for Colloids and Interfaces, Berlin, Germany,* K.Kjær, and W.G.Bouwman, *Dept. of Solid State Physics, Riso National Laboratory, Denmark*

The present investigations are focused on the influence of changes in the hydrophobic part of phosphatidylethanolamine (PE) molecules on the structure of monolayers formed at the air-water interface. In the experiments we have studied monolayers of the racemic 1-($2C_1$-18:0)-2H-PE (a), 1-($2C_{16}$-18:0)-2H-PE (b) and 1,2-Di-($2C_{16}$-18:0)-PE (c), *cf.* Fig. 1. The grazing-incidence diffraction (GIXD) measurements were performed using the liquid surface diffractometer on the undulator X-ray beamline BW1 at HASYLAB, DESY, Hamburg.
Both the introduction of a methyl branch in the acyl chain linked at C1 of the glycerol (a) and the chain length difference between the acyl and the ether (-O-) chains (b) lead to tilted phases. In the case of substance (a) the tilt is much higher than that of the nonbranched DPPE at the same pressure. The tilt direction is changed from NN (DPPE) towards NNN (a). Even at the highest pressure (41 mN/m) the monolayer of (a) shows tilted molecules with an tilt angle of 29°, whereas for DPPE a hexagonal packing with upright oriented chains was obtained. The analysis of the GIXD-data of (b) indicates self assembling of condensed domains at ~zero pressure. The chains are packed in a centred-rectangular lattice. With increasing surface pressure a phase transition to a hexagonal phase with untilted chains occurs between 4 and 14 mN/m. At lower lateral pressures and even at zero pressure the quadruple-chain PE (c) displays two diffraction peaks indicating a rectangular unit cell. The chains are tilted towards their nearest neighbours (NN). At 27 mN/m a hexagonal phase with vertical arranged chains occurs.

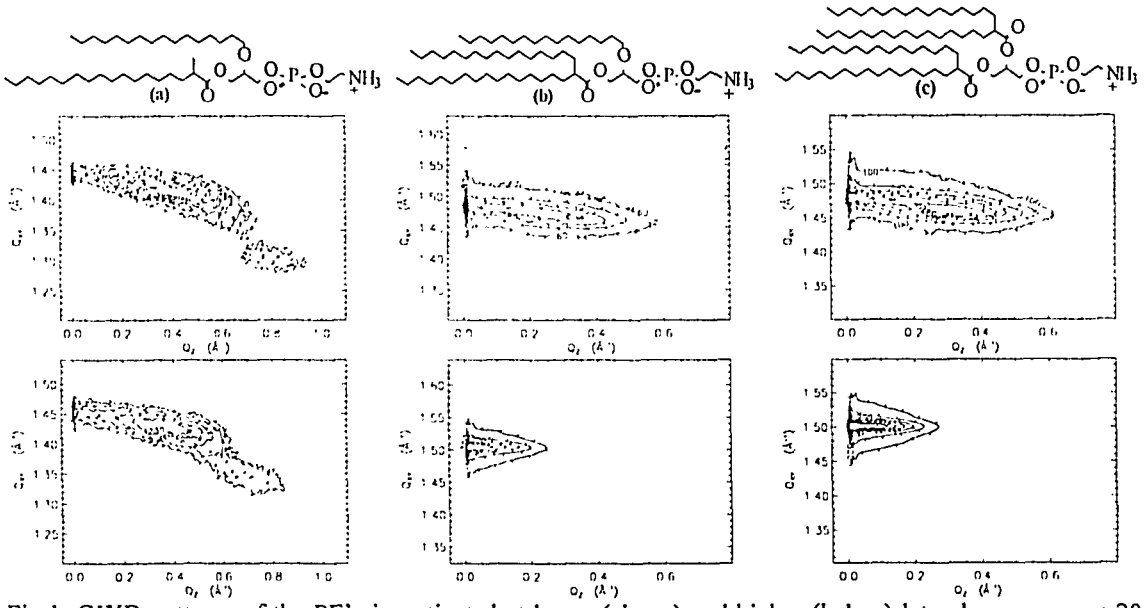

Fig.1. GIXD patterns of the PE's investigated at lower (above) and higher (below) lateral pressures. a: 20 °C, 26 mN/m and 41 mN/m, b: 15 °C, 0 mN/m and 37 mN/m, c: 15 °C, 0 mN/m and 40 mN/m.

Although (c) has four chains of equal length, the chains are tilted at low pressure. This could be an indication of a bending of the C2 acyl chain, already observed in bulk systems of double chain phospholipids using single crystal X-ray analysis. Therefore, the bending of the chains at C2 leads to an effective chain length difference. The optimization of the hydrophobic interaction results in tilted molecules at low pressure.

2.6.7 Right- and Left-handed Molecules at the Air/Solution Interface

I. Kuzmenko, R. Buller, M. Lahav, L. Leiserowitz, *Department of Materials & Interfaces, The Weizmann Institute of Science, Rehovot, Israel*, J.Als-Nielsen, *Niels Bohr Insitute, H.C.Ørsted Laboratory, Denmark*, W.G. Bouwman and K.Kjær, *Department of Solid State Physics, Riso National Laboratory, Denmark*

The self-organization of chiral molecules at the air/water interface has been studied in the past by surface pressure *vs.* molecular area (π-A) isotherms. This macroscopic method does not however provide direct information on the molecular arrangement of these thin films. We demonstrate that in some cases a comparison of isotherm behavior does not lead to an unambiguous interpretation of chiral recognition on molecular level. With the use of novel analytical tools such as grazing incidence diffraction (GIXD) and atomic force microscopy (AFM), it has become possible to explore monolayer structures on the subnanometer scale.
The present work deals with the structure of monolayers of R-*para*-pentadecylmandelic acid ($C_{15}H_{31}$-C_6H_4-CH(OH)-COOH) forming compounds at the air-solution interface with R'- or S'-phenylethylamine (C_6H_5-$CH(CH_3)$-NH_2). Thus, two *diastereomeric* systems: (R,R') and (R,S') are formed. The three-dimensional crystallization of the water-soluble analogous systems, phenylethylamine mandelates (C_6H_5-$CH(CH_3)$-NH_2, C_6H_4-CH(OH)-COOH), have been intensively studied. Although the π-A isotherms for the monolayer-solute (R,R') and (R,S') mixtures were almost identical (not shown here), GIXD data (Fig.1) provided an unequivocal evidence that (R,R') films form 2-D crystalline layers upon compression, whereas the (R,S') films did not show any diffraction at all. The GIXD pattern obtained for (R,R') layers was well explained and fitted with the use of a molecular model that is compatible with the thickness of the layers obtained by AFM for the films transferred onto mica and is very much similar to the corresponding three-dimensional structure.

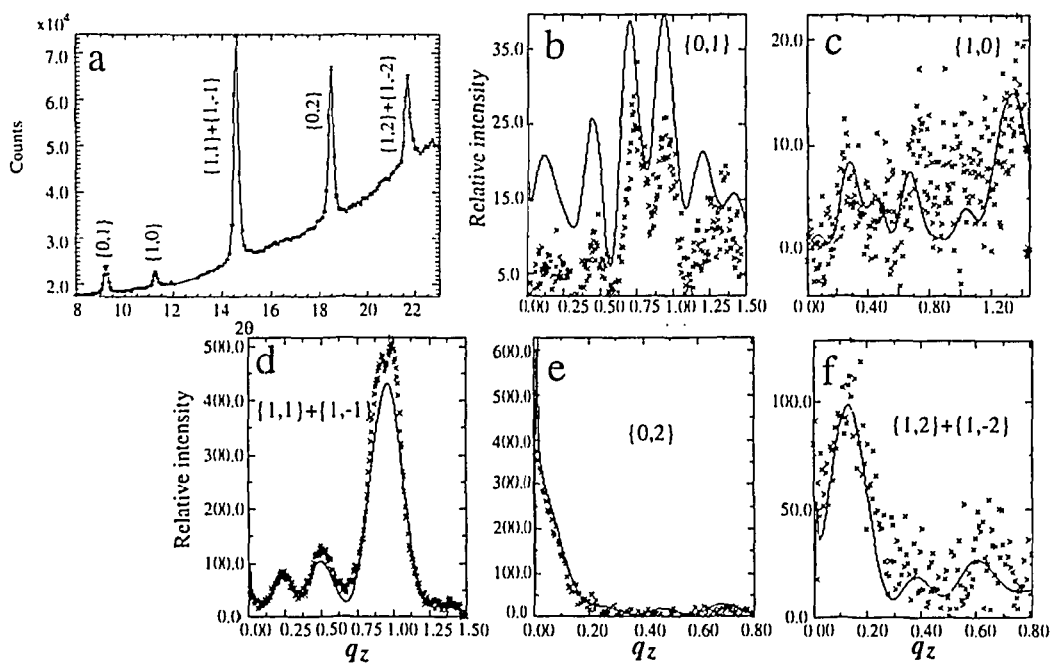

Fig.1 Grazing incidence diffraction (GID) pattern of R-pentadecyl-mandelic acid plus R-phenylethylamine
(a) - Measured Bragg peaks (b-f) - Measured and calculated (solid line) Bragg rod intensity profiles

2.6.9 Self Aggregation of Non Amphiphilic Oligo-Thiophenes into Crystalline Thin Films on the Water Surface

I. Weissbuch, M. Lahav, L. Leiserowitz, *Department of Materials & Interfaces, The Weizmann Institute of Science, Israel*, K. Kjær, *Department of Solid State Physics, Riso National Laboratory, Denmark* J. Als-Nielsen, *Niels Bohr Institute, H.C. Orsted Laboratory, Copenhagen, Denmark*, S. Isz, A. Ruaudel-Teixier, *Service de Chimie Moléculaire, DRECAM, CEA-CEN Saclay, France*

Our recent results have shown that, in contrast to previous belief, non-amphiphiles such as *n*-alkanes can form crystalline monolayer and multilayer films composed of molecules oriented vertically on the water surface. In order to understand such surface phenomena we have extended the structural study to thin films of oligo-thiophenes (molecules containing n=4, 5 or 6 unsubsituted hetero-aromatic rings, see Fig. 1) spread on water surface. The oligo-thiophenes belong to a family of π-conjugated materials which present a promising potential for fabricating organic field-effect transistors since charge transport occurs through a face-to-face intermolecular exchange.

The GIXD patterns from the oligo-thiophenes composed of four (S4), five (S5) and six (S6) rings spread on the water surface are consistent with the formation of multilayer films with the molecules oriented almost vertically on the water surface.

The diffraction pattern of S4 consists of six major Bragg peaks leading to a rectangular 2-D cell of a=6.1Å, b=7.9Å, which is very similar to that obtained in 3-D powder diffraction. Calculations of the Bragg rod intensity profiles based on atomic molecular models show the formation of a bilayer film with the molecules tilted by about 23° from the surface normal and related by twofold-screw symmetry within the layer and by inversion symmetry between the layers, in a manner similar to that in 3-D crystals of S6.

The diffraction patterns of the films obtained from very dilute spreading solutions (0.005mM as compared with standard 0.5mM) showed, as a common characteristic, the formation of monolayer/bilayer crystalline films of a different polymorph, with a rectangular 2-D cell a=5.6Å, b=7.7Å, consistent with the molecular plane being perpendicular to the water surface. The reason for such a polymorphic transition depending on the concentration of the spreading solution might be connected with known molecular aggregation effects in oligo-thiophene solutions.

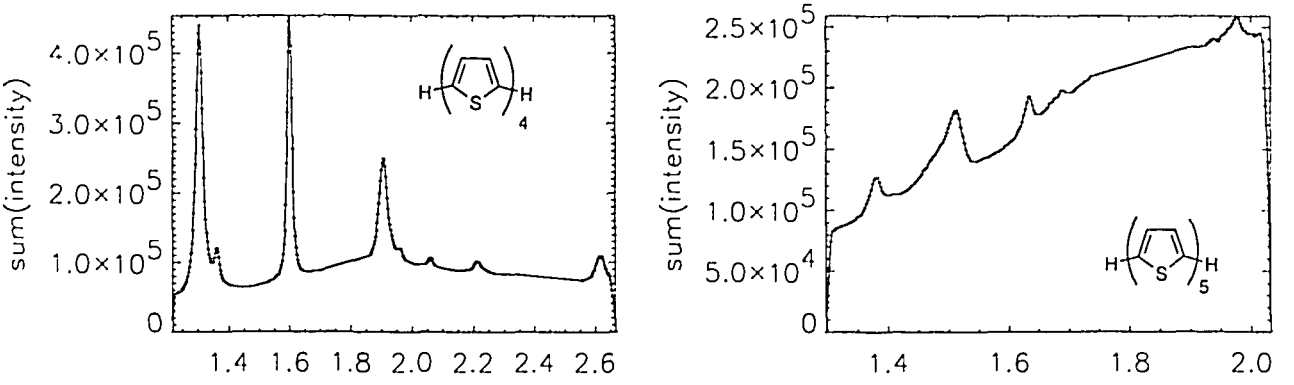

Fig. 1. GIXD patterns obtained (left) for S4 spread from 0.5mM and (right) for S5 from 0.005mM solutions.

2.6.10 Two-Dimensional Crystalline Order of Ionophores at the Surface of Aqueous Solutions

H. Rapaport, M. Lahav, L. Leiserowitz, *Department of Materials and Interfaces, The Weizmann Institute of Science, Israel* , J. Als-Nielsen, *Niels Bohr Institute, H. C. Ørsted Laboratory, Denmark*, W.G. Bouwman and K. Kjær, *Dept. of Solid State Physics, Risø National Laboratory, Denmark*

Valinomycin (Fig. 1, insert) is a naturally occurring cyclic ionophore: It selectively induces K^+ permeability through biological and artificial membranes. The cation binds to the ionophore forming a complex which enables its transport across the hydrophobic bilayer. Although the structure of valinomycin in different solvents has been extensively studied, especially by spectral means, its actual molecular conformation and architecture within a membrane have not been determined. Nonactin (Fig. 2, insert), another natural cyclic ionophore which complexes well with NH_4^+ and K^+, has been much less studied.

In order to obtain information on the complexed forms of the molecules at water- solution interfaces, grazing incidence X-ray diffraction (GIXD) measurements were performed (at 5°C). The valinomycin monolayers were studied on concentrated aqueous solutions of KCl, KBr and KI. A 1:1 mixture of valinomycin with stearic acid monolayers spread on a KCl solution was examined, as well. The resulting diffraction patterns revealed the presence of two-dimensional crystalline aggregates composed of the complexed valinomycin. Fig.1a shows the GIXD pattern obtained from valinomycin spread upon 1M KCl after compression to 180Å²/molecule. The five reflections present could be indexed in terms of a hexagonal unit cell with $a=b=13.88$Å. A very similar pattern of the valinomycin system was observed for the 1:1 mixture with stearic acid, indicating their separation into two phases. In presence of 1M KBr the K^+-valinomycin complex arranged into a slightly distorted hexagonal cell with $a=b=13.75$Å and $\gamma=119.5°$C. At least two polymorphs were formed where valinomycin was spread upon 0.5M KI (see Fig.1b).

Nonactin monolayers were studied after spreading over 1M water solutions of NH_4SCN, KSCN and KCl. Upon NH_4SCN subphase the nonactin formed two-dimensional crystalline aggregates (see Fig.2). A similar pattern was measured for nonactin over KSCN solution but the structure was much more susceptible to X-ray beam damage. Nonactin spread over KCl solution didn't diffract at all. This demonstrates the important role of the counterion in the formation and stabilization of the 2D crystallite array.

These preliminary results demonstrate the ability of the two ionophores to form two-dimensional crystalline aggregates at the air-water interface after complexation. Further investigations are required in order to determine the relative positions of the complexed molecules and the counter ions inside the unit cell.

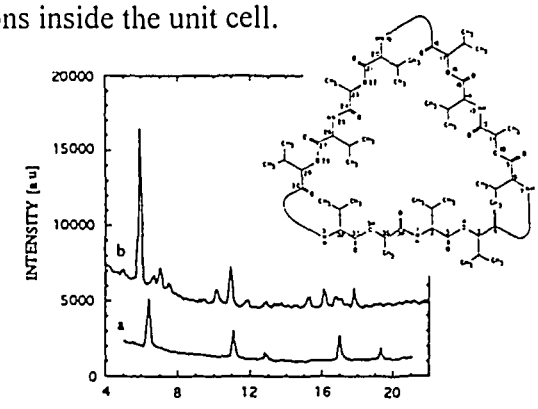

Fig. 1. GIXD pattern obtained from valinomycin spread over a) 1M KCl solution b) 0.5M KI solution.

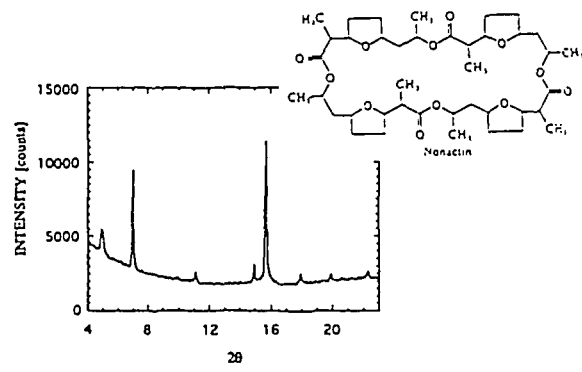

Fig. 2. GIXD pattern obtained from nonactin spread over 1M solution of NH_4SCN.

2.6.11 Structural Details of Polyelectrolyte Interface Multilayer Films

J. Schmitt, *Institute of Physical Chemistry, Johannes-Gutenberg-University, Mainz, Germany*, K. Lehmann, M. Lösche, *Experimental Physics I, University of Leipzig, Germany*, W. G. Bouwman and K. Kjær, *Department of Solid State Physics, Riso National Laboratory, Denmark*

In earlier neutron reflectivity work we have shown that the adsorption of polyelectrolytes from aqueous solution to surface charged substrates such as surface modified Si wafers leads to polymer films that are stratified on the molecular length scale.[1,2] Since then we have initiated a systematic study of the internal structure of layer-by-layer deposited polymer films. As earlier, we have deposited structured films that incorporated perdeuterated and perprotonated polyelectrolyte layers in a characteristic, one-dimensional superlattice pattern (typically a sequence of 7 protonated and 1 deuterated layer, repeated n times, where n = 6, 8, or 10). To get better reproducability of the preparation, we have used a home-built robot device for the sample preparation. Neutron reflectivity was measured at the refurbished TAS8 spectrometer which owing to its superior resolution is very well suited for the characterization of "thick" molecular multilayer films ($d \sim 2500$ Å).

In all preparations we found surprisingly complex reflectivity curves (e.g., Fig. 1) with Bragg reflections of up to the third or fourth order. A satisfactory model description of the data is achieved only if one allows for a systematic and continuous increase of the thickness of the deposited layers from the substrate toward the film/air interface. This non-uniform layer structure also remains after a dehydration-rehydration cycle applied on a sample. In rehydration experiments with D_2O, the water content, ~45 vol%, of the wet films was determined. After dehydration over P_2O_5, we have determined the void volume created by the evaporation of water molecules: the polymer shrinks only by ~50% of the lost water volume. Whereas the molecular weight of the deposited polyelectrolyte has surprisingly small influence on the layer structure, the layer thickness and internal roughness between deuterated and protonated layers depend almost linearly on the ionic strength of the deposition solution in the range between 0.5 and 3 mol/l.

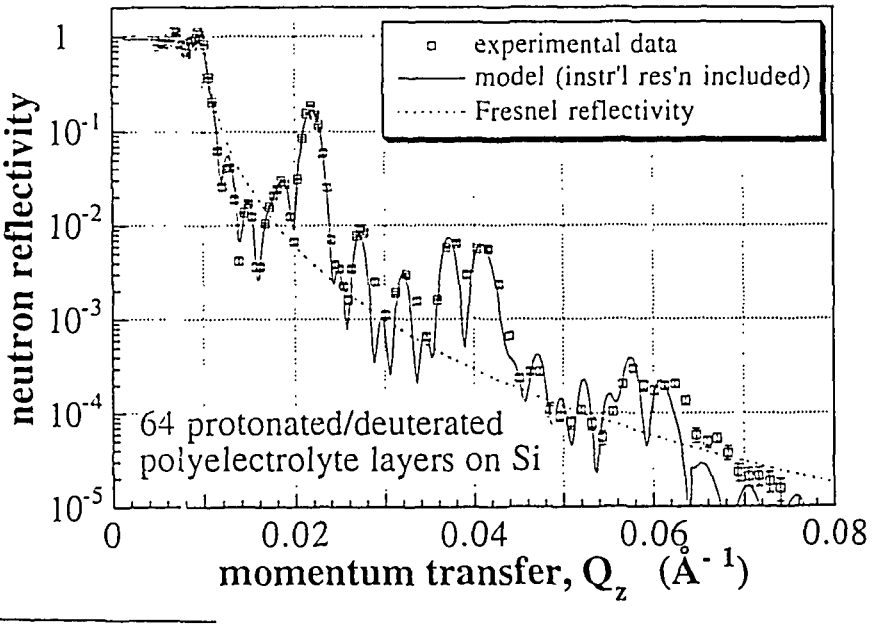

[1] J. Schmitt, T. Grünewald, G. Decher, P. S. Pershan, K. Kjær and M. Lösche, Macromolecules 26, 7058-7063 (1993).

[2] M. Lösche et al., "Internal structure of electrostatically adsorbed polyelectrolyte films," Ann. Progr. Rep. Dept. Solid State Phys. 1993, Riso Natl. Lab., Roskilde, Denmark.

2.6.12 Structure of Reassembled Molecular Bacterial S-Protein Layers at Aqueous Surface Monolayer Films

M. Weygand, M. Lösche, *Experimental Physics I, University of Leipzig, Germany*, B. Wetzer, T. Lackner, D. Pum, *Center for Ultrastructure Research, University for Agriculture, Vienna, Austria*, and K. Kjær, *Department of Solid State Physics, Riso National Laboratory, Denmark*

Surface-layer proteins constitute the outermost cell envelope component of many eu- and archeobacteria. Previously we have studied the recrystallization of S-layer proteins at lipid monolayers floating on top of aqueous surfaces with electron microscopy,[1] dual label fluorescence microscopy, and FTIR spectroscopy.[2] We found a reverse influence between the lipid and the protein components: 2D protein crystals nucleate at lipid areas that are in the gel phase and, *vice versa*, the formation of 2D protein crystals at the interface increase the order parameter of the lipid chains. Whether or not the protein, which apparently communicates with the lipid chains, interpenetrates physically into this lipid chains region could not be resolved with the techniques mentioned above.

We have investigated this question with neutron reflectometry at the new TAS9 liquid surface reflectometer in the guide hall of DR3 and with x-ray reflectometry at the beam line BW1 in HASYLAB, DESY Hamburg. The S-layer proteins of *Bacillus coagulans E38–66* or *Bacillus sphaericus CCM2177* were adsorbed to DMPE (dimyristoyl phosphatidylethanolamine) monolayers on aqueous buffer. For the neutron measurements, chain-perdeuterated DPPE-d_{62} and both H_2O or D_2O subphases were used. The x-ray measurements were conducted on protonated samples. Fig. 1 shows representative data sets for *CCM2177*: neutron reflectivity of S-layer protein under DMPE-d_{62} on H_2O, 10 mM $CaCl_2$, *pH*=9. (a) and on D_2O, same buffer (b), as well as x-ray reflectivity on H_2O, same buffer (c). The data indicate that a complex layer structure has assembled at the interface. A preliminary evaluation seems to suggest that the protein forms a molecular layer under the lipid monolayer but does not interpenetrate the lipid acyl chain region. More definite conclusions on the structure must await a more quantitative evaluation of the data.

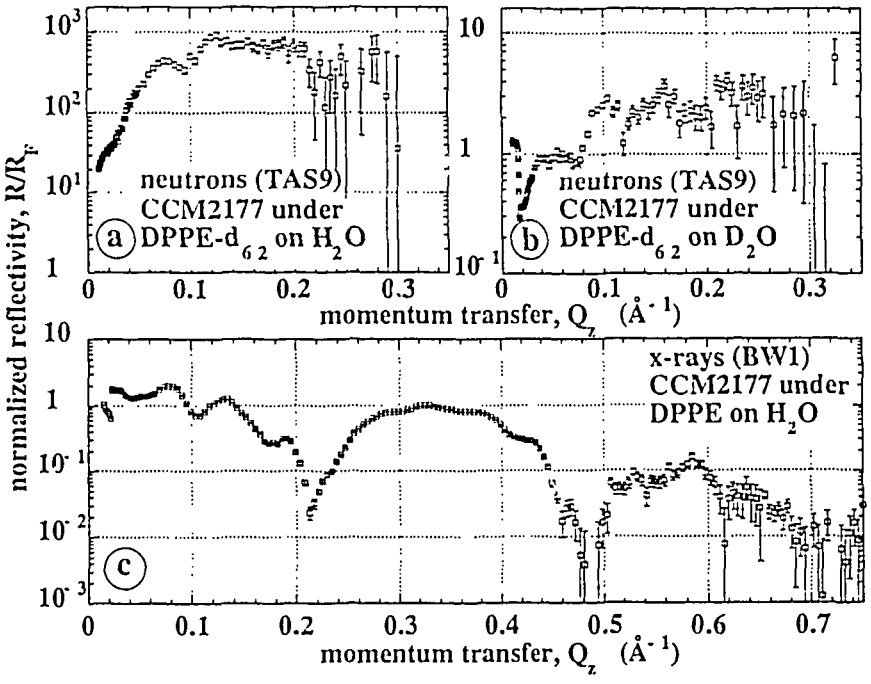

[1] D. Pum, M. Weinhandl, C. Hödl and U. B. Sleytr, J. Bacteriol. **175**, (1993).
[2] A. Diederich, C. Hödl, D. Pum, U. B. Sleytr and M. Lösche, Colloids Surf. B, submitted.

2.7 Microemulsions, Surfactants and Biological Systems

2.7.1 Micellar Ordering of the Triblock Copolymer P85 at a Solid-Liquid Interface

M.C. Gerstenberg, J. Skov Pedersen, *Department of Solid State Physics, Risø National Laboratory, Denmark,* and G. Smith, *Manual Lujan Jr. Neutron Scattering Center, LANSCE, Los Alamos National Laboratory, New Mexico, USA*

The triblock copolymer P85 consists of two symmetric outer blocks of poly(ethylene oxide) (EO) and a central block of poly(propylene oxide) (PO) with the formula H-$[EO]_{25}[PO]_{40}[EO]_{25}$-H, where the subscript of the square brackets denote the number of repeating units. EO is hydrophilic for all temperatures, whereas PO is hydrophobic for temperatures above 15°C. Consequently, various aggregates form in aqueous solution. A great number of techniques have been applied in determination of the bulk phases. In the present study the surface induced ordering of P85 in an aqueous solution (D_2O) at a quartz surface has been measured for several concentrations (5-30%(w/w)) and temperatures by neutron reflectometry at TAS8. The polymer was kept in a Teflon enclosure with a single crystal quartz lid. The neutrons traverse the quartz crystal with only slight attenuation and reflect off the solid-liquid interface. Initially the reflectivity measurements (see Fig. 2) have been analysed using a form-free method[1] and the corresponding scattering length profiles are shown in Fig. 1. The profiles can be interpreted as a water layer forming on the surface and a subsequent micellar ordering perpendicular to the surface. Each local minimum corresponds to the position of the micellar core with water interpenetrating. The decay of the scattering length density is due to the decreasing order in the layers. As the temperature is increased more disorder, i.e. a more rapid decay, occurs in the surface ordering. The micellar ordering can be modelled by a first order Spherical Bessel function of first kind with an exponential decay. The fits reveal a period of 123±3 Å and 135±1 Å for the 49°C and 61°C data, respectively. These values are slightly less than the expected bulk values[2] of 145 Å and 160 Å for the hard-sphere diameter of the micelles of the respective temperatures.

Fig. 1. and 2. 25% (w/w) Polymer concentration. The model free scattering length density (ρ) profiles and the corresponding reflectivity data.

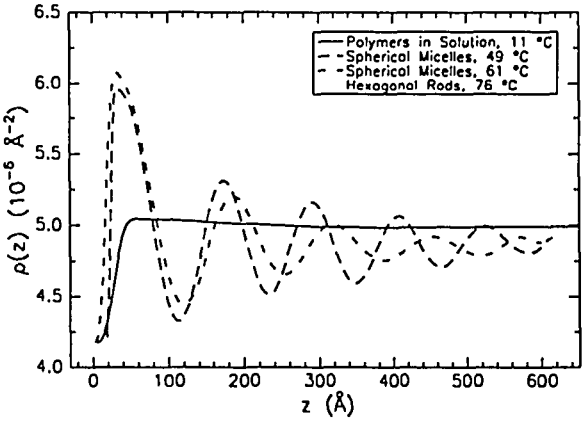

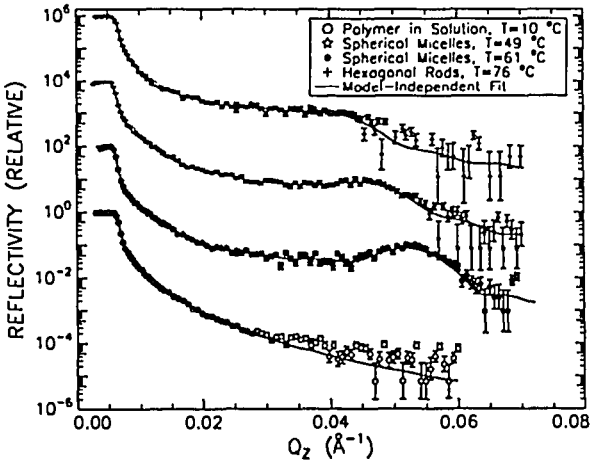

[1] J.S. Pedersen and I.W. Hamley, J. Appl. Cryst. **27**, 36 (1994).
[2] K. Mortensen and J. S. Pedersen, Macromolecules **26**, 805 (1993).

2.7.2 Neutron Reflection from Biosensors

S. Roser, *School of Chemistry, University of Bath, UK*, D. Caruana, *Department of Biomedical Sciences, University of Malta, Malta*, M. C. Gerstenberg, *Department of Solid State Physics, Riso National Laboratory, Denmark*

Neutron reflection at small angles yields structural information about interfaces at close to atomic resolution. We have used the technique at Risø to investigate the behaviour of thin films of polymers and enzymes which have potential use as in-situ electrochemical sensors. In particular we have focused on Glucose Oxidase (GOX) which can be used to detect levels of glucose in the bloodstream of diabetics. A thin layer of poly(phenol) is plated onto a gold electrode by polymerisation from an aqueous solution. The layer is self-limiting at a thickness of about 100Å, and the cigar shaped enzyme can be included in the film by adsorbing it onto the electrode surface, prior to depositing the polymer. Crucial parameters which affect the performance of the sensor will be the extent to which solvent and hence glucose can penetrate into the polymer, and the extent to which the enzyme protrudes from the film, which depends on the thickness and interfacial roughness of the polymer, as well as the orientation of the GOX with respect to the surface. In such a complex system, the amount of information that can be obtained from a single reflection profile is limited. We have therefore performed an experiment on pure poly(phenol) films with many subphase contrasts in order to deconvolute contributions from different interfaces. The figures show model profiles fitted to three different reflectivity curves from subphases of pure H_2O, D_2O and water matched to the electrode.

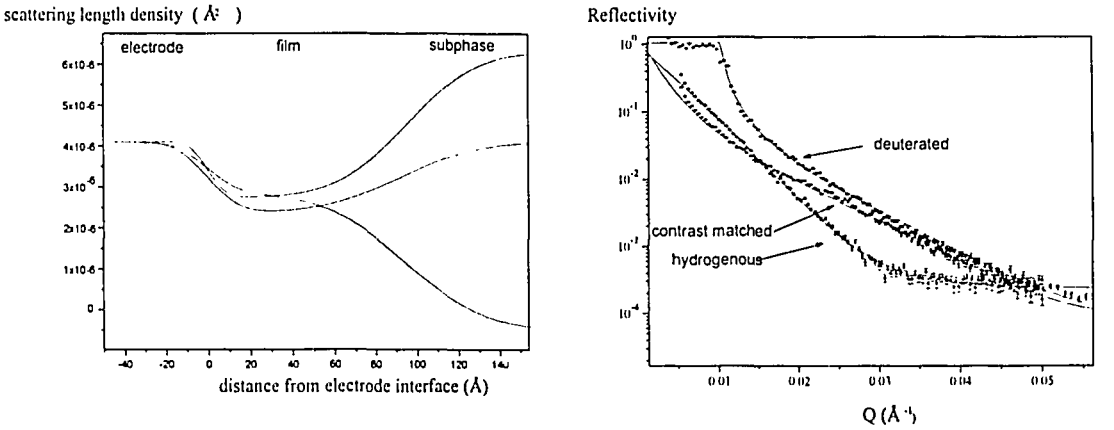

From the model fits, we can see that the polymer film has a well defined thickness, accurately and unambiguously measured by the fringes in the profiles as 95 ± 2Å. The density of the film close to the electrode surface is virtually independent of the subphase, and hence there is little or no solvent penetration in the inner half of the film. With the known structure of the GOX molecule, we can state that the active sites will only present to the solvent, and hence the glucose if the molecules are orientated with their long axis parallel to the surface normal. In further experiments, we have studied the rate of growth of the films over a time scale of 10s at constant Q, and will be making measurements with GOX preadsorbed on the electrode.

2.7.3 Scattering Formfactor of Block Copolymer Micelles

J. Skov Pedersen and M.C. Gerstenberg, *Department of Solid State Physics, Riso National Laboratory, Denmark*

When block copolymers are dissolved in a solvent which is a good solvent for only one of the blocks, micelles are formed.[1,2,3] Depending on the concentration, the temperature, and the relative length of the blocks the shape of the micelles may be spherical, elliptical, or cylindrical.[1] The structure of the spherical micelles has been suggested to consist of a spherical core of the insoluable part surrounded by a shell of dissolved polymer chains. This shell is similar to the outer region of a multi-arm star polymer or a brush consisting of end-grafted polymer chains.

The formfactor of a micelle model with a spherical core and Gaussian polymer chains attached to the surface has been calculated analytically. The calculation uses the classical Debye equation which describes the scattering intensity of particles consisting of spherical subunits, and the approaches, which are used for calculating the scattering from branched polymers. The results have been compared to Monte Carlo simulations. Excluded volume interactions between the core and the polymers were introduced in the simulations. The expansion of the coils due to this effect can be mimicked in the analytical calculations by moving the center of mass of the chains further away from the center of the core. The analytical expression for the formfactor has been used for analyzing experimental small-angle scattering[1,2] data from micelles of the triblock copolymer poly(ethylene oxide)-poly(propylene oxide)-poly(ethylene oxide) (P85) in D_2O and of micelles of d-poly(sterene)-poly(isoprene) in d-decane solutions.[3]

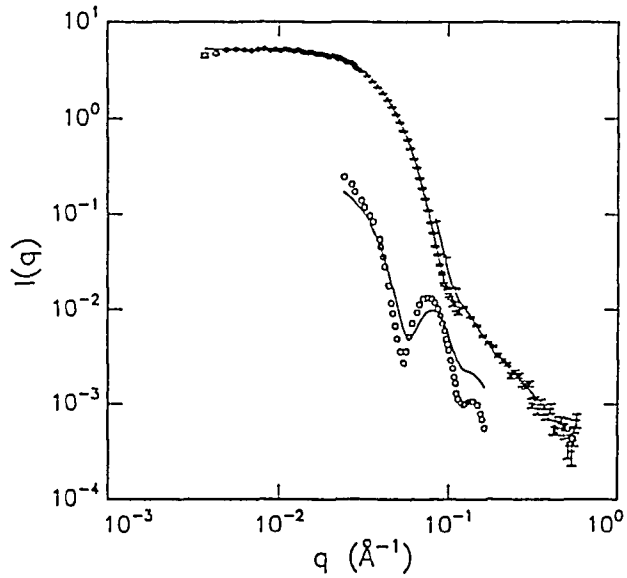

The small-angle neutron scattering data of 0.5% P85 ($EO_{25}PO_{40}EO_{25}$) in D_2O (upper data). The data were recorded using three different instrumental settings. The curve is the fit by the analytical model including polydispersity of the micelles. The lower data are SAXS results on similar micelles.[3] The curve is calculated for the results determined by fitting the SANS data.

[1] K. Mortensen and J.S. Pedersen, Macromolecules **26**, 805 (1993).
[2] B. Farago, M. Monkenbusch, D. Richter, J.S. Huang, L.J. Fetters and A.P. Gast, Phys. Rev. Let. **71**, 1015 (1993).
[3] O. Glatter, G. Scherf, K. Schillen and W. Brown, Macromolecules **27**, 6046 (1994).

2.7.4 The Effect of Shear on the Ordering of Pluronic P85 at a Solid-Liquid Interface

M.C. Gerstenberg, J. Skov Pedersen, *Department of Solid State Physics, Riso National Laboratory, Denmark*, and G. Smith, *Manual Lujan Jr. Neutron Scattering Center, LANSCE, Los Alamos National Laboratory, New Mexico, USA*

The amphiphilic triblock copolymer P85[1] has been observed to align instantaneously to shear forming a single crystal in a polycrystalline phase.[2] In order to understand the fundamental surface behaviour and determine the surface morphology in contrast to the previously investigated bulk behaviour a shear flow cell[3] was used. In a typical experiment, a neutron beam passes through a single crystal of quartz and reflects from the solid-liquid interface. The polymer is in a Teflon enclosure, where the crystal serves as a lid. By pumping a fluid across a solid-liquid interface, free or adsorbed molecules are subjected to shear stress. Neutron reflectivity studies were performed for several concentrations in the range 20-30% (w/w) and temperatures in order to investigate the occurring phases as a function of shear rate. As in the static case a form-free method[4] has been employed in the analysis of the reflectivity data. In the spherical micellar phase (44°C) at a polymer concentration of 25% (w/w) no change was observed in the scattering length density profiles for increasing shear rates. The reflectivity measurements in the hexagonal rod phase (76°C) at the same concentration and the corresponding form-free profiles are shown in Fig. 1 and 2. When shear is increased the distances between each local minimum, which can be interpreted as a characteristic length related to the diameter of the rods, changes from approximately 148 Å in the static case to 166 Å and 148 Å for 16% and 47% of maximum shear rate, respectively. Furthermore, the water layer next to the quartz surface diminishes as the shear rate is increased. The surprising indication of an increase followed by a decrease in size will be investigated further in future experiments.

Fig. 1. and 2. Reflectivity measurements of 25% (w/w) P85 at different shear rates and the corresponding form-free scattering length density (ρ(z)) profiles.

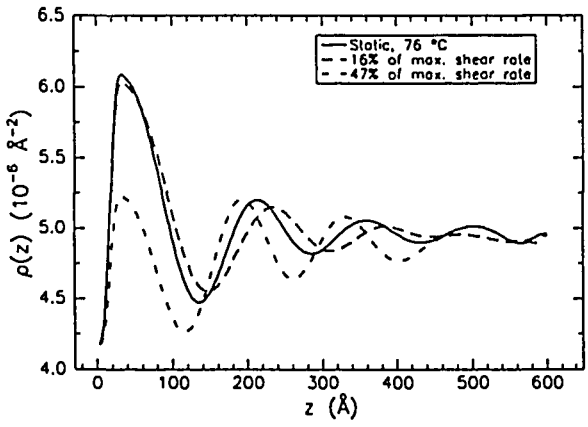

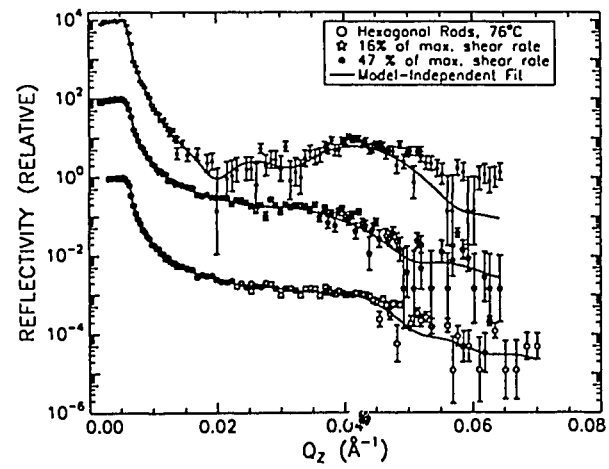

[1] See "Micellar Ordering of the Triblock Copolymer P85 at a Solid-Liquid Interface", contribution 2.7.1.
[2] K. Mortensen, Europhys. Lett. 19, 599, (1992).
[3] S.M. Baker, G. Smith, and R. Pynn, Rev. Sci. Intrum. 65, 412, (1994).
[4] J.S. Pedersen and I.W. Hamley, J. Appl. Cryst. 27, 36, (1993).

2.7.5 Structure of Graphitized Carbon Black Aggregates in Triton X-100/Water Solutions

V.M. Garamus, *Frank Laboratory of Neutron Physics, Joint Institute for Nuclear Research, Dubna, Russsia,* J. Skov Pedersen, *Department of Solid State Physics, Riso National Laboratory, Denmark*

The structure of graphitized carbon black aggregates (CB) dispersed in non-ionic surfactant/water solutions is studied by small angle neutron scattering and contrast variation by heavy/light water exchange. The presence of two different types of inhomoginities, i.e. fractal CB aggregates coated with surfactant molecules and Triton X-100 micelles, was detected. The addition of CB dispersions to Triton X-100/water mixtures shifted the critical micelle concentration to a low value. The fractal dimension near the match point (75 % heavy water) was found to decrease.

The scattering data were modelled by a complex model including fractal-like aggregates (CB+surfactant), micelles and voids in the CB particles. The data were fitted simultaneously for three different contrasts. The fractal dimension was found to decrease for increasing CB concentration from $D = 3.4$ at $h = 0.01$ to $D = 2.9$ at $h = 0.05$, where h is the volume fraction of the CB particles. The maximum size of the fractal aggregates increases from 150 Å to 200 Å. The primary CB particles have a broad size distribution and its average size (80 Å) is slightly decreasing with CB concentration. The degree of occupation of the surface of the CB particles by surfactant molecules is 10% and stays constant with varying CB and surfactant concentration. The micelle structure is found to be the same as in surfactant/water solutions. The volume fraction of voids does not exceed 1% of the CB volume fraction.

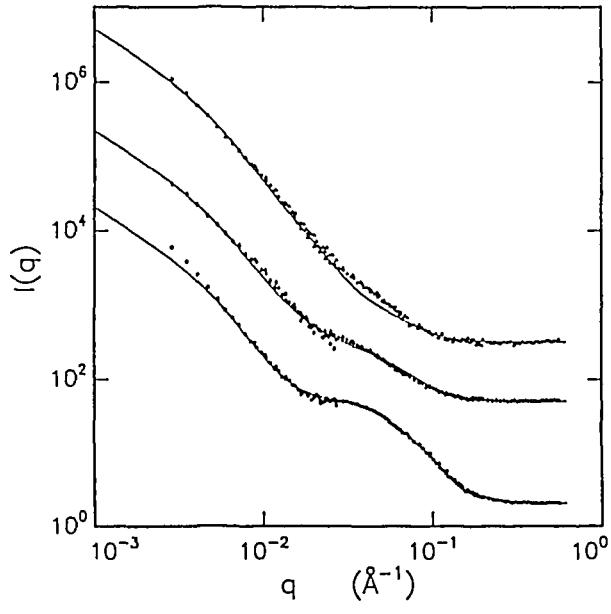

Small angle neutron scattering data from a dispersion of 10 g/l CB in 1.84 g/l Triton/water solution with different contrasts and model fits (solid lines). The lower spectrum is in 100% D_2O , the middle spectrum (multiplied by 10) in 73% D_2O, and the upper spectrum (multiplied by 100) is in 47% D_2O.

2.7.6 Contrast Variation Study of the E. Coli Ribosome

D.I. Svergun, M.H.J. Koch, *EMBL, Hamburg Outstation, Germany,* N. Burkhardt, K. Nierhaus, *Max-Planck Institute for Molecular Genetics, Berlin, Germany,* V.V. Volkov, M.B. Kozin, *Institute of Crystallography, Moscow, Russia,* I.N. Serdyuk, *Institute of Protein Research, Pouschino, Russia,* W. Merwink, H.B. Stuhrmann, *GKSS Research Centre, Geesthacht, Germany,* and J. Skov Pedersen, *Department of Solid State Physics, Risø National Laboratory, Denmark*

The aim of this study is to develop a four-phase low resolution model of the ribosome consisting of the shapes of the RNA and protein moieties in its large and small subunits. A four-phase system produces ten basic scattering functions, i.e. four scattering intensities from the different phases and six cross terms. To separate these functions, wide scale contrast variation experiments on specifically deuterated samples are required.

Solutions of the 70S E. Coli ribosome reassembled from the free subunits were measured at different concentrations of heavy water at the Risø SANS facility. Four different particle types were used:

i) 30S protonated + 50S protonated,
ii) 30S protonated + 50S deuterated,
iii) 30S deuterated + 50S protonated,
iv) 30S deuterated + 50S deuterated.

The samples were measured at 0%, 35%, 50%, 75% and 100% heavy water. Two experimental settings (sample-detector distance 4 m at the wavelength 0.62 nm and sample-detector distance 1.25 m at 0.56 nm) covered the range of momentum transfer from 0.1 to 2.5 1/nm. The concentration of the samples was around 15 mg/ml. For the low-angle setting, the lower concentration samples were measured to estimate and possibly eliminate the concentration and/or aggregation effects.

These curves were combined with the synchrotron scattering data measured at DESY, Hamburg (contrast variation with sucrose on the 70S ribosome and on the free 30S and 50S subunits) as well as with the results of the spin dependent neutron scattering experiments from the GKSS polarized target (selectively deuterated and reassembled 70S). The analysis indicates that the scattering from the free subunits is consistent with the scattering from these in the reassembled ribosome, so that all the data sets (total of 32) can be used together in the four-phase model search.

A program MONSTER (Multiphase Optimization of Neutron Solution scaTtering Experiments on Ribosome) based on the spherical harmonic technique and non-linear least-squares minimization was written to generate the low resolution model of the ribosome by simultaneously fitting all the data sets. Refinement of the model is now in progress.

2.7.7 Local Structure and Flexibility of Worm-like Micelles in Isooctane

G. Jerke, P. Schurtenberger, *Institut für Polymere, ETH Zürich, Switzerland*, J. Skov Pedersen, *Department of Solid State Physics, Riso National Laboratory, Denmark*

Long worm-like micelles can be described essentially as semi-flexible polymers. This was clearly shown in previous light scattering experiments.[1] In order to obtain additional information on local structure and flexibility we started an experimental and theoretical investigation of polymer-like water-in-oil microemulsions.[2,3,4] As a typical example of an equilibrium polymer we chose lecithin in isooctane with trace amounts of water.

In different series of experiments at the SANS instrument at Risø we studied the structural properties of these polymer-like reverse micelles as a function of concentration, c, and water to lecithin molar ratio, ω_0, over an extended q range (2.8×10^{-3} Å^{-1} $< q <$ 0.45 Å^{-1}). In combination with static light scattering experiments we thus obtained a full set of experimental data on the concentration dependence of the static structure factor, $S(q)$.

The scattering function, $S(q)$, shows all the characteristic features of classical polymers. Depending on the the various length scales and properties we can extract information about the overall size, flexibility and the cylindrical cross-sectional behaviour. The data obtained for isooctane were in quantitative agreement with the presence of a polydisperse population of polymer-like micelles.

Information on the local structure was obtained by the application of the indirect Fourier transformation method and the square-root deconvolution procedure developed by.[5,6,7,8] All experiments were performed on absolute scale. Our results are in qualitative agreement with a geometrical model of locally tubular reverse micelles. The cross-sectional radius of gyration, R_{gc}, increases slightly with water to lecithin molar ratio, ω_0, due to the swelling of the water core (approximately: 19 - 20 Å). Within the experimental error the mass per length, M_L, is neither ω_0 or concentration dependent (approximately: $0.13 - 0.14 \times 10^{-12}$ g/cm).

In a second step we aimed at a qualitative determination of the persistence length as a measure of the flexibility of the micelles. We find that on length scales where local flexibility becomes visible polydispersity has a minor effect. However, we observe a significant concentration dependence of the persistence length. This finding seems to reflect the influence of the intermicellar interaction effect on $S(q)$,which results in the determination of an apparent persistence length if expressions for single scattering functions were used to analyze the experimental data. In the limit $c \rightarrow 0$ the persistence length is in the range of 150 Å.

---

[1] P. Schurtenberger, C. Cavaco, J. Phys. II (France) **3** 1279 (1993); J. Phys. II (France) **4**, 305 (1994); Langmuir **10**, 100 (1994); J. Phys. Chem. **98**, 5481 (1994).
[2] G. Jerke, C. Cavaco, P. Schurtenberger, P. Lindner, J.S. Pedersen (1995). In preparation.
[3] J.S. Pedersen, P. Schurtenberger (1995). In preparation.
[4] J.S Pedersen, M. Laso, P. Schurtenberger (1995). Submitted.
[5] O. Glatter, J. Appl. Crystallogr. **10**, 415 (1977).
[6] O. Glatter, J. Appl. Crystallogr. **14**, 886 (1981).
[7] J.S. Pedersen, P. Schurtenberger (1995). Submitted.
[8] P. Schurtenberger, G. Jerke, C. Cavaco, J.S. Pedersen (1995). Submitted.

2.7.8 Association Behaviour of β-lactoglobulin Studied by Small-Angle Neutron Scattering

M. Verheul, C.G. de Kruif, S.P.F.M. Roefs, *Technology Department, Netherlands Institute for Dairy Research, The Netherlands*, J. Skov Pedersen, *Department of Solid State Physics, Riso National Laboratory, Denmark*

β-lactoglobulin (β-lg) is the major whey protein in bovine milk. Characterization of the native protein and heat-induced denaturation, aggregation and gelation are main issues in our research. First, we focussed on the reversible association behaviour of native β-lg in 0.1M NaCl as a function of pH, and protein concentration at 20°C. The data were analyzed using the indirect Fourier transformation method[1] yielding the distance distribution function, *p(r)*, the *z*-averaged radius of gyration, R_g, and the weight-averaged molecular mass, M_w. The distance distribution functions were calculated from crystal atom coordinates of β-lg monomers and dimers that are largely known.[2] In figure 1 the calculated and experimental *p(r)* functions of β-lg are compared and from this it is clear that the structure in solution differs markedly from both the monomeric and dimeric crystal structure for all the pH values investigated. Moreover, the pH did not have a large influence on the state of association in the pH and concentration range studied and β-lg seems to be close to the dimeric form in all cases except for pH 4.65 (close to the iso-electric point) where larger structures are present.

Some authors think that β-lg dimers dissociate if the temperature is raised above 30°C. Experimental *p(r)* functions of 2-8 mg/ml β-lg at pH 6.9 measured at 20°C and 45°C however, were almost identical. Interpretation of measurements on β-lg solutions with very low ionic strength is more complicated, since interparticle electrostatic interaction has to be taken into account. Preliminary experiments were undertaken with β-lg solutions heated *in situ* and the scattering pattern was measured as a function of time. Presently, the results are being analyzed using fractal aggregation models.[3]

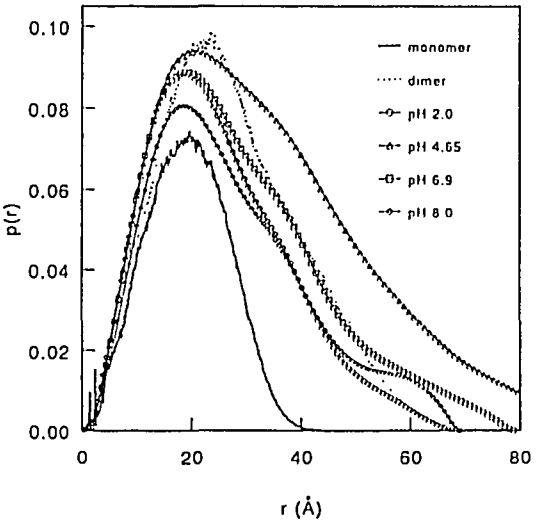

Fig. 1. *p(r)* calculated from the crystal structure[2] of β-lg monomers (full curve) and dimers (dashed curve) and *p(r)* from experiments on 8 mg/ml β-lg solutions at different pH values.

[1] O. Glatter, J. Appl. Cryst. **10**, 415 (1977).
[2] Coordinates were kindly provided by Dr. L. Sawyer, University of Edinburgh.
[3] J. Teixera, J. Appl. Cryst. **21**, 781 (1988).

2.7.9 A Small Angle Neutron Scattering Study of Orientational Ordering in the Nematic Phase of Thermotropic Liquid Crystals

I.W. Hamley, *School of Chemistry, University of Leeds, U.K.*, G.R. Luckhurst, *Department of Chemistry, University of Southampton, U.K.*, J.M. Seddon, *Department of Chemistry, Imperial College, London, U.K.*, J. Skov Pedersen, *Department of Solid State Physics, Risø National Laboratory, Denmark*, and R.M. Richardson, *School of Chemistry, University of Bristol, U.K.*

Orientational order in the nematic phase of 4,4'-dimethoxyazoxybenzene (PAA) and 4-pentyl-4'-cyanobiphenyl (5CB) has been studied using small angle neutron scattering from mixtures of unlabelled and deuterium labelled molecules.[1] Unlike spectroscopic methods, the determination of the complete singlet orientational distribution function is possible using this technique.[2] The Legendre polynomial orientational order parameters corresponding to the expansion of the singlet orientational distribution function were extracted from the anisotropic single molecule scattering isolated at small scattering angles (see figure). These order parameters were compared to those predicted from the Maier-Saupe theory of nematic ordering[3] and to second rank order parameters extracted from NMR experiments. For PAA we have also made comparisons with previous neutron scattering measurements.[4] For both nematogens, we found that only the second and fourth rank terms in the expansion of the single molecule scattering are statistically significant, which means that $\overline{P}_2$ and $\overline{P}_4$ only are significant. For the rigid nematogen PAA, the Maier-Saupe theory was found to underestimate $\overline{P}_2$ and its dependence on the reduced temperature T/T_{NI} where T_{NI} is the nematic-isotropic transition temperature. The theoretical values of $\overline{P}_4$ are, however, in remarkably good agreement with the measured values. Order parameters extracted from NMR were found to be slightly lower than those determined from the SANS experiment. For 5CB, the measured order parameters are substantially lower than the predictions of the Maier-Saupe theory, and this can be interpreted in terms of the flexibility introduced in the molecule by the terminal alkyl chain.

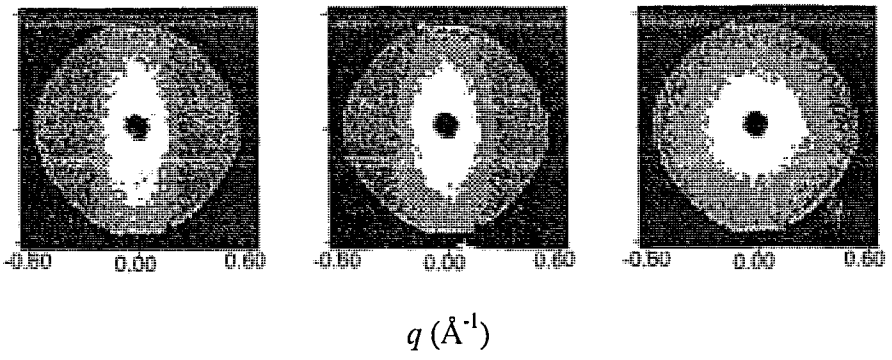

Fig. 1. Intensity contour plots of the SANS patterns for PAA. Left: Deep in the nematic phase at 108°C. Middle: In the nematic phase at 133°C, close to the nematic-isotropic transition (at 135°C). Right: In the isotropic phase at 140°C.

[1] I.W. Hamley, G.R. Luckhurst, J.M. Seddon, J.S. Pedersen and R.M. Richardson, in preparation.
[2] P.G. de Gennes, C.R. Acad. Sci. **274B**, 142 (1972).
[3] W. Maier and A. Saupe, Z. Naturforsch. **A13**, 564 (1958); **A14**, 882 (1959); **A15**, 287 (1960).
[4] R.W. Date, I.W. Hamley, G.R. Luckhurst, J.M. Seddon and R.M. Richardson, Mol. Phys. **76**, 951 (1992).

original contains color illustrations

2.7.10 Pseudo-critical Behavior and Unbinding of Phospholipid Bilayers

J. Lemmich, J.H. Ipsen, T. Hønger, O.G. Mouritsen, *Department of Physical Chemistry, The Technical University of Denmark, Lyngby, Denmark,* Kell Mortensen, *Department of Solid State Physics, Riso National Laboratory, Roskilde, Denmark* and Rogert Bauer, Department of *Physics, Royal Veterinary and Agricultural University of Denmark, Frederiksberg, Denmark*

Phospholipid bilayers in aqueous solution display thermal phase transitions, one of which is the main phase transition, which predominantly involves chain melting within the individual bilayers. Results from a variety of experimental and theoretical studies have pointed to the possibility that the main transition in saturated phospholipid bilayers, although of first order, is close to a critical point. The proximity to a critical point has dramatic consequences for the physical properties both of the individual bilayer as well as for the collective properties of a multilamellar array. Specifically near the transition temperature, T_m, response functions like the bending rigidity blow up, with particular consequence of an enhancement of the interlamellar entropic repulsion forces,[1] and an anomalous swelling behavior.[2] In the present report we present results obtained from analysis of the small-angle neutron scattering (SANS) from multilamellar arrays of bilayers of deuterated phospholipids, DMPC-d_{54} and DPPC-d_{62}, in their main transition region. The main result from the study is that the lamellar repeat distance, d, for DMPC and the total thickness of the hydrophilic aqueous layers, d_A, for both DMPC and DPPC display distinct peaks at T_m. In contrast, the hydrophobic bilayer thickness, d_L, varies monotonously with temperature through the transition region, although rather abruptly on the fluid side of T_m. The anomalous swelling in d on the fluid side of the transition can for both DMPC and DPPC be rationalized in terms of pseudo-critical behavior near the pseudo-critical temperature, T*: $d(T)-d_o \propto (T-T^*)^{-\psi}$, with $\psi=1$. d_0 is the repeat distance in the fluid phase far from the phase transition. We suggest that the observation of the onset to a power-law singularity for the lamellar repeat distance, which, however, only partially develops because of the intervention of a first-order phase transition at T_m, may be understood within the framework of the theory of critical unbinding transitions for interacting membranes.[3] We believe that our results represent the first experimental observation of a phenomenon that in a quantitative manner can be directly related to critical unbinding of interacting lipid membranes.[4]

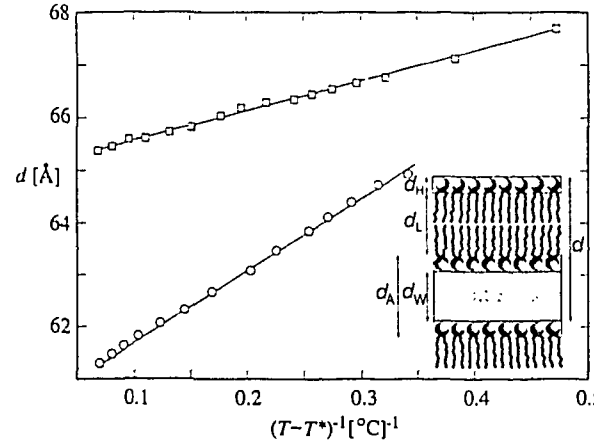

Fig.1. Plot of reduced lamellar repeat distance $d(T)$ as a function of inverse distance $(T-T^*)^{-1}$ to the pseudocritical temperature T^*. The insert shows a schematic representation of the different layers within the multilamellar stack.

[1] Helfrich, W., Z. Naturforsch. 33, 305 (1978).
[2] Honger, T., Mortensen, K., Ipsen, J.H., Lemmich, J., Bauer, R., and Mouritsen, O.G., Phys. Rev. Lett. 72, 3911 (1994).
[3] Lipowsky, R., and Leibler, S., Phys. Rev. Lett. 56, 2541 (1986).
[4] Lemmich, J., Mortensen, K., Ipsen, J.H., Hønger, T., Bauer, R., and Mouritsen, O.G., Phys. Rev. Lett. 75, 3958 (1995).

2.7.11 Micelles of Mixed Surfactants

T.-L. Lin, *National Tsing-Hua University, Hsin-Chu, Taiwan,* J. Samseth, *Institute of Energytechnology, Kjeller, Norway* and K. Mortensen, *Department of Solid State Physics, Riso National Laboratory, Denmark*

Many amphiphilic molecules (surfactants) form micellar aggregates in aqueous solutions. In practical applications, the desired properties it is often obtained by mixing different surfactants or co-surfactants. The basic understanding of association properties of micelles formed by mixing different surfactant molecules is therefore a subject which beyond general basic interests have important implication for practical use. Theoretical modelling of mixed micelles is essential for the detailed understanding. Recently, thermodynamic models have been applied to describe the aggregation behavior of mixed surfactants-alcohol aggregates, mixed nonionic micelles, and mixed ionic micelles. Some experimental studied on mixed micellar systems have also been performed in recent years.

We have made structural studies of aqueous solution on a system of mixed dihexanoylphosphatidylcholine (diC_6PC) and diheptanoyl-phosphatidylcholine (diC_7PC), which are both synthetic zwitter-ionic surfactants. In the mixed state they associate into *mixed micelles*. The structures and thermodynamic properties of pure one-component diC_6PC and one-component diC_7PC micelles have previously been extensively studied by small angle neutron scattering (SANS). diC_6PC was shown to associate in globular micelles while diC_7PC forms polydisperse rodlike micelles i aqueous solutions. Since the properties of diC_6PC and diC_7PC thus are well characterised, the mixed diC_6PC and diC_7PC micellar system is an ideal model system for studying association behavior of mixed micelles. SANS was used to study the mixed diC_6PC and diC_7PC micelles at various mixing ratios. The measured SANS spectra, which show that the mixed micelles have a rod-like form, will be analysed by using indirect transform method to determine the size distribution of the mixed micelles. It was shown previously that the formation and growth of pure diC_7PC rodlike micelles can be well described by the socalled "ladder" thermodynamic theory. A thermodynamic theory for ideally mixed two-component rodlike micelles can be derived in close analogy with this one-component theory. The SANS results will be compared with that predicted by this thermodynamic theory.

Preliminary analysis indicates that the thermodynamic theory for the developement of the mixed rodlike micelles can be successfully used in characterizing the mixed rodlike micelles formed by mixing diC_6PC and diC_7PC. The indirect transform method was used to obtain the size distribution of the rodlike micelles, and gives results which seems to be in good agreement with that predicted from the thermodynamic theory. There is also good agreements between the experimentally determined mean aggregation number of the mixed micelles and that predicted by the thermodynamic theory.

2.7.12 Microstructural Studies of Bile Salts by Small Angle Neutron Scattering

F. Lopez and J. Rouch, *University of Bordeaux, CPMOH CNRS URA283 France*, J. Samseth, *Institutt for Energiteknikk, Physics Department, Kjeller, Norway*, E Rosenqvist, *National Institute of Public Health of Oslo* and K. Mortensen, *Department of Solid State Physics, Riso National Laboratory, Roskilde, Denmark*

Scientist from the National Institute of public health of Oslo have prepared a complex vaccine against serogroup B meningococcal disease from a B : 1.7, 16 meningococcal strain (44/76) using a bio-detergent Sodium Deoxycholate (NaDC). A crucial step in the production of the vaccine consists in determining thephysico-chemical properties of Sodium Deoxycholate in aqueous solutions. The main aim of our work is then devoted to the study of the self aggregation patterns of pure NaDC and to the determination of their colligative properties. Bile salts properties in aqueous solutions were investigated by Small Angle Neutron Scattering (SANS), Quasi-elastic Light Scattering (QELS), Electrical conductivity and Time Domain Reflectometry (TDR) as a function of pH, temperature and detergent concentration. The structural investigations reveal a rod-like association which appears to be strongly dependent on the pH (as seen in Fig. 1) and ionic strength. The radius and length of such conformations compare reasonably well with the dimensions of helical models and rods previously observed by Small Angle X-Ray Scattering (SAXS) and Electron Spin Resonance (ESR). We also show the existence of two critical micellar concentrations (CMC). The lower one corresponds to an increase of the pH.

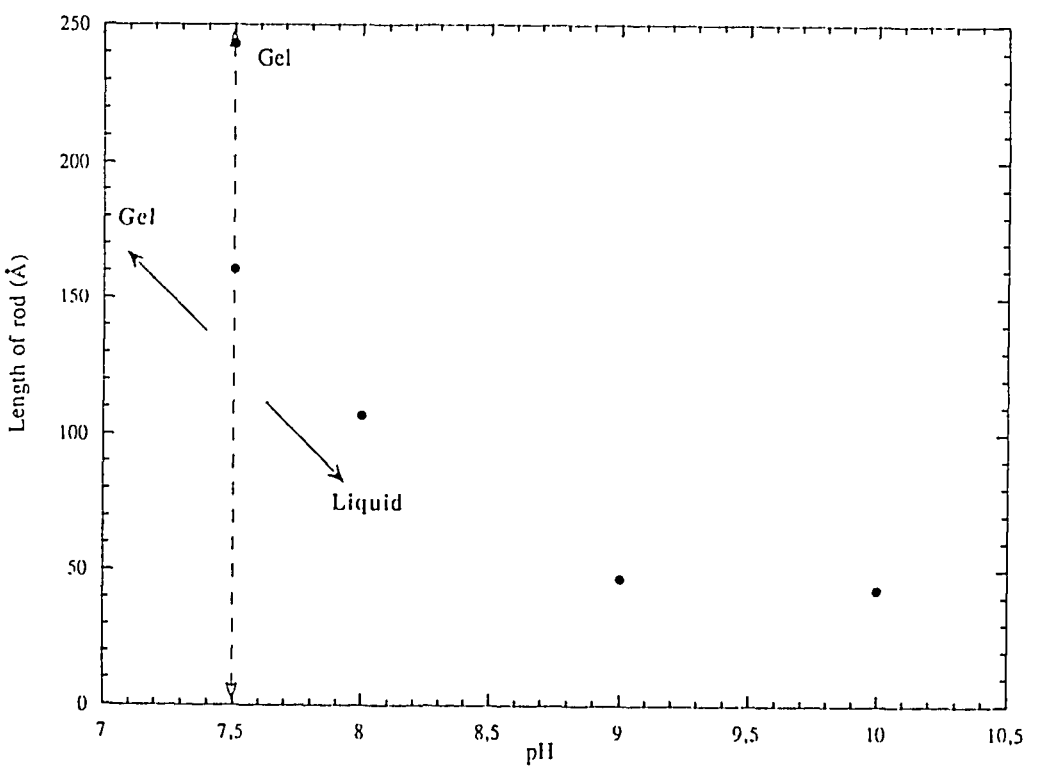

Fig. 1. Increase of the micellar rod's length fron 43Å down to 161Å as the pH of the pure NaDC solution is decreased from pH-10 toward the liquid-to-gel transition at pH-7.5. The radius of the rod-like micelles is confined within the range 8-15Å.

2.7.13 Shear Induced Orientation of a Hexagonal Phase in a Diblock Copolymer Melt

K. Almdal, K. Mortensen, *Department of Solid State Physics, Riso National Laboratory, Denmark*, T. Tepe, M.F. Schulz, J. Zhao, M. Tirrell, and F.S. Bates, *Department of Chemical Engineering and Materials Science, University of Minnesota, USA*

AB diblock copolymers, which are characterised by their overall molar mass and the volume fraction, f, of A, are known to form a range of ordered structures. In particular a phase consisting of hexagonally packed A-rich rods in a B-rich matrix exist in a range of f-values close to f=0.3. The hexagonal phase has been shown to align in flow fields with the cylinders parallel to the flow direction as first discovered by Keller et al.[1] We have investigated[2] the behaviour of a poly(ethylene)-*block*-poly(ethylene-*alt*-propylene) (PE-PEP) diblock copolymer that contains 37% by volume PE and is characterised by, M_n=1.70×10^{5}g/mol, M_w/M_n=1.05 and has an order-disorder transition temperature, T_{ODT} of 189±1°C. The block copolymer was placed in a shearing device that allows the sample to be subjected reciprocating shear while being structurally characterised by small angle neutron scattering (SANS). The geometry of the experiment was such that the shear was in the x-direction, the shear gradient and the neutron-beam in the y-direction. A 1.2 mm thick piece of the sample was placed in the device and sheared with an amplitude of the triangular wave of 100%. In an experiment at 130°C the sample was sheared for 30 min with a shear rate of 0.35s^{-1}. This produced a SANS pattern that persisted after the cessation of the shear, with two strong spot along the q_z-direction in accordance with cylinders aligned with the x-direction. Unfortunately SANS experiments with the beam along the y-direction do not permit distinction between the possible different crystallographic arrangements where the cylinders are lined up with the x-direction. The sample was therefore removed from the shearing device and quenched in liquid nitrogen. After the sample was reheated to room temperature it was cut in 1 mm thick stripes thereby making SANS analysis with the beam along the x- and z-directions, respectively, possible. These experiments revealed that the (10) plane of the hexagonal structure was parallel to the xz-plane. In another experiment a sample was sheared while cooling from 195°C to 185°C; *i.e.* while cooling through the ODT. In this case similar cutting revealed that the (10) plane was parallel to the xy-plane. Thus shearing close to and well below T_{ODT} produced different crystallographic orientations.

[1] A. Keller, E. Pedemonte, F .M. Willmouth, *Nature*, **225**, 538 (1970).
[2] T. Tepe, M. F. Schulz, J. Zhao, M. Tirell, F.S. Bates, K. Mortensen, K. Almdal, *Macromolecules*, **28**, 3008 (1995).

2.7.14 A Small-angle Scattering Study of the Shape and Structural Interactions of Microemulsion Droplets

L. Arleth and J. Skov Pedersen, *Department of Solid State Physics, Riso National Laboratory, Denmark,* T. Zemb, *Service de Chimie Moléculaire, CE Saclay, France*

At certain compositions and temperatures ternary mixtures of water, alkane and the amphiphilic molecule bis(2-ethylhexyl)sodium sulfosuccinate (AOT) form clear and thermodynamically stable solutions of almost spherical AOT-covered water droplets in alkane. The aim of the present study is to determine how the size, polydispersity and shape fluctuations of the microemulsion droplets depend on the alkane type and to investigate the influence of the shape of the droplets on the structural interactions. For this purpose small-angle neutron and x-ray scattering measurements on different AOT/water/decane and AOT/water/isooctane microemulsions are performed. In the figure below the scattering data of a microemulsion with a droplet volume fraction of 15% are shown. The different data sets corresponds to different scattering contrasts. When the microemulsions are constituted by AOT/D_2O/decane or AOT/H_2O/-deuterated decane the contrast for neutrons is close to being that of solid spheres. A shell contrast is seen for the x-ray data on AOT/D_2O/decane and for the neutron data on AOT/D_2O/deuterated decane. The bulk and shell contrasts are reflected in the slope of the scattering data at high scattering angles. For the bulk contrasts the slope is q^{-4} and for the shell contrasts it is q^{-2}. The large amount of information obtained by measuring the same concentrations with different contrasts should allow a very precise determination of the size, polydispersity and shape fluctuations of the microemulsion droplets. Similar data sets obtained on dilution series of the droplets show that the AOT microemulsions are also very well suited as model systems for the study of structural interactions in dense solutions of objects being close to spherical.

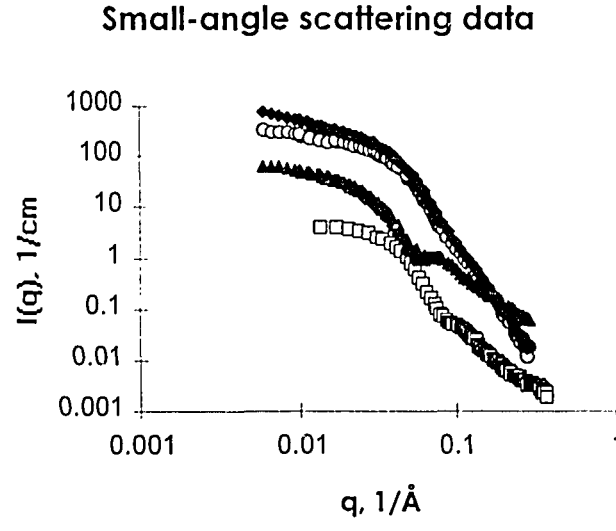

Fig. 1. Normalized small angle scattering data for different contrasts of an AOT/water/decane micro-emulsion having a droplet volume fraction of 15%. ◆ neutron data of AOT/H_2O/deuterated decane. ○ neutron data of AOT/D_2O/decane. ▲ neutron data of AOT/D_2O-/deuterated decane. □ x-ray data of AOT/D_2O-/decane. The x-ray data are divided by a factor of 10.

2.8 Polymers

2.8.1 Neutron Reflection from Lithographic Polymers

C. Moore and S. Roser, *School of Chemistry, University of Bath, UK*, M. C. Gerstenberg, *Department of Solid State Physics, Riso National Laboratory, Denmark*

Lithography is a printing method that utilises differences in surface chemical properties to provide a contrast between image and non-image regions. Thin mixed films based upon the novolak-diazoquinone resin are used extensively in the printing and photoresist industries as positive resists.

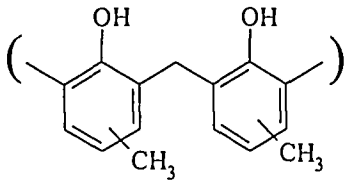

Novolak

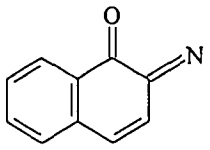

Diazoquinone

Exposure of the diazoquinone in UV radiation leads to the formation of an indene carboxylic acid, thereby significantly increasing the solubility of the film in the developer, which then leads to the image formation. As both components are soluble in the developer to some degree, a detailed knowledge of the dissolution process is desirable to both achieve maximum resolution and new film technology.

Thin novolak films (approximate 600Å thickness) were prepared by spin coating onto a single crystal silicon wafer. The thickness of the coated novolak film was determined to approximately 630Å by neutron reflection at Risø. Further reflectivity profiles were obtained for the same sample in 3 different solvent systems, H_2O, D_2O and 0.4×10^{-5} contrast H_2O / D_2O. Results suggest that there was significant retention of solvent in coated films, however baking for 5 minutes at 100°C was sufficient to remove this. Immersion of baked films into H_2O and D_2O systems produced a decrease in thickness of the film whilst in contact with water of approximately 10% of the original film thickness. This is believed to be due to compression of the polymer film. Film/air reflectivity profiles after being removed from the aqueous systems show an increase in film thickness over the original value due to the immersion process. This would imply that there is water penetration into the film to some degree.

Future studies will include a comprehensive investigation into partially dissolved baked novolak films. This will be achieved by immersing the film into a dilute basic developer (KOH) and subsequenly drying. The developed interface will then be probed by reflectivity on the film/air and a range of film/solution systems.

2.8.2 Artificial Muscles: Polymerbased Materials for Actuator Purposes

P. Sommer-Larsen, I. Johannsen and K. Bechgaard, *Department of Solid State Physics, Riso National Laboratory, Denmark,* K. West, *Department of Physical Chemistry, The Technical University of Denmark,* S. Skaarup, *Physics Department, The Technical University of Denmark,* P. Gravesen and P. E. Pedersen, *Corporate Technology and Research, Danfoss A/S, Denmark*

The actuation of robots and mobile machines is at present preferentially performed with pneumatics, hydraulics and electric motors. Although these actuators are usually powerful, they are nonetheless imprecisely controlled. An area like dexterous robotics grippers will require more versatile actuators that allow for a high degree of motoric control based on microprocessor technology. There is a need for an versatile electrically controlled actuator, capable of expanding or contracting linearly and performing in a manner that resembles the natural skeleton muscles. Actuators based on polymeric materials may be able to fulfill this need.

A project aimed at studying the feasibility of using polymers as basic materials in the construction of such actuators is carried out in collaboration between the industrial company Danfoss A/S, The Technical University of Denmark and Risø National Laboratory. The main emphasis is on actuators for robotics grippers, but the project also focuses on industrial valves and microanalysis systems (valves and pumps). The project is given the acronym ARTIST.

The aim of the project is to obtain knowledge about polymer-based actuators to enable the participants to judge whether such materials have the potential to form the basis for a new actuator technology. This knowledge will also enable the partners to decide on their participation in future development and research projects in the field. In a longer perspective, the project is also of value in its potential for initiating a national Danish research effort in this area.

The feasibility project involves a series of activities: A report has been prepared that specifies requirements to be fulfilled for both actuators and actuator materials for different applications.

An important aspect of the project is the retrieval, systematizing and analyzing of scientific material, data and information on applications of known polymeric materials with actuator properties. A database containing 1500 references to articles and patents in the area has been established. Leading research institutions and companies working in the area will be contacted

Part of the project consists of converting the knowledge that is acquired and generated during the project into new concepts for actuators of practical use. Known systems as well as new ideas for concepts and materials generated in the project will be analyzed with respect to the requirements established in the above-mentioned report.

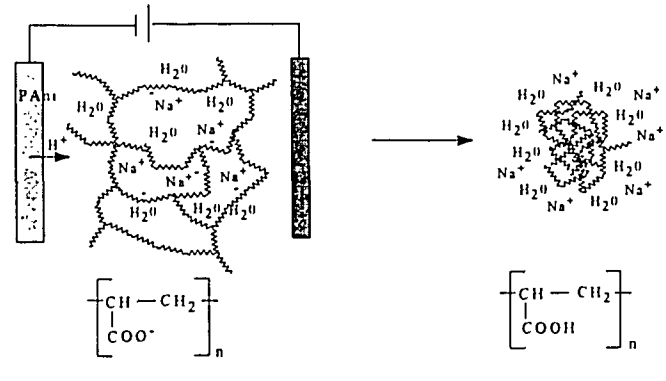

Fig. 1. Polymeric system with actuator properties.
Partly ionised poly(acrylic acid) swollen in aqueous solution will contract strongly in acidic solution. Flexible electrodes made from conducting polyaniline (PAni) may produce the necessary change in pH.

2.8.3 Molar-Mass Dependence of the Lamellar Thickness in Symmetric Diblock Copolymers

C. M. Papadakis and D. Posselt, *IMFUFA (Institute of Mathematics and Physics), University, Denmark,* K. Almdal, *Department of Solid State Physics, Riso National Laboratory, Denmark*

Diblock copolymers in the bulk state are known to undergo a phase transition, the so-called order-disorder transition (ODT), from a disordered state to an ordered state where various morphologies exist, *e.g.* spheres forming a cubic lattice, hexagonally packed rods or, in case of symmetric diblock copolymers a lamellar structure.[1] The lamellar thickness, D, is by mean-field theories predicted to scale with the chain length of the polymers, N: $D \propto N^{\delta}$ where $\delta=2/3$ deep in the ordered state.[2] In the disordered state and in the weak segregation limit the chains are assumed to be Gaussian: $R_g \propto N^{1/2}$.

In the present study, a homologous series of ten symmetric polystyrene-*block*-polybutadiene (SB) samples was synthesized anionically[3] yielding polymers with narrow molar mass distributions covering a large range of molar masses: 9200-183000g/mol. SB was chosen because of its relatively large Flory-Huggins interaction parameter, χ, which allows measurements deep in the ordered state. Different methods for sample preparation were used (annealing, solvent-casting with a good, non-selective solvent and shear-alignment) in order to ensure thermal equilibrium. Solvent-casting and shear-alignment lead to oriented samples, whereas the annealed samples are 'polycrystalline'. The values of the lamellar thickness at a fixed temperature (150°C) were determined by small-angle X-ray scattering using IMFUFA's Kratky compact-camera.[4] High molar-mass samples were investigated with small-angle neutron scattering at Risø.

The following conclusions can be drawn:

1) The resulting lamellar thicknesses for the different preparation methods were found not to differ more than 3% (Fig. 1).
2) An exponent $\delta=0.72\pm0.01$ is found in the ordered state, *i.e.* a slightly higher value than the mean-field prediction.
3) Also in the disordered state the chains are non-gaussian in accordance with dynamic light scattering results where stretching was found to set in deep in the disordered state ($\chi N \approx 5$).[5]

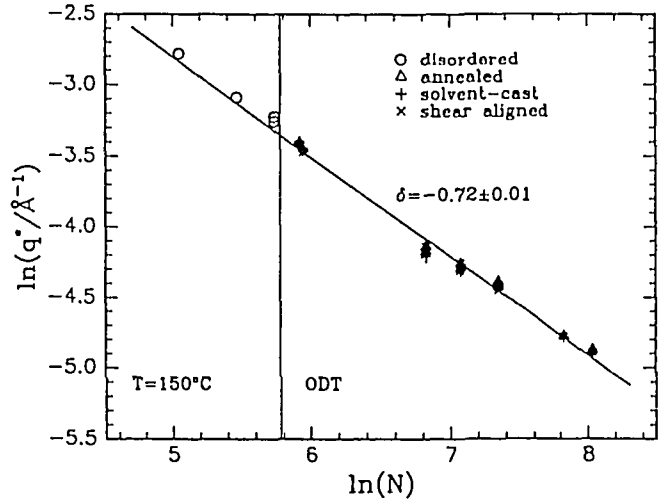

Fig. 1: Scaling of the peak position, $q^* = 2\pi/D$, with the chain length, N. The vertical line indicates the ODT as determined in dynamic mechanical measurements.

[1] F.S.Bates and G.H.Fredrickson, Annu.Rev.Phys.Chem. **41**, 525 (1990).
[2] E.Helfand and Z.R.Wasserman, Macromolecules **9**, 879 (1976). A.N.Semenov, Sov.Phys.JETP **61**, 733 (1985).
[3] S.Ndoni, C.M.Papadakis, F.S.Bates, and K.Almdal, Rev.Sci.Instrum. **66**, 1090 (1995).
[4] C.M.Papadakis, K.Almdal, and D.Posselt, Il Nuovo Cimento **D16**, 835 (1994).
[5] C.M.Papadakis, W.Brown, R.M.Johnsen, D.Posselt, and K.Almdal, to be published in J.Chem.Phys **1** (1996).

2.8.4 Laboratory-scale Setup for Living Anionic Polymerization under Inert Atmosphere

S. Ndoni, K. Almdal, *Dept. of Solid State Physics, Riso National Laboratory, Denmark*; C. M. Papadakis, *Dept. of Mathematics and Physics, University of, Denmark* and F. S. Bates, *Dept. of Chemical Engineering and Materials Science, Minneapolis, Minnesota, USA*

Since the discovery by Szwarc[1] that anionic polymerization, under certain conditions can be 'living', that is termination-free, the technique has been developed to allow controlled synthesis of polymers with a variety of structures. Thus living anionic polymerization is the reaction mechanism of choice for the preparation of very well-controlled homo- or co -polymers having very narrow molar mass distributions in a wide range of molar masses, architectures (linear, star-shaped, macrocycles, etc.) and chemical structures. Such samples are vital in experimental polymer physics and the technique of living anionic polymerization under inert atmosphere[2] offers a readily feasible and self-sufficient method for the synthesis of such samples. As the synthesis of one sample (easily up to 100g) by the inert atmosphere technique takes only a few days, quick feedback between synthesis and physical characterization is possible.

The main parts of the setup are the vacuum-argon (or nitrogen) distribution line (called the fixed part, see Fig.1) and the polymerization system. The vacuum-argon distribution line provides vacuum of the order of 10^{-3} mbar or lower and very pure argon (impurity less than 1ppm). In many cases the active centres at the growing chain-ends are very reactive (organometallic strong bases that react with water, alcohols and with oxygen, terminating the polymerization). Therefore a thorough drying and purification of all the components coming into contact in the polymerization process, is imperative for a well controlled synthesis. The drying procedures of the glassware combine heat treatment with vacuum-argon flashing; the purification of argon, solvents and monomers comprises reactions with powerful drying agents combined with reflux/distillation operations under vacuum or argon. The polymerization reaction is carried out in a specially designed glass reactor under slight overpressure of argon. Examples of typical monomers (co)polymerized by the use of the inert atmosphere technique are styrene, dienes (f.ex. 1,3-butadiene and isoprene), alkyl methacrylates, cyclic ethers (f.ex. ethylene oxide), siloxanes (f.ex. the cyclic trimer of dimethyl siloxane), etc. The degree of reaction control is similar to that achieved by the more traditional high vacuum technique, but the time required to prepare one (co)polymer is roughly ten times shorter.

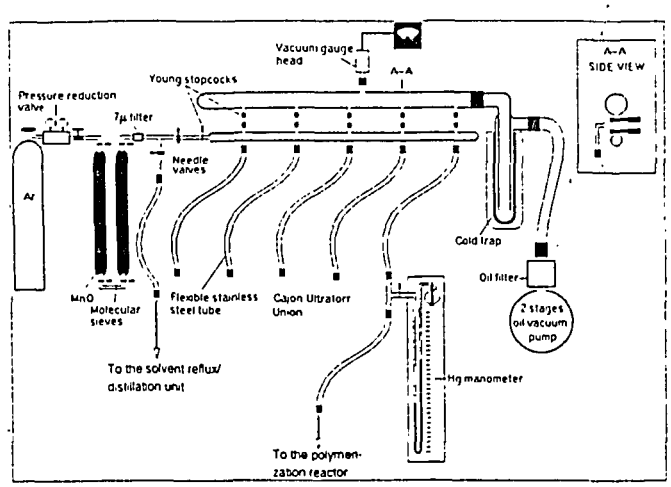

Fig.1. Drawing of the fixed part of the setup. From left to right: argon purification and flow-control system, vacuum-argon distribution manifold and pumping system. The insert shows the cross-section A-A in the main figure.

[1] M. Szwarc, Nature, **178**, 1168 (1956).
[2] S. Ndoni, C. M. Papadakis, F. S. Bates and K. Almdal, Rev. Sci. Instrum. **66** (2), 1090 (1995).

2.8.5 Side-Chain Liquid Crystalline Polyesters for Optical Information Storage

S. Hvilsted, *Department of Solid State Physics, Riso National Laboratory, Denmark*, P.S. Ramanujam, *Optics and Fluid Dynamics Department, Riso National Laboratory, Denmark*, H.W. Siesler, *Department of Physical Chemistry, University of Essen, Germany*, P. Magagnini, *Chemical Engineering Department, University of Pisa, Italy*, and F. Andruzzi, *CNR, Chemical Engineering Department, University of Pisa, Italy*

LICRYPOIS is a collaborative focused fundamental research performed by the above consortium with the objective to develop materials for optical information storage. The project is supported financially in part by the European Economic Community in the framework of the Brite/EuRam programme and the project management is in the department.

The holographic storage achieved in thin films of cyanoazobenzene side-chain liquid crystalline polyesters have now been permanent for almost 4 years. The stored information can be erased by heating the films to about 80°C and after cooling to room temperature, the film can be reused.[1]

New polyesters including copolyesters employing a mixture of two diacid precursors or a mixture of two diols have been prepared, characterized and investigated with respect to the optical storage potential. X-rays from synchrotron radiation have been used to characterize irradiated polyester films. Fourier-Transform infrared polarization spectroscopy has been applied to investigate on-line laser induced orientational behaviour and thermal stability of the photo-induced alignment.

The biphotonic high density storage of text and gratings as holograms with a typical size of 1 mm was investigated in a side-chain liquid crystalline polyester. This required the use of two wavelengths, typically 488 nm from an Argon ion laser and 633 nm from a HeNe laser or 670 nm from a diode laser, in a cyanoazobenzene side-chain polyadipate. It was also observed that the red laser could be turned on several minutes after the Argon laser was switched off still creating a grating in a polarization holographic set-up. Since this involves two photons separated as much as 10 minutes in time, we call this a biphotonic process, in order to distinguish it from a non-linear two-photon process, which requires the simultaneous presence of two photons. An explanation has been found on the basis of experimental observations of optical and FTIR absorption spectra.[2] It has been shown experimentally for the first time that a red laser beam at 633 nm causes *cis-trans* (Z-E) transitions in azobenzene. The lifetime of the *cis* state has been measured using both optical and infrared spectroscopy and has been found to approximately 120 minutes in the cyanoazobenzene polyadipate.

Atomic force and scanning near-field optical microscopic investigations on thin polyester films exposed to two orthogonally circularly polarized laser beams have revealed that, immediately following laser radiation, a topographic surface grating structure appears.[3] The time development of the grating structure was followed by atomic force microscopy for 20 hours by repeatedly scanning the same area of the film. A pronounced increase of surface roughness has been found to take place, which can be attributed to a reordering of the aggregated phase preserving the stored information. A near-field optical microscopic scanning of the grating reveals that the structure is also optically anisotropic.

---

[1] S. Hvilsted, F. Andruzzi, C. Kulinna, H.W. Siesler, P.S. Ramanujam, Macromolecules **28**, 2172 (1995).
[2] P.S. Ramanujam, S. Hvilsted, I. Zebger, H.W. Siesler, Macromol. Rapid Commun. **16**, 455 (1995).
[3] P.S. Ramanujam, N.C.R. Holme, S. Hvilsted, submitted to Appl. Phys. Lett.

2.8.6 The Optical Anisotropic Potential in New Azobenzene Side-Chain Polyesters

M. Pedersen, S. Hvilsted, *Department of Solid State Physics, Riso National Laboratory, Denmark*, N.C.R. Holme, P.S. Ramanujam, *Optics and Fluid Dynamics Department, Riso National Laboratory, Denmark*, and J. Kops, *Department of Chemical Engineering, The Technical University of Denmark, Denmark*

A number of new potentially mesogenic azobenzene based diols have been synthesized with the aim to undertake a systematic study of the influence of the substituent in the 4-position of the azobenzene photochromic moiety. It is well-known that the "electronic" properties of the substituent being either a single atom or an ensemble of atoms forming an entity or a group effectively contributes the acceptor part of the particular azobenzene chromophore and thus plays a decisive role in the dipole moment of the chromophore. However, at present the influence of the chromophore dipole moment on the laser induced anisotropy in the polyesters is unknown. Neither does a model predicting the behaviour or the correlation exist.
The choice of substituents was originally based on theoretical computer calculations of dipole moments of the *trans* 4-substituted azobenzene side-chain diols by use of *HyperChem*™. A large variation in dipole moments was sought. The diol dipole moments range between 3.3 Debye (**H**-substituted) and 9.3 Debye (NO_2-substituted) with the reference **CN**-substituted in between (5.5 debye). In addition, attempts to research the influence of symmetry, steric hindrance and bulkiness motivated choices of substituents; finally the influence of halogens was investigated. The entire list of substituents now comprises: **CN**, NO_2, OCH_3, **H**, CF_3, CH_3, n-C_4H_9, C_6H_5, **F**, **Cl** and **Br**. After going through an elaborate purification procedure for the diols the polyesters were prepared in a stepwise polycondensation.
The acceptor properties of the particular substituents are indirectly reflected in the visible absorption maximum, λ_{max}, since the rest of the chromophore and for that matter the rest of the polyester matrix is exactly the same. It should be pointed out that the absorption behaviour of as well the phenolic azobenzenes as the azobenzene side-chain diols is very similar to that of the corresponding polyester. This, of course, is expected since the azobenzene chromophore is carried through from the phenolic azobenzenes to the polyesters. The eleven azobenzene side-chain polyesters have λ_{max} in the range from 348 nm (**H**-substituted = "**H**") to 377 nm ("NO_2"). The effective spectral window is thus only 30 nm in all these 4-substituted azobenzene side-chain polyesters. All new 4-substituted azobenzene side-chain polyesters could be prepared in medium to high molar masses. From the determined values it can be concluded that none of the new substituents precludes the formation of polyester materials with high molar masses. In fact, all the new polyesters have molar masses comparable to all previously prepared "**CN**" polyesters. It is therefor concluded that neither the visible light absorption nor the molar masses of these new polyester materials prevent the laser induced optical anisotropy necessary for optical information storage. Inital investigations on holographic storage were performed on thin films of the new "NO_2", "**CN**", "OCH_3", "**H**", "CF_3", "CH_3", "**F**", and "C_6H_5" polyesters. These investigations clearly show that "**CN**" is the best for holographic storage at room temperature. In addition, anisotropy measurements have been performed in the films as a function of temperature. The induced anisotropy at room temperature is superior in "**CN**". However, a new computerized set-up for analyzing the laser induced optical anisotropy as a function of temperature reveals a surprising behaviour: Films of several new polyesters which have negligible anisotropy at room temperature show a reasonably high anisotropy at elevated temperature, typically in the temperature range 35 - 40 °C.

2.8.7 Ferroelectric Side-Chain Liquid Crystalline Polyesters

S. Hvilsted, E.T. Kristensen, *Department of Solid State Physics, Riso National Laboratory, Denmark*, and P.S. Ramanujam, *Optics and Fluid Dynamics Department, Riso National Laboratory, Denmark*

In the framework of The Danish Polymer Centre under the project dealing with polymers for optical applications an activity with potentially ferroelectric side-chain liquid crystalline polyesters has been initiated. This activity is aiming at the design of a photoactive polyester material with the necessary requirements for a potentially external and electrically stimulated fast phase change. One such basic requirement for ferroelectrical properties is chiral mesogenic moieties close to the photo addressable functionality. It is anticipated that optical information written in thin films based on these materials can be locally erased by applying an electric field in contrast to the global thermal heating utilized at present.

The synthetic strategy for the preparation of the necessary, chiral monomer building block was based on a commercially available optically active alcohol, S(-)-2-methyl-1-butanol. This was conventionally converted to the corresponding tosylat which was substituted with 4-nitrophenol at relatively moderate temperature. The formed crude product could as implied in literature not be purified by vacuum distillation. A number of attempts to optimize the purification by preparative liquid chromatography furnished a method which allowed purification in acceptable quantities by batch column chromatography. The optically active nitro compound was then reduced catalytically to the corresponding amine. This was conventionally diazotised and coupled with phenol to provide the chiral azophenol which again was coupled with either a bromohexyl or a bromodecyl ketal-protected diol precursor. After deprotection by acidolysis the chiral azobenzene diols were obtained.

Polyesters with both long, medium and short main-chain methylene spacing have been prepared in a melt transesterification between the chiral hexyl-spaced diol and the corresponding diphenyl esters. The initial optical storage investigations performed by use of polarizing two beam holography have demonstrated that diffraction gratings can be induced into thin films of these chiral polyesters. Moreover, the grating efficiency in the adipate based polyester (short main-chain spacing) is unexpectedly high and comparable to the best polyester architectures produced so far. The opto-electrical investigations have not been started yet.

2.8.8 Optical Storage in Peptide-Based Materials

R. H. Berg, S. Hvilsted, *Department of Solid State Physics, Riso National Laboratory, Denmark*, and P. S. Ramanujam, *Optics and Fluid Dynamics Department, Riso National Laboratory, Denmark*

In recent work, we have demonstrated that small peptide-based molecules offer a new framework for the design of photoanisotropic organic materials for use in holographic storage of information.[1] These molecules, referred to as DNO oligomers, are made up of ornithine units oligomerized by solid-phase synthesis through the δ-amino groups and with azobenzene side chains attached to the α-amino groups (Fig. 1). By a number of measures, they perform better than polymers currently available. Diffraction efficiencies near 100% of the maximum achievable were obtained from laser-induced holographic gratings formed in thin films of DNO oligomers containing two or more residues. The values measured are, by far, the largest found in a photoanisotropic organic material in zero electric field. The holograms formed are exceptionally stable and are not erased after exposure to 150^{0}C for extended periods. They can, however, be erased (locally) by exposure to circularly polarized light and reused several times without fatigue.

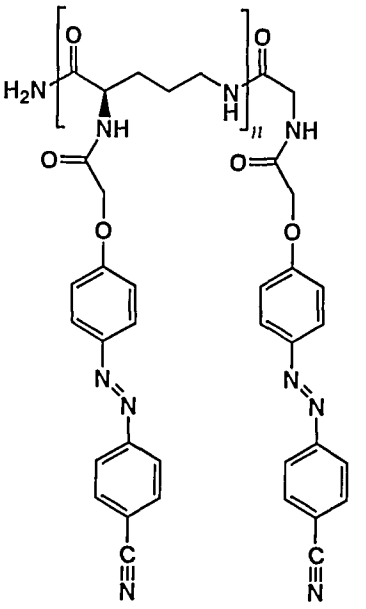

Fig. 1. Chemical structure of DNO oligomers.

[1] R. H. Berg, S. Hvilsted, and P. S. Ramanujam, (1995) submitted for publication.

2.8.9 Selectively Deuterium Labelling as a Tool for the Investigation of Laser Induced Segmental Orientation in Azobenzene Side-Chain Polyesters

C. Kulinna, S. Hvilsted, *Department of Solid State Physics, Riso National Laboratory, Denmark*, P.S. Ramanujam, *Optics and Fluid Dynamics Department, Riso National Laboratory, Denmark*

Holographic optical data storage performed in thin azobenzene side-chain polyester films is based on a light induced orientation of the photosensitive chromophores, resulting in a macroscopic optical anisotropy.
Storage capability, diffraction efficiency, long term stability as well as film-casting properties are highly sensitive to structural variations, effecting the motional flexibility of the attached chromophores and the polymer backbone.[1]
In order to optimize the mechanical and optical properties of these azobenzene side-chain polyesters through adjusting the variable structural parameters, a detailed characterization of the photoinduced alignment process on a molecular basis is essential.
For most analytical techniques (e.g. FTIR, Solid State NMR, SANS), deuterium - located at specific sites in a molecule - has proved to be a universal nucleus for selectively probing molecular orientation and dynamics, without considerably influencing chemical and physical sample properties.[2,3] Therefore, specifically deuterated precursors and monomers, carrying a deuterium content of more than 93 % were synthesised using exchange and reduction techniques. Subsequently, various side-chain polyesters have been prepared by a melt transesterification procedure from the available set of labelled monomers based on diphenyl adipate, diphenyl tetradecanedioate and 2-[ω-[4-[(4-cyanophenyl)azo]phenoxy]alkyl]-1,3-propanediols.
A complete characterization of monomers and polymers have been carried out by a combination of thermal (DSC, POM), chromatographic (SEC) and spectroscopic (NMR, FTIR) techniques.
Only an insignificant isotope effect could be observed.

FTIR spectroscopy with polarized radiation has been employed to monitor the photoinduced alignment of the individual structural polymer units. By focusing on the dichroic behaviour of (CD_2) vibrational modes and remaining (CH_2) absorptions, it became possible for the first time to perform a detailed analysis of the segmental orientation in adipate and tetradecanedioate based azobenzene side-chain polyesters upon irradiation. From the FTIR polarization spectra it is apparent that besides the azobenzene chromophore, the flexible aliphatic side-chain spacer as well as the polyester main chain experience a macroscopic alignment with respect to the laser beam polarization and therefore contribute to the observable optical anisotropy.[4]
Furthermore, evaluation of *trans-cis* configuration sensitive absorption bands, previously being superimposed by (CH_2) modes, offers experimental evidence for the photoinduced "rotational diffusion" process, supposed to be the basic mechanism responsible for the laser induced segmental orientation.

---

[1] S. Hvilsted, F. Andruzzi, C. Kulinna, H.W. Siesler, P.S. Ramanujam, Macromolecules **28**, 2172 (1995).
[2] H.W. Spiess, Pure & Appl. Chem. **57**, 1617 (1985).
[3] R.G. Kirste, H.G. Ohm, Makromol. Chem., Rapid Commun. **6**, 179 (1985).
[4] S. Hvilsted, C. Kulinna, P.S. Ramanujam, Nordic Polymer Meeting 1995, Helsinki, 14-16 Nov. 1995, Abstract p. 46.

2.8.10 Order and Disorder in Symmetric Diblock Copolymer Melts

J.H. Rosedale, F.S. Bates, *University of Minnesota, MN, USA,* K. Almdal and K. Mortensen, *Department of Solid State Physics, Riso National Laboratory, Denmark,* and G. Wignall, *Oak Ridge National Laboratury, TN, USA*

The thermodynamics and dynamic properties of symmetric diblock copolymer melts have been studied in the vicinity of the order-to-disorder (ODT) transition. In the homogeneous phase at high temperatures such melts are uniform in composition and the diblock chains obey Gaussian statistics. As the temperature is lowered, increasing incompatibility between the two blocks causes a microphase separation into lamellar mesophase. We have studied several partially deuterated symmetric diblock copolymers of PE-PEP and PEP-PEE, where PE, PEE and PEP are poly(ethylene), poly(ethyl-ethylene) and poly(ethylene-propylene), respectively.[1] A lamellar morphology was established for all temperatures below the ODT using small-angle neutron scattering (SANS) measurements with shear aligned specimens. As T_{ODT} is approached, the lamellar order weakens as evident by the loss of higher order SANS reflections (Fig.1) and azimuthal smearing of the principal equitorial scattering peaks (Fig.2). SANS and rheology experiments also provide evidence of composition fluctuations above the order-to-disorder transition temperature. The temperature range of these fluctuations in the disordered state depends on the degree of polymerization, in accordance with fluctuation theory. Coincident with the temperature where the fluctuations become apparent rheologically id a transition between slightly and highly stretched coils was observed by scattering.

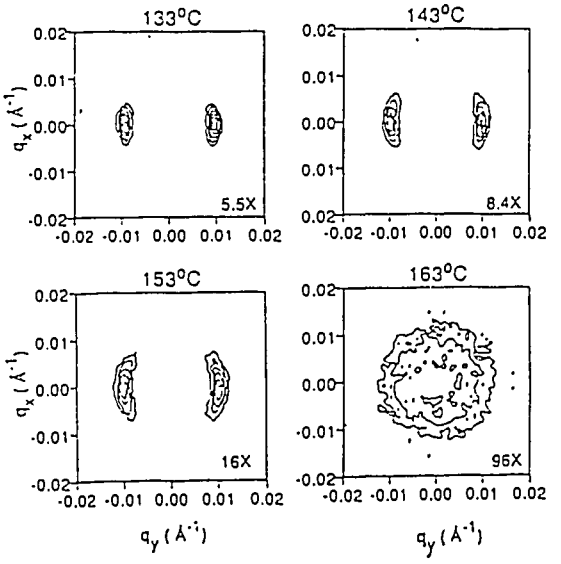

Fig. 1 Scattering function of shear oriented symmetric (f=0.50) PE-PEP (sample 6H) at several temperatures below T_{ODT}=139°C. The steady decrease in the number and intensity of the higher order reflections as T_{ODT} is approached indicates a softening of the composition profile, and weakening of long range correlations.

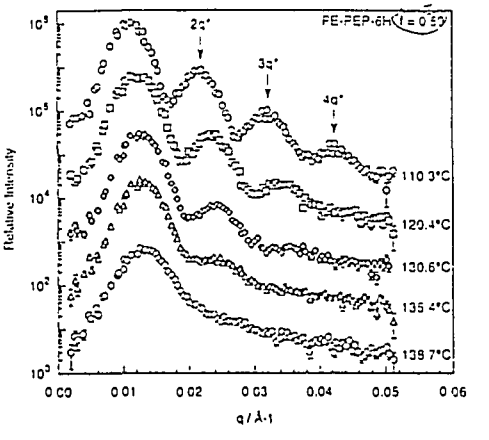

Fig. 2 Evolution of the diffraction peaks of shear oriented symmetric (f=0.49) PE-PEE diblock copolymer (sample 3D) in the q_x-q_y scattering plane while heating. The total intensity decreases and the diffraction peaks spread azimuthally as T_{ODT} is approached.

[1] Rosedale, J.H., Bates, F.S., Almdal, K. and Mortensen, K. Macromolecules **28**, 1429-1443 (1995).

2.8.11 Complex Layered Phases in Asymmetric Diblock Copolymers

I.W. Hamley, M.D. Gehlsen, A.K. Khandhur, K.A. Koppi, J.H. Rosedale, M.F. Schulz and F.S. Bates, *Chemical Engineering and Materials Science, University of Minnesota, USA*, K. Almdal and K. Mortensen, *Department of Solid State Physics, Riso National Laboratory, Denmark*

The phase behavior of mesomorphic systems has been the subject of intense interests over the last quarter century. Thermotropic liquid crystal phases have been investigated in detail since the late 1960's and extensive experimental data and theoretical description is available for the structure and ordering mechanism. The mesomorphism of lyotropic liquid crystals is less well understood. In particular the driving forces for the formation of complex bicontinous phases, which appear between the classical lamellar, hexagonally packed cylinders and body-centred cubic phase of spherical micelles have not yet been elucidated in detail. Block copolymers are a class of mesomorphic materials which beyond their attractive properties by their own, may provide important new insight into the general phase behavior of mesomorphic systems. In the classical picture, a diblock copolymer can form lamellar, hexagonally packed cylinder, or body centred cubic phases, depending on the volume fraction of the two blocks. Experimental studies on diblock copolymers near the order-disorder transition temperature (i.e. in the weak-segregation limit), have however shown a much richer polymorphism.[1] We have studied a series of polyolefin diblock copolymers with volume fraction f of the block with the larger segment length in the range of f= 0.63-0.75. Based on small-angle neutron scattering (SANS) and electron microscopy (EM) is it shown that the transition from lamellae (LAM) to hexagonally packed cylinder (HEX) phases normally occurs *via* intermediate complex layered phases that is characterised by in-plane hexagonal order.[2] One class of diblock forms a hexagonally modulated lamellar (HML) phase, then a hexagonally perforated (HPL) phase upon heating from lamellae, while another class in addition forms a hexagonally packed phase of modulated cylinders (MHEX). In the figure is these various phases illustrated. It is concluded that the detailed phase diagrams for diblocks copolymers depend on the molecular weight, which is important for the fluctuation, and on the conformational asymmetry between the two blocks.

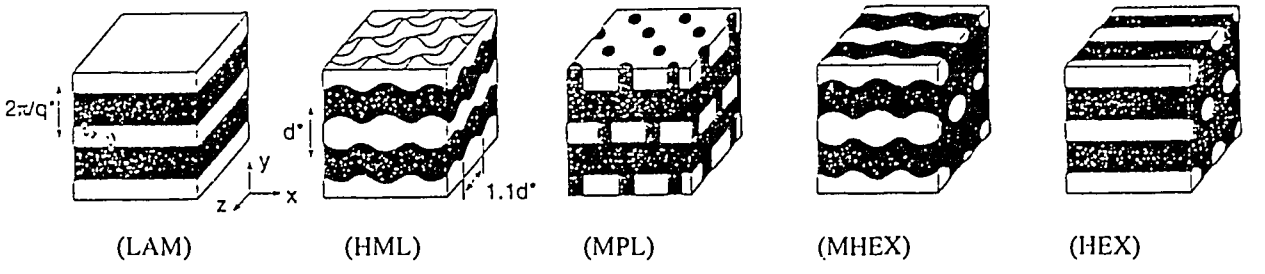

Fig. 1 Sketches of morphologies of diblock copolymers with f>0.5. LAM: lamellar; HML: hexagonally modulated lamellar; HPL: hexagonally perforated lamellar; MHEX modulated hexagonally packed cylinders; and HEX: hexagonally packed cylinders.

[1] Bates, F.S., Schulz M.F., Khandpur, A.K., Förster, S, Rosedale, J.H., Almdal, K., and Mortensen, K., Trans. Faraday Soc. 98 ,7-18 (1994).

[2] Hamley, I.W., Gehlsen, M.D., Khandpur, A.K., Koppi, K.A., Rosedale, J.H., Schulz, M.F., Bates, F.S., Almdal, K., and Mortensen, K., J. Physique II 4, 2161-2186 (1994).

2.8.12 Evidence of L_3-sponge Phase in a A(A/B)B-Triblock Copolymer Melt

R.J. Spontak, J.H. Laurer, *North Carolina State University, Raleigh, NC, USA,* J. Samseth, *Institute of Energy Technology, Kjeller, Norway,* and K. Mortensen, *Department, of Solid State Physics, Riso National Laboratory, Denmark*

Block copolymers, consisting of at least two contiguous sequences ("blocks") of covalently bonded, yet chemically dissimilar, monomer species, order into a variety of periodic morphologies when the blocks are sufficiently incompatible. Repulsion between adjoining blocks occurs at the shared junction site which, at equilibrium, resides within the interface between adjacent microdomains. Most conventional studies of AB diblock copolymers control interblock incompatibility through the temperature dependence of χ or by adjusting the molecular length N. In this study, we demonstrate that manipulation of monomer sequencing provides a viable means of varying χ while holding temperature and N constant. Chemical incorporation of a random A/B segment between the A and B endblocks reduces incompatibility without altering the overall copolymer composition. By varying the size of the A/B block, we have probed the spatial dependence of χ with a series of A(A/B)B triblock copolymers, composed of poly(styrene) (A) and poly(isoprene) (B), in which the midblock fraction (f_m) varies from 0 to 40 wt%. The morphological behavior of the neat copolymers and blends with homopolystyrene (hPS) has been characterized by transmission electron microscopy (TEM) and small-angle neutron scattering (SANS). Direct imaging of the morphologies exhibited by the blends has been provided by TEM studies performed at North Carolina State University, Raleigh, North Carolina, USA. Since TEM alone provides only a measure of local ordering in the blend system, SANS has been performed at Risø National Laboratory, Denmark. The results obtained corroborate the overall TEM observations, and provide a means of quantitatively determining the blend morphologies. In particular, the SANS results verify the development of the L_3 (sponge) phase in this block copolymer system. Quantitative measurements of the microdomain periodicity's, coupled with recent theoretical developments, permit evaluation of an effective χ as a function of f_m for the neat copolymers. We observe that at low f_m, the A/B segment acts to broaden the interface and enhance phase mixing, a trend that continues until a minimum in χ at f_m=0.3 is observed. Additionally, the effect of the random A/B block on blend morphologies is shown to be significant. Blends of the diblock (f_m=0.0) with a parent homopolymer form classic morphologies (lamellae, cylinders, and disordered micelles), while blends containing A(A/B)B copolymers with midblocks f_m>0.20 exhibit morphologies indicative of weakly-segregated copolymers.

2.8.13 Butterfly Pattern in an Uniaxially Stretched Triblock Copolymer Gel

N. Mischenko, K. Reynders, H. Reynaers, *Molecular Structure Chemistry, Catholic University of Leuven, Belgium,* and K. Mortensen, *Department of Solid State Physics, Riso National Laboratory, Denmark*

Triblock copolymers gels constitutes a relative new class of materials with promising properties. They are physical gels formed on the basis of self-assembling into a three-dimensional polymer network when mixed with a solvent which is good only for the mid-block polymer. We have studied the structural characteristics of various architecture (i.e. various relative volume fraction of each block) triblock copolymers with poly(styrene) as the outer blocks, and either poly(ethylene propylene), PEP, or poly(ethylene buthylene), PEB, as the soluble midblock. The block copolymers form a gel when dissolved in a homogen mixture of saturated aliphatic and alicyclic hydrocarbons (M_W=500) which is good only for the PEP and PEB. It was previously shown, that the triblock copolymers associate in spherical micelles with a dense core of PS, thus forming a network.[1,2] The glassy-state of PS makes the network permanent, resulting in a highly elastic material which can be stretched more than 1000% reproducible. When these type of materials are stretched uniaxially with a small amount, the network response is homogeneous as evident from the scattering pattern: the characteristic correlation peak changes from azimuthally isotropic to an ellipsoidal form, which however is not affine with the external axes-ratio.[3] Further stretching up to of the order of 100% causes the development of well resolved Bragg-like reflections, resembling a stretched induced ordering on the mesoscopic level. When the material is stretched beyond 100-500%, depending on polymer concentration, the scattering pattern develop into a new type, namely the 'butterfly' pattern as shown in the figure. I the highly stretched state, the inter-micellar correlation's perpendicular to the stretching axis is lost. Somewhat similar butterfly patterns have been observed in inhomogeneous polymer networks. We conclude from the scattering data that the micellar network consists of clusters of highly correlated micelles connected by a less regular system of polymer links.

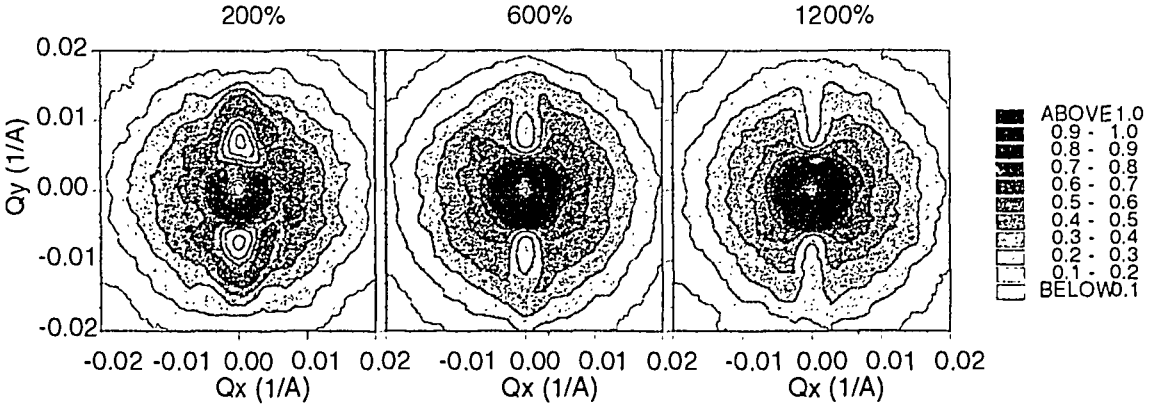

Fig. 1 Two dimensional scattering pattern of PS-PEP-PS gel when stretched 200-1000%.

[1] Mischenko, N., Reynders, K., Scherrenberg, R., Mortensen, K., Fontaine, F., Reynaers, H., Macromolecules **27,** 2345 (1994).
[2] Mischenko, N., Reynders, K., Koch, M.H.J., Mortensen, K., Pedersen, J.S., Fontaine, F., Gralus, R., and Reynaers, H., Macromolecules **28,** 2054 (1995).
[3] Reynaers, K., Mischenko, N., Mortensen, K., and Reynaers, H., Macromolecules *in the press.*

2.8.14 Composition Fluctuations and Coil Conformation in the Poly(Ethylene-Propylene)-Poly(Ethyl Ethylene) Diblock Copolymer as a Function of Temperature and Pressure

H. Frielinghaus, D. Schwahn and T. Springer, *Forschungszentrum Jülich, Germany*, K. Mortensen and K. Almdal, *Department of Solid Sate Physics, Riso National Laboratory, Denmark*

It is well established that many diblock copolymer melts undergo an order-to-disorder transition upon increasing temperature. The driving force for this transition is temperature dependence of the degree of incompatibility of the two blocks. In analogy with phase separation dynamics of binary polymer blends, this microphase separation is described using the Flory-Hyggins theory. Recently it was shown that pressure studies provide important additional information on the phase behavior of polymer blends. For example, it was shown in a scattering study witn an *in situ* pressure device how the pressure affects the phase behavior of polymer blends, mainly as a result of changes in free volume, and thereby changes in the fluctuations.[1] In diblock copolymers the influence of fluctuations is expected to have even more significant effects on the dynamics near the (microphase) separation temperature, since fluctuations completely changes the phase diagram. In the attempt to provide additional experimental data on the dynamics and thermodynamics near the microphase (or order-to-disorder) transition in diblock copolymers, we have accordingly conducted pressure dependent structural studies on the diblock copolymer melt poly(ethylene-propylene)-poly(ethyl ethylene) (PEP-PEE), which is a system that already has been extensively studied as a function of temperature.[2] The measurements showed that pressure markedly changes the order-to-disorder transition temperature: T_{ODT} increases with increasing pressure with a slope of 0.02K/bar. The PEP-PEE copolymer exhibit at lower temperatures an order-to-order transition, which however have only negligible pressure dependence. From the peak-position in the structurefactor, we can calculate the coil-dimension and thereby provide information on the microscopic compressibility. Such analysis shows that the coil compressibility decreases with increasing temperature and shows a maximum at T_{OOT}.

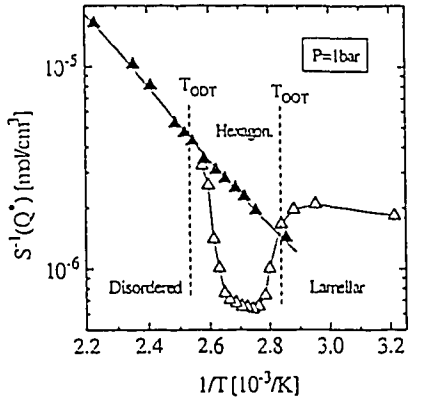

Fig.1 Inverse structure factor at the peak position for $q=q^*$ versus 1/T for P=1bar. Open symbols represents shear aligned samples, the solid symbols represents quenched samples

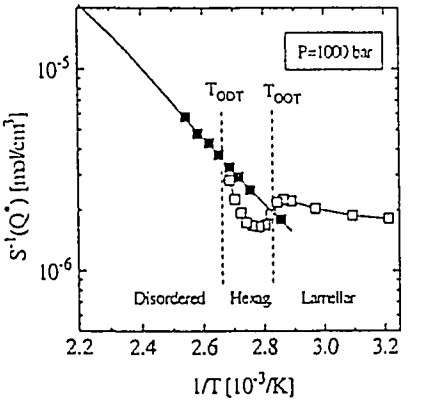

Fig. 2 Inverse structure factor at the peak position for q=q* versus 1/T for P=1000bar. Open symbols represents shear aligned samples, solid symbols represents quenched samples.

[1] Janssen,S.; Schwahn,D.; Mortensen,K.;Springer,T. Macromolecules **26**, 5587 (1993). Macromolecules **28**, 2555 (1995).

[2] Bates, F.S., Schulz, M.F., Khandpur, A.K., Förster, S., Rosdale, J.H., Almdal, K., Mortensen, K Faraday Discuss. **98**, 7 (1995).

2.8.15 Bicontinous L_3-Sponge Phase in a Binary Block-Copolymer - Water System

E. Hecht and H. Hoffmann, *Physical Chemistry, University of Bayreuth, Germany,* and K. Mortensen, *Department of Solid State Physics, Riso National Laboratory, Denmark*

Many block copolymers of poly(ethylene oxide)-poly(propylene oxide)-poly(ethylene oxide) PEO-PPO-PEO associate into micelles when mixed with water, as a result of the hydrophobic nature of PPO. Most studies on PEO-PPO-PEO in water have revealed spherical micelles, but also cylinder or worm like aggregates have been observed. The micellar form, as well as the critical micellation temperature and concentration can to a large extend be controlled by the detailed chemical design, i.e. overall molecular weight and the ratio between propylene oxide and ethylene oxide. Like small-molecular weight hydrocarbon surfactants, the PEO-PPO-PEO micelles can form a variety of lyotropic liquid crystalline phases, like lamellar, hexagonal and cubic phases. In small surfactant systems, the spontaneous curvature have important influence on the phase behavior. For ionic surfactants this curvature can be controlled by addition of electrolyte or cosurfactant, whereas nonionic surfactants often shows a temperature dependence. If the curvature of the polar/apolar interface is toward the hydrophobic part, spherical or (if the curvature is small) rod-like micelles are formed: the L_1-phase. Zero spontaneous curvature results in flat lamellae (L_α), while a small curvature toward the apolar part often leads to the L_3 phase which is a complex three dimensional bicontinuous phase. High curvature toward the hydrophobic part results in inverted micelles (L_2-phase). The phases therefore follows the sequence $L_1 \rightarrow L_\alpha \rightarrow L_3 \rightarrow L_2$. With the aim to possibly reveal a corresponding phase sequence for polymeric surfactants, have we studied an aqueous solutions of PEO-PPO-PEO triblock copolymers with relative small PEO-blocks, $EO_6PO_{36}EO_6$ abbreviated PE6200.[1] The measurements include small-angle neutron scattering, dynamic light scattering, DC-conductivity and calorimetry. The measurements clearly showed that also block-copolymer surfactants form complex phase rather similar to ordinary surfactants, even though the interface is expected to have different characteristics. The structural measurements reveals for the first time an L_3 in a block copolymer surfactant system.[1] The observed phase sequence, $L_1 \rightarrow L_\alpha \rightarrow L_3$, is similar to the corresponding observations in ordinary surfactant systems. The figure shows the scattering pattern in the L_3-sponge phase and the adjacent L_α-lamellar phase.

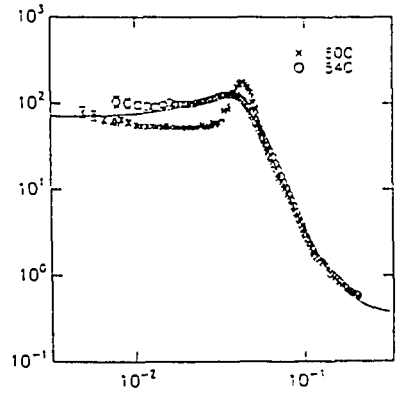

Fig. 1 Scattering function of 30% PE6200 in D_2O at T=50°C and T=54°C. The solid line represents a least square fit to the Teubner Strey function

[1] Hecht, E., Mortensen, K., and Hoffmann, H., Macromolecules **28**, 5465-6476 (1995).

2.8.16 Structural Studies of a New Poly(Ethylene Oxide) Based Triblock Copolymer in the Bulk and when Dissolved in Water

K. Mortensen, *Department of Solid State Physics, Riso National Laboratory, Denmark,* Gao, B., Kops, J., *Department of Chemical Engineering, Technical University of Denmark, Denmark,* and Y. Talmon, *Department of Chemical Engineering, Technion-Israel Institute of Technology, Haifa, Israel*

Amphiphilic macromolecules have in recent years attracted lots of interests within applied science as well as in basic research. The topic is extremely rich and offers great potential because of the amphiphilic character leads to association behavior which in many respect is an important extension of that of soaps and surfactants of small molecules. Amphiphilic macromolecules have already importance for a wide range of modern products, ranging from medicine and pharmaceutics products, to paints which is least harmful to the environments. The self-association of amphiphilic macromolecules gives in selective solutions rise to a wide range of phase behavior, including micelles of various form and size, complex structured microemulsions, and liquid crystalline phases. When block-copolymers are mixed in a solvent which is good for only one of the blocks, they self-associate into specific structures to avoid direct contact between solvent and the blocks which are not soluble. Most of the polymers which have been studied in relation to aqueous solutions, are based on poly(ethylene oxide), PEO, as the water soluble block. In particular the Pluronics, which have a hydrophobic poly(propylene oxide) mid-block, have been extensively studied[1] and have found widespread application. In recent years some related block-copolymers have been developed with the aim to provide an even broader range of amphiphilic materials for specific application. This include a new system with poly(isobutylene), PIB, as the hydrophobic mid-block.[2] We have performed structural studies on both bulk polymer samples and dilute aqueous solutions. In the bulk, PEO-PIB-PEO is dominated by an order-disorder transition at T=30°C resulting from melting of the PEO-blocks. In the disordered phase the material shows strong composition fluctuations. In the dilute solutions the PEO-PIB-PEO polymers associate in micellar aggregates. Both small angle scattering data and cryo-TEM studies show that these micelles are dominantly in form of worm-like micelles. The cryo-TEM pictures shows, however, that spherical micelles coexist with these dominating worm-like micelles. The diameter of these two types of aggregates are similar. In the figure is shown the scattering pattern of a sample of bulk PEO-PIB-PEO.

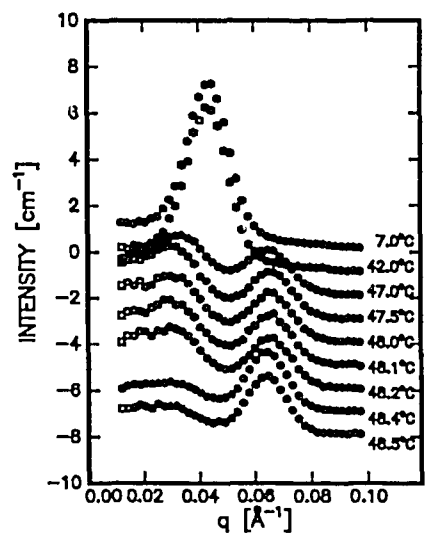

Fig. 1 Small-angle neutron scattering pattern of bulk PEO-PIB-PEO (the molecular weight is M_w=6000, 2000 for each of the three blocks). The correlation peak below T=30°C reflects the lammellar of alternating amorphous PIB and crystalline PEO. Above T=30°C, the correlation peak is due to incompatibility between PEO and PPO.

[1] K. Mortensen, J. Physics: Condensed Matter. *to be published.*
[2] B. Gao and J. Kops, Polymer Bulletin, 34, 279 (1995).

2.8.17 Structural Studies of the Bulk phase of Deuterated Pluronics: PEO-dPPO-PEO

K. Mortensen, *Riso National Laboratory, Denmark,* C. Booth, G.-E. Yu, T. Ryan and I.Hamley, *University of Manchester, UK,* W. Brown, *University of Uppsala, Sweden*

Triblock copolymers based on poly(ethylene oxide), PEO, and poly(propylene oxide), PPO, have in recent years attracted lots of interests, both within application and as model systems for polymeric surfactants. The systems are commercial available in a wide range of molecular architectures and sizes, under the names Pluronics or Poloxamers. Recently, we observed that bulk materials of these type of molecules, both the PEO-PPO-PEO type and the reverse PPO-PEO-PPO form lamellar phases at low temperature as a result of the crystallisation of the PEO blocks.[1,2] The periodicity of the lammellar phase is very large, revealing that the PEO chains are highly stretched in their crystalline layered domains. Extended studies on a wide range of PEO-based diblock copolymers also shows this special type of crystallisation induced lamellar mesophase.[3] But also above the PEO crystallisation temperature were there indications of major composition fluctuations. These were observed in dynamic light scattering, but could not be observed in neutron or X-ray scattering because of the almost equal scattering length density of PEO and PPO. In the attempt to get direct and better understanding of these composition fluctuations was a material synthesised with a deuterated midblock PPO. The initiator for the dPPO was hydrogenous 1,2-butane diol, $HOCH_2CH(C_2H_5)OH$. The resulting formula was $EO_{33}dPO_{42}EO_{33}$ with a narrow polydispersity: M_w/M_n=1.10. In Fig.1 is shown the scattering function for temperatures both above and below the PEO-crystallisation temperature. The lamellar structure at low temperatures are, due to the enhanced contrast, much better resolved in original Pluronics, and both 2. and 3. order harmonics are clearly visible. Above the crystallisation induced order-disorder transition, the scattering function shows the type of correlation functions typical for block-copolymers relative close to the micro-phase separation temperature.

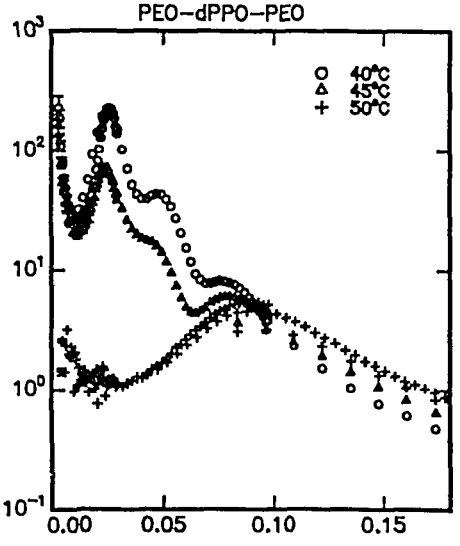

Fig. 1 Scattering function of bulk PEO-dPPO-PEO revealing a lamellar structure at low temperatures and marked composition fluctuations at higher temperatures. The micro-phase separation temperature cannot be reached because of the first order transition into lamellar structure induced by the PEO-crystallisation.

[1] K. Mortensen, W. Brown and E. Jorgensen, Macromolecules, **28**, 1458 (1995).
[2] K. Mortensen, W. Brown and E. Jorgensen, Macromolecules, **27**, 5654 (1994).
[3] M. Hillmyer, F.S. Bates, K. Almdal, K. Mortensen and A. Ryan, Science *in the press.*

2.8.18 Small-Angle Neutron Scattering of Poly(propyleneimine) Dendrimers

R. Scherrenberg, *DSM-Research, Geleen, The Netherlands*, and K. Mortensen, *Department of Solid State Physics, Risø National Laboratory, Denmark*

Dendrimers are synthesised by stepwise repetitive reaction sequences, yielding regularly branched macromolecules that emanate from a central core and have a defined number of functional end-groups. Apart from the unique architecture, these macromolecules exhibit, in contrast to linear polymers, a maximum in the intrinsic viscosity as a function of the molar mass. The recent possibility to produce poly(propyleneimine) dendrimers on a kilogram scale up to the fifth generation gave new impulses to the development of specific applications in this field.

The poly(propyleneimine) dendrimers are synthesised by a repetitive reaction sequence of Michael additions of acrylonitrile to the amine endgroups and nitrile reductions using diaminobutane (DAB) as core. The reactions proceed with a selectivity higher than 99%. Five generations with both amine endgroups DAB-dendr-$(NH_2)_x$ and nitrile end-groups DAB-dendr-$(CN)_x$ (x=4,8,16,32,64) were synthesised.[1]

Small-angle neutron scattering (SANS) experiments has been performed at the Risø National Laboratory to investigate the molecular characteristics of both DAB-dendr-$(NH_2)_x$ and DAB-dendr-$(CN)_x$ as a function of the generation number. The obtained results for 1% (v/v) solutions of DAB-dendr-$(NH_2)_x$ in D_2O are illustrated in Figure 1, using a Guinier representation. For both DAB-dendr-$(NH_2)_x$ and DAB-dendr-$(CN)_x$, a linear relationship is found between the radius of gyration (R_g) and the generation number (Figure 2).

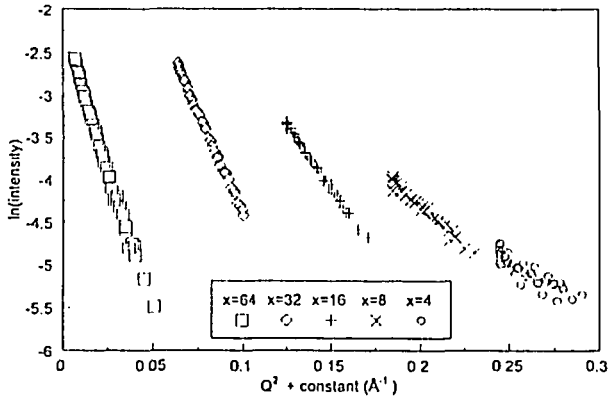

Fig. 1 Guinier plots of 1% (v/v) solution of DAB-dend-$(NH_2)_x$ in D_2O as a function of the generation number

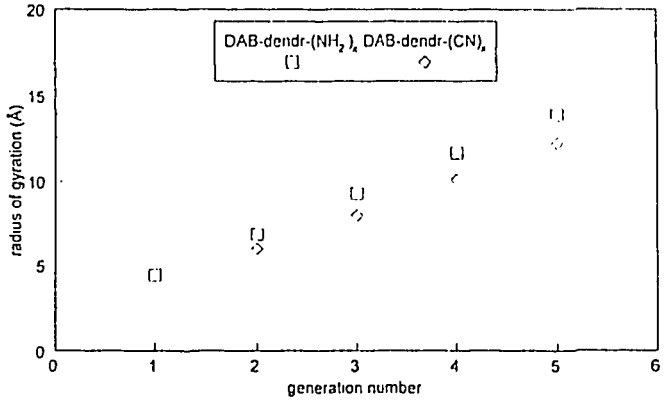

Fig. 2 Radius of the gyration (R_g) of polyproyleneimine dendrimers as a function of the generation number

[1] E.M.M de Brabander van den Berg and E.W.Meijer, Angew.Chem. **105**, 1370 (1993).

2.8.19 Characterisation and Modification of Polymer Surfaces

W.B. Petersen and I. Johannsen, *Riso National Laboratory, Denmark*

This Materials Technology Development Programme (MUP-2) was initiated mid 1994 with the aim to study different surface modification processes and to correlate the functional surface properties with the results registered by mean of different surface characterisation methods. The partners in this project are Coloplast A/S, NKT Research Center, Nunc A/S, Radiometer A/S, Danish Technological Institute and Risø National Laboratory.

As a core activity in this programme chemical characterisation of surface composition by means of X-ray Photoelectron Spectroscopy, XPS is carried out at a newly established facility at Risø. I this instrument, which is dedicated to the study of macromolecular surfaces, the elements present in the outermost molecular layers (0-5 nm) are determined from the binding energy of core electrons. In this way elements except H and He can be quantified. Furthermore, the spectra con give some information on the chemical surrounding of the elements. Carbon bound to carbon or hydrogen gives C 1s = 284 eV, while the presence of other atoms bound to carbon induces a small shift to higher energies.

Experiments have shown that a good correlation with the theoretical elemental composition is found for uncontaminated surfaces, see table.

From the appearance of characteristic binding energies surface modifications such as oxidation or contamination are easily detected, see Fig. 1.

A large number of samples from the partners have been analysed, and the results obtained have convincingly demonstrated the importance of XPS for surface analysis of polymeric materials.

Sample		C	N	O	F	Si
Kapton	Meas.	76,2	6,5	17,1		
	Calc.	75,9	6,9	17,2		
Teflon	Meas.	32,8			67,3	
	Calc.	33,3			66,7	
Mylar	Meas.	71,5		28,5		
	Calc.	71,4		28,6		
PDMS	Meas.	49,9		24,9		25,2
	Calc.	50,0		25,0		25,0
PC	Meas.	83,9		16,1		
	Calc.	84,3		15,7		

Table: XPS quantification's of polymers.

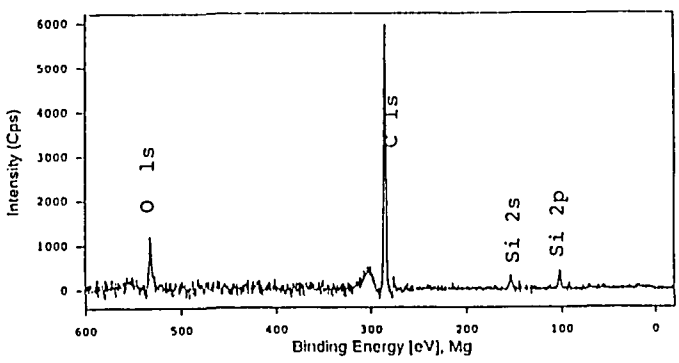

Fig. 1: XPS spectrum of a polymer surface contaminated with silicone oil.

2.8.20 Improved Polymeric Materials through Control of Interface Interaction

W.B. Petersen, N.B. Madsen, K. Almdal, P. Sommer-Larsen, I. Johannsen, *Riso National Laboratory, Denmark*

A Materials Technology Development Programme (MUP2) with this subject was initiated mid 1994. NKT Cables A/S, Wolff & Kaaber A/S, University of Copenhagen - Department of Chemistry and Risø National Laboratory form a working group with the focus on a study of the effect of interface interactions in polymer/polymer as well as polymer/inorganic filler systems.

The contribution from Risø includes a fundamental study of interactions across an interface in different model systems. The results will be generalised by means of advanced modelling techniques. Polymer modelling software from BIOSYM and other sources have been implemented for this purpose in the department. Preliminary results for total atomistic modelling of the interaction between polymers and inorganic surfaces have been obtained. See Fig. 1.

Different analytical techniques have been tented for the applicability of identification and quantification of the chemical structure on bare inorganic fillers and surface modified fillers. Diffuse reflectance FT-IR spectroscopy was found to be the most versatile technique to study chemical modifications.

The modification of inorganic fillers in traditionally performed by using short chain coupling agents. Coupling agents with a chain length above the chain entanglement length may improve the mechanical properties of filled polymers. Therefore, the synthesis of block copolymers with a long block compatible with the polymer matrix and a smaller block containing chemical groups reactive towards inorganic surfaces have been initiated.

For the highly filled polymer systems of special interest for the industrial partners, the rheological properties are very important. A rheological characterisation of a model systems containing metal spheres or a real systems containing SiO_2 particles showed that dynamic mechanical measurements in the shear mode failed to give meaningful number due to slip in the specimen. Preliminary results using a constant strain geometry indicate that this geometry may be used as a quantitative measure of the rheological properties of highly filled polymer systems.

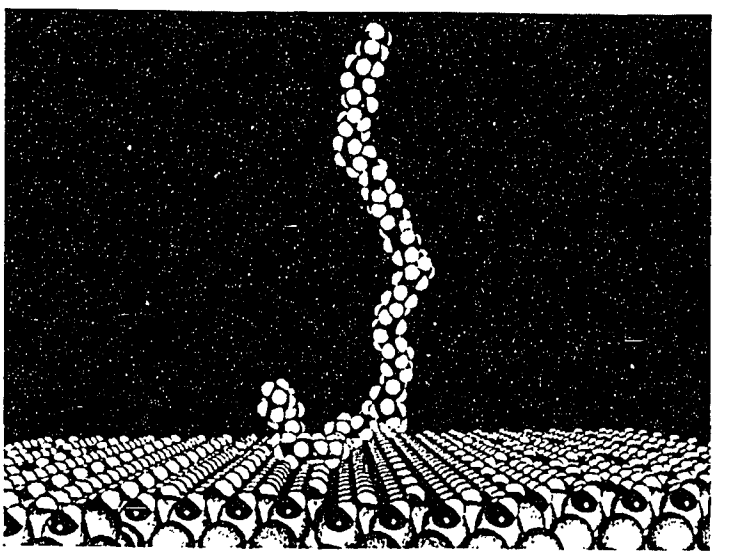

Fig. 1. Atomistic simulation of polyethylene adsorbed to a (1-1 0)-surface of quartz terminated with hydroxyl group. The polymer is in amorphous state. Only one polymer chain is shown.

2.9 Organic Chemistry

2.9.1 Synthesis of a Saccharide Sensor based on Calix[4]arene Diboronic acid

M. Larsen, M. Jørgensen and K. Bechgaard, *Department of Solid State Physics, Riso National Laboratory, Denmark*

The development of receptor molecules that can precisely recognize and specifically bind guest molecules has been the focus of much attention. Specially the design of a receptor molecule that can bind saccharide molecules selectively are interesting. The interaction between the receptor molecule and the target molecule can be hydrogen bonding, covalent bonding or ionic bonding. Boronic acids are known to react with 1,2-diols and 1,3-diols forming new covalent bonds and in saccharides with the *cis*-diol groups. These cyclic boronic esters are quite stable which is why the boronic acids are used in the synthesis of a saccharide sensor. We have chosen the calix[4]arene as the platform molecule because of its structure. Calix[4]arene is a cyclic tetramer of phenolic units and belong to a class of molecules called *cyclophanes*. The first step in our research was to synthesize the calix[4]arene tetraboronic acid by standard procedures, but it turned out that this compound could not be synthesized in this way. In our attempt to synthesized the calix[4]arene tetraboronic acid we discovered a new reaction which leads to calix[4]arene diboronic acid (fig.1a) instead and quite good yield. The ^{1}HNMR and ^{13}CNMR are used for the study of the complexation with D(-)-fruktose, D(+)-glucose and D(+)-galactose. ^{13}CNMR indicates that the saccharide binds to the calix[4]arene diboronic acid, because of the large differences in the chemical shift values for the saccharide part. In the ^{1}HNMR spektrum the signals for the aromatic protons in the complexed/uncomplexed are different. Before anything could be said about the structure of the complex we have to determine the stoichiometry of the saccharide/calix[4]arene complex. MALDI-TOF spectrometry are used to determine the stoichiometry.

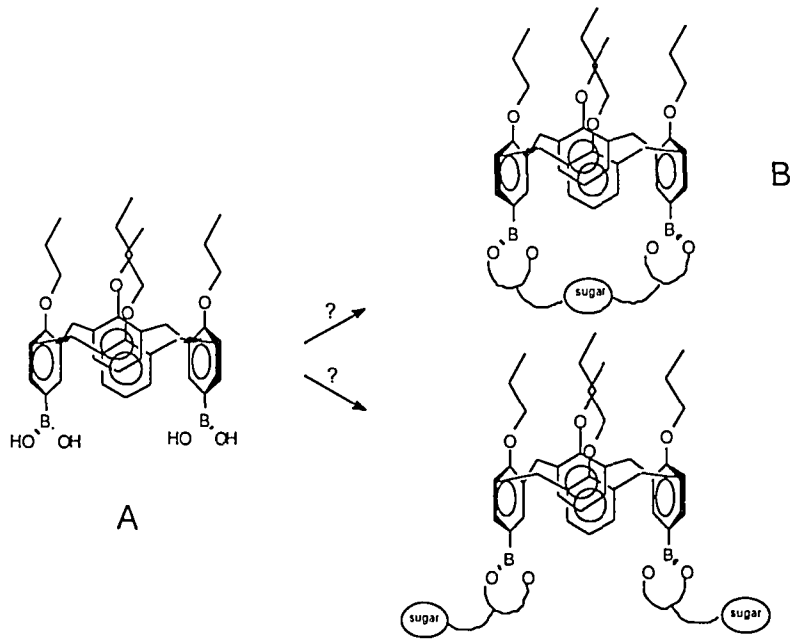

Fig. 1.

2.9.2 Synthesis and Characterization of a Supramolecular Sensor Compound

M. Jørgensen, M. Larsen and W. B. Petersen, *Department of Solid State Physics, Riso National Laboratory, Denmark*

Large molecules with an internal cavity capable of including guest molecules are of great interest as novel materials for sensors. The sensing ability is based on the same principles that is used by Nature in enzymes and antibodies: supramolecular interactions between molecules. We have synthezised macro molecules based on so called calixarenes with an internal cavity large enough to accommodate organic molecules like anthracene and bind these guests *via* π-π interactions. The new sensor molecules were prepared from a calixarene diacid chloride and 1,4-diamino-benzene as outlined in Fig. 1. Characterization of the product with laser desorption mass spectroscopy (MALDI-TOF MS) revealed that it was a mixture of oligomers with *n* calixarene and *n* 1,4-diamino-benzene units (*n*=1,2,3,4,5,6,7 and 8). The **Dimer** (*n*=2) predominated with the next most abundant species being the tetramer (*n*=4). Size exclusion chromatography (SEC) confirmed the oligomer distribution with the **Dimer** in about 50 % yield. Improvements in synthesis has brought the yield of **Dimer** up to 74 %. The **Dimer** was then purified by preparative SEC until oligomer free. This material was shown by high resolution FAB mass spectroscopy to have the isotope distribution and exact mass expected for the **Dimer**. ^{1}H-NMR titration experiments have shown that the **Dimer** indeed interacts with anthracene in solution to form a host-guest pair.

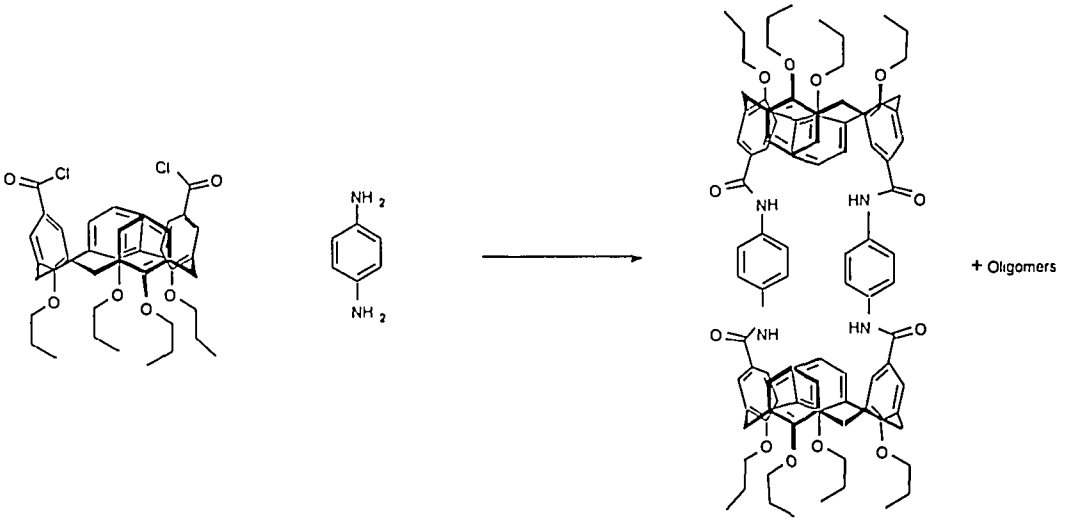

Fig. 1. Calixarene diacid chloride and 1,4-diamino-benzene reacts to give the **dimer**.

2.9.3 Synthesis of an Azo-Bridged Double Calixarene. A Photo-Controlable Cavitant

M. Jørgensen, *Department of Solid State Physics* and P. S. Ramanujam, *Department of Optical and Fluid Dynamics, Riso National Laboratory, Denmark*

The azo-benzene functionality has been introduced into crownethers to modify binding of cations *via* the light induced *trans* to *cis* isomerization. We have used a similar strategy to prepare a double calixarene joined by a single azo bridge. The calixarene parts resemble bowls and in the most stable *trans* isomer they are held apart. On irradiation with an ultraviolet laser, the azo functionality adopts the *cis* form and the two bowl shaped calixarenes come together to form a more closed semi-spherical molecule. The closed form is suitable to trap small molecules in the internal cavity. The *cis* isomer can revert back to the *trans* isomer either thermally or by irradiation with longer wavelength light, thus creating a photo controllable cavitant type molecule.

The synthesis was carried out by mono-nitration of a suitable calixarene tetraether and then reductive formation of the azo function. Characterization by ^{1}H and ^{13}C NMR and by HPLC with a UV-vis detector confirmed the identity of the product, as the *trans* isomer. Irradiation with the ultraviolet laser of the compound in solution, followed by HPLC clearly demonstrated convertion of a major proportion to the *cis* isomer. In ^{1}H and ^{13}C NMR the two species could also be clearly distinguished. Further work has to be done to clarify whether solvent molecules are actually trapped in the interior cavity.

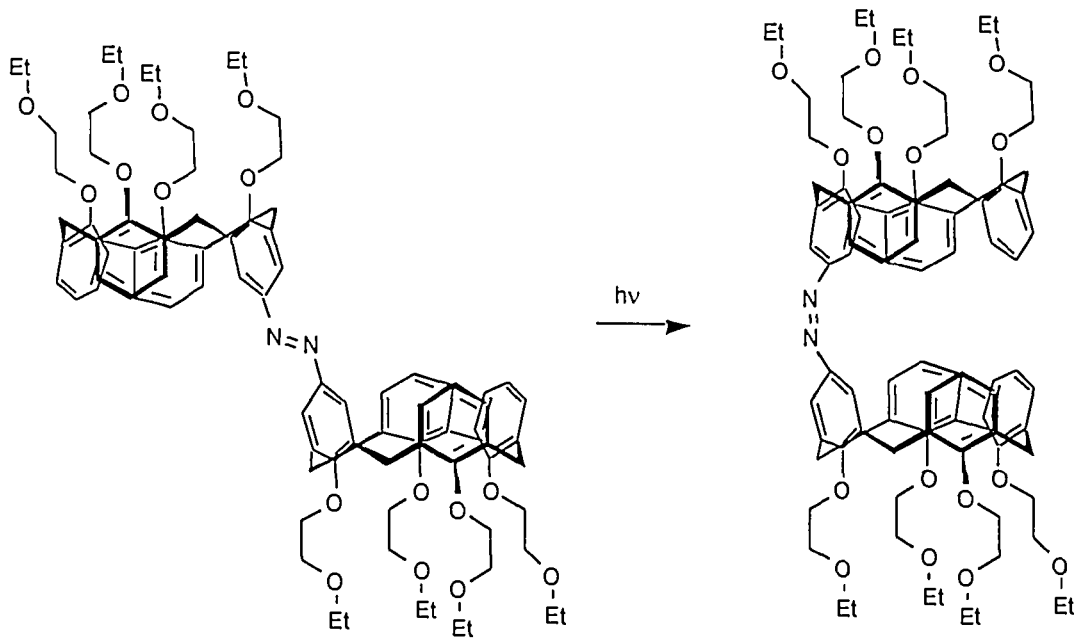

Fig. 1. Photo induced *trans* to *cis* isomerization of the azo-bridged double calixarene.

2.9.4 Synthesis of Calix[4]arene Crown Ethers

J. Svejstrup, M. Jørgensen, and I. Johannsen, *Department of Solid State Physics, Riso National Laboratory, Denmark*

Calix[*n*]arenes are macrocyclic molecules containing *n* phenol units bridged in the *ortho* position with a methylene unit. They are easily obtained from the condensation of formaldehyde with *p-tert*-butylphenol under alkaline conditions. Depending on how the phenol units are aligned, calix[4]arene, **1**, can adopt four conformations, namely the *cone* (all four hydroxy groups pointing downwards), the *partial cone* (three hydroxy groups pointing downwards, one upwards), the *1,2-alternate* (two geminal hydroxy groups pointing downwards, two upwards), and the *1,3-alternate* (two distal hydroxy groups pointing downwards, two upwards). In the cone conformation, **1** contains a bowl-shaped cavity which is able to act as a receptor for guest molecules and has therefore received an increasing amount of attention in the field of host-guest chemistry. By proper modifications it is possible to change the selectivity properties of the calixarene and hence design calixarenes which can specifically bind other molecules. It is well known that by increasing the rigidity of the calixarene moiety it is possible to increase the specificity towards guest molecules. By reacting molecules of the type **1** with oligoethyleneglycol ditosylates under alkaline conditions it is possible to create rigid calixarenes bridged with ethylene units either *intra-* or *inter*-molecularly[1] depending on the reaction conditions (*eg.* type of base, number of ethylene units, stoichiometry of reactants and solvent used). In our efforts to synthesize calixarene crowns (*calixcrowns*) in the 1,3-alternate conformation by using the usual '1,3-alternate conditions' (Cs_2CO_3 as base in DMF or CH_3CN)[2,3], an unsual calixarene, **2**, in the 1,2-alternate conformation has been isolated. The same approach using a 1,3-disubstituted calixarene, **3** (prepared *via* 1,3-dialkylation of **1**) and a longer ethyleneglycol chain, afforded the calixcrown **4.**

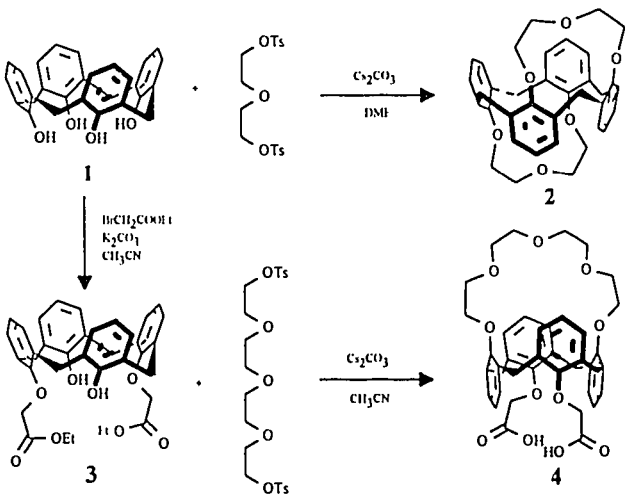

[1] Z. Asfari, S. Wenger and J. Vicens, *J. Incl. Phenom.* 19, 137 (1994).
[2] W. Verboom, S. Datta, Z. Asfari, S. Harkema and D.N. Rheinhoudt, *J. Org. Chem.*, 57, 5394 (1992).
[3] A. Casnati, A. Pochini, R. Ungaro, F. Ugozzoli, F. Arnaud, S. Fanni, M.-J. Schwing, R.J.M. Egberink, F. deJong and D.N. Rheinhoudt, *J. Am. Chem. Soc.*, 117, 2767 (1995).

2.9.5 Thiaheterohelicenes. Synthesis and Properties of Thia[5]-, [9]- and [13]Heterohelicenes

J. Larsen and K. Bechgaard *Department of Solid State Physics, Risø National Laboratory, Denmark*

In order to investigate the donor properties of a series of thiahelicenes and in turn derived conducting solids we have prepared thiaheterohelicenes, such as **1**, We have made extensive use of the classical routes to these structures as developed by H. Wynberg.
Photocyclization of *cis* -stilbenes followed by *in situ* iodine oxidation is a crucial step in the synthesis of helicenes and heterohelicenes. That reaction is problematic because it normally requires very dilute solutions, typically in toluene, and more important, the product acts as a filter for the incoming radiation. We have found a convenient oxidative cyclisation procedure for mixtures of *cis* - and *trans* -1,2-bis-benzothiophen-2-yl-ethylenes to give the thiahelicenes. Where possible, a procedure involving $FeCl_3$ was the simplest to perform considering that the product does not have to be separated from the supporting electrolyte which had to be present in the electrochemical analogue.
The donor properties of a series of thiaheterohelicenes were investigated by cyclic voltammetry. The thiaheterohelicenes are oxidised to the corresponding cation radicals at potentials from 1.03 V to 1.45 V vs. SCE.
Compound **1** can be oxidised to a rather unstable semiconducting salt: $(\mathbf{1})_2PF_6$, Treatment of racemic **1** with 7,7',8,8'- tetracyanoquinodimethane (TCNQ) gave a 1:1 semiconducting solid.
Work is in progress in order to separate the enantiomers.

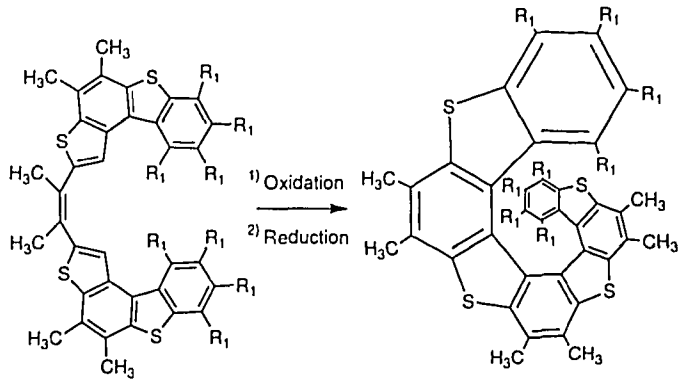

1

2.10 Human Capital and Mobility - Access to Large Installations

K.N. Clausen, *Department of Solid State Physics, Riso National Laboratory, Denmark*

The CEC Large Installation Programme was initiated in order to make large national facilities available to users from the whole EU, to promote European collaboration and to make more facilities available to the less favoured regions in the EU. The cold neutron facilities at DR3 has been included in this programme since early 1992. The present HCM programme expires early 1996 and at present a contract for the continuation under the Training and Mobility of Researchers programme - Access to Large-scale facilities is being negotiated. The new programme will be on the same level as before for access to Risø, but will be extended with access to the thermal neutron scattering facilities at Studsvik in Sweden. News about the programme, information about the facilities and deadline for proposals can be found on WWW pages: http://www.risoe.dk/fys/lip.html and http://www.studsvik.uu.se

Proposals for experiments are refereed by a group of four international experts. A.R. Mackintosh acts as a Risø independent user representative in the management of the programme, and participates in beam allocation meetings, which are held 3 times every year. The HCM programme covers marginal expenses in connection with neutron scattering experiments at Risø. These expenses are (1) Travel and subsistence for the users, (2) salaries to staff employed to run the user programme, (3) consumables and other running costs in connection with the experiments, (4) purchase of auxiliary equipment requested by the users and (5) a contribution to the continued modernisation and upgrade of the facilities

During 1995 the 9T magnet has entered routine user operation, and the vertical scattering reflectometer TAS9 for studies of liquid surfaces and interfaces was commissioned. On the internal strain spectrometer TAS8 and the triple axis spectrometer TAS6 the μ-Vax controle computers were replaced by DEC-α workstations. The facilities for the users were improved by new office facilities in the neutronhouse.

During 1995 a total of 618 instrument days (88 beam weeks) were used by 71 scientists from 7 different European countries. In total 68 experiments were performed, and 107 visits were supported by the programme.

The experiments carried out at Risø with support from the Commission of the European Communities during 1995 are listed below in chronological order. The column marked applicant is the name of the principal applicant.

Applicant	Title
Hetch Edgar	Ternary Phase Behaviour of block copolymer/surfactant/water mixtures
Dr. D.J. Smith	Measurement of the redistribution of residual stresses after mechanical loading
Götz Jerke	Size, Flexibility and Local Structure of Polymerlike Micelles
Prof. Roy Taylor	Measurement of internal stresses in thick plasma sprayed thermal barrier coatings
Dr. M.R. Wells	Magnetic order in $BaLn_2F_8$, where Ln=Ho,Er,Dy and extended measurements in HoF_3
Dr Miguel Gregorkiewitz	The accurate position of lithium in the new ionic conductor $Li(AlSiO_4)$
Prof. K.A. McEwen	Magnetic Field Dependence of Structures and Excitations in Pr
Prof. K.A. McEwen	Magnetic excitations and magnetic structure of $Pr_{0.9}Tm_{0.1}$
Geetha Balakrishnan	Investigations on the new $(RE)Ni_2B_2C$ superconductors below T_c
Jörg Pohl	Structure and magnetism of Cr/delta-Mn and Fe/delta-Mn-superlattices
Dr. S.J. Roser	Solvent Penetration in Lithographic Polymers
Prof. Gomez-Sal	Structural and magnetic SANS study of the $Fe_{90-x}Zr_{10+x}$ amorphous ribbons
Prof. Don McK Paul	Spin Peierls Transition in doped $CuGeO_3$
Prof. R.A. Cowley	Magnetic Structure of Rare Earth Multilayers
Prof. H.W. de Wijn	Ordering of Frustrated two dimensional magnetic systems
Prof. G. Albertini	Texture measurements in a welded steel
Prof. G. Caglioti	Texture analysis in highly deformed Al alloys
Dr. Paul Müller	Spin structure determination of Na_6MnSe_4 and DySI
Dr. S.J. Roser	Neutron Reflection from Biosensors
Dr. J.P. Goff	Magnetic field dependence of spin excitations in the S=1/2 1D Heisenberg Antiferromagnet Cs_2CuCl_4
Prof. Don McK Paul	Spin Peierls Transition in doped $CuGeO_3$
C.G. de Kruif	Protein Interactions: Aggregation or crystallization of β-lactoglobulin
Prof. R.A. Cowley	Phase diagram of magnetic multilayers
Prof. Don McK Paul	Spin Peierls Transition in doped $CuGeO_3$
Dr. A.T. Boothroyd	The magnetic structure in $PrBa_2Cu_3O_{6+x}$
Prof. E.M. Forgan	Studies of vortex structures in the high temperature superconductors $Bi_2Sr_2CaCu_2O_{8+y}$ and $YBa_2Cu_3O_{7-4}$
Dr. A.T. Boothroyd	The magnetic structures in Al-free crystals of $PrBa_2Cu_3O_{6+x}$
Dr. D. Schwahn	The pressure and temperature dependence of the Flory-Huggins parameter
Jason S. Gardner	Magnetic Diffraction in the highly Doped $La_{2-x}SrCoO_4$
Dr G.J. Nieuwenhuys	Low energy excitations in the frustrated antiferromagnet UNi_4B
Dr. M. Stamm	Phase behavoir of polystyrene polyparamethylstyrene block copolymers and blends near the microphase separation
Dr. D. Svergun	Contrast Variation Study of the 30S Subunit of the E.Coli Ribosome
Dr. D. Svergun	Contrast variation study of the 50S subunit of the E.coli ribosome
Prof. F.J. Bermejo	Temperature dependence of the inelastic scattering intensity in vitreous boron trioxyde

Prof. K.A. McEwen	Magnetic excitations and magnetic structure of $Pr_{0.9}Tm_{0.1}$
Dr. S.J. Roser	Solvent Penetration in Lithographic Polymers
Dr. S.J. Roser	Neutron Reflection from Biosensors
Prof. R.A. Cowley	Magnetic Structure of Rare Earth Multilayers
Dr. G.F. Modlen	Preferred orientation in cold-drawn high-carbon steel
Dr. A.T. Boothroyd	The magnetic structure in $PrBa_2Cu_3O_{6+x}$
A.R. Wildes	Magnetic Structures of $MnPS_3$
Prof. R.A. Cowley	Magnetic Structure of Rare Earth Multilayers
Dr. M. Loewenhaupt	Magnons in the different phases of $NdCu_2$
Dr. Mathias Lösche	Structure of reassembled monomolecular bacterial S-protein layers at air/water interfaces
Prof. Don McK Paul	Spin Peierls Transition in doped $CuGeO_3$
Dr. U. Steigenberger	Magnetic excitations of UPd_3 in a field
Prof. Dr.-Ing. habil. P. Klimanek	Correlation between texture and grain size during isothermal grain growth in zinc
Prof. K.A. McEwen	Magnetic Field Dependence of Structures and Excitations in Pr
Dr. I.W. Hamley	Orientational order in thermotropic liquid crystals by isotope labelling
Mark Miodownik	Secondary recrystallisation of ODS alloys - kinetics and the role of solute pinning
Prof. Miguel Alario Franco	Structural study of room temperature chemically oxidized $La_{2-x}Nd_xCuO_{4+y}$ and $La_{2-x}Dy_xCuO_{4+y}$, $0< x<0.15$
Dr. Thierry Magnin	Effect of Nitrogen content on the phase coupling and low cycle fatigue in alpha-gamma duplex steels
O. Stockert	Magnetic order of the heavy fermion alloy $CeCu_{6-x}Au_x$ near the critical concentrations $x>=x_c=0.1$
Dr Miguel Gregorkiewitz	The accurate position of lithium in the new ionic conductor $Li(AlSiO_4)$
Dr Jon Samseth	Microstructural studies of bile salts by small angle neutron scattering
Dr. C.V. Tomy	Magnetic ordering above Tc in superconducting $DyNi_2B_2C$
O. Stockert	Magnetic order of the heavy fermion alloy $CeCu_{6-x}Au_x$ near the critical concentrations $x>=x_c=0.1$
John M Martin	Magnetic properties of the heavy fermion $CeCuAl_3$ and the associated compounds $CeCu_{1-x}Ag_xAl_3$
Dr. Mathias Lösche	Structure of reassembled monomolecular bacterial S-protein layers at air/water interfaces
Federica Malizia	Morphological characterization of partially crystallized $Fe_{78}Si_9B_{13}$ amorphous alloy
Dr. Mathias Lösche	Structure of reassembled monomolecular bacterial S-protein layers at air/water interfaces
Jason S. Gardner	Single crystal diffraction of $LaCoO_4$
Martin R. Daymond	In situ Strain Monitoring During Thermal Cycling of Whisker Reinforced Metal Matrix Composites
Prof. R.A. Cowley	Magnetic Structure of Rare Earth Multilayers
Dr. J.P. Goff	Magnetic field dependence of spin excitations in the S=1/2 1D Heisenberg Antiferromagnet Cs_2CuCl_4
Ulf Olsson	Structure and dynamics of surfactant fluid surfaces

3 Publications, Educational and Organizational Activities, Colloqia

3.1 Publications

Barholm-Hansen, C., Bentzon, M.D., Vigild, M.E., Findeisen, E.,Feidenhans'l, R.,Hansen, J.B., Process control by optical emission spectroscopy during growth of a-C:H from a CH_4 plasma by plasma-enhanced chemical vapour deposition. Surf. Coat.Technol. (1994) **68/69,** 702-707.

Barker, J.G., Pedersen, J.S., Instrumental smearing effects inradially symmetric small-angle neutron scattering by numerical and analytical methods. J. Appl. Cryst. (1995) **28,** 105-114

Bartels, V.T., Stamm, M., Abetz, V., Mortensen, K., Direct measurement of chain stretching in diblock copolymers at the microphase separation transition. Europhys. Lett. (1995) **31,** 81-86.

Bates, F.S., Schulz, M.F., Khandpur, A.K., Förster, S., Rosedale, J.H., Almdal, K., Mortensen, K., Fluctuations, conformational asymmetry and block copolymer phase behaviour. Faraday Discuss. (1994) **98,** 7-18.

Bates, F.S., Maurer, W., Lodge, T.P., Schulz, M.F., Matsen, M.W., Almdal, K., Mortensen, K., Isotropic Lifshitz Behaviour in Block Copolymer-Homopolymer Blends. Phys. Rev. Let. (1995) **75 (24),** 4429-4432.

Bermejo, F. J., Garcia-Hernandez, M., Mompean, F. J., McMorrow, D. F., Martinez, J. L., Nature of the First Diffraction Peak in Glassy Selenium, Phys. Rev. B. (1995) **51,** 11932.

Brecht, E., Schmahl, W.W., Fuess, H., Casalta, H., Schleger, P., Lebech, B., Andersen, N.H., Wolf, T., Significance of Al doping for antiferromagnetic AFII ordering in $YBa_2Cu_{3-x}Al_xO_{6+\delta}$ materials: A single-crystal neutron-diffraction study. Phys. Rev. B (1995) **52,** 9601-9610.

Brecht, E., Schmahl, W.W., Fuess, H, Casalta, H., Lebech, B., Andersen, N.H., Schmenn, S., Lütgemeier, H., und Wolf, Th., Mechanismus des AFI ↔ AFII Phasenübergangs von Al dotierten, reduzierten $YBa_2Cu_{3-x}M_xO_{6+\delta}$ Einkristallen. Z. Krist. Suppl. (1995) **9,** 30.

Brecht, E., Schmahl, W.W., Miehe, G., Rodewald, M., Gonschorek, W., Fuess, H., Andersen, N.H., und Th. Wolf, Einfluss vom Wârmebehandlungen in unterschiedlichen Atmosphären auf die strukturellen Eigenschaften von Al dotierten Y-Ba-Cu-O Einkristallen, Z. Krist. Suppl. (1995) **9,** 148.

Brezesinski, G., Dietrich, A., Struth, B., Böhm, C., Bouwman, W.G., Kjær, K., Möhwald, H., Influence of ether linkages on the structure of double-chain phospholipid monolayer. Phys. Lipids (1995) **76,** 145-157.

Brezesinski, G., Rietz, R., Kjær, K., Bouwman, W.G., Möhwald, H., Separation of enantiomers in a diol monolayer studied by fluorescence microscopy and grazing incidence x-ray diffraction. Nuovo Cimento Soc. Ital. Fis. D (1994) **16,** 1487-1492.

Böhringer, M., Molinàs-Mata, P., Zegenhagen, J., Falkenberg, G., Seehofer, L., Lottermoser, L., Johnson, R.M., Feidenhans'l, R., Possible Mechanism for the Room-Temperature Stabilization of the Ge(111) T>300^{0} C Phase by Ga. Phys. Rev. B (1995) **52 (3),**

Casalta, H., Schleger, P., Montfrooij, W., Andersen, N.H., Lebech, B., Liang, R. Hardy, W.N., Antiferromagnetism in reduced $YBa_2Cu_3O_{6+x}$. J. Magn. Magn. Mater. (1995) **140-144,** 1297-1298.

Christensen, M. J., Feidenhans'l, R. Nielsen, M., Fe/V superlattices: X-ray and neutron-scattering investigations. Vacuum (1995) **46,** 1113-1115.

Christensen, L., Fitzpatrick, R., Gildea, B., Petersen, K.H., Hansen, H.F., Koch, K., Egholm, M., Buchardt, O., Nielsen, P.E., Coull, J. and Berg, R.H., Solid-phase synthesis of peptide nucleic acids (PNA). J. Peptide Sci. (1995) **3,** 175-183.

Chirstensen, L., Nielsen, P.E., Buchardt, O., Egholm, M and Berg, R.H. Film-supported PNA synthesis. In: Peptides 1994, Maia, H.L.S. (ed.), Escom, Leiden (1995), 283-284.

Clausen, K.N., Aagaard Sorensen, S., McEwen, K.A., Jensen, J., Mackintosh, A.R., Crystal fields and conduction electrons in praseodymium. J. Magn. Magn. Mater. (1995) **140-144,** 735-738.

Cowley, R.A., McMorrow, D.F., Simpson, J. A., Jehan, D., Swaddling, P., Ward, R.C.C., Wells, M.R., Magnetic structures and interactions in Ho/Y, Ho/Lu, and Ho/Er . J. Appl. Phys. (1994) **76,** 6274-6377.

Cowley, R.A., McMorrow, D.F., Simpson, J.A., Swaddling, P.P., Ward, R.C.C., Wells, M.R., Magnetic structure and excitations of rare earth superlattices. Indian J. Pure Appl. Phys. (1995) **33,** 509-515.

Crevecoeur, R., Schepper, I.M. de, Graaf, L.A. de, Montfrooij, W., Svensson, E.C., Carlile, C., Angular- and time-resolution of neutron time of flight spectrometers. Nucl. Inst. and Meth. (1995) **A356,** 415.

Crevecoeur, R., Verberg, R., Schepper, I.M. de, Graaf, L.A. de, Montfrooij, W., Overdamped phonons in fluid helium at 4K. Phys. Rev. Lett. (1995) **74,** 5052.

Cubitt, R., Forgan, E.M., Wylie, M.T., Yang, G., Lee, S.L., Keller, H., McK Paul, D., Mook, H.A., Yethiraj, M., Kes, P.H., Li, T.W., Menovsky, A.A., Tarnawski, Z., Mortensen, K., Small angle neutron diffraction studies of vortex structures in high temperature superconductors. Physica C (1994) **235-240,** 2583-2584.

Dolbecq, A., Boubekeur, K., Batail, P., Canadell, E., Aubansenzier, P., Coulon, C., Lerstrup, K., Bechgaard, K., Organic-inorganic molecular aggregates and their association within long-range ordered crystalline assemblies: Relevance to the template effect in solid-state chemistry. J. Mater. Chem. (1995) **5,** 1707-1718.

Ellouze, C., Takahashi, M., Wittung, P., Mortensen, K., Schnarr, M., Nordén, B., Evidence for Elongation of the Helical Pitch of RecA-ADP Filament Upon ATP and ADP Binding Using Small-angle Neutron Scattering. Eur. J. Biochemistry (1995) **233,** 579-583

Enderle, M., Kakurai, K., Clausen, K.N., Steiner, M., Inami, T., Tanaka, H., Excitations of $CsMnI_3$ (S=5/2) in magnetic field, in comparison to $CsNiCl_3$ (S=1): A test of the Haldane conjecture. Physica B (1995) **213-214,** 158-160.

Fetters, L.J., Balsara, N.P., Huang, J.S., Jeon, H.S., Almdal, K., Lin, M.Y., Aggregation in living polymer solutions by light and neutron scattering: A study of model ionomers. Macromolecules (1995) **28,** 4996-5005.

Fiig, T., Andersen, N.H., Berlin, J., Lindgård, P.-A., Theory and computer simulation of diffuse scattering from lattice-gas models: Structure-factor calculations for the high-temperature superconductor $YBa_2Cu_3O_{6+x}$. Phys. Rev. B (1995) **51** 12246-12255.

Gammel, P.L., Yaron, U., Huse, D.A., Kleiman, R.N., Batlogg, B., Oglesby, C.S. Bucher, E., Bishop, D.J., Mason, T.E., Mortensen, K., Small angle neutron scattering from the vortex lattice in $2H$-$NbSe_2$. J. Appl. Phys. (1994) **76,** 6789.

Gibaud, A., McMorrow, D.F., Swaddling, P.P., Determination of the x-ray scattering lineshape from a Nb thin film using synchrotron radiation. J. Phys. Condens. Matter (1995) 7, 2645-2654.

Grübel, G., Als-Nielsen, J., Vettier, C., Gibbs, D., Bohr, J., Pengra, D., Resonant magnetic scattering in holmium at an undulator source. International conference on magnetism. J. Magn. Magn. Mater. (1995) **140-144,** 755-756.

Hamley, I.W., Gehlsen, M.D., Khandpur, A.K., Koppi, K.A., Rosedale, J.H., Schultz, M.F., Bates, F.S., Almdal, K., Mortensen, K., Complex layered phases in asymmetric diblock copolymers. J. Phys. II France (1994) **4,** 2161-2186.

Harris, P., Lebech, B., Pedersen, J.S., The three-dimensional resolution function for small-angle scattering and Laue geometries. J. Appl. Cryst. (1995) **28,** 209-222.

Harris, P., Lebech, B., Hae Seop Shim, Mortensen, K., Pedersen, J.S., Small-angle neutron-scattering studies of the magnetic phase diagram of MnSi. Physica B (1995) **213-214,** 375-377.

Hecht, E., Mortensen, K., Gradzielski, M., Hoffmann, H., Interaction of ABA block copolymers with ionic surfactants: Influence on micellization and gelation. J. Phys. Chem. (1995) **99,** 4866-4874.

Hecht, E. Mortensen, K., Hoffmann, H., L_3 phase in a binary block copolymer/water system. Macromolecules (1995) **28,** 5465-5476.

Hvilsted, S., Andruzzi, F., Kulinna, C., Siesler, H.W., Ramanujam, P.S., Novel side-chain liquid crystalline polyester architecture for reversible optical storage. Macromolecules (1995) **28,** 2172-2183.

Hvilsted, S.; Kulinna, C.; Ramanujam, P.S., New azobenzene polymers for optical information storage. In: 45th Finnish chemical congress and exhibition and Nordic polymer meeting. Abstracts. KEMIA 95, Helsinki (FI), 14-16 Nov 1995. (Association of Finnish Chemical Societies, Helsinki (1995) 46.

Janssen, S., Schwahn, D., Springer, T., Mortensen, K., Coil and melt compressibility of polymer blends studied by SANS and pVT experiments. Macromolecules (1995) **28,** 2555-2560.

Janssen, S., Schwahn, D., Springer, T., Mortensen, K., Hasegawa, H., Investigation of the pressure dependence of the Gibbs potential for polymer blends by means of SANS. Physica B (1995) **213-214,** 691-693.

Kawano, S., Sorensen, S.Å., Lebech, B., Achiwa, N., High pressure neutron diffraction studies of the magnetic structures of erbium. J. Magn. Magn. Mater. (1995) **140-144,** 763-764.

Kleiman, R.N., Aeppli, G., Bishop, D.J., Bucher, E., Stüchelli, N., Yaron, U. Clausen, K.N., Howard, B., Mortensen, K., Pedersen, J.S., Neutron diffraction from the vortex lattice in the heavy fermion superconductor UPt_3. J. Appl. Phys. (1994) **76,** 6788.

Koch, T., Næsby, M., Wittung, P., Jorgensen, M., Larsson, C., Buchardt, O., Stanly, C.J., Norden, B., Nielsen, P.E., Ørum, H., PNA Peptide chimerae. Tetrahedron Lett. (1995) **36,** 6933-6936.

Langridge, S., Stirling, W.G., Nuttall, W.J., Lander, G.H., Lebech, B., Vogt, O., Neutron scattering study of the magnetic phases of $USb_{0.8}Te_{0.2}$. Physica B (1995) **213-214,** 122-124.

Larsen, N.B., Bjornholm, T., Garnæs, J., Als-Nielsen, J., Kjær, K., Structural studies of Langmuir and Langmuir-Blodgett films of functionalized surfactants. Synth. Met. (1995) **71,** 1985-1988.

Lebech, B., Modulated magnetic structures and their relations to the crystal structure. In: Symmetry and structural properties of condensed matter. Lulek, T., Florek, W., Walcerz, S. (eds.), (World Scientific, Singapore, 1995) 39-55.

Lebech, B., Magnetic structure determination by neutron diffraction. In: Magnetic neutron scattering. Furrer, A. (ed.), (World Scientific, Singapore, 1995) 58-69.

Lebech, B., Harris, P., Pedersen, J.S., Mortensen, K., Gregory, C.I., Bernhoeft, N.R., Jermy, M., Brown, S.A., Magnetic phase diagrams of MnSi. International conference on magnetism. J. Magn. Magn. Mater. (1995) **140-144,** 119-120.

Lemmich, J., Hjort Ipsen, J., Honger, T., Jorgensen, K., Mouritsen, O.G., Mortensen, K., Bauer, R., Soft and repulsive: Relationship between lipid membrane in-plane fluctuations, bending rigidity, and repulsive undulation forces. Mod. Phys. Lett. B (1994) **8,** 1803-1814.

Lemmich, J., Mortensen, K., Ipsen, J. H., Honger, T., Bauer, R., Mouritsen, O., Mean-Field like Pseudo-Critical Behavior of Phospholipid Bilayers. Phys. Rev. Lett. (1995) **75,** 3958-3961.

Lindgård, P. -A., What determines the Martensitic transition temperature in alloys? J. Phys. IV France (1995) **5(C2),** 29-34.

Lindgård, P.-A., Bohr, H., How many protein fold classes are to be found? In: Protein folds: a distance based approach. Bohr, H., Brunak, S. (eds.), (CRC Press, Boca Raton, FL, 1995) 98-102.

Loewenhaupt, M., Reif, T., Arons, R.R., Gratz, E., Rotter, M., Lebech, B., The magnetic structures of $NdCu_2$ determined by single crystal neutron diffraction. Z. Phys. B (1995) **96,** 491-496.

Lussier, J.G., Coad, S.M., McMorrow, D.F., Paul, D.M., Observation of the Néel state in doped $CuGeO_3$. J. Phys. Condens. Matter (1995) 7 L325-L330.

Majewski, J., Edgar, R., Popovitz-Biro, R., Kjær, K., Bouwman, W.G., Als-Nielsen, J., Lahav, M., Leiserowitz, L., Structure determination in the twilight region between monolayers and 3-D crystals, a grazing incidence x-ray diffraction study of nanocrystalline aggregates of α,ω -Docosanediol at the air-water interface. Angew. Chem. Int. Ed. Engl. (1995) **34,** 649-652.

Majewski, J., Popovitz-Biro, R., Bouwman, W.G., Kjær, K., Als-Nielsen, J., Lahav, M., Leiserowitz, L., The structural properties of uncompressed crystalline monolayers of alcohols $C_nH_{2n+1}OH$(n=13-31) on water and their role as ice nucleators. Chem. Eur. J. (1995) **1,** 304-311.

Mason, T.E., Petersen, T., Aeppli, G., Buyers, W.J.L., Bucher, E., Garrett, J.D., Clausen, K.N., Menovsky, A.A., Magnetic fluctuations in heavy-fermion metals. Physica B (1995) **213-214,** 11-15.

McEwen, K.A., Steigenberger, U., Clausen, K.N., Bi, Y.J., Walker, M.B., Kappler, C., Neutron scattering study of the antiferroquadrupolar structure and order parameter of UPd_3. Physica B (1995) **213-214,** 128-130.

McMorrow, D.F., Simpson, J.A., Cowley, R.A., Jehan, D.A., Ward, R.C.C., Wells, M.R., Thurston, T.R., Gibbs, D., The magnetic structure of holmium/erbium superlattices. J. Magn. Magn. Mater. (1995) **140-144,** 779-782.

Mischenko, N., Reynders, K., Koch, M.H.J. Mortensen, K., Pedersen, J.S., Fontaine, F., Graulus, R., Reynaers, H., Small-angle x-ray and neutron scattering from bulk and oriented triblock copolymer gels. Macromolecules (1995) **28,** 2054-2062.

Molinàs-Mata, P., Böhringer, M., Artacho, E. Zegenhagen, J., Seehofer, L. Buslaps, T., Johnson, R.L. Findeisen, E., Feidenhans'l, R., Nielsen, M., The phase diagram of annealed Ge(111)/Ga. Phys. Stat. Sol. (a) (1995) **148,** 191-212.

Montfrooij, W., Schepper, I. de, Relationship between the roton minimum and T_λ in ^{4}He. Phys. Rev. B (1995) **51,** 15607-5609.

Mortensen, K., Almdal, K., Bates, F.S., Koppi, K., Tirrell, M., Nordén, B., Shear devices for in situ structural studies of block copolymer melts and solutions. Physica B (1995) **213/214,** 682-684.

Mortensen, K., Brown, W., Jorgensen, E., Lamellar mesophase of poly(ethylene oxide) poly(propylene oxide) poly(ethylene oxide) melts and water-swollen mixtures. Macromolecules (1995) **28,** 1458-1463.

Nad, F., Monceau, P., Bechgaard, K., Low-frequency permittivity of spin-density wave in $(TMTSF)_2PF_6$ at low temperatures. Solid State Commun. (1995) **95,** 655-660.

Ndoni, S., Papadakis, C.M., Bates, F.S., Almdal, K., Laboratory-scale setup for anionic polymerization under inert atmosphere. Rev. Sci. Instrum. (1995) **66,** 1090-1095.

Norby, P., Krogh Andersen, I.G., Krogh Andersen, E., Andersen, N.H., The crystal structure of lanthanum manganate(III), $LaMnO_3$, at room temperature and at 1273 K under N_2. J. Solid State Chem. (1995) **119,** 191-196.

Nuttall, W.J., Langridge, S., Stirling, W.G., Lander, G.H., Lebech, B., Vogt, O., Resonant x-ray and neutron diffraction study of $USb_{0.8}Te_{0.2}$. Phys. Rev. B (1995) **52,** 4409-4419.

Olsson, U., Mortensen, K., Shear melting and orientation of a lyotropic cubic phase. J. Phys. II France (1995) **5,** 789-801.

Papadakis, C.M., Almdal, K., Posselt, D., Molar-mass dependence of the lamellar thickness in symmetric diblock copolymers. Nuovo Cimento Soc. Ital. Fis. D (1994) **16,** 835-842.

Paul, D.M., Forgan, E.M., Cubitt, R., Lee, S.L.,Wylie, M., Mook, H.A., Yethiraj, M., Mortensen, K., Neutron scattering from the flux-line lattice in $Bi_2Sr_2CaCu_2O_{8+\gamma}$. Physica B (1995) **213-214,** 107-109.

Pedersen, J.S., Instrumentation for small-angle scattering. In: Modern aspects of small-angle scattering. Brumberger, H. (ed.), (Kluwer Academic Publishers, Dordrecht, 1995) (NATO Advanced Science Institutes Series C: Mathematical and Physical Sciences, 451) 57-91.

Pedersen, J.S., Egelhaaf, S.U., Schurtenberger, P., Formation of polymerlike mixed micelles and vesicles in lecithin-bile salt solutions: A small-angle neutron-scattering study. J. Phys. Chem. (1995) **99,** 1299-1305.

Pedersen, J.S., Hansen, S. Bauer, R., Scaling in the aggregation behaviour of zinc-free insulin studied by small-angle neutron scattering. Nuovo Cimento Soc. Ital. Fis. D (1994) **16,** 1447-1455.

Pedersen, M., Hvilsted, S. Andruzzi, F. Ramanujam, P.S., New side-chain liquid crystalline polyesters for optical storage. Materialenyt (1995) **2,** 57-58.

Peters, G.H., Toxværd, S., Larsen, N.B., Bjørnholm, T., Schaumburg, K., Kjær, K., Structure and dynamics of lipid monolayers: Implications for enzyme catalysed lipolysis. Nature Struct. Biol. (1995) **2,** 395-401.

Peters, G.H., Toxværd, S. Larsen, N.B. Bjørnholm, T., Schaumburg, K., Kjær, K., Phase transitions in diglyceride monolayers studied by computer simulations, pressure-area isotherms and x-ray diffraction.. Nuovo Cimento Soc. Ital. Fis. D (1994) **16,** 1479-1485.

Popovitz-Biro, R., Majewski, J., Wang, J.L., Leiserowitz, L., Lahav, M., Kjær, K., Als-Nielsen, J., Langmuir films of amphiphilic alcohols and surfaces of polar crystals as templates for ice nucleation. In: Organic thin films and surfaces: Directions for the nineties. Ulman, A. (ed.), (Academic Press, San Diego, 1995) (Thin Films, 20) 145-181.

Ramanujam, P.S., Andruzzi, F., Hvilsted, S., Optical storage in side-chain liquid crystalline polyesters. Opt. Rev. (1994) **1(1),** 30-32.

Ramanujam, P.S., Holme, C., Hvilsted, S., Pedersen, M., A compact holographic storage system based on novel polyesters. In: Optics and information. (Cercle SFO/SEE d'Opto-Informatique, Mulhouse, 1995) (European Optical Society Topical Meetings Digests Series, 6) Paper 4.14.

Ramanujam, P.S.; Holme, C.; Hvilsted, S.; Pedersen, M.; Andruzzi, F.; Paci, M.; Tassi, E.L.; Magagnini, P.L.; Zebger, I.; Siesler, H.W., Holographic storage in side-chain azobenzene polyesters. In: Third international symposium on polymers for advanced technologies. Conference programme. PAT '95, Pisa (IT), 11-15 Jun 1995. (CNR, Pisa) (1995) 52.

Ramanujam, P.S., Hvilsted, S., Zebger, I., Siesler, H.W., On the explanation of the biphotonic processes in polyesters containing azobenzene moieties in the side chain. Macromol. Rapid Commun. (1995) **16,** 455-461.

Ranlov, J., Lebech, B., Nielsen, K., Neutron diffraction investigation of the atomic defect structure of Y-doped $SrCeO_3$, a high temperature protonic conductor. J. Mater. Chem. (1995) **5,** 743-747.

Rial, C., Morán, E., Alario-Franco, M.A., Amador, U., and Andersen, N.H., Structural and superconducting properties of $La_{2-x}Sr_xCuO_{4+y}$ ($0 < x < 0.15$) prepared by room temperature chemical oxidation, Physica C (1995) **254,** 233-248.

Rosedale, J., Bates, F.S., Almdal, K. Mortensen, K., Wignall, G.D., Order and disorder in symmetric diblock copolymer melts. Macromolecules (1995) **28,** 1429-1443.

Schins, A.G., Nielsen, M., Arts, A.F.M. and Wijn, H.W. de, Neutron study of the two-dimensional random-exchange antiferromagnet $Rb_2Cu_{0.12}Co_{0.88}F_4$, J. Magn. Mat. (1995) **140-144**, 1715.

Schins, A.G, Nielsen, M., Arts, A.F.M., Wijn, H.W. de, Neutron-scattering study of the two-dimensional frustrated antiferromagnet $Rb_2Cu_{0.12}Co_{0.88}F_4$. Phys. Rev. B (1994) **49**, 8911-8919.

Schins, A.G., Nielsen, M., Arts, A.F.M., Wijn, H.W. de, Neutron scattering study of the two-dimensional random-exchange antiferromagnet $Rb_2Cu_{0.12}Co_{0.88}F_4$. J. Magn. Magn. Mater. (1995) **140-144,** 1715-1716.

Schiodt, N.C., Sommer-Larsen, P., Bjornholm, T., Nielsen, M.F., Larsen, J., Bechgaard, K., Preparation and electronic structure of substituted aromatic dithiolene complexes of gold (III). Inorg. Chem. (1995) **34,** 3688-3694.

Schleger, P., Casalta, H., Hadfield, R., Poulsen, H.F., Zimmermann, M. von, Andersen, N.H., Schneider, J.R., Liang, R.X., Dosanjh, P., Hardy, W.N., Observation of Ortho-III correlations by neutron and hard x-ray scattering in an untwinned $YBa_2Cu_3O_{6.77}$ single crystal. Physica C (1995) **241,** 103-110.

Schleger, P., Hadfield, R.A., Casalta, H., Andersen, N.H., Poulsen, H.F., Zimmermann, M. von, Schneider, J.R., Liang, R.X., Dosanjh, P., Hardy, W.N., Random-field structural transition in $YBa_2Cu_3O_{6.5}$. Phys. Rev. Lett. (1995) **74,** 1446-1449.

Schwahn, D., Janssen, S., Willner, L., Schmackers, T., Springer, T., Mortensen, K., Takeno, H., Hasegawa, H., Jinnai, H., Hashimoto, T., Imai, M., Critical crossover phenomena in compatible polymer blends studied with SANS. Physica B (1995) **213-214,** 685-687.

Schwahn, D., Schmackers, T., Mortensen, K., Ginzburg criterion for the mean-field to three-dimensional Ising crossover in polymer blends. Phys. Rev. E (1995) **52,** R1288-R1291.

Sequeira, A.D., Calderon, H.A., Kostorz, G., Pedersen, J.S., Bimodal size distributions of γ ' precipitates in Ni-Al-Mo. I. Small-angle neutron scattering. Acta Metall. Mater. (1995) **43,** 3427-3439.

Sequeira, A.D., Calderon, H.A., Kostorz, G., Pedersen, J.S., Bimodal size distributions of γ ' precipitates in Ni-Al-Mo. II. Transmission electron microscopy. Acta Metall. Mater. (1995) **43,** 3441-3451.

Sequeira, A.D., Pedersen, J.S., Kostorz, G., The anisotropy of metallic systems - analysis of small-angle scattering data. In: Modern aspects of small-angle scattering. Brumberger, H. (ed.), (Kluwer Academic Publishers, Dordrecht, 1995) (NATO Advanced Science Institutes Series C: Mathematical and Physical Sciences, 451267-297.

Seto, H., Schwahn, D., Yokoi, E., Nagao, M., Komura, S., Imai, M., Mortensen, K., The crossover from mean-field to 3D-Ising critical behaviour in a 3-component microemulsion. Physica B (1995) **213-214,** 591-593.

Simpson, J.A., McMorrow, D.F., Cowley, R.A., Jehan, D.A., The low-temperature magnetic structure of holmium. International conference on magnetism. J. Magn. Magn. Mater. (1995) **140-144,** 751-752.

Simpson, J.A., McMorrow, D.F., Cowley, R.A., Jehan, D.A., Trigonal interactions in holmium. Phys. Rev. B (1995) **51,** 16073-16082.

Simpson, J.A., McMorrow, D.F., Cowley, R.A., Ward, R.C.C., Wells, M.R., Short-range magnetic order in holmium-praseodymium superlattices. J. Phys.: Condens. Matter (1995) **7,** L417-L423.

Struth, B., Scalas, E., Brezesinski, G., Möhwald, H., Bringezu, F., Bouwman, W.G., Kjær, K., Influence of a hydrophilic spacer on the structure of phospholipid monolayer. Nuovo Cimento Soc. Ital. Fis. D (1994) **16,** 1545-1550.

Svergun, D.I., Pedersen, J.S., Serdyuk, I.N., Koch, M.H.J., Solution scattering from 50S ribosomal subunit resolves inconsistency between electron microscopic models. Proc. Nat. Acad. Sci. USA (1994) **9,** 11826-11830.

Swaddling, P.P., McMorrow, D.F., Cowley, R.A., Simpson, J.A., Wells, M.R., Ward, R.C.C., Clausen, K.N., Collins, M.F., Buyers, W.J.L., The magnetic phase diagram and zero field structure of holmium-lutetium superlattices. International conference on magnetism. J. Magn. Magn. Mater. (1995) **140-144,** 783-784.

Tassi, E.L., Paci, M., Magagnini, P.L., Yang, B., Rustichelli, F., Andruzzi, F., Hvilsted, S., Ramanujam, P.S., Pedersen, M., Zebger, I., Hendann, C., Siesler, H.W., Caratterizzazione de polipropilenadipati liquido-cristallini contenenti gruppi laterali azobenzenici. (Associazione Italiana di Scienza e Tecnologia delle Macromolecole, Palermo, 1995) 164-167.

Tepe, T., Schulz, M.F., Zhao, J., Tirrell, M., Bates, F.S., Mortensen, K., Almdal, K., Variable shear-induced orientation of a diblock copolymer hexagonal phase. Macromolecules (1995) **28,** 3008-3011.

Thoft, N.B., Bohr, J., Buras, B., Johnson, E., Johansen, A., Andersen, H.H., Sarholt-Kristensen, I., Melting and solidification of bismuth inclusions in aluminium. J. Phys. D (1995) **28** 539-548.

Tomy, C.V., Chang, L.J., Paul, D.M., Andersen, N.H., Yethiraj, M., Neutron diffraction from $HoNi_2B_2C$. Physica B (1995) **213-214,** 139-141.

Tuoriniemi, J.T., Nummila, K.K., Vuorien, R.T., Lounasmaa, O.V., Metz, A., Siemensmeyer, K., Steiner, M., Lefmann, K., Clausen, K.N., and Rasmussen, F.B., Neutron Experiments on Antiferromagnetic Nuclear Order in Silver at Picokelvin Temperatures. Phys. Rev. Lett. (1995) **75,** 3744-3747.

Weinbach, S.P., Weissbuch, I., Kjær, K., Bouwman, W.G., Als-Nielsen, J., Lahav, M., Leiserowitz, L., Self-assembled crystalline monolayers and multilayers of n-alkanes on the water surface. Adv. Mater. (1995) **7,** 857-862.

Weissbuch, I., Berkovic, G., Yam, R., Als-Nielsen, J., Kjær, K., Lahav, M., Leiserowitz, L., Structured nuclei of 4-(octadecyloxy)benzoic acid monolayer for induced nucleation of 4-hydroxybenzoic acid monohydrate as determined by grazing incidence x-ray diffraction on the aqueous solution. J. Phys. Chem. (1995) **99,** 6036-6045.

Wolny, J., Lebech, B., Magnetic modulation vectors in Nd rich Nd-Pr alloys. J. Magn. Magn. Mater. (1995) **140-144,** 741-742.

Yaron, U., Gammel, P.L., Huse, D.A., Kleiman, R.N., Oglesby, C.S., Bucher, E., Batlogg, B., Bishop, D.J., Mortensen, K., Clausen, K., Bolle, C.A., Cruz, F. de la, Neutron diffraction studies of flowing and pinned magnetic flux lattices in 2H-$NbSe_2$ (Erratum to Phys. Rev. Lett. 1994, **73,** 2748). Phys. Rev. Lett. (1995) **74,** 1700.

Yaron, U., Gammel, P.L., Huse, D.A., Kleiman, R.N., Oglesby, C.S., Bucher, E., Batlogg, B., Bishop, D.J., Mortensen, K., Clausen, K.N., Structural evidence for a two-step process in the depinning of the superconducting flux-line lattice. Nature (1995) **376,** 753-755.

Yaron, U., Gammel, P.L., Huse, D.A., Kleiman, R.N., Oglesby, C.S., Bucher, E. Batlogg, B., Bishop, D.J., Mortensen, K., Clausen, K.N., Bolle, C.A., Cruz, F. de la, Translational order and neutron diffraction studies of magnetic flux lattices. (Reply). Phys. Rev. Lett. (1995) **75,** 3373.

Yethiraj, M., Mook, H.A., Forgan, E.M., Cubitt, R., Wylie, M.T., Paul, D.M., Lee, S.L., Ricketts, J., Kes, P.H., Mortensen, K., Small-angle neutron scattering study of the flux-line lattice in a single crystal of $Bi_{2.15}Sr_{1.95}CaCu_2O_{8+x}$. J. Appl. Phys. (1994) **76,** 6784-6787.

Zebger, I., Kulinna, C., Siesler, H.W., Andruzzi, F., Pedersen, M., Ramanujam, P.S., Hvilsted, S., The influence of substitutents on the orientational behaviour of novel azobenzene side-chain polyesters. Macromol. Symp. (1995) **94,** 159-170.

Österberg, R., Mortensen, K., Ikai, A., Direct observation of humic acid clusters, a nonequilibrium system with a fractal structure. Naturwissenschaften (1995) **82,** 137-139.

Ørum, H., Nielsen, P.E., Jorgensen, M., Larsson. C., Stanley, C. and Koch, T., Sequence-Specific Purification of Nucleic Acids by PNA-Controlled Hybrid Selection. Biotechniques (1995) **19(3),** 472-479.

3.2 Other Publications

articles for a broader readership, theses and reports

Bohr, H. Lindgård, P.-A., Fysikken i proteiners foldningsklassifikation. Kvant (1995) **6**, 3-7.

Feidenhans'l, R., Performance of the HASYLAB BW2 beamline, Synchrotron Radiation News (1995) 8(2), 37.

Jorgensen, M., Fremtidens avancerede sensorer er baseret på naturens egne principper. Risønyt (1995) (2), 2-3.

Lebech, B., Antiferromagnet, Den Store Danske Encyklopædi, Lund, J., (ed.), København, Danmarks National Leksikon A/S, (1994) **1**, 455.

Lefmann, K., Nuclear Magnetic Ordering in ^{109}Ag, Risø-R-850(EN) (thesis).

Lindgård, P.-A., Bechgaard, K., Clausen, K.N., Feidenhans'l, R., Johannsen, I. (eds.), Annual progress report of the Department of Solid State Physics, 1 January - 31 December 1994. Risø-R-779(EN) (1995) 162 pp.

Mortensen, K., Almdal, K., Blandinger af polymerer giver fysikerne nye udfordringer. Risonyt (1995) (3), 13-15.

Ndoni, S., Rubber Networks with Controlled Viscoelastic Properties. Dept. of Chemistry, University of Copenhagen (1994).

Thoft, N.B., Annealing studies of Bi and Kr inclusions in Al. Risø-R-783(EN) (1995) 82 pp.

Tuoriniemi, J. T., Lefmann, K., Nummila, K. K., Metz, A., Neutron Studies of Highly Polarized Silver Nuclei Extended to Nanokelvin Temperatures, Report TKK-F-A744, Helsinki University of Technology, Espoo (1995).

Winther, L., Hydrophilic support materials for peptide synthesis. (Technical University of Denmark. Department of Chemical Engineeing, Lyngby (1995).

3.3 Conferences

presentations at conferences and workshops

Almdal, K., Rotationsreometri. Polymerteknisk Selskab. Møde om polymerer - anvendt reologi, København (DK) (April).

Almdahl, K., Rotational Rheometry. Meeting on Polymer Applied Rheology. Danish Society for Polymer Technology (DK) (April).

Andersen, N.H., Magnetic and structural phases of YBaCuO. NORDITA Conference on The Physics of the 2D Electron Gas, Copenhagen (DK) (June).

Andersen, N.H., Structural and magnetic phases of the YBaCuO system, 5th Workshop on: The Influence of the Local Structure on the Superconducting Properties for Samples in the Y-Ba-Cu-O and Related Systems, Blois (FR) (June).

Andersen, N.H., Structural phase transitions in YBCO type high T_c materials. International Workshop on Scattering Experiments with High Energy Synchrotron Radiation, Schwerin (DE) (October).

Arleth, L., Pedersen, J.S., Mortensen, K., Posselt, D., Gazeau, D., Lapent, C. and Zemb, T., Characterization of tetraaza-AC8. A surfactant with cation complexing potential. DFS 95. Danish Physical Society Spring Meeting, Odense (DK) (May - June).

Baker, J. and Lindgård, P.-A., Structure of surface layers of KBr on NaCl studied by Monte Carlo simulation. DFS 95. Danish Physical Society Spring Meeting, Odense (DK) (May - June).

Baker, J. and Lindgård, P.-A., Atomic structure of interface layers between mismatched crystals studied by continuous Monte Carlo simulation. NATO Advanced Study Institute on statics and dynamics of alloy phase transformations, Corfu (GR) (June - July).

Bartels, V.T., Stamm, M., Abetz, V., Mortensen, K., Small-Angle Neutron Scattering Study of the Microphase separation in Poly(styrene-b-paramethylstyrene) Block Copolymers German Neutron Scattering Meeting, Hamburg (DE) (August).

Berg, R. H., DNO: A Peptide-Based Structure for Optical Storrage, Danish Optical Society Annual Meeting, Espergærde (DK) (December).

Blesa, M.C., Morán, E., Amador, U., Andersen, N.H., Structural properties of nickel ferrite obtained by ionic exchange from α - $NaFeO_2$. Vth European Conference on Solid State Chemistry, Montpellier (FR) (September).

Brecht, E. Schmahl, W.W., Fuess, H., Casalta, H., Schleger, P., Lebech, B., Andersen, N.H., Schemenn, S., Lütgemeier, H., Wolf Th., Significance of Al-doping for antiferromagnetic reordering in $YBa_2Cu_{3-x}Al_xO_{6+\delta}$ single crystals. 5th Workshop on: The Influence of the Local Structure on the Superconducting Properties for Samples in the Y-Ba-Cu-O and Related Systems, Blois (FR) (June).

Chang, L.J., Tomy, C.V., Paul D.McK., Andersen, N.H., and Yethiraj, M., Neutron diffration studies of $Ho_{1-x}Y_xNi_2B_2C$ compounds. SCES'95 Goa Conference, Goa (IN) (September).

Clausen, K. N., RITA- Re Invented Triple Axis Spectrometer - Project at Risø. Ersten Arbeitstreffen zur Instrumentierung des FRM II, Bernried (DE) (May).

Everitt, B.A.; Salamon, M.B.; Park, B.J.; Flynn, C.P.; Borchers, J.A.; Erwin, R.W.; McMorrow, D.; Rhyne, J.J., Novel magnetic structures of epitaxial Nd/Y systems. 1995 March meeting of the American Physical Society, San Jose, CA (US) (March).

Fernandez Barquin, L.; Gomez Sal, J.C.; Kaul, S.N.; Barandiaran, J.M.; Gorria, P.; Pedersen, J.S.; Heenan, R., SANS behaviour of $Fe_{91}Zr_9$ under magnetic field. International conference on magnetism and magnetic materials, Philadelphia, PA (US) (October).

Frello, T., Hadfield, R., and Andersen, N.H., Mass spectrometry and neutron diffraction on BiSCCO powder synthesis. Workshop on Applications of High Temperature Superconductors. The Technical University of Denmark, Lyngby (DK) (September).

Gerstenberg, M.C., Pedersen, J.S., Mortensen, K., Smith, G., Investigation of The Surface induced Ordering of P85 on Quartz. Fourth International Conference on Surface X-ray and Neutron Scattering, Lake Geneva, Wisconsin (US) (July).

Gerstenberg, M. C., Pedersen, J.S., Mortensen, K., Smith, G., Investigation of The Surface induced Ordering of P85 on Quartz. Danish Physical Society Spring Meeting, Odense (DK) (June).

Goff J. P., Bryn-Jacobsen, C., McMorrow, D. F., Ward, R. C. C., Wells, M. R., The Magnetic Structure of Nd/Pr Superlattices. 2nd International Conference on Metallic Multilayers, Cambridge (UK) (September).

Götz, J.; Pedersen, J.S.; Schurtenberger, P., Micelles as equilibrium polymers; Light and neutron scattering experiments. 9. European Colloid and Interface Society conference, Barcelona (ES) (September).

Götz, J.; Pedersen, J.S.; Laso, M.; Schurtenberger, P., Die statische Strukturfaktor von Gleichgewichtpolymeren. Frühjahrstagung der Deutschen Physikalische Gesellschaft. Fachverband Polymerphysik: Streuung an Polymeren, Jülich (DE) (March).

Hussain, A.M.; Pedersen, J.S.; Mortensen, K.; Vigild, M., A new small-angle x-ray scattering (SAXS) spectrometer utilizing and image plate detector system. DFS 95. Danish Physical Society Spring Meeting, Odense (DK) (May - June).

Hvilsted, S., FTIR til undersøgelse af polymerer. Analytiker-Ringen. Danish Pharmaceutical University, Copenhagen (DK) (March).

Larsen, J., Bechgaard, K., Synthesis and Properties of Thiahelicenes, ISCOM '95,Mittelberg (AT) (August).

Lebech, B., Magnetic structure determination by neutron diffraction. Third Summer Scool on Neutron Scattering, Zuoz, (CH) (August).

Lefmann, K., Nummila, K.K., Tuoriniemi, J.T., Vuorinen, R., Metz, A., Clausen, K. N., Lounasmaa, O.V., Rasmussen, F.B., Siemensmeyer, K., Steiner, M. Nuclear Magnetic Ordering in 109-Ag Studied by Neutron Diffraction. Joint Meeting of the American Physical Society, San Jose, CA (US) (March).

Lefmann, K., Nummila, K.K., Tuoriniemi, J.T., Vuorinen, R., Metz, A., Clausen, K. N., Lounasmaa, O.V., Rasmussen, F.B., Siemensmeyer, K., Steiner, M. Nuclear Magnetic Ordering in 109-Ag Studied by Neutron Diffraction. Danish Physical Society Spring Meeting, Odense (DK) (June).

Lefmann, K., Rasmussen, F. B., Thorsen, P. A., Shabanovna, E., Schaumburg, K., Pedersen, E.J., Nuclear Magnetism of C-13 Diamond. 2nd Emil Warburg Symposion, Bayreuth (DE) (October).

Lindgård, P.-A., Ab initio calculation of the RKKY interaction. Symposium on electronic structure of solids, Luntern (NL) (September).

Lindgård, P.-A.; Bohr, H., Towards a structural classification of protein foldings: A simplified model approach. DFS 95. Danish Physical Society Spring Meeting, Odense (DK), (May - June).

Loewenhaupt, M., Reif, T., Svoboda, P., Gratz, E. and Lebech, B., Spin structure and dynamics of $NdCu_2$. LIP - Users Meeting, Copenhagen, (DK) (September).

McMorrow, D. F., High Q resolution studies of condensed matter systems. International workshop on high-energy x-ray scattering. Schwerin (DE) (November).

Mortensen, K., Small angle scattering from Polymers. Swedish Neutron Scattering Society Annual Meeting, Studsvik, (SE) (May).

Mortensen, K., Schwahn, D., Janssen, S., Meier, G., and Schmackers, T., Scaling Law of the Ginzburg Number in Polymer Blends. Danish Physical Society Annual Meeting, Odense, (DK) (June).

Mortensen, K., Block copolymer micellar mesophases and networks. American Chemical Society Colloid and Surface Science Symposium, Salt Lake City (US) (June).

Mortensen, K., Structural Charaterization of Polymers using Small-Angle Scattering. IDA-Symposium on Polymer Characterization, Copenhagen (DK) (October).

Mortensen, K., Introduction to Small-Angle Neutron Scattering. Workshop on Small-Angle Neutron Scattering, Bangi, (MY) (November).

Mortensen, K., Small-Angle Neutron Scattering Data Reduction and Analysis. Workshop on Small-Angle Neutron Scattering, Bangi (MY) (November).

Mortensen, K., Examples on the use of Small-Angle Neutron Scattering with Industrial Relevance. Workshop on Small-Angle Neutron Scattering, Bangi, (MY) (November).

Nielsen, M., Smilgies, D.-M., Feidenhans'l, R., Landemark, E., Falkenberg, G., Lottermoser, L., Seehofer, L., Johnson, R.L., Hut Clusters on Ge(001) Surfaces Studied by STM and Synchrotion X-ray Diffraction. ECOSS 15 European Conf. on Surf. Science, Lille (FR) (September).

Nielsen, M., Hut Clusters on Ge(001) and Si(001) Surfaces Studied by Synchrotron X-ray Diffraction, DFS 95, Danish Physical Society Spring Meeting, Odense (DK) (May-June).

Paolosini, L., Lander, G. H., Shapiro S., Caciuffo R., Regnault L. P., Lebech B. and Fournier J. M., Magnetic response function of UFe_2 single crystal. Journeé des Actinides, Aquilla, (IT) (April).

Paolosini, L., Lander, G. H., Shapiro S., Caciuffo R., Regnault L. P., Lebech B. and Fournier J. M., Magnetic excitations in the UFe_2 single crystal. LIP - Users Meeting, Copenhagen, (DK) (September).

Pedersen, J.S., Small-angle scattering studies of fractal and porous materials. Norwegian Chemical Society. Section for Analytical Chemistry, Oslo (NO) (April).

Pedersen, J.S., Small-angle scattering studies of fractal and porous materials. Meeting on porous materials: Structure and transportproperties. Dansk Selskab for Katalyse, Kobenhavn (DK) (May).

Pedersen, J.S.; Hansen, S.; Bauer, R., Equilibrium aggregation of zinc-free insulin studied by small-angle neutron scattering. NATO Advanced Study Institute on physics of biomaterials: Fluctuations, self assembly and evolution, Geilo (NO) (Mar - April).

Pedersen, J.S.; Hansen, S.; Bauer, R., Equilibrium aggregation of zinc-free insulin studied by small-angle neutron scattering. Annual meeting of the American Crystallographic Association, Montreal (CA) (July).

Pedersen, J.S.; Hansen, S.; Bauer, R., Equilibrium aggregation of zinc-free insulin studies by small-angle neutron scattering. DFS 95. Danish Physical Society Spring Meeting, Odense (DK) (May - June).

Pedersen, J.S.; Laso, M.; Schurtenberger, P., Monte Carlo simulation studies of semi-flexible polymers with excluded volume interactions. 9. European Colloid and Interface Society conference, Barcelona (ES) (September).

Pedersen, W. B. HPLC and SEC as Tools in Polymer Analysis. IDA-Symposium on Polymer Characterization, Copenhagen, (DK) (October).

Poulsen, H.F., Fisker, R., Bentzon, M., Frello, T., Andersen, N.H., Süssenbach, J., and Nowikow, D., In -situ texture determinations of superconducting tapes using synchrotron radiation. Workshop on Applications of High Temperature Superconductors. The Technical University of Denmark, Lyngby (DK) (September).

Raju, N.P.; Greedan, J.E.; Pedersen, J.S.; Simon, C.; Maignan, A.; Niraimathi, A.M.; Gmelin, E.; Subramanian, M.A., Magnetic ordering in pyrochlore $Ho_2Mn_2O_7$. International conference on magnetism and magnetic materials, Philadelphia, PA (US) (October).

Rial, C., Morán, E., Alario-Franco, M.A., Amador, U., and Andersen, N.H., Room temperature chemically oxidized $La_{2-x}M_xCuO_{4+y}$ (M = Sr, Ba; $0 \leq x \leq 0.15$). Crystal structure and physical properties. Vth European Conference on Solid State Chemistry, Montpellier (FR) (September).

Rump, P.J., Arts, A.F.M., Wijn, H.W. de and Nielsen, M., Dynamics of coupled electron-phonon modes in $LiHo_{1-x}Y_xF_4$, Combined 4th Int. Conf. Phonon Physics and 8th Int. Conf. Phonon Scattering in Condensed Matter, Sapporo (JP) (July).

Schröder, A., Aeppli, G., Mason, T. E., Bucher, E., Metal Insulator Transition in Ce(Ni,Cu)Sn. DFS 95, Danish Physical Society Spring Meeting, Odense (DK) (May) .

Smilgies, D.-M., Epitaxy of High-Temperature Superconductor Films on $SrTiO_3$ Substrates. HASYLAB User Meeting, Hamburg, (DE) (January).

Smilgies, D.-M., Epitaxy of High-Temperature Superconductor Films on $SrTiO_3$ Substrates. DPG Frühjahrstagung, Berlin, (DE) (March).

Smilgies, D.-M., In-situ X-ray Diffraction Study of Dynamic Scaling in Sputtering of Ge(001). Gordon Research Conference on X-ray Physics, Plymouth, New Hampshire, (US) (July).

Sørensen, S. Aa. and Lebech, B., Neutron diffraction studies of MnSi. Third Summer Scool on Neutron Scattering, Zuoz, (CH) (August).

Tepe, T.R., Bates, F.S., Tirell, M., Almdal, K., and Mortensen Isotropic-to-lamellar transition under oscillatory shear. Bulletin of the American Physical Society APS-March Meeting, San Jose (US) (March).

Vigliante, A.; Hill, J.P.; Gibbs, L.D.; Helgesen, G.; McMorrow, D.F.; Cowley, R.A.; Wells, M.R.; Ward, R.C.C., Element specific x-ray magnetic scattering from Ho-Pr thin film alloys. 1995 March meeting of the American Physical Society, San Jose, CA (US) (March).

Vigild, M. E., Mass Density and Hydrogen Content of a a-C:H DLC Films Related to the Preparation by PE-CVD. March meeting of the American Physical Society. San Jose (US) (November).

Yaron, U., Gammel, P.L. Huse, D.A., Kleinman, R.N., Oglesby, C.S., Bucher E., Batlogg, B., Bishop, D., Mortensen K., Clausen K.N. , Neutron Diffraction Studies of Flowing and Pinned Vortex Lattices in $NbSe_2$ Bulletin of the American Physical Society APS-March Meeting, San Jose (US) (March).

Zebger, I.; Hendann, C.; Hoffmann, U.; Czarnecki, M.A.; Völkl, N.; Siesler, H.W.; Andruzzi, F.; Paci, M.; Tassi, E.L.; Magagnini, P.L.; Holme, C.; Hvilsted, S.; Kulinna, C.; Pedersen, M.; Ramanujam, P.S., Fourier-transform infrared spectroscopy of side-chain liquid crystalline polyesters under external fields. 10. International conference on Fourier transform spectroscopy, Budapest (HU) (August - September).

Zhao, J., Bates, F.S., Schulz, M., Majumdat, D., Lipic, P., Almdal, K. and Mortensen, K., Bicontinous Cubic Phase in Block Copolymer Blends Bulletin of the American Physical Society APS-March Meeting, San Jose (US) (March).

3.4 Lectures

Andersen, N.H., Højtemperatur superledere (High temperature superconductors), University Extension in Holbæk: Two double-lectures given at Risø National Laboratory, Roskilde (DK) (November).

Andersen, N.H., Magnetic ordering in $YBa_2Cu_3O_{6+x}$ and $PrBa_2Cu_3O_{6+x}$. University of Hamburg (DE) (November).

Batsberg, W.P., Chromatographic Methods. Roskilde University Centre, Roskilde (DK) (April).

Bechgaard, K., Molekylær Kemi på Afdelingen for Faststoffysik, Risø, Danish Chemical Society General Assembly, Copenhagen (DK) (November).

Feidenhans'l, R., Surfaces and Interfaces. Structure Determination Using Synchrotron Radiation. Bern, (CH) (January).

Feidenhans'l, R., Surfaces and Interfaces. Swiss Synchrotron Radiation Spring School, Grimnetz (CH) (March).

Feidenhans'l, R., The Structure Factor. Danish Technical University (DK) (December).

Feidenhans'l, R., X-ray Scattering from Surfaces and Interfaces. University of Odense (DK) (March).

Gerstenberg, M. C., Pedersen, J.S., Mortensen, K., Smith, G., Investigation of The Surface induced Ordering of the Triblock-Copolymer P85 at a Solid-Liquid Interface. Winter School in Physics, Sandbjerg (DK) (January).

Gerstenberg, M. C., Pedersen, J.S., Mortensen, K., Smith, G., Investigation of The Surface induced Ordering of the Triblock-Copolymer P85 at a Solid-Liquid Interface. Ph. D. Course in Methods in Soft Materials Science, RUC, Roskilde (DK) (March).

Johannsen, I., Polymer Research at Risoe National Laboratory- an Interdisciplinary effort. Chalmers Technical University, Göteborg (SE) (October).

Kjær, K., Synchrotron X-ray Scattering. Roskilde University Centre, Roskilde (DK) (March).

Lefmann, K., Studies of the S=1/2 One-dimensional Antiferromagnet Copper Benzoate., Low Temperature Laboratory, Helsinki University of Technology, Espoo (FI) (February).

Lefmann., K., Nuclear Magnetic Ordering in ^{109}Ag Studied by Neutron Diffraction. Neutron Scattering Dept., NIST, Gaitersburg, MD (US) (March).

Lefmann., K., Nuclear Magnetic Ordering in ^{109}Ag Studied by Neutron Diffraction. Institute of Physics and Astronomy, Johns Hopkins University, MD (US) (March).

Lefmann., K., Nuclear Magnetic Ordering in ^{109}Ag (Thesis defence). Niels Bohr Institute, University of Copenhagen (DK) (October).

Lindgård, P.-A., Electronic and Magnetic Properties of Small Magnetic Clusters., Ph.D. Course in Nano-scale Materials, Danish Technical University (DK) (September) and H. C. Ørsted Institute, University of Copenhagen (DK) (October).

McMorrow, D. F., Kunstigt Fremstillede Magnetiske Materialer. Dept. of Solid State Physics, Risø (DK) (February).

Mortensen, K., Structural Investigations of Materials Ungdommens Naturvidenskabelige Forening, Copenhagen (DK) (January).

Mortensen, K., and Posselt, D., Small Angle Scattering Ph-D cource in Methods in Soft Material Science, RUC, Roskilde (DK) (March).

Mortensen, K. and Skov Pedersen, J., Small Angle Scattering and its Data Analysis Study Class on Modern Aspects in X-ray and Neutron Scattering, Risø (DK) (March).

Nielsen, M., Hut Clusters on Ge(100) and Si(100) Surfaces Studied by STM and Synchrotron X-ray Diffraction. Max-Planck-Institute für Festkörperforschung, Stuttgart (DE) (March).

Nielsen, M., Hut Clusters on Ge(100) and Si(100) Surfaces Studied by STM and Synchrotron X-ray Diffraction. MIC, DTU, Lyngby (DK) (April).

Pedersen, W. B., Chromatographic Methods, Ph.D. Course in Methods in Soft Materials Science, Risø (DK) (April).

Smilgies D.-M., Structural Studies of Surfaces, Interfaces, and Thin Films Using Synchrotron X-ray Diffraction. National Institute of Standards and Technology, Gaithersburg, Maryland (US) (February).

Smilgies, D.-M., Study of Surface Roughness Using Synchrotron X-ray Diffraction. University of Maryland, College Park, Maryland (US) (February).

Smilgies, D.-M., Structure and Dynamics of Surfaces, Interfaces, and Thin Films, European Synchrotron Radiation Facility, Grenoble (FR) (November).

Smilgies D.-M., Dynamic Scaling in Sputtering of Ge(001), (September).

3.5 Organisation of Meetings and Courses

3.5.1 HCM - Access to Large Scale Facilities Users' Meeting

22-23 September, Grand Hotel, Copenhagen, Denmark.
The third annual users' meeting of the HCM programme was attented by 58 scientists from the EU member states. The programme consisted of 9 plenary lectures listed below and a poster session with 17 contributions.

Organization

McMorrow, D.F., Clausen, K.N., *Riso National Laboratory, Denmark* and Mackintosh, A.R. *Niels Bohr Institute, University of Copenhagen, Denmark.*

Programme

Paul, D.McK., *Department of Physics, University of Warwick, Coventry, England.* Breaking the chains in $CuGeO_3$.

Goff, J.P., *Clarendon Laboratory, Oxford Physics, Oxford, England.* Magnetic interactions in Nd/Pr superlattices.

de Cavalho Paixão, J.A., *Dept.de Fisica, Fac.Ciencias e Technologia, Univ. de Coimbra, Portugal.* Neutron and magnetic X-ray scattering studies of actinide and rare-earth compounds with the $ThMn_{12}$ structure.

Svergun, D., *EMBL Hamburg Outstation, c/o DESY, Hamburg, Germany.* Structural studies of ribosomes in solution by contrast variation.

Olsson, U., *Phys. Chem. 1, Chemical Center, Lund University, Sweden.* Phase behaviour of nonionic microemulsions.

Roser, S., *University of Bath, Claverton Down, England.* Neutron reflectivity from biosensors.

Hutchings, M.T., *521.1 Harwell, AEA Technology, Didcot, England.* Stress measurement by neutron diffraction - a challenge to the physicist and materials scientist.

Brecht, E., *Forschungszentrum Karlsruhe, Institut für Nukleare Festkörperphysik, Germany.* The effect of Al-doping on antiferromagnetic AFII ordering in $YBa_2Cu_{3-x}Al_xO_{6+\delta}$.

Nieuwenhuys, G., *Kamerlingh Onnes Lab., Leiden University, The Netherlands.* The unique magnetic structure of UNi_4B.

3.5.2 Polymer Characterization

31 October, Domus Technica, Copenhagen, Denmark.
This Symposium under the auspices of Danish Society for Polymer Technology was dedicated to advanced methods and instrumentation for characterization of polymer materials. Six lecturers described state-of-art within selected and sometimes complementary methods and the Symposium had 50 participants with the majority from industry and 8 from the Department of Solid State Physics.

Organization

Hvilsted, S., *Riso National Laboratory, Denmark*, Clausen, L.D., *Radiometer Medical A/S, Denmark*

Programme

Siesler, H.W., *University of Essen, Germany.* Vibrational Spectroscopy in Short Time Intervals and Over Long Distances: From Time- Resolved Measurements to Remote Analysis.

Nielsen, N.C., *Aarhus University, Denmark.* Quantitative Solid-State NMR Spectroscopy on Polymers.

Mortensen, K., *Riso National Laboratory, Denmark.* Structural Characterization of Polymers Using Small-Angle Scattering.

Pedersen, W.B., *Riso National Laboratory, Denmark.* HPLC and SEC as Tools in Polymer Analysis.

Badyal, J.P., *University of Durham, England.* XPS Characterization of Polymer Surfaces.

Warkentin, P., *Linköping University, Sweden.* Adsorption Behaviour of IgG on Methylated Silicon Surfaces Studied by Tapping Mode Atomic Force Microscopy.

3.5.3 Danish Polymer Centre Meeting

24 October, Technical University of Denmark.
Presentation of research projects within Danish Polymer Centre attended by 41 scientists. The programme consisted of 12 lectures.

Organization

Johannsen, I, *Riso National Laboratory, Denmark* and Hassager, O., *Department of Chemical Engeneering, Technical University of Denmark.*

Programme

Hassager, O., *Department of Chemical Engeneering, Technical University of Denmark* and Almdal, K., *Riso National Laboratory, Denmark.* Polymer Rheology and Processing.

Jørgensen, M., *Riso National Laboratory, Denmark.* Functional Polymers and Surfaces.

Berg, R.H. and Kulinna, C., *Riso National Laboratory, Denmark.* Optical Polymers.

Lyngaae-Jørgensen, J. and Strøbech, E., *Department of Chemical Engeneering, Technical University of Denmark.* Structure and Phase behaviour of Polymer Systems.

Gregorius, K., *Mouritsen & Elsner A/S, Denmark.* Modification of Plast Surfaces.

Christensen, S.F., *Coloplast A/S, Denmark.* Rheology of Adhesion.

Melamed, M., *Danfoss A/S, Denmark* and Larsen, T.S., *Grundfos A/S, Denmark.* Chemical and Thermical Deterioriation of Plast Composites.

Rasmussen, *S.E., Nunc A/S, Denmark.* Use of Polymer Blends for Surface Functionalisation of Injection Moulded Parts.

Buch-Rasmussen, T., *Novo-Nordisk A/S, Denmark.* Development and Charactarisation of Materials for Packaging of Medical Products.

Lambertsen, E., *ABB I.C.Moller, Denmark.* Charactarisation of Foamed Plastics.

Urban, C., *Hempel's Marine Paints A/S, Denmark.* Study of Epoxy Networks for use in Coating Applications.

Iván, B., *Institute of Physical Chemistry, University of Mainz, Germany.* Synthesis and Properties of New Microphase Separated Polymer Systems.

3.5.4 Design and Development of Catalytic Processes, Modecs Meeting

9-10 November 1995, Hotel Frederiksdal, Lyngby, Denmark.
Modecs meeting on Catalysis. The programme consisted of 9 lectures and 1 plenary discussion.

Organization
Johannsen, I., *Risø National Laboratory, Denmark.*

Programme

Heterogeneous Catalysis
Henrik Topsøe, *Haldor Topsøe Research Laboratories, Denmark.* Catalysis Research: From Fundamentals to Development.

Nan-Yu Topsøe, *Haldor Topsøe Research Laboratories, Denmark* Nature of Surface Sites and Reaction Mechanism for the Selective Catalytic Reduction of Nitric Oxide by Ammonia over Vanadia/Titania Catalysts.

Peter Mikal Holmblad, *Physics Institute, The Technical University of Denmark.* Designing metal surfaces for heterogeneous catalytic reactions.

Homogenous Catalysis
John M. Brown, *Oxford University, Dyson Perrins Laboratory, England.* Novel Catalysts and Reaction Paths in Asymmetric Synthesis.

Karl Anker Jørgensen, *Aarhus University, Denmark.* Metal-Catalyzed Asymmetric Reactions.

Søren Rasmussen, *Environmental Science and Technology Department, Risø National Laboratory, Denmark.* PCR-techniques - Theory and Applications.

Discussion
Ove Poulsen, *Ministry of Research, Denmark* and Haldor Topsøe, *Haldor Topsøe A/S, Denmark,* National Research Strategy. Does it work ?

Enzymatic Catalysis
Itamar Willner, *Institute of Chemistry, The Hebrew University of Jerusalem, Israel.* Enzyme and Immunosensor Electrodes and Optobioelectronic Devices.

Morten Meldal, *Carlsberg Laboratory, Copenhagen, Denmark.* Specificity of Enzymatic Catalysis and Inhibition Monitored by Internally quenched Peptide Libraries.

Jens Sigurd Okkels, *Enzyme Screening, NOVO-Nordisk, Copenhagen, Denmark.* Protein Engineering of Industrial Interesting Lipases.

3.5.5 Ph.D. Course in Modern Aspects of X-ray and Neutron Scattering.

Feb.-June, Riso National Laboratory, Denmark, as a series of 2x45 min lectures.

Organization

Feidenhans'l, R., Clausen, K.N. and Mackintosh, A. *Riso National Laboratory, Denmark*

Programme

Als-Nielsen, J.	Dynamical Diffraction
Als-Nielsen, J.	Dynamical Diffraction
Spiller, E.	Multilayer Optics
Mackintosh, A	Magnetic Neutron Scattering
Spiller, E.	X-ray Imaging and Multilayers II
Mortensen, K., and Pedersen, J.S.	Small Angle Scattering and its Data Analysis
Spiller, E.	X-ray Coherency and Holography
Clausen, K.N.	Neutron Sources
Gerstenberg, M.C.	Filters for Polarisation of Neutrons
Aagaard, S.	Polarized Neutron Scattering
Eskildsen, M.R.	X-ray Wave Guides
Holme, C.	Bragg-Fresnell Lenses
Ramanujam, P.S.	X-ray Lasers
Feidenhans'l, R.	Application of X-ray Lasers

3.6 Membership of Committees and Boards

Andersen, N.H.,

Consultant for the Swedish Superconductivity Consortium.

Bechgaard, K.,

Chairman of the Danish National Commitee for Chemistry.
Member of the Advisory Board of Journal of Materials Chemistry.
Member of the EEC COST D-4 Committee.
Member of the Academy Council of the Danish Academy of Technical Sciences.
Member of the NATO Special Programme Panel on Supramolecular Chemistry.
Chairman of the "Mindship Foundation".

Berg, R. H.,

Member of the Editorial Advisory Board, Journal of Peptide Science.
Councillor of the European Peptide Society.

Clausen, K. N.,

Risø Board of Governors
ESS Science Working Group

Feidenhans'l, R.,

Secretary for the National Commitee for Crystallography
Member of the Forschungsbeirat Synchrotronstrahlung HASYLAB, DESY, Hamburg.

Hvilsted, S.,

Treasurer of The Danish Society for Polymer Technology.

Lebech, B.,

IURC Commision on Neutron Scattering
Den Danske National Kommite for Krystallografi
Danish Representative in ENSA, the European Neutron Scattering Assiciation

Lindgård, P.-A.,

Vicechaiman of the Magnetism Section of International Union of Pure and Applied Physics (IUPAP).
Chairman of the Condensed Matter Commitee at NORDITA.

Mortensen, K.,

Member of the Board of Solid State Dicision of the Danish Physical Society.
Member of the European Spallation Source Scientific Working group on Large Scale Structures.

Pedersen, J. S.,

Coeditor of Journal of Applied Crystallography.

3.7 Colloquia

Papadakis, C., IMFUFA, Roskilde University, Denmark. Mean Field and Scaling Theories of Polymers and Block-copolymers (January).

Moij, G.C.A., The Technical University of Denmark, Denmark. Simulation of Polymer Phase Equilibria (February).

Wolf, T., Kernforschungszentrum Karlsruhe, Germany. Growth and Physical Properties of Large $YBa_2Cu_3O_7$ single Crystals (February).

Pohl, J., Universität Konstanz, Germany. Growth and Structure of δ-Mn in superlattices: A summary of experimental results (March).

Høghøj, P., Institute Laue-Langevin, France. Multilayer for X-ray and Neutron Optics (February).

Yaron, U., AT&T Bell Laboratories, USA. Small-Angle Neutron Scattering of Pinned and Flowing Magnetic Flux Lattices in Type II Superconductors (March).

Day, P., The Royal Institution of Great Britain, England. New Physics From Molecular Conductors and Magnets (March).

Aono, M., Surface and Interface Lab., RIKEN Inst., Japan. Producing and measuring extreme high vacuum (XHV), much better than UHV (April).

Gatteschi, D., Department of Chemistry, University of Firenze, Italy. Metal Ions and Organic Radicals for Magnetic Materials (May).

Motokawa, M., Institute for Materials Research, Tohuku University, Japan. The Strange Magnetic Properties of $Y_2Cu_2O_5$ (June).

Stecki, J., Institute of Physical Chemistry, Polish Academy of Science, Poland. Correlations in planar liquid interfaces by Molecular Dynamics simulations (June).

Bilderback, D., Cornell University, USA. X-ray microscience opportunities with micron diameter beams produced from capillary optics (September).

Noolandi, J., Xerox Research Center of Canada, Canada. Rod-coil Mixing by Acid-base Interactions and Metal/Polymer Compatibilizers (September).

Lindegaard-Andersen, A., The Technical University of Denmark, Denmark. 100 years of X-ray Radiography (October).

Nummila, K., Helsinki University of Technology, Low Temperature Laboratory, Finland. Neutron Transmission Techniques Applied to Spin Lattice Relaxation Measurements on Highly Polarized Silver Nuclei (October).

Rieu, J.P., Laboratoire de Spectrométrie Physique, Université Joseph Fourier, France. An X-ray Diffraction Study of Melting of Short Alcohol Monolayers on Water (October).

Eng, P., Advanced Photon Source, USA. Achromatic Micro-Focused X-ray Beams at 2nd and 3rd Generation Synchrotron (October).

Iván, B., University of Mainz, Institute of Physical Chemistry, Germany. Amphiphilic Networks and Gels: A New Class of Crosslinked Polymers and Potential Biomaterials (October).

Siesler, H.W., Department of Physical Chemistry, University of Essen, Germany. Time-resolved Spectroscopy of Segmental Mobility in Liquid Crystals (November).

Bergström, M., Department of Chemistry, Division of Physical Chemistry, Royal Institute of Technology, Sweden. Reversibly Formed Bilayer Vesicles: Energetics and Polydispersity (November).

Lehmann, M.S., Institut Laue-Langevin, France. Macromolecular Crystallography with Cold Neutrons and a Large Image Plate Detector (December).

Steinfort, A.J., University of Delft, The Netherlands. Study of Thin Layers and Interfaces with X-ray Diffraction (December).

Skriver, H., Physics Department, The Technical University of Denmark, Denmark. Possible Ferromagnetism in Pd-Ag Superlattices (December).

4 Participants in the Work in the Department

4.1 Staff

Aeppli, Gabriel (Consultant)
Almdal, Kristoffer
Als-Nielsen, Jens (Until April 1)
Andersen, Niels Hessel
Bechgaard, Klaus (Head of the Department)
Berg, Rolf Henrik
Clausen, Kurt N. (Head of Research Programme)
Feidenhans'l, Robert (Head of Research Programme)
Hvilsted, Søren
Johannsen, Ib (Head of Research Programme)
Jørgensen, Mikkel
Kjær, Kristian
Lebech, Bente
Lebech, Jens
Lindgård, Per-Anker
McMorrow, Des
Mortensen, Kell
Nielsen, Mourits
Pedersen, Jan Skov
Pedersen, Walther Batsberg
Sommer-Larsen, Peter

Ph.D. Students and Students

Christensen, Morten Jagd
Eskildsen, Morten Ring
Krebs, Frederik (From July 1)
Gerstenberg, Michael C.
Hviid, Lene (Until August 1)
Krog, Thomas
Larsen, John Greibe
Larsen, Mogens (From May 1)
Madsen, Anders (From February 1)
Madsen, Jesper
Madsen, Nils Berg (From July 1)
Pedersen, Marianne
Petersen, Thomas (Until January 30)
Schmidt, Ole (From October 1)
Sørensen, Steen Aagaard
Vigild, Martin
Wang, Christian
Zhou, Ji (From February 1)

Technical Staff

Bang, Steen
Berntsen, Allan Nørtoft
Breiting, Bjarne
Hansen, Dorthe (Apprentice from September 1)
Hansen, John Erik (Temporary until December 31)
Hedeboe, Vivi
Hubert, Lene
Jensen, Birgit
Johansen, Arne (Temporary from April 3)
Jørgensen, Ole
Jørgensen, Ole Emil (Temporary from August 28)
Kjær, Torben
Kristensen, Eva Tulin
Lund, Morits
Nielsen, Anne Bønke
Nielsen, Carina (Apprentice from December 1)
Nielsen, Lotte
Nielsen, Steen
Rasmussen, Helle Demant (Apprentice from September 15)
Rasmussen, Ove
Saxild, Finn
Sonberg, Tina Sonne (Apprentice until September 14, temporary from September 15)
Stahl, Kim
Theodor, Keld

Temporary Student Assistants

Bøgetoft, Morten (From November 25 to November 30)
Frederiksen, Line (From February 8 to February 28)
Kofod, Guggi (From June 26 to August 20)
Hansen, Per Mørkegaard (From June 26 to July 31)
Nørgaard, Lillian Gilsgaard (From June 26 to July 21)

Secretaries

Byrdal, Christina (Apprentice from November 1)
Frederiksen, Lajla
Schlichting, Bente Overgaard
Studinski, Ca Thi

Guest Scientists, Temporary Staff, Long Time Visitors and Post Docs

Arleth, Lise (Temporary from March 1)
Bouwman, Wim (Until March 31)
Bødker, Franz (Temporary from January 2 to February 28 and October 1 to December 31)
Frello, Thomas (Temporary from June 12)
Fischer, Erik (Temporary until September 30)
Hendann, Claudia
Hussain, Ahsen (Temporary until September 30)
Käll, Mikael (From September 1)
Kulinna, Christian
Landemark, Erik
Larsen, Jan (Temporary until October 14)
Lefmann, Kim (Temporary until June 30)
Lussier, Jean-Guy
Misaki, Yohji (From September 1)
Ndoni, Sokol (From January 16)
Nielsen, Niels Chr. (Temporary from August 15)
Schröder, Almut
Smilgies, Detlef
Svejstrup, Jens (Temporary until December 31)
Wilkes, Stephen

Awards and Degrees

Foss, Morten Ph.D., University of Aarhus
Lefmann, Kim Ph.D., University of Copenhagen
Mortensen, Kell, Research professor
Thoft, Nina Bjørn Ph.D., University of Aalborg
Winter, Lars Ph.D., Danish Technical University

4.2 Short Time Visitors

Baker, J.	University of Florida, Physics Dept., Thallahassee, U.S.A.
Bates, F.S.	Department of Chemical Engeneering and Materials Science, University of Minnesota, USA.
Benevides, H.	Departamento de Ingeniera Metalurgica, ESIQIE, IPN, Mexico
Bishop, D.	AT&T Bell Laboratories, Murray Hill, NJ, U.S.A.
Broholm, C.	The Johns Hopkins University, Physics & Astronomy Dept., Baltimore, U.S.A.
de Jesus Cruz, J.	Departamento de Ingeniera Metalurgica, ESIQIE, IPN, Mexico
Dender, D.	The Johns Hopkins University, Physics & Astronomy Dept., Baltimore, U.S.A.
Dorantes, H.	Departamento de Ingeniera Metalurgica, ESIQIE, IPN, Mexico
Gammel, P.	AT&T Bell Laboratories, Murray Hill, NJ, U.S.A.
Gidalevitz, D.	Weizman Institute, Israel
Gilhøj, H.	FKI, The Technical University of Denmark, Denmark
Hayden, S.	H.H. Wills Physics Lab., University of Bristol, England
Hillemeyer, M.	Department of Chemical Engeneering and Materials Science, University of Minnesota, USA.
Hutchings, M.	NDT Materials Characterization, NDT Dept., 521 Harwell, England
Lee, S.	The Johns Hopkins University, Physics & Astronomy Dept., Baltimore, U.S.A.
Lulek, T.	Adam Mickiewicz Univ., Inst. of Physics, Poznán, Poland
Mason, T.	Physics Department, University of Toronto, Canada
Olsson, U.	Physical Chemistry 1, Lund University, Sweden
Österberg, R.	Dept. of Chemistry, Univ. of Agricultural Science, Uppsala, Sweden
Rajagopalan, V.	Physical Chemistry 1, Lund University, Sweden
Reich, D.	The Johns Hopkins Univ., Physics & Astronomy Dept., U.S.A.
Richards, H.	University of Florida, Physics Dept., Thallahassee, U.S.A.
Salansky, J.	Academy of Sciences of Czech Republic, Physics Institute, Za Slovankow 3, Praha 8, Tjekkiet, Czech Republic
Schurtenberger, P.	ETH-Zürich, Institut für Polymere, Switzerland
Schwendler, M.	Inst. für Physikalische Chemie, Johannes Gutenberg Universität, Mainz, Germany
Sinclair, R.	NDT Materials Characterization, NDT Dept., 521 Harwell, England
Svoboda, P.	Charles University, Dept. of Metal Physics, Praha 2, Czech Republic
Tepe, T.	Department of Chemical Engeneering and Materials Science, University of Minnesota, USA.
Weimann, P.	Departamento de Ingeniera Metalurgica, ESIQIE, IPN, Mexico
Windsor, C.	NDT Materials Characterization, NDT Dept., 521 Harwell, England
Yaron, U.	AT&T Bell Laboratories, Murray Hill, NJ, U.S.A.
Zebger, I.	University of Essen, Dept. of Physical Chemistry, Germany

4.3 Short Time Visitors under the CEC-HCM programme

Abetz, V.	Max-Planck-Inst. für Polymerforschung,Mainz, Germany
Bartels, V.	Max-Planck-Inst. für Polymerforschung,Mainz, Germany
Berbessou, D.	Université de Bordeaux I, Talence, France
Bonner, N.W. University	Department of Manufacturing Engineering, Loughborough of Technology, England
Boothroyd, A.	Clarendon Laboratory, Oxford University, England
Bryn-Jacobsen, C.	Clarendon Laboratory, Oxford University, England
Burkhardt, N.	EMBL c/o DESY, EMBL Hamburg Outstation, Germany
Caruana, D.	School of Chemistry, University of Bath, England
Chakkalakal, T.	Department of Physics, University of Warwick, England
Chang, L.T.	Department of Physics, University of Warwick, England
Coad, S.M.	Department of Physics, University of Warwick, England
Coldea, R.	Clarendon Laboratory, University of Oxford, England
Cowley, R.	Clarendon Laboratory, University of Oxford, England
Cubitt, R.	School of Physics and Space Research, Univ.of Birmingham, England
Dawidowski, J.	Instituto de Estructura de la Materia, C.S.I.C., Spain
Daymond, M.	Univ.of Cambridge, Dept.of Materials Science & Metallurgy, England
de Kruif, G.	Netherlands Institute for Dairy Research, EDE, The Netherlands
de Wijn, H.	Faculty of Physics and Astronomy, University of Utrecht, Holland
Deriu, A.	Dipartimento di Fisica, Universita di Parma, Italy
Elizondo, U.J. A.	Dpt. Quimica Inorga nica, Fac. C. Quimicas, Universidad Complutense de Madrid, Spain
Falcao, A.	INETI/ICEN, Physics Department, Sacavém, Portugal
Fernandez, L.	Facultad de Ciencias, Universidad de Cantabria, Spain
Finnegan, M.	School of Chemistry, University of Bath, England
Fiori, F.	Politecnico Di Milano, Dipartimento di Ingegneria Nucleare - CESNEF, Italy
Forgan, E.M.	School of Physics and Space Research, Univ.of Birmingham, England
Forsyth, B.	Clarendon Laboratory,Oxford University, England
Frielinghaus, H.	Inst. f.Festkörperforschung,Forschungszentrum Jülich mbH,Germany
Gardner, J.	Physics Department, University of Warwick, England
Goff, J.	Clarendon Laboratory, Oxford University, England
Gomez Sal, J. C.	Facultad de Ciencias, Universidad de Cantabria, Spain
Gomez, D.	Facultad de Ciencias, Universidad de Cantabria, Spain
Gorria, P.	Facultad de Ciencias, Universidad de Cantabria, Spain
Gregorkiewitz, M.	Dip. Scienza della Terra Universita, Italy
Hamley, I.	University of Durham, Department of Physics, Durham, England
Hecht, E.	Dept. of Physical Chemistry I, University of Bayreuth, Germany
Henn, G.	Max-Planck-Inst. für Polymerforschung,Mainz, Germany
Lackner, T.	Zentrum für Ultrastrukturforschung, Der Universität für Bodenkultur, Wien, Austria
Lee, S.	School of Physics and Space Research, Univ.of Birmingham, England

Lloyd, S.	School of Physics and Space Research, Univ.of Birmingham, England
Loewenhaupt, M.	Inst. f. Festkörperforschung, Forschungszentrum Jülich GmbH, Germany
Longmore, A.	Department of Physics, Clarendon Laboratory, England
Lopez, C. R.	Dpt. Quimica Inorganica, Fac. C. Quimicas, Universidad Complutense de Madrid, Spain
Lopez, F.	Université de Bordeaux I, Talence, France
Lösche, M.	Universität Leipzig, Fakultät f. Physik und Geowissenschaften, Germany
Luckhurst, G.	University of Durham, Department of Physics, Durham, England
Magnin, T.	Centre SMS, Ecole des Mines Saint-Etienne, Saint-Etienne, France
Malang, U.	Fakultät für Physik, LS Prof.Dr. E. Bucher, Universität Konstanz, Germany
Malizia, F.	Dipartimento di Fisica, Universita di Parma, Italy
Martin, J.	University of Warwick, Department of Physics, England
Martinez, J.L.	Instituto de Estructura de la Materia, C.S.I.C., Spain
McEwen, K.	Birkbeck College, Univ. of London, Dept. of Physics, England
Mentik, S.	Kamerligh Onnes Laboratory, Leiden University, The Netherlands
Mills, G.	Department of Manufacturing Engineering, Loughborough University of Technology, England
Miodownik, M.	Oxford University, Materials Department, Parks Road, England
Moolenaar, A.	Birkbeck College, Univ. of London, Dept. of Physics, England
Moore, C.	School of Chemistry, University of Bath, England
Müller, G.	Institut für Festkörperforschung, Forschungszentrum Jülich GmbH, Germany
Müller, P.	Institut für Anorg. Chemie der RWTH Aachen, Aachen, Germany
Nieuwenhuys, G. J.	Kamerligh Onnes Laboratory, Leiden University, The Netherlands
Nutley, M.	School of Physics and Space Research, Univ.of Birmingham, England
Olsson, U.	Chemical centre, Lund University, Sweden
Pohl, J.	Fakultät für Physik, LS Prof.Dr. E. Bucher, Universität Konstanz, Germany
Reif, T.	Institut für Festkörperforschung, Forschungszentrum Jülich GmbH, Germany
Riseman, T.	School of Physics and Space Research, Univ.of Birmingham, England
Roefs, S.	Netherlands Institute for Dairy Research, EDE, The Netherlands
Roser, S.	School of Chemistry, University of Bath, England
Rotter, M.	Institut für Festkörperforschung, Forschungszentrum Jülich GmbH, Germany
Rump, P.	Faculty of Physics and Astronomy, University of Utrecht, Holland
Sabin, T.	University of Cambridge, Dept. of Materials Science & Metallurgy, England
Schalke, M.	Universität Leipzig, Fakultät f. Physik und Geowissenschaften, Germany
Schwahn, D.	Institut für Festkörperforschung, Forschungszentrum Jülich GmbH, Germany
Schwingel, D.	UMIST, Materials Science Centre, England

Seddon, J.	University of Durham, Department of Physics, Durham, England
Serrano, M.	Dip. Scienza della Terra Universita, Italy
Simpson, A.	Clarendon Laboratory, Oxford University, England
Smith, D.	Dept. of Mechanical Engineering, University of Bristol, England
Stamm, M.	Max-Planck-Inst. für Polymerforschung,Mainz, Germany
Steigenberger, U.	ISIS Science Division, Rutherford Appleton Laboratory, England
Stockert, O.	Physikalisches Institut, Universität Karlsruhe, Germany
Svergun, D.	EMBL c/o DESY, EMBL Hamburg Outstation, Germany
Tennant, A.	Clarendon Laboratory, University of Oxford, England
Verheul, M.	Netherlands Institute for Dairy Research, EDE, The Netherlands
Viviani, L.	Politecnico Di Milano, Dipartimento di Ingegneria Nucleare - CESNEF, Italy
Vogel, S.	TU Bergakademie Freiberg, Inst. für Metallkunde, Germany
Vogt, J.B.	Université de Lille 1, Laboratoire Métallurgie Physique, Villeneuve d'Ascq, France
Wells, M.	Clarendon Laboratory, Oxford University, England
Wetzer, B.	Zentrum für Ultrastrukturforschung, Der Universität für Bodenkultur, Wien, Austria
Weygand, M.	Universität Leipzig, Fakultät f. Physik und Geowissenschaften, Germany
Wildes, A.	Oxford Physics, Clarendon Laboratory, England
Zhu, W.	Dept. of Mechanical Engineering, University of Bristol, England
Zimmerman, M.	HASYLAB, c/o DESY, Hamburg, Germany

Bibliographic Data Sheet **Riso-R-863(EN)**

Title and author(s)

Annual Progress Report of the Department of Solid State Physics
1 January - 31 December 1995

Edited by M. Jørgensen, K. Bechgaard, K.N. Clausen, R. Feidenhans'l, and I. Johannsen

ISBN
87-550-2142-5

ISSN
0106-2840
0907-0249

Dept. or group
Department of Solid State Physics

Date
January 1996

Groups own reg. number(s)

Project/contract no.

Pages	Tables	Illustrations	References
173	5	135	163

Abstract (Max. 2000 char.)
Research in the department is concerned with "Materials with Distinct Physical and Chemical Properties". The principal activities of the department in the period from 1 January to 31 December, 1995, are presented in this Progress Report.

Neutron and x-ray diffraction techniques are used to study a wide variety of problems in condensed matter physics and include: two- and three-dimensional structures, magnetic ordering, heavy fermions, high T_c superconductivity, phase transitions in model systems, precipitation phenomena, and nano-scale structures in various materials. The research in chemistry includes chemical synthesis and physico-chemical investigation of small molecules and polymers, with emphasis on polymers with new optical properties, block copolymers, surface modified polymers, and supramolecular structures. Related to these problems there is work going on in theory, Monte Carlo simulations, computer simulation of molecules and polymers and methods of data analysis.

Descriptors INIS/EDB
MAGNETISM, POLYMERS, PROGRESS REPORT, RESEARCH PROGRAMS, RISOE NATIONAL LABORATORY, SOLID STATE PHYSICS, SUPERCONDUCTIVITY

Available on request from:
Information Service Department,
Riso National Laboratory (Afdelingen for Informationsservice, Forskningscenter Riso)
P.O. Box 49, DK-4000 Roskilde, Denmark
Phone (+45) 46 77 46 77, ext. 4004/4005 - Telex 43 116 - Telefax (+45) 46 75 56 27

Direct phone numbers, fax numbers and e-mail addresses of the scientific staff of the Department of Solid State Physics:

Name	Phone number	Fax number	e-mail address
Almdal, Kristoffer	+45 4677 4785	+45 4675 5330	almdal@risoe.dk
Als-Nielsen, Jens	+45 4677 4728	+45 4237 0115	als@xray.fys.dk
Andersen, Niels Hessel	+45 4677 4711	+45 4237 0115	hessel@risoe.dk
Arleth, Lise	+45 4677 4720	+45 4237 0115	fys-liar@risoe.dk
Bechgaard, Klaus	+45 4677 4701	+45 4237 0115	fys-klbe@risoe.dk
Berg, Rolf Henrik	+45 4677 4782	+45 4675 5330	
Christensen, Morten Jagd	+45 4677 4712	+45 4237 0115	morten@fys-hp-1-risoe.dk
Clausen, Kurt N.	+45 4677 4704	+45 4237 0115	clausen@risoe.dk
Eskildsen, Morten Ring	+45 4677 4713	+45 4237 0115	eskild@risoe.dk
Feidenhans'l, Robert	+45 4677 4708	+45 4237 0115	fys-rofe@risoe.dk
Frello, Thomas	+45 4677 4719	+45 4237 0115	frello@risoe.dk
Gerstenberg, Michael C.	+45 4677 4741	+45 4237 0115	gerstenberg@risvx1.risoe.dk
Hvilsted, Søren	+45 4677 4784	+45 4675 5330	hvilsted@risoe.dk
Johannsen, Ib	+45 4677 4747	+45 4675 5330	ibj@risoe.dk
Jørgensen, Mikkel	+45 4677 4717	+45 4675 5330	fys-mijq@risoe.dk
Käll, Mikael	+45 4677 4713	+45 4237 0115	
Kjær, Kristian	+45 4677 4709	+45 4237 0115	kkjaer@risoe.dk
Kulinna, Christian	+45 4677 4778	+45 4675 5330	kulinna@risoe.dk
Larsen, Mogens	+45 4677 4261	+45 4675 5330	fys-mlar@risoe.dk
Lebech, Bente	+45 4677 4705	+45 4237 0115	lebech@risoe.dk
Lebech, Jens	+45 4677 4761	+45 4237 1594	fys-jens@risoe.dk
Lindgård, Per-Anker	+45 4677 4706	+45 4237 0115	pal@risoe.dk
Lussier, Jean-Guy	+45 4677 4726	+45 4237 0115	lussier@fys-hp-1.risoe.dk
Madsen, Nils Berg	+45 4677 4743	+45 4675 5330	mak-nibm@risoe.dk
McMorrow, Des	+45 4677 4723	+45 4237 0115	mcmorrow@fys-hp-1.risoe.dk
Misaki, Yohji	+45 4677 4779	+45 4675 5330	mak-yomi@risoe.dk
Mortensen, Kell	+45 4677 4710	+45 4237 0115	mortensen@risoe.dk
Ndoni, Sokol	+45 4677 4746	+45 4675 5330	fys-sond@risoe.dk
Nielsen, Mourits	+45 4677 4703	+45 4237 0115	fys-moun@risoe.dk
Nielsen, Niels Chr.	+45 4677 4776	+45 4675 5330	
Pedersen, Jan Skov	+45 4677 4718	+45 4237 0115	skov@risoe.dk
Pedersen, Marianne	+45 4677 4779	+45 4675 5330	marianne.pedersen@risoe.dk
Pedersen, Walther Batsberg	+45 4677 4783	+45 4675 5330	
Schröder, Almut	+45 4677 4720	+45 4237 0115	almut@fys-hp-1.risoe.dk
Smilgies, Detlef	+45 4677 4719	+45 4237 0115	detlef@risoe.dk
Sommer-Larsen, Peter	+45 4677 4744	+45 4675 5330	mak-pesl@risoe.dk
Sørensen, Steen Aagaard	+45 4677 4722	+45 4237 0115	sqrensen@risvxq.risoe.dk
Svejstrup, Jens	+45 4677 4753	+45 4675 5330	jens.svejstrup@risoe.dk
Vigild, Martin	+45 4677 4712	+45 4237 0115	martin.vigild@risoe.dk
Wilkes, Stephen	+45 4677 4753	+45 4675 5330	steve.wilkes@risoe.dk
Zhou, Ji	+45 4677 4754	+45 4675 5330	

RISØ

Objective

Risø's objective is to provide society and industry with new opportunities for development in three main areas:

- *Energy technology and energy planning*
- *Environmental aspects of energy, industrial and agricultural production*
- *Materials and measuring techniques for industry*

In addition, Risø advises the authorities on nuclear issues.

Research profile

Risø's research is strategic, which means that it is long-term and directed toward areas which technological solutions are called for, whether in Denmark or globally. The reasearch takes place within 11 programme areas:

- *Wind energy*
- *Energy materials and energy technologies for the future*
- *Energy planning*
- *Environmental impact of atmospheric processes*
- *Processes and cycling of matter in ecosystems*
- *Industrial safety*
- *Environmental aspects of agricultural production*
- *Nuclear safety and radiation protection*
- *Structural materials*
- *Materials with special physical and chemical properties*
- *Optical measurement techniques and information processing*

Transfer of Knowledge

Risø's research results are transferred to industry and authorities through:

- *Co-operation on research*
- *Co-operation in R&D consortia*
- *R&D clubs and exchange of researchers*
- *Centre for Advanced Technology*
- *Patenting and licencing activities*

And to the world of science through:

- *Publication activities*
- *Network co-operation*
- *PhD education and post docs*

Key Figures

Risø has a staff of more than 900, including more than 300 researchers and 100 PhD students and post docs. Risø's 1996 budget totals DKK 471 m, of which 45 % come from research programmes and commercial contracts, while the remainder is covered by government appropriations.

Risø-R-863(EN)
ISBN 87-550-2142-5
ISSN 0106-2840
ISSN 0907-0249

Available on request from:
Information Service Department
Risø National Laboratory
P.O. Box 49, DK-4000 Roskilde, Denmark
Phone +45 46 77 46 77, ext. 4004/4005
Telex 43116, Fax +45 46 75 56 27
http://www.risoe.dk
e-mail: risoe@risoe.dk

Klebel s offset tryk a s